Appraisal of Relative Sea Level Rise Scenarios for Venice

Final Project Report

NBMG-RP-VEN3

January 10, 2006

Prepared by:
Nevada Bureau of Mines and Geology,
University of Nevada, Reno
Mail Stop 178
Reno, NV 89557
USA

Reference:

Plag, H.-P., Tsimplis, M. N., Hammond, W., and Pugh, D, 2006. Appraisal of the relative sea level rise scenario for Venice. Final Project Report, Nevada Bureau of Mines and Geology, University of Nevada, Reno, Report NBMG-RP-VEN3, 134pp.

Contents

Executive Summary **6**

1 Introduction **10**

1.1 Objectives . . . 10

1.2 Organization of the report . . . 10

2 Concepts in sea-level studies **12**

2.1 Definition of basic terms . . . 12

2.2 The local sea-level equation . . . 14

2.3 The global ocean mass balance . . . 18

2.4 Relations between GOM, GOV and LSL . . . 19

3 The data base and models **21**

3.1 Tide gauge records . . . 21

3.1.1 Hourly tide gauge records . . . 21

3.1.2 Monthly sea-level records . . . 23

3.2 Satellite altimetry . . . 24

3.3 Meteorological data . . . 25

3.3.1 Local, *in-situ* observations . . . 25

3.3.2 Global reanalysis data sets . . . 29

3.4 Oceanographic data . . . 30

3.4.1 Global data sets . . . 30

3.4.2 Oceanographic data sets in the Mediterranean Sea . . . 31

3.5 Observations of vertical land motion . . . 32

3.5.1 Leveling . . . 32

3.5.2 GPS data . . . 33

3.5.3 Interferometric Synthetic Aperture Radar . . . 35

3.6 Model predictions of forcing factors . . . 36

3.6.1 Predictions of atmospherically forced sea level . . . 36

3.6.2 Predictions of post-glacial rebound . . . 36

3.6.3 Predictions of contributions from the large ice sheets . . . 37

3.6.4 Predictions of other contributions due to mass exchange . . . 38

3.7 Proxy data . . . 40

3.7.1 Sun spot observations . . . 40

3.7.2 Atmosphere-ocean oscillation indices . . . 42

3.8 Overview . . . 44

4 Observed sea-level variations **47**

4.1 Introduction . . . 47
4.2 Tides . . . 47
4.3 Long-period spectrum . . . 49
4.4 Seasonal cycle . . . 51
4.5 Interannual to decadal variability . . . 53
4.6 Secular trends . . . 56
4.7 Extreme sea levels . . . 59
4.7.1 Background to estimating probabilities of extreme sea levels . . . 59
4.7.2 Total observed sea levels . . . 60
4.7.3 Trends in individual components of sea levels: Mean sea levels . . . 62
4.7.4 Trends in individual components of sea levels: Tidal variations . . . 62
4.7.5 Trends in individual components of sea levels: Meteorological components and extreme sea levels . . . 63
4.7.6 Studies of extreme sea levels in nearby locations . . . 64
4.7.7 Issues for further assessments and some limitations . . . 64
4.8 Conclusions . . . 65

5 Local forcing of sea-level variations in the upper Adriatic Sea **67**

5.1 Introduction . . . 67
5.2 Atmospheric forced variations . . . 67
5.2.1 Seiches . . . 68
5.2.2 Storm surges . . . 68
5.2.3 Seasonal variations . . . 68
5.2.4 Interannual to decadal variations . . . 69
5.2.5 Secular trends . . . 69
5.3 Oceanographic contribution . . . 69
5.3.1 Tides . . . 69
5.3.2 Oceanic circulation of the Mediterranean Sea . . . 70
5.3.3 Exchange through Straits . . . 70
5.3.4 Effect of local air-sea interaction on the circulation in the Adriatic . . . 71
5.3.5 The influence of oceanic circulation on sea-level variability . . . 72
5.3.6 Multidecadal trends in water mass characteristics in the Adriatic and the Eastern Mediterranean . . . 72
5.3.7 The Eastern Mediterranean Transient . . . 73
5.3.8 The signature of water mass and circulation changes at the tide gauges of the Northern Adriatic . . . 74
5.4 Contributions from local vertical land motion . . . 75

5.4.1 Regional Tectonics . . . 75
5.4.2 Postglacial rebound . . . 75
5.4.3 Present-day mass movements . . . 76
5.4.4 Water extraction . . . 77
5.4.5 Gas Extraction . . . 77
5.4.6 Biological/Chemical Soil Processes . . . 77
5.4.7 Sediment compaction and loading . . . 77
5.5 Overview . . . 78

6 Global sea-level changes and their effect on the upper Adriatic Sea 81
6.1 Introduction . . . 81
6.2 The global ocean mass balance . . . 81
6.3 Steric contribution . . . 82
6.4 Overview . . . 83

7 Reanalysis of the vertical land motion in the upper Adriatic area 84

8 Reanalysis of the sea-level variations in the upper Adriatic Sea 93

9 Appraisal of sea-level rise scenarios for Venice 99
9.1 Critical review of the current sea-level rise scenario for Venice . . . 99
9.2 Critical review of global sea-level rise scenarios . . . 100
9.3 Possible future sea-level scenarios for Venice over the 21st century . . . 101
9.3.1 Scenario components . . . 102
9.4 Impact of mean LSL rise on high water levels . . . 107
9.5 Reducing the uncertainties . . . 108
9.6 A local integrated sea-level monitoring system . . . 109
9.6.1 Tide gauges . . . 109
9.6.2 Oceanographic and meteorological measurements . . . 110
9.6.3 GPS . . . 110
9.6.4 Leveling . . . 112
9.6.5 InSAR . . . 112
9.7 Future updates of the sea-level rise scenarios . . . 112

10 Main conclusions and recommendations 114
10.1 Conclusions . . . 114
10.2 Main recommendations . . . 114
10.2.1 Observations . . . 114
10.2.2 Database related recommendations . . . 115

10.2.3 Data analysis 115
10.2.4 Research studies 115
10.2.5 Updates of the LSL Scenarios 116

References **117**

A Acronyms and Abbreviations **133**

Executive Summary

What does this report contain?

This document is the final report on the project *Appraisal of relative sea-level rise scenarios for Venice*, which was carried out by the Nevada Bureau of Mines and Geology, University of Nevada, Reno.

The design of the Venice flood barrier and its operation has been based on a local sea-level rise estimate of 23 cm over the 21st century. The choice of this particular scenario is based on a study carried out by the *Consortium for Coordination of Research Activities in the Venice Lagoon System* (Co.Ri.La) in 1999 (Co.Ri.La, 1999). That study resulted in a number of scenarios covering the range from 0.20 to 0.53 m in sea-level rise by 2100. After the adoption of the 0.23 m scenario, it was decided to monitor new information and literature (experimental data and model results) on sea-level changes. This report is the result of the first appraisal of the sea-level rise scenarios after they were set up in 1999.

This document reports on studies and considerations relevant for sea-level scenarios for the city of Venice and the Lagoon. The material compiled in this report provides a basis for assessing the uncertainties in the sea-level scenarios.

Since the current sea-level rise scenario for Venice was adopted in 1999, results of extensive research on local conditions in the Adriatic, several studies of regional processes in the Mediterranean, studies of the global processes affecting sea level, and new assessments of the potential future development of sea level have been reported. These new results permit a reevaluation of the uncertainties in future sea-level change.

Why is sea level important in the context of climate change?

Local Sea Level (LSL) is the quantity that describes the impact of global and regional changes in climate and sea level in a given area. LSL results from a number of forcing processes acting on a wide range of spatial and temporal scales. LSL can be viewed, in principle, as the sum of four terms: (1) local changes in the sea surface due to mass exchanges in the global water cycle, (2) local changes in the volume of the sea water due to temperature and salinity changes, (3) vertical motion of the land with respect to the center of mass of the Earth system, (4) changes in the local sea level due to changing atmospheric forcing (air pressure, wind, evaporation, precipitation and radiation). Most of the processes affecting sea level contribute to more than one of these terms, leading to a complex situation with respect to modeling past and, even more so, future LSL variations.

The Upper Adriatic is an area where all local, regional and global factors are of importance for the variations and trends in LSL. Moreover, global forcing factors are biased due to the semi-enclosed nature of the Mediterranean and the particular setting of the Adriatic. Consequently, LSL will follow a complex trajectory over time, depending on the specific, local mix of the various forcing factors, and potentially posing considerable threats to low-lying coastal areas.

How has sea level changed in the past?

Based on an analysis of the available sea-level observations, it can be stated that over the 20th century, sea level in Venice and Trieste has increased by an average rate of 2.4 mm/yr and 1.2 mm/yr, respectively. However, over the interval from 1960 to 2003, sea level in the Adriatic has been very stable with rates close to 0.0 mm/yr for stations along the eastern coast and maximum rates of 0.5 mm/yr and 0.4 mm/yr in Venice and Trieste, respectively. The larger than average LSL rise in the first half of the 20th century and the relatively stable LSL in the second half is a feature that deserves particular attention. In Venice, this non-linearity arises partly from man-made changes in local subsidence, while in Trieste, other factors have to be identified, which most likely also contribute partly to the non-linearity in Venice.

Within the last fifteen years, the LSL trend in Venice appears to be consistent with the sea-level trend at most of the Adriatic stations, with the exception of Trieste, where the LSL trend in that period is somewhat lower than at the other available observation sites. However, the coherency of the trend in Venice with those trends found elsewhere cannot be taken as an indication that the land motion in Venice is consistent with the land motion in the other part of the Adriatic. The complex interplay of land subsidence, spatially variable changes in atmospheric forcing, and contributions from changes in ocean circulation preclude conclusions with respect to the underlying processes based only on the correlations of LSL records from different locations.

How have the different processes contributed to past sea-level changes?

Based on a review of the evidence for vertical land motion, it is first shown that the City of Venice over the time period from 1980 to 2000 was subsiding with respect to more northern locations (close to the Alps) by 2.0 ± 1.5 mm/yr, while the adjacent areas south-west and north-east of the City of Venice appear to experience larger relative subsidence. The analysis of the available continuous GPS data reveals that the area around Venice over the period from 2001 to 2004 was moving with -2.00 ± 1.2 mm/yr in a geocentric reference frame, and thus appears to be subsiding with respect to the geocenter.

With respect to the factors causing the vertical land motion, it is argued in the literature that the land motion in Venice results from a tectonic contribution associated with the nearby plate boundary (of the order of -1 ± 0.5 mm/yr), a component due to sediment loading and compaction (-0.5 ± 0.5 mm/yr), a contribution from post-glacial rebound (0.0 ± 0.3 mm/yr), and a temporally and spatially highly variable anthropogenic contribution due to water, gas and oil extraction. The latter is difficult to assess and introduces a large uncertainty in the overall budget. Moreover, other potential contributions to vertical uplift result from a visco-elastic response to deloading of the crust due to the past and present melting of alpine glaciers, past removal of groundwater, and past and present removal of oil and gas in the region. Nevertheless, the quantitative estimates considered here are in agreement with the geocentric estimate based on GPS. However, due to the large non-linear man-made contribution to vertical land motion, it is not clear whether the GPS estimates can be considered representative for the geocentric motion of the Venice area over longer time scales than the actual GPS observation period of only 3.5 years. Continued measurements and analysis are necessary to better understand the trends.

Based on a review of the atmospheric forcing, it is concluded that atmospheric pressure has been increasing over the last 40 years causing sea-level reduction in the whole of the Adriatic. These changes appear to be linked to atmospheric variations on time scales of several decades to centuries as expressed in the long period variations of the *North Atlantic Oscillation* (NAO). The Bora wind appears to be reducing in strength while more Sirocco events have been noticed. However, the ageostophic character of the wind field requires high spatial resolution for the field to be represented accurately for the purpose of storm surge modeling. The combined wind and pressure forcing over the Mediterranean and in particular the pressure forcing over the Adriatic has contributed a negative trend over the interval from 1960 to the end of the 20^{th} century, lowering sea level by up to 2.5 cm over these 40 years. This feature may be part of a long-period oscillation of the coupled atmosphere-ocean system with a period of six decades or more, which could temporarily offset or even reverse a secular rising trend.

Based on a review of the circulation in the Adriatic and the Mediterranean Sea, it is argued that the effects of the thermohaline circulation, dense water formation, and the presence of straits all affect the mean sea level of the Adriatic basin. These variations contribute to the decadal and inter-decadal variability observed in the tide-gauge records. A cooling of the upper water layers over the last 40 years is found to have lowered sea level on the order of 5 to 10 mm over that period, thus reducing the sea-level trend by about 0.1 mm/yr.

Based on a review of the published results on studies of extreme sea levels, it is argued that the observed wind reduction and atmospheric pressure increases have reduced the size of the largest surges. However, this reduction is balanced by sea-level rise giving a near to no change situation for extreme events over the time interval from 1960 to 2000. None of the published studies appears to be addressing all relevant aspects systematically. In order to facilitate such studies, a comprehensive, quality-controlled database should be made available. A difficulty arises from the fact that most of the observed trends in the distribution of the sea-level values may be due to cyclic variations (with multi-decadal periods) rather than secular unidirectional trends. Therefore, scenarios for the future development of extremes are rather uncertain and will remain so if the nature and contribution of the cyclic behavior is not better clarified.

Summarizing all factors, the LSL trend balance can be presented as

Observed LSL trend = mass comp. + steric comp. − land − motion comp. + atmospheric comp.

Over the best documented period, that is, approximately 1960 to 2002, this leads to the quantitative balance (in mm/yr) of

$$0.5 = x + (-0.1 \pm 0.1) + (-0.8 \pm 0.1) - (-2.0 \pm 1.2)$$
$$0.5 = (1.1 \pm 1.4) + x,$$

where x is the unknown contribution from mass changes in the global water cycle and the associated effects on the geoid. These numbers leave room for a contribution of the mass term, that is, global, regional and local changes mainly in the water cycle, of $x = -0.6 \pm 1.4$ mm/yr. The order of magnitude of the mass term appears to be reasonable considering the current understanding of this term. It is emphasized here that the large uncertainty of the vertical land motion results mainly from the uncertainty of the relation between reference frame origin and center of mass of the Earth system.

How will sea level in Venice change by the end of the 21^{st} century?

In order to elucidate the uncertainties in scenarios of future sea levels, a set of possible scenarios for the future local sea level at the end of the 21^{st} century is synthesized from a combination of the various processes contributing to sea level in Venice and the upper Adriatic. A difficulty arises from the fact that the global mean sea-level scenarios provided in the Third Assessment Report (TAR) of IPCC need to applied with great care, allowing for all the relevant sub-global processes. In general, this is true for any coastal location, due to the spatially highly variable fingerprints of all forcing factors on sea level. For the upper Adriatic, it is even more so due to the semi-enclosed character of the Mediterranean, with the Strait of Gibraltar biasing all forcing coming from the Atlantic Ocean, as well as the difficulties encountered in the interpretation of past contributions. Based on the understanding of the past sea-level changes in the Adriatic and the IPCC scenarios provide in the TAR a set of mean local sea-level scenarios has been derived, taking into account the considerable uncertainties. The set of plausible mean local mean sea-level scenarios for Venice considered here turns out to cover a wide range of possible sea levels by 2100. The uncertainties in the individual scenarios are large and of the order of ±0.60 m to ±0.75 m. The rise in maximum flood levels could be higher due to an increase in tidal range as well as an increase of storm surges and waves associated with climate change.

Main uncertainties result not only from the contribution of global processes (ice-sheet melting and ocean warming) but also from local contributions such as local vertical land motion, changes in the local meteorology and regional processes in the Mediterranean. For the vertical land motion, the main uncertainty is attributed to the relation of the origin of the global geodetic reference frame to the center of mass of the Earth system.

For the scenarios considered here it was assumed that the current regulations of local groundwater extractions are sustained up to 2100. If groundwater extraction is resumed due to future water

shortages, then the maximum scenario might easily increase by 0.5 m or more. This shows the importance of current groundwater extraction regulations.

The current scenario fails to inform coastal managers and planners of the large range of plausible future sea-level trajectories and their uncertainties. These uncertainties, which are confirmed in other, similar studies, need to be considered as an integral part of the plausible futures and cannot be neglected in the discussion of potential impacts and the most appropriate adaptation strategy.

How can the uncertainties be reduced?

Based on a detailed review of the sea-level variations and trends in the Upper Adriatic over the last 100 years and a summary of the contributing factors, it is shown that the current knowledge of the different forcing factors for the local sea-level variations is still too uncertain to synthesize the decadal and multi-decadal variation in sea level from available observations and models of the forcing factors conclusively. On a local scale, an appropriate observation system to monitor the current sea-level trend in the Upper Adriatic is a crucial prerequisite required to ensure that the uncertainties in the future local sea-level scenarios can be reduced over time. This system needs to combine tide gauges measuring LSL *in situ* with a sufficiently developed component to monitor the vertical land motion. Well maintained tide gauges in the upper Adriatic are crucial components of this observing system (which is to a large extent in place). Moreover, temporally homogeneous time series of key meteorological and oceanographic parameters are necessary in particular for assessing the oceanic contribution to LSL change and the trend in extreme sea levels. Of particular importance for the monitoring of vertical land motion are a (low) number of continuously recording *Global Navigation Satellite System* (GNSS) sites combined with a sufficient number of well distributed and established markers for campaign-type GNSS measurements. Moreover, in the analysis of the data, full use should be made of a combination of InSAR and GNSS observations, particularly in the future, where significant improvements in the availability of InSAR are expected.

A sufficient sea-level observing system is also required for the Mediterranean to support studies of the regional climate and oceanographic processes that influence the Adriatic sea level. On a global scale, a better understanding of the global water cycle and its effect an global, regional and local sea level will help to reduce the uncertainties in the mass term. In order to improve the understanding of the past changes in extremes and to provide a basis for future scenarios of extremes, more elaborate studies of the statistics of the extreme sea levels and meteorological events are required for the whole Adriatic considering sea level and meteorological parameters simultaneously. Improved storm surge models would help to study extremes under past and future climate conditions.

An improved sea-level monitoring system will also provide a basis to reduce the uncertainties in the future sea-level rise scenarios produced here, particularly if combined with local studies and improved models. Moreover, it is expected that numerous scientific studies of the global and regional forcing processes will improve the understanding of these process and allow IPCC to improve the global and regional scenarios in the near future considerably.

1 Introduction

The currently adopted sea-level rise scenario for Venice is based on an assessment carried out by the *Consortium for Coordination of Research Activities in the Venice Lagoon System* (Co.Ri.La) in 1999. Since then, extensive research on local conditions in the Adriatic, several studies of regional processes in the Mediterranean, studies of the global processes affecting sea level as well as new assessments of the potential future development of sea level have been carried out.

This report contains the results of the analysis of past sea-level variations in Venice and the Adriatic, as well as studies of future sea-level scenarios and their uncertainties for Venice and the Lagoon by the end of the 21st century.

1.1 Objectives

The objective of the project *Appraisal of relative sea level rise scenarios for Venice* was the appraisal of the currently adopted sea-level rise scenario for Venice in order to provide a solid basis for decision with respect to necessary mitigation of potential hazards. The appraisal is based on a comparison of the current scenario with a number of scenarios of plausible future *Local Sea Level* (LSL) rise in Venice and the Lagoon derived in the frame of the project. In order to be able to set up these scenarios, it was necessary to assess the estimates of the past and current LSL trends as well as to discuss the list of forcing factors considered to be relevant for the LSL variations in the Adriatic.

In order to set up scenarios for future LSL in Venice, it is also necessary to understand the regional and local forcing mechanisms for sea-level variations and secular change. To a large extent, this knowledge will have to be based on studies of observations, which best cover the interval from approximately 1960 to present. In addition, knowledge about the expected changes in these forcing mechanisms is required. The existing global scenarios are to a large extent based on the assumption that heat expansion of the oceans and ice-sheet melting would be major global mechanisms contribution to sea-level rise (Church et al., 2001). However, these two processes lead to spatially highly variable fingerprints in sea level (e.g., Church et al., 2001; Plag, 2006a). Moreover, they combine with other local and regional factors including changes in atmospheric and oceanic circulation and vertical land motion to form a complex spatial pattern of future LSL trends. Thus, it is necessary to understand the contributions to LSL of the important mechanisms acting on different spatial and temporal scales to considerably better than 1 mm/yr in order to provide realistic regional and local sea-level scenarios. Once these scenarios have been deduced, they provide a solid basis for the appraisal of the existing scenarios and, in particular, the one accepted for Venice.

1.2 Organization of the report

For sea-level studies, and particularly for studies and projections of secular sea-level trends, it is extremely important to define the basic terms properly and to ensure that the concepts of global, regional and local contributions to local sea level are consistently treated. Therefore, in Section 2 we introduce first the basic terms and discuss the underlying concepts. This section is intended to provide a set of well-defined terms which are then used consistently throughout this report. The section also emphasizes the problems inherent in the relation of global scenarios for the ocean's mass and volume changes to scenarios of local sea level at any given coastal location.

In Section 3 we give a comprehensive description of the available database and the models for various factors contributing to local or regional sea-level variations. Besides the tide gauge and satellite altimetry observations of sea level and sea surface, respectively, this section also gives an overview of

the meteorological, oceanographic and geodetic data available for the Adriatic region. A number of forcing factors acting on regional to global scale have to be predicted by models, and these include post-glacial rebound, and present-day changes in the large ice sheets.

Section 4 gives a description of the observed sea-level variations in the upper Adriatic region. This description is to a large extent based on published material. However, the available sea-level observations have been analyzed in a preliminary processing and these results are also reported here.

Section 5 summarizes the present state of the knowledge with respect to local and regional forcing of sea-level variations in the Upper Adriatic region. In particular, in this section we consider the atmospheric and oceanographic forcing as well as the contribution from vertical land motion.

Section 6 will reviews the state of knowledge with respect to sea-level variations caused by global processes, and focuses on their fingerprints in the Adriatic region. This section is will be based to a large extent on the IPCC assessment reports, as well as own studies.

Section 7 reports on the reanalysis of the available GPS observations of vertical land motions. For scenarios of future secular changes in sea level, global predictions of sea-level rise have to be combined with local vertical land motion in the same, global geocentric reference frame. For that, knowledge of the local land motion in a well determined global reference is crucial.

Section 8 describes the reanalysis of the available sea-level observations in the upper Adriatic. The goal of this reanalysis was to determine the decadal to interdecadal oscillations that may introduce significant transient trends in mean sea level as well as the extreme sea level over periods of several decades.

The synthesis of the material presented in these sections into a number of LSL scenarios for Venice is presented in Section 9. Here we discuss the possible scenarios including their uncertainties, and we compare them to the Co.Ri.La (1999) scenarios. In order to reduce the considerable uncertainties, we give recommendations for a monitoring system appropriate to provide an increasingly better database for future assessments. The section also includes suggestions for future updates of the sea-level rise scenario.

Finally, in Section 10 we summarize the main conclusions and recommendations of the report.

2 Concepts in sea-level studies

In the frame of the project, it is necessary to link global scenarios for the ocean's mass and volume balance to scenarios for local sea-level changes in the Adriatic and at Venice. Therefore, it is of crucial importance, that these widely different scenarios are considered in the frame of a consistent concept. Moreover, local sea-level variations have to be analyzed in terms of their forcing factors, which also requires that these forcing factors are considered in a conceptually consistent frame. Based on the considerations given by Plag (2006a), this section provides a critical overview of the terms and concepts used in studies of local sea-level changes as well as studies of the global ocean's mass and volume balance. As a result, we provide the underlying concept as well as the set of well define terms and equations to be used throughout the report.

2.1 Definition of basic terms

We define the quantity "*Local Sea Level*" (LSL) for all locations on the Earth's surface as the height $h(\phi, \theta)$ of the ocean surface above the underlying solid Earth, that is,

$$h(\phi, \theta, t) = \begin{cases} r_1(\phi, \theta, t) - r_0(\phi, \theta, t) & : \text{ in the ocean} \\ 0 & : \text{ on land} \end{cases} , \tag{1}$$

where r_0 and r_1 are the geocentric positions of the sea floor and sea level, respectively (Plag, 2006b). ϕ and θ are the geographical longitude and latitude, respectively.

LSL as defined through eq. (1) is the quantity relevant for impact studies as well as for the adaptation to sea-level rise. Therefore, in order to assess the impact of global climate change and the induced changes in global sea level on any given coastal region, the processes affect LSL in that region need to be understood and the future development of each of these processes need to be modeled. In particular, the complex relation between global and regional processes and LSL have to be taken into account.

It is strongly emphasized that the LSL defined here is an absolute[1] quantity, independent of the reference frame used for r_0 and r_1. Therefore, the term *Relative Sea Level*, which is often used to refer to this quantity is a mis-nomer and not used here. It gives the wrong impression that coastal sea level is a relative quantity, which it is not. Tide gauges carefully maintained (that is, making sure that the relative movement of the tide gauge with respect to the benchmarks are known and that the benchmarks are representative for the land movement under the tide gauge) are the only tool to measure local absolute sea-level changes directly. Therefore, correcting tide gauge measurements of LSL for local vertical land motion does not lead to 'sea level' or even 'absolute sea level changes' but to a different quantity, which is not easy to interpret.

We also define the geocentric position of the sea surface $H(\theta, \lambda)$ as the distance of the sea surface from the geocenter. This quantity is a relative quantity because it is not directly measurable and has to be given with respect to a geocentric reference frame, for example ITRF2000. Using another reference frame, for example ITRF97, results in another sea surface position. Therefore, the sea surface position (which is not a sea level as defined above) needs the frame information to be attached to it. Moreover, changes in the geocentric position of the (local) sea surface only coincide with sea-level changes as defined above if the ocean floor at this position does not move vertically.

[1] We refer here to quantities as *absolute quantities* if they do not depended on a specific reference frame chosen to refer them to.

The geocentric sea surface position as measured by, for example, satellite altimetry, is often referred to as 'geocentric sea level' or 'absolute sea level'. We consider these terms as mis-nomer and will not use them here.

For the global water cycle and climate change discussions, it is important to define two global absolute quantities, namely the mass of the ocean water M_{O} and the volume V_{O} of the ocean water, for which we will use the acronym GOM (*Global Ocean Mass*, Plag, 1998) and GOV (Global Ocean Volume), respectively. GOM is an important quantity in the mass balance equation of the global water cycle, while GOV is a complex function of GOM, the heat and salinity content of the ocean, and the distribution of the mass in the ocean.

GOV is defined by

$$V_{\mathrm{O}} = \int_{\mathrm{O}} \mathrm{d}V, \tag{2}$$

$$= \int_0^{2\pi} \int_0^{\theta} \left(\int_{r_0(\theta,\phi)}^{r_1(\theta,\phi)} r^2 dr \right) \sin\theta \mathrm{d}\theta \mathrm{d}\phi \tag{3}$$

that is, the volume integral taken over the complete ocean volume.

GOM is defined by

$$M_{\mathrm{O}} = \int_{\mathrm{O}} \rho \mathrm{d}V \tag{4}$$

$$= \int_0^{2\pi} \int_0^{\theta} \left(\int_{r_0(\theta,\phi)}^{r_1(\theta,\phi)} \rho(\theta,\phi,r) r^2 dr \right) \sin\theta \mathrm{d}\theta \mathrm{d}\phi \tag{5}$$

that is, the integral over the density of the ocean water taken over the complete ocean volume. It has to be noted that both the density and the volume of the ocean are functions of time.

The governing equation for GOM changes is the global water cycle mass balance

$$0 = \sum_{i=1}^{n} \frac{\mathrm{d}M_i}{\mathrm{d}t}, \tag{6}$$

where M_i is the total mass of the water in reservoir i and n the number of reservoirs in the global water cycle. Changes in GOM are solely determined by the scalar changes in the masses of the other reservoirs, independent of where the mass fluxes comes from or go to. GOM just counts the number of kilograms of water in the ocean.

Changes in V_{O} result from the sum of steric changes, that is, changes caused by temperature and salinity changes of the sea water, and mass changes due to mass added to or subtracted from the ocean. Thus

$$\text{GOV changes} = \text{steric changes} + \text{mass changes}. \tag{7}$$

However, there is no simple balance equation to relate changes in GOV to changes in the global water cycle. In fact, GOV depends not only on GOM but also the total heat and salinity contents of the ocean. Moreover, due to the complex equation of state of the sea water (see, e.g., Gill, 1982), the density ρ_w depends non-linearly on temperature, salinity and pressure. Consequently, GOV depends both on the amount and the distribution of heat, mass and salinity in the ocean.

In many studies of global sea-level changes, the underlying concepts are not clear. In particular, the mass balance given by eq. (6) is often expressed in global sea level equivalents (e.g., Church et al., 2001). This leads to interpretations, which do not take into account that the spatial pattern of sea-level changes depends on where the mass added to the ocean is coming. This complicates the determination of a global sea-level rise and the relation between sea-level changes and the mass balance. Therefore, it is important to set up a LSL equation accounting for both global, regional and local factors.

2.2 The local sea-level equation

The LSL measured by a tide gauge is the result of a number of forcing factors acting on a wide range of spatial and temporal scales (see, e.g., Chelton & Enfield, 1986; Trupin & Wahr, 1990). The factors include but are not limited to waves, tides, meteorological forcing, ocean currents, mass and heat changes of the ocean, geophysical and geochemical processes affecting the land level and the geoid, and man-made processes. In some locations, seiches and tsunamis can contribute at the high-frequency end, too.

Instrumental effect can bias the sea-level measurements (for an overview of these effect see, e.g., Pugh, 2004; IOC, 2000). Changes in instrumentation and/or location of the tide gauge can introduce offsets in the records. Errors in the clock can lead to oscillations particularly in the residual after removal of the ocean tides. On longer time scales, slow vertical motion of the tide gauge with respect to the benchmark can introduce erroneous long-period or secular variations. A benchmark with a vertical motion not representative for the vertical motion of the land close to the tide gauge also introduces a biases in the vertical motion deduced for the tide gauge.

At the high frequency end of the sea-level spectrum, the main contributions come from waves, tides, atmospherically forced surges and depressions, and at some locations, seiches and tsunamis. Thus, the high-frequency part of the LSL variations at a given location can be described as

$$h_{\mathrm{hf}}(t) = w(t) + h_{\mathrm{tidal}}(t) + h_{\mathrm{atmos}}(t) + h_{\mathrm{seiches}}(t) + h_{\mathrm{tsunami}}(t). \tag{8}$$

We assume here that the fluctuations $w(t)$ due to waves are eliminated from the LSL measurements of tide gauges by appropriate filtering.

h_{tidal} is in fact composed of high frequency parts as well as long period contributions. The astronomical tidal potential (for a full description see, e.g., Cartwright & Edden, 1973; Tamura, 1987) contains harmonic constituents with significant frequencies at the ter-diurnal, semi-diurnal and diurnal bands, as well as longer period tides at fortnightly, monthly, semi-annual and annual frequency band. Moreover, the nodal tide adds a long-period tide with a period of 18.6 years. At diurnal and sub-diurnal frequencies, the ocean responds dynamically and therefore, ocean tides contain non-linear constituents in addition to those found in the astronomical potential. Nevertheless, the diurnal and sub-diurnal ocean tides can be computed accurately from the astronomical tidal potential and tidal constituents determined from an analysis of, for example, a yearly record (e.g., Doodson & Warburg, 1941; Schureman, 1958). The tides with periods of fourteen days and more are generally considered to be equilibrium tides (Proudman, 1959). Nevertheless there are indications that these constituents exhibit considerable temporal variations (e.g., Plag, 1988) and they may not be fully in equilibrium. Potentially, these apparent variations may be due to an interaction with atmospheric forcing. The semi-annual and annual astronomical tides are small (of the order of 5 to 10 mm) compared to the sea-level variations induced by climatological forcing, and they can be assumed to be equilibrium tides.

The atmospherically forced sea-level variations are more difficult to compute and normally require a hydrodynamical model, if an accuracy of the order of 10 cm or better is to be achieved. The atmospheric forcing contains virtually all temporal scales from wind-driven waves, over air-pressure

and wind-driven variations at the typical time scales of weather variations with a maximum at 2 to 5 days, climatological variations at intraseasonal and seasonal time scales up to phenomena such as the *North Atlantic Oscillation* (NAO) (see, e.g., Hurrell, 1995; Hurrell & van Loon, 1997), the *Northern Hemisphere Annular Mode* (NAM, Thompson & Wallace, 2001), and the *El Niño/Southern Oscillation* (SO, see, e.g., Philander, 1990) with typical periods of several years to decades. Oscillations in the climate system with periods of several decades to a century as described by, for example, Schlesinger & Ramankutty (1994) may also be associated with long-period variations in sea level captured by tide gauge records (e.g., Plag, 2000).

The contributions $h_{\text{seiches}}(t)$ and h_{tsunamis} from seiches and tsunamis, respectively, normally will be zero. However, due to specific atmospheric forcing, seiches can be excited particularly in semi-enclosed sees, but also in larger ocean basins. Once triggered they can last for several days, depending on the geometry of the particular basin. Tsunamis are infrequently triggered as part of submarine earthquakes, volcanic eruptions or landslides, and can have very large and devastating amplitudes when they hit coastal areas.

The seasonal cycle is mainly composed of an annual and semi-annual constituent, which are to a large extent caused by the combined effect of steric and wind- and pressure driven variations. Averaged over several years, these constituents appear to be fairly stable, but Plag & Tsimplis (1999) found indications of changes in amplitude and phase particularly in Northern Europe in the last two decades with respect to previous decades.

For the discussion of secular trends, we will consider monthly mean sea-level values. We denote monthly mean sea levels at a tide gauge located at a point $\vec{x}$ on the Earth surface by $h_{\text{M}}(\vec{x},t)$. The variations h_M in LSL can be approximated as a sum of several factors, namely

$$\begin{aligned} h_{\text{M}}(\vec{x},t) = {} & S(\vec{x},t) + C(\vec{x},t) + A(\vec{x},t) + I(\vec{x},t) + G(\vec{x},t) + \\ & T(\vec{x},t) + P(\vec{x})(t-t_0) + V_0(\vec{x})(t-t_0) + \delta V(\vec{x},t) \end{aligned} \tag{9}$$

where t is time, t_0 an arbitrary time origin, and where we have considered the contributions to LSL changes for the processes summarized in Table 1. All these contributions depend on the location, and most of them display a wide range of spatial and temporal scales (for a detailed discussion, see, e.g., Emery & Aubrey, 1991; Chelton & Enfield, 1986). Moreover, the local contributions to LSL from mass-dependent terms are the result of an integral equation and depend not only on local processes but rather the mass transport in the global water cycle (see Section 2.4 for a more detailed discussion).

The factors in eq. (9) can be separated in those originating mainly from local forcing and those resulting from regional or global forcing (Table 1). The global and regional factors that contribute to local secular trends with a fingerprint exhibiting large spatial variations on long to global scales are the post-glacial rebound signal P, the steric signal S, the contribution I from the two large ice sheets in Antarctica and Greenland, and the mass exchange T and G with the remaining terrestrial hydrosphere and the continental glaciers, respectively.

The complex interaction between the different processes is depicted in Figure 1. Mass movements in the terrestrial hydrosphere (groundwater, rivers, lakes, and reservoirs) and land-based cryosphere (glaciers and ice sheets) and mass exchange with the ocean load and deform the solid Earth and affect the gravity field. The deformations and the associated gravitational changes result in LSL changes, depending on where mass has been relocated. Ocean mass changes change the sea surface position, similar to ocean volume changes caused by heat and salinity changes. The latter also affect the ocean currents and thus change the DST. Atmospheric circulation forces regional, wind-driven currents affecting the DST. DST and sea surface changes caused by regional and global processes change LSL in any location. The atmosphere also acts locally on the sea surface and thus changes sea level. Past changes in the ice sheets and glaciers lead to post-glacial rebound, which affects sea level

Table 1: Main characteristics of processes influencing LSL on decadal to secular time scales. *From Plag (2006a).*

Sy.	Process	Description, Observations, Models	LSL fingerprint
S	Steric changes	Volume changes due to variation in temperature and salinity of sea water. Can be computed on the basis of sea water temperature and salinity observations (Levitus et al., 2000; Ishii et al., 2003).	Considerable seasonal to inter-decadal variations and secular trends. Large spatial variability.
C	Changes in ocean currents	Long-period changes mostly caused by variations of the dynamic sea surface topography. Mostly accounted for by S.	
A	Changes in atmospheric circulation	Results in changes in mean air-pressure distribution and wind field. On longer time scales, sea level responds to air-pressure variations as inverted barometer; changes in wind stress affect ocean currents and coastal upwelling. Wind field and air-pressure field can be computed from meteorological observations.	Inter-decadal changes in the distribution of mean air pressure are expected to be small. Locally, variations in coastal wind may be much larger.
I	Changes in the mass of large ice sheets	The large ice sheets respond to climate variations, though with considerable time lag. For known ice mass changes, the LSL fingerprint can be computed using the sea-level equation. Uncertainties in the mass balance of the ice sheets are large, with potential contributions of the Antarctic and Greenland ice sheets to sea-level rise over the last 50 years being ± 1 mm/yr and ± 0.4 mm/yr level, respectively (Warrick et al., 1996; Church et al., 2001).	The ice masses change seasonally as well as on decadal to longer time scales. The LSL fingerprint is dominated by global scales with larger gradients close to the ice sheet.
G	Changes in the mass of glaciers	Continental glaciers display large mass variations due to climate-induced variations of the mass balance. Affects the ocean similar to I. Global models are available (e.g., Meier, 1984), but there are considerable deficiencies in global coverage and mass balance of individual glaciers (see Church et al., 2001, for a detailed discussion).	The spatial distribution of the glaciers and their individual dimension results in an overall LSL fingerprint of small amplitudes and small spatial wavelength.
T	Changes in the terrestrial hydrosphere	Due to various natural and man-made processes affecting groundwater and surface water storage. Are expected to contribute to global sea-level trends on the level of 0.5 mm/yr (Sahagian et al., 1994; Gornitz et al., 1996; Warrick et al., 1996; Church et al., 2001). Currently, no reliable model available for the prediction of the LSL fingerprint.	LSL fingerprint is mainly dominated by short wave lengths. Larger scales due to changes in mean snow cover, permafrosts, and deforestation.
P	Post-glacial rebound	Due to visco-elastic deformations of the solid Earth induced by the large cryospheric mass variations during the last ice age. Elaborate geophysical models for the present-day post-glacial signal in LSL exist. Inter-model differences are still considerable, depending both on the ice history and the earth model. Considerable uncertainties due to the uncertain history of the Antarctic ice sheet during the last glaciation and changes in the Antarctic and Greenland ice sheets over the last several thousand years.	Local trends are considered to be linear on time scales of centuries. In the near-field to the former ice sheets, P reaches values in excess of 10 mm/yr while in the far-field, it seldom exceeds 1 mm/yr.
V_0	Tectonic vertical land motion	Large parts of the ocean's coasts are in deformation areas associated with plate tectonics (see, e.g., Fig. 6 in Stein, 1993) and experience vertical land motion on spatial scales ranging from 30 to 100 km (see, e.g., Emery & Aubrey, 1991) at the lower end to the size of the plates on the high end. Currently, no global model or observational database exists that would allow the derivation of the resulting LSL fingerprint.	Dominated by short spatial scales but can also be consistent over large regions with passive continental margins mainly subsiding and regional uplift and subsidence at active plate boundaries.
δV	Nonlinear vertical land motion	Results from tectonic processes such as pre-, co- and post-seismic motion, as well as a number of man-made processes (groundwater, oil and gas extraction). Can currently only be described on the basis of observations, which are often lacking.	Temporal scales from instantaneous offsets (co-seismic) to interannual transients. Mostly small spatial scales; for great earthquakes up to 1000 km and more.

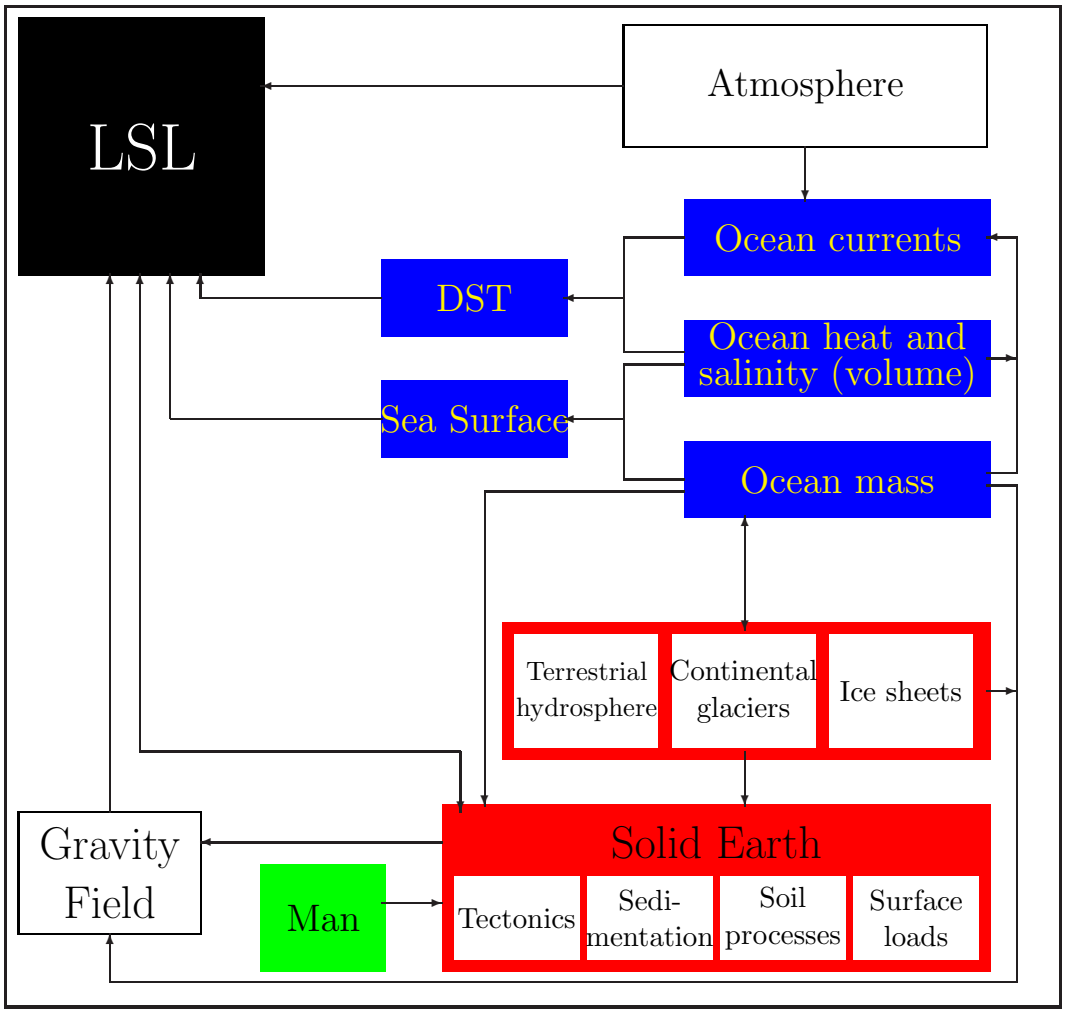

Figure 1: Interaction of processes controlling LSL.

For a discussion of the interactions, see text. From Plag (2006b).

through vertical land motion and geoid changes. Tectonic processes in the solid Earth both result in vertical land motion, changes in the size of the ocean basins, and changes in the geoid. In areas where sedimentation takes place, the compaction of the sediments and their load on the solid Earth introduce vertical land motion. Moreover, changes in LSL feedback on the solid Earth and can cause the destruction of peat through oxidation and thus lead to subsidence.

Finally, man-made vertical land motion associated with exploitation of groundwater, oil and gas as well as changes in sedimentation affect the solid Earth and can change the Earth surface position. Variations in sedimentation due to river regulation (reduction) or land use (increase) also affect LSL particularly in the vicinity of river deltas.

For any given coastal location, all these interacting processes need to be assessed in order to understand past sea-level changes and to set up scenarios of future sea-level changes. For studies of impacts, the combined effects of equations (8) and (9) are important.

For the understanding of past sea-level changes at a given location, an alternative equation based on observations may be written as

(10)

$$\begin{aligned} h_{\mathrm{obs}}(t) &= h_{\mathrm{land}}(t) + h_{\mathrm{atmos}}(t) + h_{\mathrm{ocean}}(t) \\ &= h_{\mathrm{land}}(t) + h_{\mathrm{atmos}}(t) + h_{\mathrm{steric}}(t) + \tilde{h}_{\mathrm{mass}}(t) \end{aligned}$$

where $h_{\rm obs}$ are the LSL variations observed by a tide gauge. The vertical land motion $h_{\rm land}$ can be directly observed with, for example, GPS. The contribution $h_{\rm atmos}$ due to atmospheric forcing can be approximated base on local atmospheric observations or by a hydrodynamical model forced by air pressure and wind. The remaining oceanic contribution $h_{\rm ocean}$ is more complex. The steric contribution $h_{\rm steric}$ can be derived from oceanographic measurements of temperature and salinity. The contribution $\tilde{h}_{\rm mass}$ only includes the contribution due to mass changes in the global water cycle and the associated geoid changes but not the vertical land motion caused by the loading. The latter is already absorbed by the vertical land motion $h_{\rm land}$. If the mass changes in the global water cycle are known, then the contribution $\tilde{h}_{\rm mass}$ can be computed from the sea-level equation (16) discussed in Section 2.4. However, it is important to point out that the Green's function in that equation has to be modified to give sea-level changes relative to the geocenter and not relative to the deformable surface of the Earth, since the vertical land motion is already accounted for in the $h_{\rm land}$ term.

2.3 The global ocean mass balance

The global ocean mass balance is discussed in detail by Plag (2006b). On the highest level, the global water cycle can be separated in three main reservoirs, namely the ocean, the atmosphere, and the terrestrial hydrosphere. The first two reservoirs are relatively simple to quantify. For the ocean, the total mass is given by eq. (6). It is pointed out here that sea ice is not considered as separate reservoir but included in GOM. However, for GOV, the amount of sea ice is important since the density of ice and water are different and therefore the same GOM can result in different GOVs, depending on the fraction of sea ice.

For the atmosphere, the total mass of the water in the atmosphere, $M_{\rm A}$, is given by the integral

$$M_{\rm A} = \int_{\rm A} \rho_{wv} {\rm d}V \tag{11}$$

that is, the integral over the density ρ_{wv} of the water suspended in the air.

For the terrestrial hydrosphere, the situation is far more complex, and we need to separate this reservoir in a number of reservoirs with different characteristics. At a minimum, we need to distinguish (t1) surface water (rivers, lakes, and land surface), (t2) soil moisture, and (t3) groundwater, (t4) snow, (t5) water stored in vegetation, and (t6) water stored in the interior of the solid Earth. The cryosphere is considered separately below. It also makes sense to separate (t7) man-made reservoirs as an individual reservoir of the terrestrial hydrosphere. Furthermore, water stored in other man-made magazines such as (t8) rice fields may also have to be considered separately. For the cryosphere, it makes sense to separate this further into (c1) continental glaciers, (c2) Greenland ice sheet, and (c3) Antarctic ice sheet. Thus the full mass balance can be written as

$$0 = \dot{M}_{\rm O} + \dot{M}_{\rm A} + \sum_{i=1}^{8} \dot{M}_{{\rm T}_i} + \sum_{j=1}^{3} \dot{M}_{{\rm C}_i}. \tag{12}$$

Quantifying the effect of global changes on LSL requires the estimation of the secular trends in the mass balance over the last 100 years. In order to estimate the uncertainties in this, we first look at the fluxes between the different reservoirs. For that, we rewrite eq. (12) as

$$\vec{\dot{M}} = F \cdot \vec{u} \tag{13}$$

where $\vec{M}^T = (M_{\rm O}, M_{\rm A}, M_{{\rm T}_1}, ..., M_{{\rm T}_7}, M_{{\rm C}_1}, ..., M_{{\rm C}_1})$ and $\vec{u}^T = (1, ..., 1)$. This is equivalent to

$$\vec{M}(t) = \vec{M}_0 + \int_{t_0}^{t} F(t) \cdot \vec{u} {\rm d}t' \tag{14}$$

where t_0 is an arbitrary time origin.

The antisymetric matrix F contains all fluxes between the different pairs of reservoirs. For our definition of the reservoirs in the global water cycle, F is given by

$$F = \begin{pmatrix}
0 & F_{\mathrm{OA}} & F_{\mathrm{OT}_1} & F_{\mathrm{OT}_2} & F_{\mathrm{OT}_3} & F_{\mathrm{OT}_4} & F_{\mathrm{OT}_5} & F_{\mathrm{OT}_6} & F_{\mathrm{OT}_7} & F_{\mathrm{OC}_1} & F_{\mathrm{OC}_2} & F_{\mathrm{OC}_3} \\
-F_{\mathrm{OA}} & 0 & F_{\mathrm{AT}_1} & F_{\mathrm{AT}_2} & F_{\mathrm{AT}_3} & F_{\mathrm{AT}_4} & F_{\mathrm{AT}_5} & F_{\mathrm{AT}_6} & F_{\mathrm{AT}_7} & F_{\mathrm{AC}_1} & F_{\mathrm{AC}_2} & F_{\mathrm{AC}_3} \\
-F_{\mathrm{OT}_1} & -F_{\mathrm{AT}_1} & 0 & F_{\mathrm{T}_1\mathrm{T}_2} & F_{\mathrm{T}_1\mathrm{T}_3} & F_{\mathrm{T}_1\mathrm{T}_4} & F_{\mathrm{T}_1\mathrm{T}_5} & F_{\mathrm{T}_1\mathrm{T}_6} & F_{\mathrm{T}_1\mathrm{T}_7} & F_{\mathrm{T}_1\mathrm{C}_1} & F_{\mathrm{T}_1\mathrm{C}_2} & F_{\mathrm{T}_1\mathrm{C}_3} \\
-F_{\mathrm{OT}_2} & -F_{\mathrm{AT}_2} & -F_{\mathrm{T}_1\mathrm{T}_2} & 0 & F_{\mathrm{T}_2\mathrm{T}_3} & F_{\mathrm{T}_2\mathrm{T}_4} & F_{\mathrm{T}_2\mathrm{T}_5} & F_{\mathrm{T}_2\mathrm{T}_6} & F_{\mathrm{T}_2\mathrm{T}_7} & F_{\mathrm{T}_2\mathrm{C}_1} & F_{\mathrm{T}_2\mathrm{C}_2} & F_{\mathrm{T}_2\mathrm{C}_3} \\
-F_{\mathrm{OT}_3} & -F_{\mathrm{AT}_3} & -F_{\mathrm{T}_1\mathrm{T}_3} & -F_{\mathrm{T}_2\mathrm{T}_3} & 0 & F_{\mathrm{T}_3\mathrm{T}_4} & F_{\mathrm{T}_3\mathrm{T}_5} & F_{\mathrm{T}_3\mathrm{T}_6} & F_{\mathrm{T}_3\mathrm{T}_7} & F_{\mathrm{T}_3\mathrm{C}_1} & F_{\mathrm{T}_3\mathrm{C}_2} & F_{\mathrm{T}_3\mathrm{C}_3} \\
-F_{\mathrm{OT}_4} & -F_{\mathrm{AT}_4} & -F_{\mathrm{T}_1\mathrm{T}_4} & -F_{\mathrm{T}_2\mathrm{T}_4} & -F_{\mathrm{T}_3\mathrm{T}_4} & 0 & F_{\mathrm{T}_4\mathrm{T}_5} & F_{\mathrm{T}_4\mathrm{T}_6} & F_{\mathrm{T}_4\mathrm{T}_7} & F_{\mathrm{T}_4\mathrm{C}_1} & F_{\mathrm{T}_4\mathrm{C}_2} & F_{\mathrm{T}_4\mathrm{C}_3} \\
-F_{\mathrm{OT}_5} & -F_{\mathrm{AT}_5} & -F_{\mathrm{T}_1\mathrm{T}_5} & -F_{\mathrm{T}_2\mathrm{T}_5} & -F_{\mathrm{T}_3\mathrm{T}_5} & -F_{\mathrm{T}_4\mathrm{T}_5} & 0 & F_{\mathrm{T}_5\mathrm{T}_6} & F_{\mathrm{T}_5\mathrm{T}_7} & F_{\mathrm{T}_5\mathrm{C}_1} & F_{\mathrm{T}_5\mathrm{C}_2} & F_{\mathrm{T}_5\mathrm{C}_3} \\
-F_{\mathrm{OT}_6} & -F_{\mathrm{AT}_6} & -F_{\mathrm{T}_1\mathrm{T}_6} & -F_{\mathrm{T}_2\mathrm{T}_6} & -F_{\mathrm{T}_3\mathrm{T}_6} & -F_{\mathrm{T}_4\mathrm{T}_6} & -F_{\mathrm{T}_5\mathrm{T}_6} & 0 & F_{\mathrm{T}_6\mathrm{T}_7} & F_{\mathrm{T}_6\mathrm{C}_1} & F_{\mathrm{T}_6\mathrm{C}_2} & F_{\mathrm{T}_6\mathrm{C}_3} \\
-F_{\mathrm{OT}_7} & -F_{\mathrm{AT}_7} & -F_{\mathrm{T}_1\mathrm{T}_7} & -F_{\mathrm{T}_2\mathrm{T}_7} & -F_{\mathrm{T}_3\mathrm{T}_7} & -F_{\mathrm{T}_4\mathrm{T}_7} & -F_{\mathrm{T}_5\mathrm{T}_7} & -F_{\mathrm{T}_6\mathrm{T}_7} & 0 & F_{\mathrm{T}_7\mathrm{C}_1} & F_{\mathrm{T}_7\mathrm{C}_2} & F_{\mathrm{T}_7\mathrm{C}_3} \\
-F_{\mathrm{OC}_1} & -F_{\mathrm{AC}_1} & -F_{\mathrm{T}_1\mathrm{C}_1} & -F_{\mathrm{T}_2\mathrm{C}_1} & -F_{\mathrm{T}_3\mathrm{C}_1} & -F_{\mathrm{T}_4\mathrm{C}_1} & -F_{\mathrm{T}_5\mathrm{C}_1} & -F_{\mathrm{T}_6\mathrm{C}_1} & -F_{\mathrm{T}_7\mathrm{C}_1} & 0 & F_{\mathrm{C}_1\mathrm{C}_2} & F_{\mathrm{C}_1\mathrm{C}_3} \\
-F_{\mathrm{OC}_2} & -F_{\mathrm{AC}_2} & -F_{\mathrm{T}_1\mathrm{C}_2} & -F_{\mathrm{T}_2\mathrm{C}_2} & -F_{\mathrm{T}_3\mathrm{C}_2} & -F_{\mathrm{T}_4\mathrm{C}_2} & -F_{\mathrm{T}_5\mathrm{C}_2} & -F_{\mathrm{T}_6\mathrm{C}_2} & -F_{\mathrm{T}_7\mathrm{C}_2} & -F_{\mathrm{C}_1\mathrm{C}_2} & 0 & F_{\mathrm{C}_2\mathrm{C}_3} \\
-F_{\mathrm{OC}_3} & -F_{\mathrm{AC}_3} & -F_{\mathrm{T}_1\mathrm{C}_3} & -F_{\mathrm{T}_2\mathrm{C}_3} & -F_{\mathrm{T}_3\mathrm{C}_3} & -F_{\mathrm{T}_4\mathrm{C}_3} & -F_{\mathrm{T}_5\mathrm{C}_3} & -F_{\mathrm{T}_6\mathrm{C}_3} & -F_{\mathrm{T}_7\mathrm{C}_3} & -F_{\mathrm{C}_1\mathrm{C}_3} & -F_{\mathrm{C}_2\mathrm{C}_3} & 0
\end{pmatrix} \tag{15}$$

where F_{ij} gives the net flux from reservoir j to reservoir i. Filling this matrix with the quantitative fluxes and their associated uncertainties will give a full quantitative overview of our knowledge of the mass transport in the global water cycle. Unfortunately, most of the elements of F are not well known and observations to quantify the elements are often missing.

2.4 Relations between GOM, GOV and LSL

It is emphasized here that the deduction of changes in GOM and, to a slightly lesser extent, GOV from observations of LSL is a rather complicated task (Plag, 2006a). To convert LSL changes into GOV changes requires for example knowledge of the changes in ocean bottom elevation relative to the surrounding land caused by current mass exchanges of the ocean with the terrestrial hydrosphere and cryosphere, post-glacial rebound, plate tectonics, sedimentation and man-made subsidence. Moreover, mass movements in the terrestrial hydrosphere also cause spatially variable motion of the ocean bottom. Since our knowledge of ocean bottom elevation changes is rather limited, GOV changes derived from LSL observations are inherently associated with large uncertainties.

Converting GOV changes in GOM changes requires detailed knowledge on density changes in the ocean. The observational database for that is rather limited, thus increasing the uncertainties of changes in GOM even more compared to the GOV changes.

Similarly, estimates of global changes in GOM or GOV as provided by, for example, the IPCC assessments (Warrick et al., 1996; Church et al., 2001) cannot be simply converted into LSL changes. Particularly LSL changes due to mass exchange of the ocean with the terrestrial hydrosphere depend crucially on where the exchanged mass originates from, and the LSL changes at a given location can only be predicted on the basis of an integral equation. This equation, which is often denoted as the sea-level equation, was first introduced by Farrell & Clark (1976) in a simplified version:

$$\xi(\vartheta,\lambda,t) = c(t) + O(\vartheta,\lambda,t)\int_{-\infty}^{t}\int_{0}^{\pi}\int_{0}^{2\pi} G(\vartheta,\lambda,\vartheta',\lambda',t-t') \tag{16}$$

$$\frac{\mathrm{d}}{\mathrm{d}t'}\left\{O(\vartheta',\lambda',t')\rho_{\mathrm{W}}\xi(\vartheta',\lambda,t') + \left[1-O(\vartheta',\lambda',t')\right]\rho_{\mathrm{L}}\eta(\vartheta',\lambda,t')\right\}\sin\vartheta'\mathrm{d}\lambda'\mathrm{d}\vartheta'\mathrm{d}t'.$$

where ξ is the local sea-level change (that is, the distance to the deformable surface of the solid Earth), G is the Green's function for sea level, O the ocean function (which is 1 over the ocean and 0 over land), η the cumulated water or ice load change due to mass added or removed from land, ρ_{W} and ρ_{L}

are the densities of the ocean water and the load (water or ice), respectively, and $c(t)$ is a quantity included to ensure mass conservation. The Green's function accounts for the vertical motion of the land, the geoid changes caused by both the mass movements and the deformation of the solid Earth, and for the mass movements itself. The equation is solved assuming a spherically symmetric Earth model. Moreover, the equation assumes instantaneous distribution of the water in the global ocean and thus is only valid for interannual or longer time scales. A fully consistent treatment would have to include dynamic effects including the response of the rotating solid Earth to the loading. A more complete sea-level equation is discussed by, for example, Milne et al. (1999).

Eq. (16) has been applied extensively to studies of sea-level changes caused by the ice ages and the subsequent post-glacial rebound (see, e.g., Clark et al., 1978; Quinlan & Beaumont, 1982; Nakada & Lambeck, 1987; Tushingham & Peltier, 1992; Peltier, 1998). However, using the same equation to describe the relation between present-day mass changes and LSL is restricted to a few examples (see, e.g., Plag & Jüttner, 2001; Mitrovica et al., 2001; Plag, 2006a). It is emphasised here, that this equation gives the fundamental relationship between any mass transport in the global water cycle and the LSL. To illustrate this, we consider the case where the Greenland ice sheet increases while the Antarctic ice sheet melts with the two changes being exactly in balance. This mass movement will not induce a global sea-level change since the mass of the ocean is constant (and no volume change is caused), but LSL will change significantly with a LSL fall close to Antarctica and probably as far as 50°to 40°S and a LSL increase over large parts of the northern hemisphere. It is obvious that the complex relation between LSL and GOM changes cannot be neglected in the interpretation of LSL observations in terms of global sea-level changes (see Plag, 2006a, for a detailed discussion).

Considering the complexity of the relation between changes in the global water cycle and LSL, extreme caution has to be taken when deriving global sea-level changes from LSL observations covering only a small part of the ocean's surface (Plag, 2006a). Likewise, extreme caution has to be taken when down-scaling the global scenarios into a region or even a local area such as the Upper Adriatic. Only if the global contribution due to mass exchange is handled correctly, can we expect to get a realistic scenario of the future changes. Thus, our understanding of the governing physics need to be taken into account. As an example, we point out here that melting of the same ice mass on Antarctica and Greenland, respectively, will have rather different effects on the sea level in Venice, due to the complex combined effect of geoid changes and Earth surface displacements.

3 The data base and models

3.1 Tide gauge records

Sea level has been recorded with tide gauges in several locations of the Adriatic regions for many years (Figure 2). For many of these gauges, monthly mean values have been submitted by the responsible authorities to the *Permanent Service for Mean Sea Level* (PSMSL), while hourly data are not generally available. The *European Sea Level Service* (ESEAS) is currently making an effort to make a comprehensive database of quality controlled hourly data available, but this work is still in progress.

For the tide gauges in Venice and Trieste, hourly data have been made available for the project by CVN. In the following section, we will first discuss these two time series of hourly data. Subsequently, we will give an overview of the records of monthly mean sea levels available in the PSMSL database.

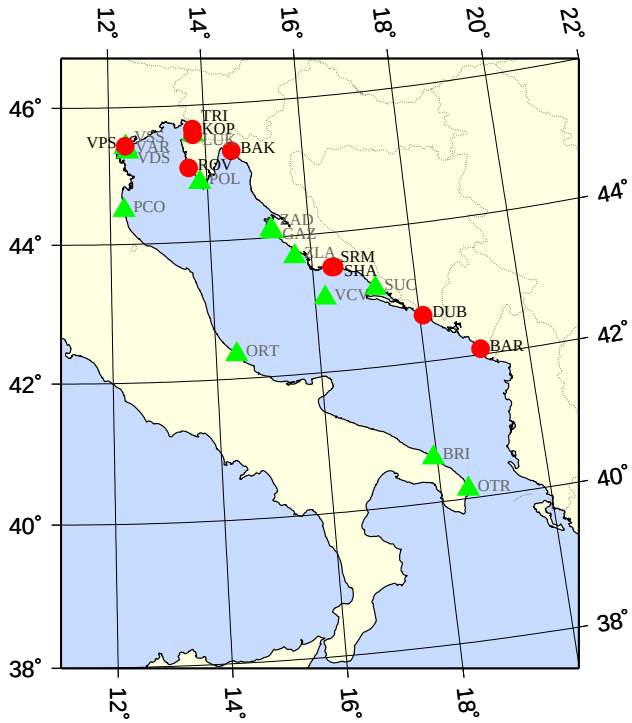

Figure 2: Tide gauge locations in the Upper Adriatic region

Tide gauge locations are taken from the PSMSL data base. Red circles are those with more than 20 years of RLR records. Green triangles indicate tide gauges with shorter records or longer Metric records (PCO and VDS). Full station names are given in Table 2 on page 25.

3.1.1 Hourly tide gauge records

For the tide gauge at Punta della Salute in Venice, hourly values are available for the period from 1955 to 2003 (Figure 3). At this tide gauge, sea-level measurements are referred to the datum, which is called the "tidal zero of Punta della Salute" and designated Z.M.P.S. Rusconi (1993) states that the mark has never varied with respect to the ground level of the city.

For the tide gauge in Trieste, the hourly values cover the period from 1939 to 2004 (Figure 3). At that tide gauge, the sea level is referred to a local reference that is approximately 150 cm above mean sea level.

In Figure 4, the differences of the hourly values at the tide gauges in Venice and Trieste are shown. Most differences are of the order of a few tens of centimeter and at least partly due to small differences of the tides between these two sites. For the years from 1955 to 1963, the difference are slightly but

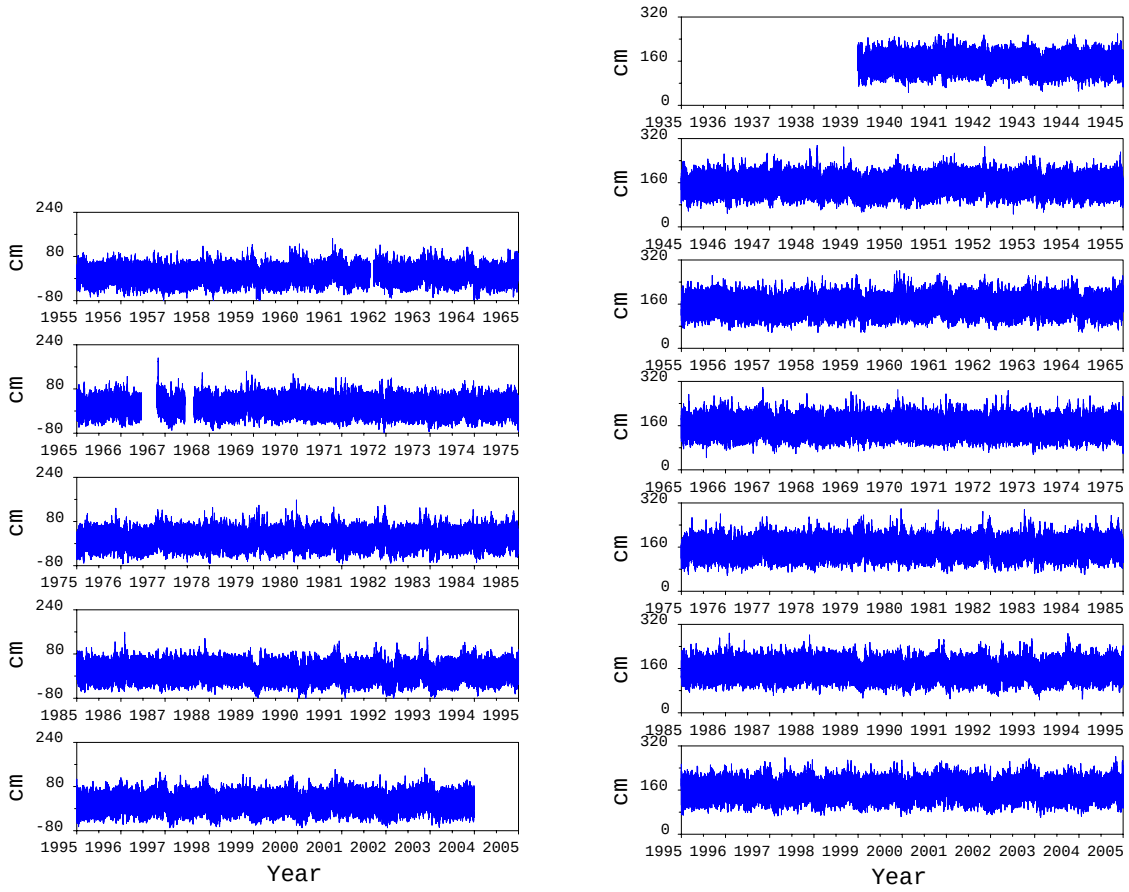

Figure 3: Hourly records of the Venice and Trieste tide gauges.

Left: Record of the tide gauge at Punta Salute in Venice, right: record of the tide gauge at Trieste Molo Sartorio. The records with monthly means can be found in Figure 26 on page 53.

significantly larger than for the following years. This might be due to a poorer quality of one of the two time series during that period, which is underlined by the long-period variation in the difference during 1955. The annual *Root Mean Square* (RMS) of the difference (Figure 5) and the annual regression and correlation coefficients also reflect a steady increase in data quality and coherency between Venice and Trieste over the interval from 1955 to approximately 1970. The annual minima and maxima underline the spikes in the differences, which most likely are caused by data errors.

It is interesting to note here that the annual mean of the differences shows decadal to multi-decadal variations with a range of approximately 8 cm (Figure 5). Over the interval from 1955 to approximately 1972, the sea level in Venice was rising faster than in Trieste, reaching a maximum in the early 1970s. After that, and until the late 1980s, sea level in Venice was rising slower than in Trieste. Over the last 15 years, sea level in Venice seems to be rising again faster than in Trieste, with the mean in Venice having increased by nearly 3 cm with respect to the mean in Trieste, which is equivalent to an excess rise in Venice of the rise in Trieste of approximately 2 mm/yr. Moreover, there also are inter-annual to decadal variations with a range of more than 6 cm within a decade. These variations and their spatial pattern will be discussed further in Sections 4.3 and 4.5.

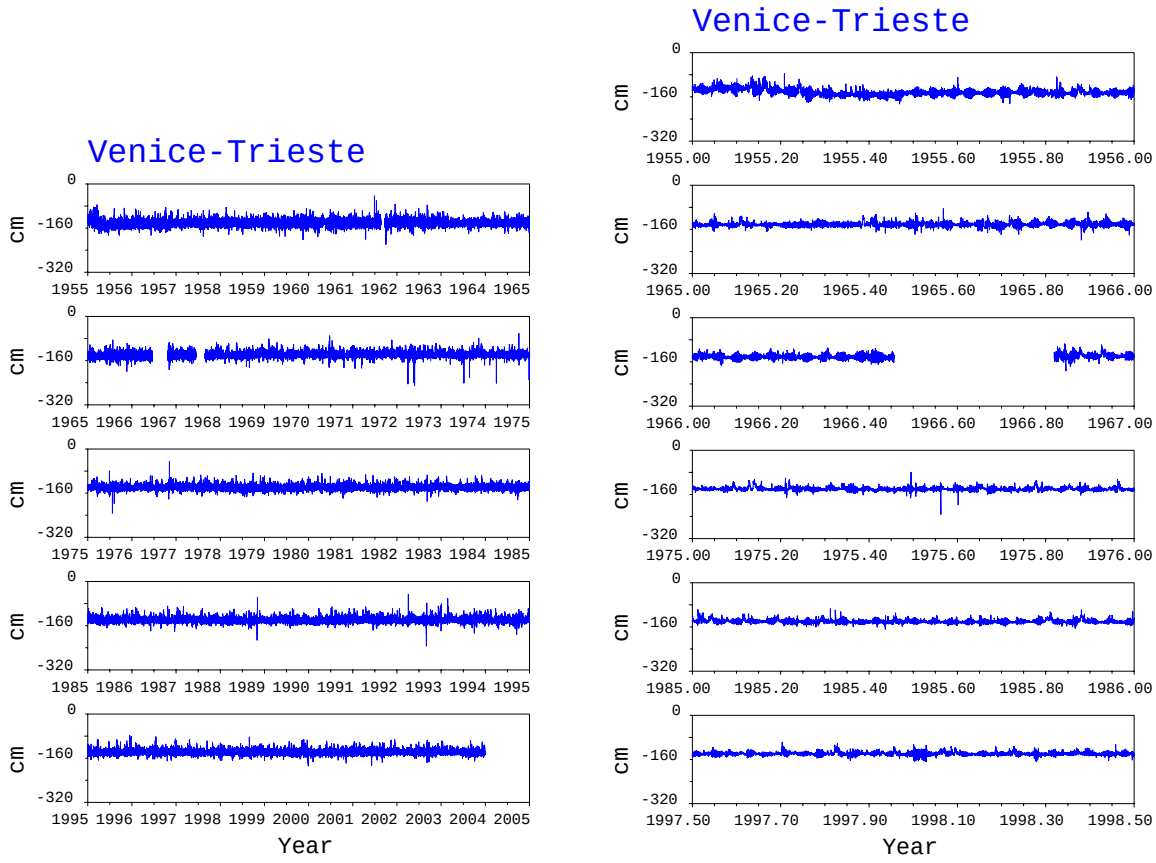

Figure 4: Differences of the hourly sea-level values at Venice and Trieste.

The difference shown are those for Venice minus Trieste. Left: Differences for the complete overlapping records. Right: differences for selected years.

3.1.2 Monthly sea-level records

The database of monthly mean sea levels collected by the PSMSL is a major source of sea-level data used in many of the studies on long-period and secular sea-level variations. The database is quality controlled (Spencer & Woodworth, 1993; Woodworth & Player, 2003), and for a large number of records, a well documented history of the relation between the tide gauge zero level and the benchmark on land exists. These latter records are those that are referred to as *Revised Local Reference* (RLR) series, while those without a well documented history to a single benchmark are denoted as Metric series. It is generally recommended that only the RLR series should be used for studies of secular trends, while the Metric series are useful for studies of seasonal and intraseasonal variations.

The PSMSL database currently contains at total of 154 stations in the Mediterranean and Black Sea. However, many of these have only short records of one to less than ten years. The number of long records covering nearly a century is small and the stations are limited to the northern coast of the Mediterranean and the Black Sea.

The Adriatic in fact is the part of the Mediterranean best covered with longer records (Table 2). 21 stations have records of more than 5 years, and 13 of these have records longer than 20 years (though two only with Metric data).

The quality of the long records and their interpretation in terms of secular sea-level trends has been discussed in a number of publications (see, e.g., Emery & Aubrey, 1991; Woodworth, 2003, and the reference therein). For the two series from the tide gauges at Venice P.S. and Trieste, quality is

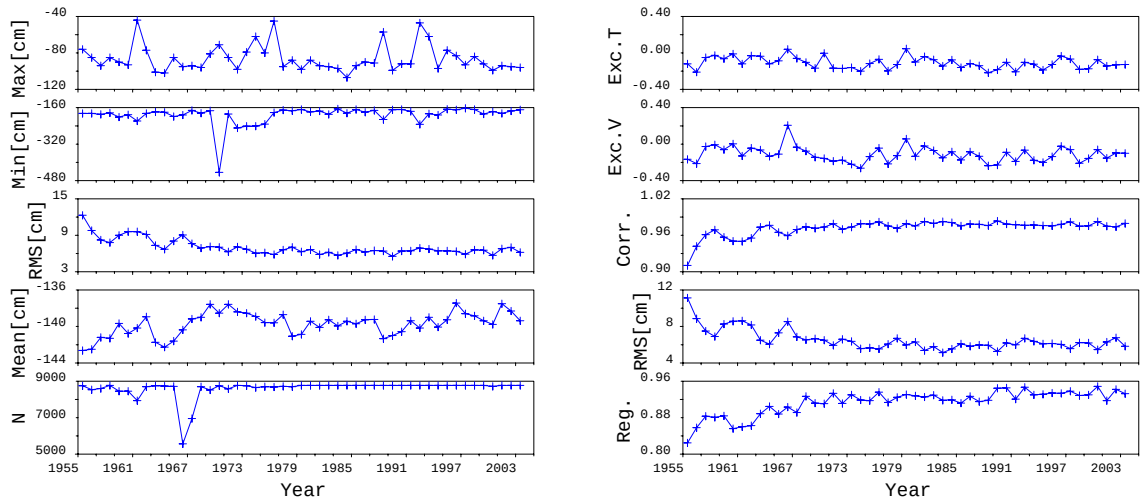

Figure 5: Annual statistics of the differences of the hourly sea-level values at Venice and Trieste.
The difference are those for Venice minus Trieste. All parameters are given for a moving, non-overlapping window of a year. A year is defined to have 8766 hours. Left: from bottom to top: Number of hourly values in a year (N); mean of the differences, root mean square of the difference; minimum of the difference; maximum of the difference. Right: From bottom to top: Regression coefficient for the equation $h_{\mathrm{V}} = a + b \cdot h_{\mathrm{T}}$*, with* h_{V} *and* h_{T} *the sea level in Venice and Trieste, respectively; root mean square of the residual* $\delta h_{\mathrm{V}} = h_{\mathrm{V}} - (a + b \cdot h_{\mathrm{T}})$*; correlation coefficient between the sea level in Venice and Trieste; skewness for Venice; skewness for Trieste (see, e.g., Press et al., 1992, for the definition of the terms).*

generally found to be good.

It is interesting to note here that Pirazzoli (1986) and subsequently a number of authors claimed that long sea-level records are needed to give reliable estimates of secular trends. Based on a similar reasoning, Douglas (1991) and several subsequent studies (see Douglas, 1997, and the references therein) choose a number of long records to determine secular trends, which he considered representative for a global sea-level rise. However, the two long records in the Adriatic illustrate nicely that long records contain significant non-linear contributions (see Tables 10 and 11 on page 51) from both local vertical land motion and atmospheric forcing (see Section 8, page 93). Therefore, for understanding the contributions to LSL, long records may not be the most important ingredients but rather a better spatial coverage. This coverage is provided for the Adriatic particularly through the gauges along the northern and eastern coast, while gauges on the western coast are lacking (see Figure 2 on page 21).

3.2 Satellite altimetry

Satellite altimetry measures the geocentric position of the sea surface in a global reference frame such as ITRF2000. For the determination of long-period trends, individual satellite altimetry missions have the disadvantage of covering only relatively short time windows of slightly more than a decade (Topex/Poseidon), while the combination of different mission is hampered by inter-mission difference. Moreover, satellite altimetry is inherently weak in coastal ares such as the upper Adriatic. A main uncertainty in the position of the sea surface determined by satellite altimetry is due to an uncertainty of the relation of the origin of the reference frame to the actual geocenter. For ITRF2000, this uncertainty is estimated to be of the order of 1 to 2 mm/yr. Therefore, satellite altimetry needs to be constraint by tide gauges co-located with GPS. However, this does not actually remove the uncertainty with respect to the geocenter.

Considering the large uncertainty, the short data span, and the inherent problems in coastal areas, we

Table 2: Monthly mean sea-level records in the Adriatic.

*The records are those currently available in the PSMSL database (see http://www.pol.ac.uk/psmsl/). Only records longer than 5 years have been included. Records marked with * and ** have more than 20 years of RLR and Metric data, respectively. The column denoted by Abbr. give the station abbreviations used throughout this report. The column Months gives the number of monthly values actually available in the record.*

Name		Abbr.	Longitude	**latitude**	**Start**	**End**	**Months**
OTRANTO		OTR	18.50000	40.13334	1961	1970	48
BRINDISI		BRI	17.93333	40.63334	1978	1991	156
ORTONA		ORT	14.40000	42.35000	1960	1972	75
PORTO CORSINI	**	PCO	12.28333	44.50000	1896	1972	688
VENEZIA (DIGA SUD DI	**	VDS	12.38333	45.35000	1917	1987	398
VENEZIA (ARSENALE)	*	VAR	12.35000	45.41667	1889	1913	287
VENEZIA (S.STEFANO)	*	VSS	12.33333	45.41667	1872	1920	576
VENEZIA (PUNTA DELLA	*	VPS	12.33333	45.43333	1909	2000	1039
TRIESTE	*	TRI	13.75000	45.65000	1905	2001	1092
POLA		POL	13.85000	44.86666	1897	1913	192
KOPER	*	KOP	13.75000	45.56667	1962	1991	344
LUKA KOPER		LUK	13.75000	45.56667	1992	2001	120
ROVINJ	*	ROV	13.63333	45.08333	1955	1999	532
BAKAR	*	BAK	14.53333	45.30000	1930	1999	708
ZADAR		ZAD	15.23333	44.11666	1994	1999	65
GAZENICA		GAZ	15.26667	44.08333	1983	1988	73
ZLARIN		ZLA	15.66667	43.70000	1983	1988	65
SPLIT RT MARJANA	*	SRM	16.38333	43.50000	1952	1999	558
SPLIT HARBOUR	*	SHA	16.43333	43.50000	1930	1999	550
VIS-CESKA VILA		VCV	16.20000	43.06667	1983	1991	97
SUCURAJ		SUC	17.20000	43.13334	1987	1999	153
DUBROVNIK	*	DUB	18.06667	42.66667	1955	1999	523
BAR	*	BAR	19.08333	42.08333	1964	1991	319

have decided not to use satellite altimetry data for the present study.

3.3 Meteorological data

Meteorological data is available from a few local observing sites as well as from global reanalysis data sets. There are several reanalysis data set available (e.g., from NCEP, ECMWF), and we have accessed the ECMWF set.

Here we use mainly the global reanalysis dataset for studies, while the local data is used to valid the station time series interpolated from the global data sets.

3.3.1 Local, *in-situ* observations

From Tessera Airport, air-pressure and temperature observations are available for the period March 1961 to December 2002 (Figure 6). These observations have a sampling interval of three hours. For the time interval from 1900 to 1960, air pressure and temperature at Tessera Airport have been estimated from Cavanis observations, taking into account the trend, the average and the RMS of the observations

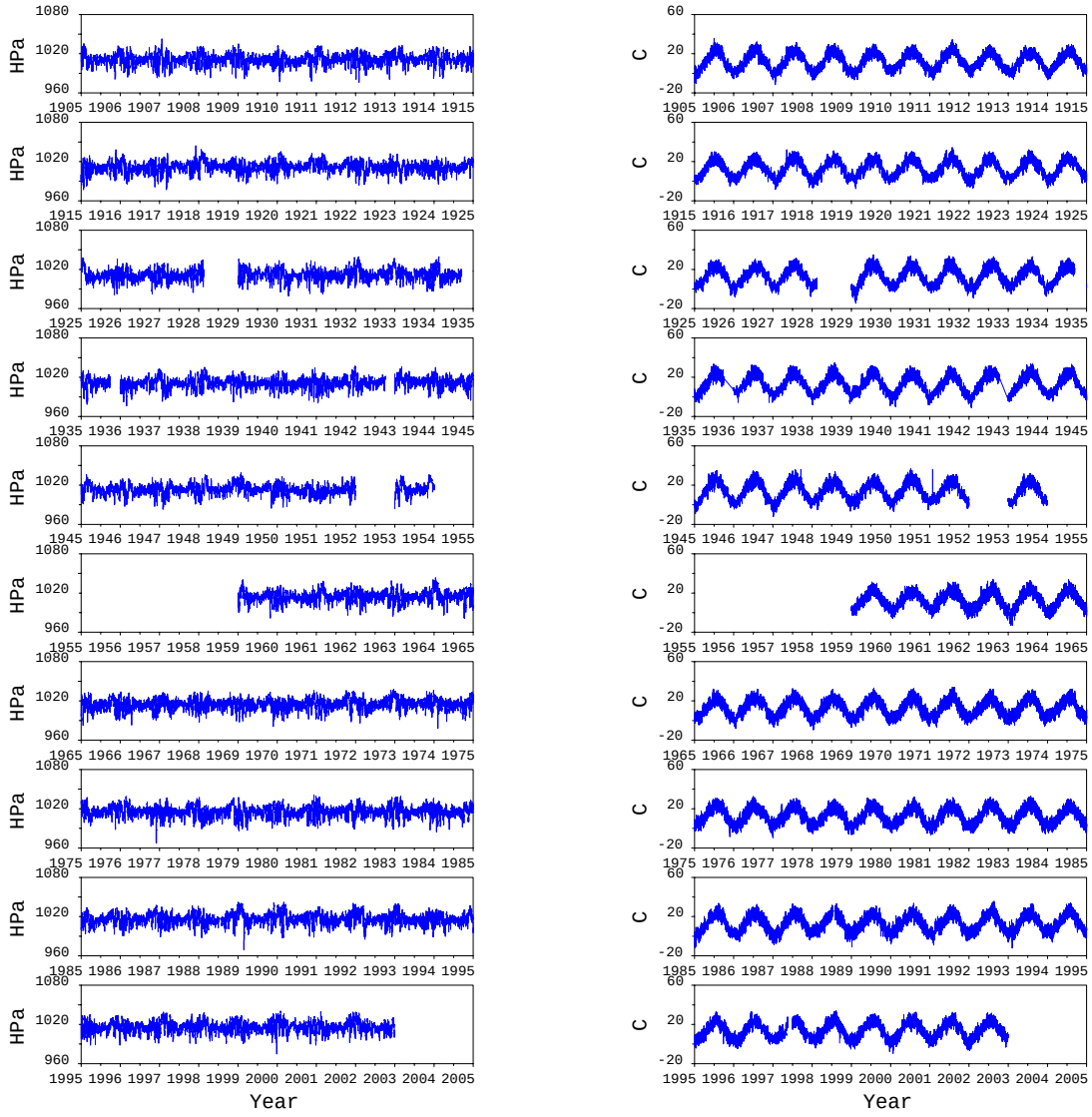

Figure 6: Air-pressure and temperature observations at Tessera airport.

Left: air pressure, right: air temperature. Note that only the data in the time window from 1961 to 2002 are actual observations, while the data prior to 1961 are estimated from the observations at Cavanis.

at the two sites (also shown in Figure 6). The estimate values are given at up to six non-equidistant time points in a day (e.g., 6:00, 12:00 and 21:00 hours).

The air-pressure record is dominated by a seasonality which mainly consists of larger variability in the winter months. There is also some interannual to decadal variability in the pattern of the seasonality. In order to emphasize long-period variations, we have integrated the time series over time, that is, we computed

$$\hat{h}(t) = \int_{t_0}^{t} h(t')dt'. \tag{17}$$

Integration acts as a low-pass filter, with the transfer function being proportional to $1/f$, where f is the frequency. It is noted here that a linear trend component $a \cdot t$ in the time series will result in a quadratic term $a \cdot t^2$ after integration. In the integration, gaps introduce a problem, which is solved by

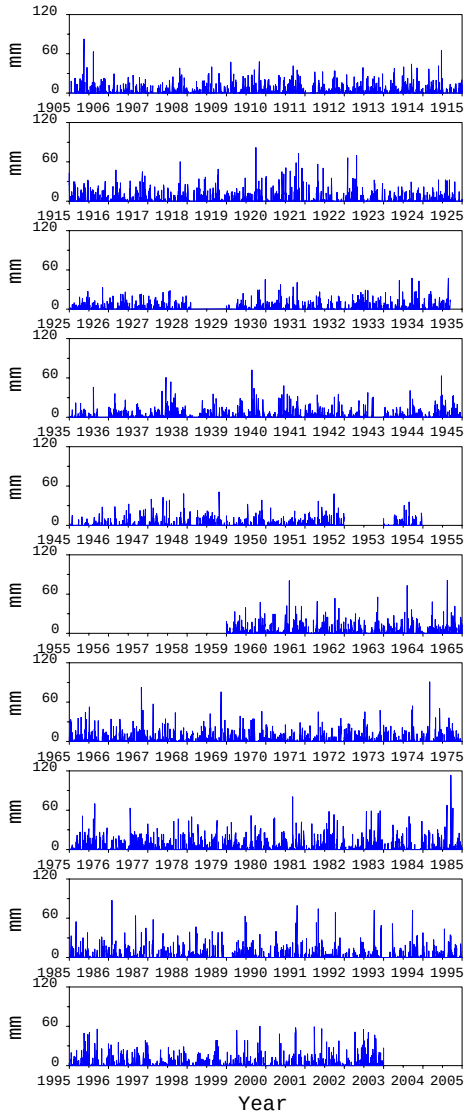

Figure 7: Precipitation at Cavanis.
The observations are from the station at Cavanis Institute. Note that the Institute changed location in 1959, which introduces an inhomogeneity in the time series.

linear interpolation. However, large gaps can easily lead to large offsets in the integrated time series.

Integrating the air-pressure time series after 1960 (in order to avoid the effects of the gaps on integration) over time reveals a significant quadratic term (Figure 8) resulting from a positive trend in air pressure. This positive trend in air pressure can expect to have had a negative effect on sea level.

As expected, the air temperature (Figure 6) is dominated by a strong seasonal signal, with only very little temporal variations in the seasonality. However, besides the still visible seasonal variation, the integrated temperature (integrated for times after 1960, in order to avoid an effect of the large gaps) shows a quadratic term (Figure 8) consistent with an increase in temperature.

Daily precipitation values are available from the Cavanis Institute for the time window from 1900 to 2002 (Figure 7). The Institute changed location in 1959, which introduced an inhomogeneity in the time series. The daily data show some interannual variability in the pattern. Integrating the deviation from the mean after 1960 (to avoid effects of the large gaps on the integration) reveals that the precipitation is remarkably stable in time, with only small interannual to decadal variations

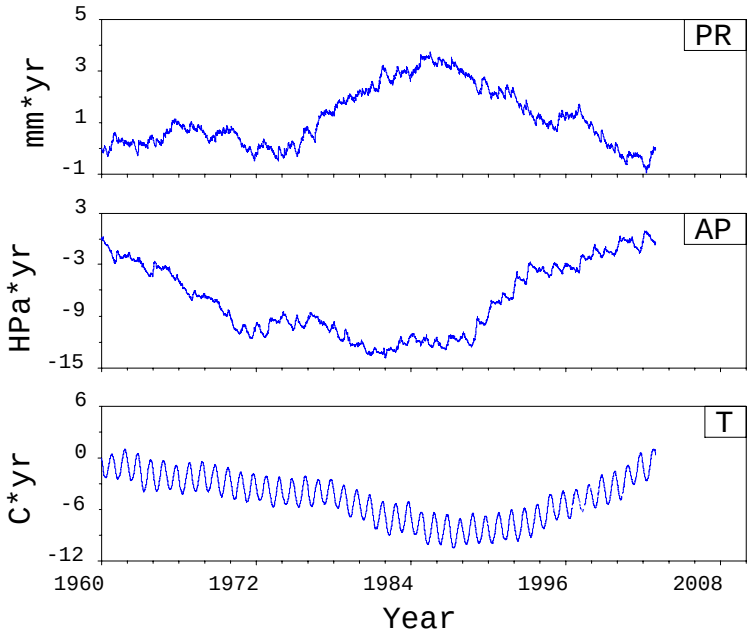

Figure 8: Integrated air pressure, temperature and precipitation observations at Tessera airport.

*The observations of air pressure and temperature are shown in Figure 6 and of precipitation in Figure 7. Observations are integrated over the time time window from 1960 to 2002 using eq. (17). Top: integrated precipitation in mm*yr; middle: integrated air pressure in HPa*yr, bottom: integrated air temperature in °C*yr.*

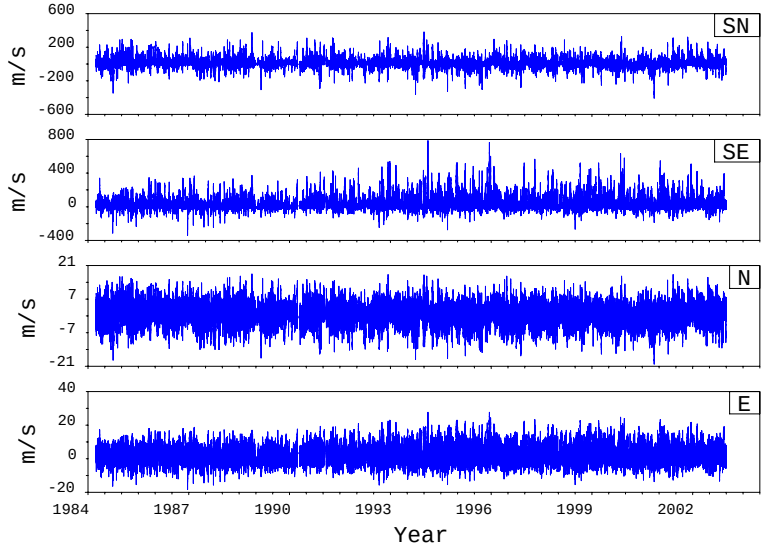

Figure 9: Wind observations and wind stress at Piattaforma.

Observations are from Piattaforma, about 15 km out in the sea. Upper diagrams give the wind stress computed with eq. (18), lower diagrams the wind speed. From top to bottom: SN: north component of wind stress; SE: east component of wind stress; N: north component of wind; E: east component of wind.

(Figure 8), and no clear trend. A maximum deviation from the mean was reached around 1985.

Wind has been measured at an hourly sampling interval at the platform Piattaforma CNR in the sea about 15 km outside the lagune from 1983 to nov 2004 (Figure 9). From that platform, wave data are also available with a sampling rate of three hours from 1987 to 2004.

The wind component in east and north are dominated by high day-to-day variability with little long-period variations discernible in the plot of the hourly observations (Figure 9). The envelop of the north component shows some seasonality while the envelop of the east component does not have this pattern. The east component shows a slightly larger variability than the north component. Integrating the wind components over time (Figure 10) emphasizes the seasonal pattern in the north component, while for the east component more interannual variability becomes visible. Both components contain

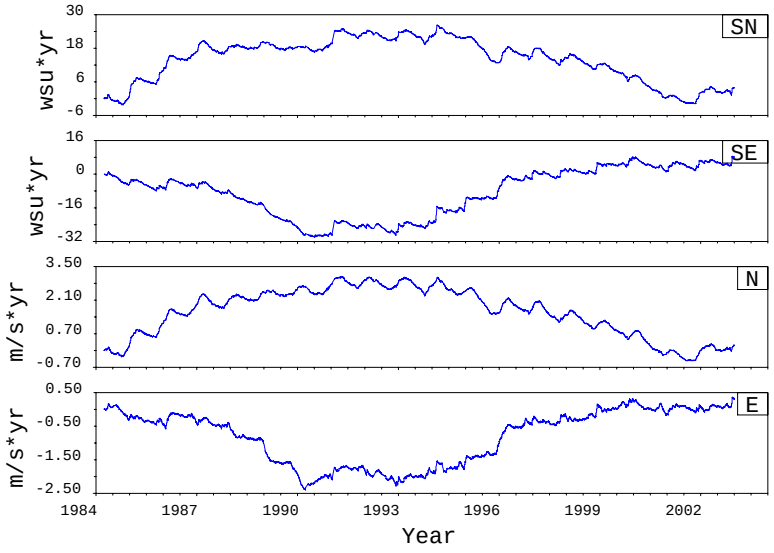

Figure 10: Integrated wind observations and wind stress at Piattaforma.

Observations are those shown in Figure 9. The observation have been integrated over time using eq. (17). From top to bottom: SN: north component of integrated wind stress; SE: east component of integrated wind stress; N: north component of integrated wind; E: east component of integrated wind. Wsu stands for wind-stress units.

a quadratic term, indicating a trend, which for the east component is positive and for the north component is negative. A negative trend in the north component is expected to have a negative affect on sea level along the northern Adriatic coast. A positive trend in the east component has a negative effect on sea level in Venice while it has a positive effect on sea level in the north-eastern most part of the Adriatic.

For sea level, wind stress is more important that the wind itself. The wind effect on sea level can be expected to be proportional to the tangential wind-stress components. The east and north components of the wind-stress component are given by

$$\sigma_{\mathrm{E}} = w_{\mathrm{E}}\sqrt{w_{\mathrm{E}}^2 + w_{\mathrm{N}}^2} \tag{18}$$

$$\sigma_{\mathrm{N}} = w_{\mathrm{N}}\sqrt{w_{\mathrm{E}}^2 + w_{\mathrm{N}}^2} \tag{19}$$

respectively. The daily wind stress for Piattaforma (Figure 9) is dominated by large high-frequency variability, though intraseasonal variability is more pronounced than in the wind components themselves. Integrating the wind-stress time series (Figure 10) reveals a pattern similar to the integrated wind components, with the quadratic components clearly visible.

A quantity related to precipitation is the river influx particularly from the river Po. Figure 11 shows the monthly mean influx measured at Pontelagoscuro. The integrated time series shows some large decadal fluctuations, which seem to be correlated to similar fluctuations in the sea level. Therefore, the river influx can be considered as a proxy for the fresh water forcing of the Adriatic, which may induce some decadal fluctuations. However, the regression results discussed in Section 8 rule out an instantaneous control of sea-level variations in the Adriatic through fresh water influx. Nevertheless, a time-lagged influence may still exist.

3.3.2 Global reanalysis data sets

The ECMWF has carried out a reanalysis of the observational data for the time period from September 1957 to August 2002. A three dimensional variational technique was applied to produce analyzes every six hours on the basis of a comprehensive global set of *in situ* observations, as well as satellite data when they became available. These so-called era40 data have been widely used for climatological, geophysical and oceanographic studies and are considered to be validated.

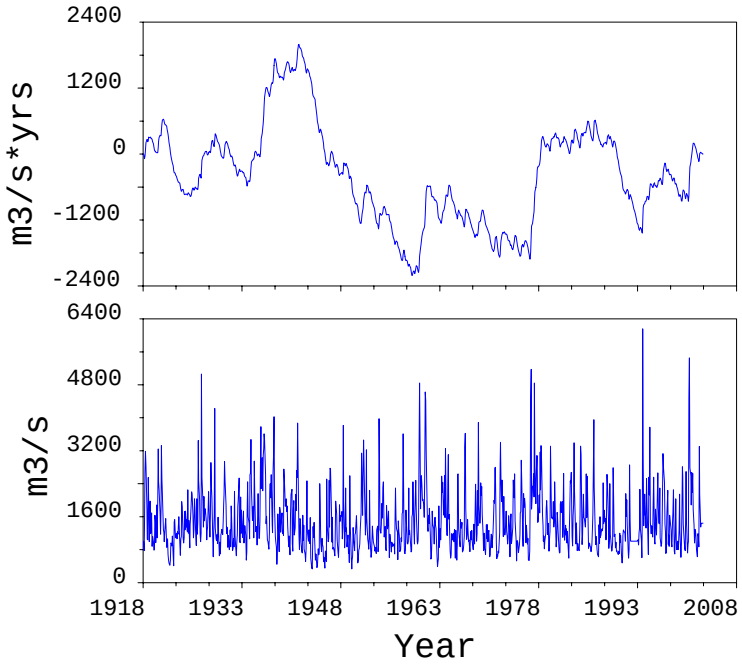

Figure 11: Monthly flux of the river Po.

The era40 data are available with a sampling interval of 6 hours and can be downloaded freely from http://data.ecmwf.int/d/era40/daily/. The parameters available include a large number of meteorological parameters given both as surface data as well as for 23 pressure levels ranging from 1000 HPa to 1 HPa. For this study, we have down-loaded the global set of sea surface pressure, sea surface temperature and the eats and north wind components for the complete era40 time window and a sampling rate of 6 hours. The spatial resolution of the datasets is 2.5 by 2.5 degrees. Time series for all long Adriatic tide gauges were interpolated for air pressure, air temperature and the east and north component of the wind stress (the latter according to eq. (18)) and then monthly mean values were computed for the regression on sea level.

3.4 Oceanographic data

3.4.1 Global data sets

To a certain extent, thermosteric sea-level variations can be computed from observations of the subsurface temperature field. Currently, two global data sets are available, namely Levitus et al. (2000) and Ishii et al. (2003) with a temporal resolution of 1 year and 1 month, respectively. Both data sets have spatial resolution of 1° in longitude and latitude. The former is given for the interval 1945 to 1998 and the latter for the interval 1950 to 1998. The two data sets are, to a large extent, based on the same observations; however, different analysis schemes are used to create the gridded data sets. The sea-level trends derived from these two data sets display considerable differences (Figure 12), with the former having more short wavelength variations and a larger range of local trends. The differences in the two data sets are studied in detail by, for example, Lombard et al. (2005). They point out that for the 1990s, the Levitus et al. (2000) data set shows a global trend nearly three time larger than the Ishii et al. (2003) data, and attribute this to errors in the processing. Moreover, according to them, the I500 dataset is likely to underestimate the thermosteric contribution due to an omission of XBT

Table 3: Data sets for thermosteric sea-level variations

All thermosteric sea-level heights were provided by Cazenave (2002, 2003, personal communication). N is the number of grid cells. A is the surface of the grid in % of the total Earth surface. See Lombard et al. (2005) for details of the computation of the steric sea-level heights.

Symbol	Oceanographic data	Depth	Temporal resolution	N	A
I500	Ishii et al. (2003)	500 m	1 month	40779	68.08
L500	Levitus et al. (2000)	3000 m	1 year	41191	68.56
L3000	Levitus et al. (2000)	500 m	1 year	41163	68.51
L700	Levitus et al. (2000)	700 m	1 year		

depth correction.

Here, we will use four sea-level heights derived from both data sets in order to estimate the uncertainty in the steric sea-level contribution (Table 3). For the steric sea-level heights denoted as L500 and L3000 only time series of annual means can be created. I500 is given as monthly means, and therefore, the time series can be directly compared to monthly mean sea levels.

However, it is pointed out here that use of the global oceanographic data sets can easily lead to misinterpretations (see, e.g., the discussion of the Cabanes et al., 2001 paper in Miller & Douglas, 2004). Therefore, proper selection of the relevant observations from both the local and global datasets will be used to provide realistic estimates of the uncertainties and thus avoid over interpretations.

3.4.2 Oceanographic data sets in the Mediterranean Sea

In addition to the global climatologies described above coordinated efforts between various research institutions led to the development of much needed regional oceanographic databases, initially the Mediterranean Oceanographic Data Base (MODB) (Brasseur, 1995) and subsequently the MEDATLAS (Maillard et al., 2001; MEDATLAS Group, 1997). Moreover, the inclusion of ex-USSR data (Hecht & Gertman, 2001) which cover areas in the Gulf of Libya were previously large gaps existed further improved the dataset. On the basis of these data the Mediterranean Climatology Medar was developed (Rixen et al., 2001). Medar as well as the Levitus and the Ishii climatologies contain almost the same Mediterranean dataset. Thus their differences arise because of the interpolation techniques in time and space. No complete comparison has yet been made. However, Medar has the advantage that the original measurements are directly available thus permitting independent tests on the climatology. One should also be aware of the limitations of the database. Regular repeated sampling of the water column was not common until the late 1940's or in many cases the late 1950's to early 1960's (Painter & Tsimplis, 2003). In almost all basins a few measurements exist which were made during the early part of the 20^{th} century (1900 to 1930). However after these early measurements gaps of up to 40 years can be found in the MEDATLAS (for example, Aegean Winter temperature records first start in 1908 but the next subsequent measurements are not made until 1948). Use of these early points can introduce a strong bias into the trends by elevating their importance. To compensate for this, trends have been based upon the mid to late 20^{th} century measurements where only a few years may separate the data. It is also a feature of the MEDATLAS that hydrographic stations have not been occupied regularly but only as part of particular expeditions which may have had diverse research interests (Painter & Tsimplis, 2003). As a result a particular area of one basin may have been sampled extensively with a large number of casts during a particular season while other areas may not have been sampled during the same period. Thus a "mean" value would not be representative of the whole basin. Moreover, due to the difficulties in obtaining the salinity measurements systematic errors per

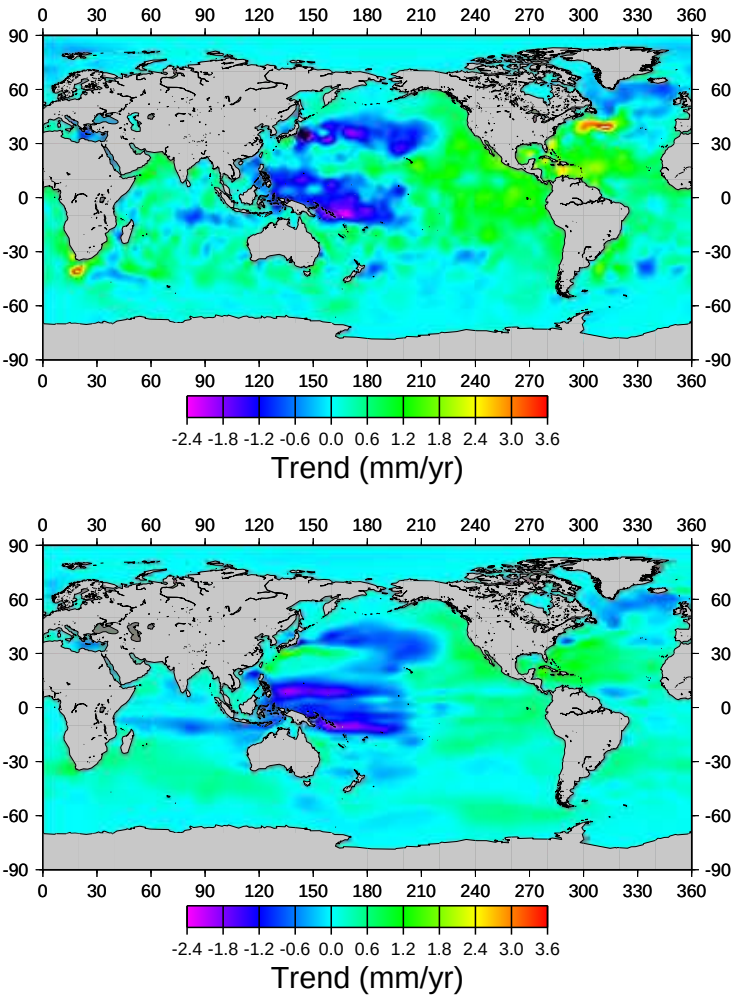

Figure 12: Spatial fingerprint of the thermosteric sea-level trend for the interval 1950 to 1998.
Upper diagram: trends for L500; lower diagram: trends for the I500.

cruise or even per cast exist which increase the noise in the salinity records. Consequently relevant results should be considered with caution. Nevertheless the MEDATLAS is our most complete source of in-situ observations and therefore the best information available.

Since all databases are essentially based on the same datasets the deficiencies are common. However, intercomparison of steric sea level variability indicates that the Medar contains more variability than the Ishii and Levitus datasets discussed above.

3.5 Observations of vertical land motion

3.5.1 Leveling

Leveling is a direct measurement of vertical offsets between adjacent benchmarks acquired through visual contact from one benchmark to a vertical measuring rod at the next. Thus, leveling does not require clean visibility of space satellites, and can be used independent of sky conditions that are required by GPS. High precision results can be obtained over short distances, however, as the length of the line increases, uncertainties accumulate and compound. Closed circuits can reduce the impact of uncertainty accumulating over a route. However, an important limitation is that the measurements are local and not tied to an external reference frame, leaving vertical motion of the entire network unconstrained. Removing this rank deficiency can be achieved by combining future surveys of the

Table 4: Some Geodetic Datasets in the Adriatic Region

Location	**Type**	**Reference**
Dinerides	GPS campaign	Altiner (2001)
Italy, N. Africa	GPS campaign	Anzidei et al. (2001)
Alpine-Pannonian	GPS continuous+campaign	Grenerczy & Fejes (2000)
S. Apennines	GPS continuous+campaign	Serpelloni (2002); Serpelloni et al. (2005)
Anatolia	GPS campaign	et al. (2000)
S. Adriatic	GPS continuous+campaign	Oldow et al. (2002)
N. Adriatic	GPS semi-continuous	RETREAT study in progress
Venice Lagoon	leveling	Carbognin et al. (2004)

leveling network with a component of three-dimensional GPS positioning on a subset of the leveling marks. This will facilitate the integration of the leveling results with other measurements, and ease the development of more complete surface deformation models.

The present leveling network around the Lagoon of Venice consists of $\sim$ 1000 benchmarks over 850 km. These have been observed in 1973, 1993, 2000 (Carbognin et al., 2004). For both the 1973-1993 and 1993-2000 intervals it has recorded a similar subsidence pattern that is greatest at the northern and southern ends of the Lagoon (approximately -4 mm/yr), and a rate near -1 mm/yr at Venice. Its only tie outside the immediate vicinity of the Lagoon is a northern line through Treviso that extends to the alpine foothills, and thus these measures of subsidence are relative to other points within the leveling network only. This one line however does indicate a relative subsidence of Treviso, Venice and the Industrial zone of approximately -1 cm in 1993-2000, suggesting that the entire network is subsiding with respect to the Alps. Results from leveling surveys across the entire eastern Po Plain (Bondesan et al., 2000) indicate that in some localities subsidence exceeds -2.5 meters since 1943 (Bologna), suggesting an average rate of at least -60 mm/yr. However, in many places the rate of subsidence declined drastically after 1970, when a shift to surface water delivery reduced the amount of groundwater pumping. This is similar to the Venice hinterland where groundwater extraction is now strictly limited. For Chioggia and Mestre, they report an average of at least -3.5 mm/yr subsidence between 1950 and 1970 with respect to the rest of their network, and slowing substantially between 1970 and 1988 to rates possibly under -1 mm/yr.

3.5.2 GPS data

GPS data have been used to identify processes at play on a wide range of temporal and spatial scales. The have been crucial in quantifying the rates of motion and deformation in and around the Adriatic, and in developing seismoteconic models that explain the pattern of crustal deformation (see references in Table 4). Generally, GPS rates are similar to those that have been inferred from to be at play for millions of years (e.g., DeMets et al., 1994). On shorter time scales, GPS has been used to infer slip rates on specific faults (Hammond & Thatcher, 2004), identify transient magmatic events in the Earths deep crust (Smith et al., 2004), and oscillations in aquifers affected by municipal water usage (e.g., Bawden et al., 2001). In general, GPS data are useful in quantifying surface motions because of their high precision, long term stability, and ease of deployment. Furthermore, the uncertainties in positions and velocities can be obtained independent of baseline length, and results can be put into global or local reference frames as demanded by particular needs.

In addition to GPS campaigns (infrequent, temporary deployments) that have been undertaken in the vicinity of the city and Lagoon of Venice, GPS data have also been acquired using permanently

Table 5: SOPAC holdings within 300 km of Venice, Italy

For an overview of the networks, see Table 6. Note that the station TREP according to information provided by CVN is an experimental station and therefore will not be considered further.

Station	Affiliation	Archive	Start	End	Comment
ACOM	FREDNET	FREDNET	5-Jul-03	19-May-04	
AFAL	FREDNET	FREDNET	22-Jun-03	19-May-04	
BZRG	EUREF	SOPAC	30-Nov-00	21-Apr-05	
CANV	FREDNET				No Data Found
CAVA	Venice	SOPAC	18-Jul-01	18-Jun-05	
COMO	EUREF				No Data Found
GENO	EUREF	SOPAC	23-Jul-98	18-Jun-05	
GRAA	EUREF	SOPAC	30-May-98	30-May-01	
GRAB	EUREF	SOPAC	2-Oct-99	29-Mar-04	
GRAZ	EUREF	SOPAC	1-Jan-97	18-Jun-05	
HFLK	EUREF	SOPAC	21-Jan-97	18-Jun-05	Listed as now inactive by EUREF
IBK2	EUREF	SOPAC			No P1 data found.
LINZ	EUREF	SOPAC			No P1 data found.
MDEA	FREDNET	FREDNET	24-Jan-03	15-May-04	
MEDI	EUREF	SOPAC	1-Jan-97	18-Jun-05	
MPRA	FREDNET	FREDNET	9-Aug-02	19-May-04	
OBE2	EUREF	SOPAC	5-Aug-01	15-Jun-05	
OBER	EUREF	SOPAC	28-Aug-97	3-Aug-01	Replaced by OBE2
OBET	IGS	SOPAC	9-Jun-03	9-May-05	
OSJE	EUREF	SOPAC			Only one file found
PADO	IGS	SOPAC	27-Nov-01	18-Jun-05	
PATK	EUREF	SOPAC	17-Oct-98	29-Mar-04	
PFAN	EUREF	SOPAC	26-Apr-98	18-Jun-05	
RTMN	EUREF	SOPAC	1-Oct-99	28-Mar-04	
SBGZ	EUREF	SOPAC	23-Dec-98	18-Jun-05	
SFEL	Venice	SOPAC	18-Jul-01	18-Jun-05	
STPO	EUREF	SOPAC	27-Jun-99	29-Mar-04	
TREP	Venice	SOPAC	23-Nov-04	18-Jun-05	
TRIE	FREDNET	FREDNET	8-Feb-03	19-May-04	
UDIN	FREDNET	FREDNET	13-Jun-02	19-May-04	
UPAD	EUREF	SOPAC	1-Jan-97	21-Nov-01	Replaced by PADO
VENE	EUREF	SOPAC	10-Feb-97	18-Jun-05	
VOLT	Venice	SOPAC	23-Jul-01	18-Jun-05	
WETB	*	SOPAC			Not found in Archive
WETM	*	SOPAC			Not found in Archive
WETT	EUREF	SOPAC	1-Jan-97	2-Feb-97	Replaced by WTZR
WTZA	EUREF	SOPAC	21-Nov-99	18-Jun-05	WTZ* and WET* sites co-located
WTZJ	IGS	SOPAC	10-Jun-02	18-Jun-05	
WTZR	EUREF	SOPAC	1-Jan-97	3-May-05	
WTZT	IGS	SOPAC	16-Apr-98	17-May-05	
WTZZ	IGS	SOPAC	10-Jun-02	3-May-05	
ZIMM	EUREF	SOPAC	1-Jan-97	18-Jun-05	
ZOUF	FREDNET	SOPAC	15-May-03	18-Jun-05	

Table 6: Existing Continuous GPS Networks

Location	Agency	Number of Sites
N. Italy	INGV	8
Europe	EUREF	173 throughout Europe and N. Africa
Central Europe	CEGRN	31 (some overlap with EUREF)
Venice Lagoon Region	SOPAC	5 (VENE, CAVA, SFEL, VOLT)
Fabriano	RETREAT	1 ELCI

monumented, continuously recording sites. Continuous sites include 36 stations that are within 300 km of the city, 7 of which are within 50 km (UPAD, VENE, PADO, CAVA, SFEL, VOLT, see Table 5). These stations belong to a number of regional or global networks (Table 6). Most of these data are freely available on the Internet through the SOPAC website (http://sopac.ucsd.edu/) and have continuous data time series that vary in length from 1 to 11 years (Table 5). Other continuous or semi-continuous GPS data not archived at SOPAC may be available. Campaign data has been collected across the Adriatic region for tectonic studies (see Table 4) and also in the vicinity of the Venice Lagoon (Strozzi et al., 2003; Carbognin & Tosi, 2003) starting in 1999.

3.5.3 Interferometric Synthetic Aperture Radar

The Interferometric Synthetic Aperture Radar (InSAR) technique compares the phase information between two radar snapshots of the surface of the Earth. Differences in the phase can be related to range change between the surface and satellite along the line between them. A significant advantage of InSAR imagery is its high spatial resolution and blanket coverage over the radar scene, which is approximately 100 km wide. Disadvantages of InSAR include its sparse temporal resolution, which is limited by the frequency of passage of the satellite over the region of interest. Also, the radar scattering characteristics of the surface are not always favorable to coherent changes in phase from scene to scene, which can cause parts of an image to be unresolved. Successfully combining pairs of radar scenes also requires precise control of the satellite orbits to achieve small baselines between successive satellite passes.

Successful generation of InSAR images has been achieved from 6 scenes that include the city of Venice (Strozzi et al., 2001, 2003). A large fraction of the surface area of the interferograms is incoherent or unusable, most likely because the surface cover is composed of vegetation and/or used for agriculture which can alter the land surface between radar acquisitions. However, where coherence is achieved, the InSAR results characterize the pattern and quantify the subsidence rates surrounding and on the littorals of the Lagoon. Subsidence rates of ~ 1 mm/yr in Venice and ~ 3 to 5 mm/yr to the north and south of the Lagoon are in agreement with leveling results (Carbognin et al., 2004). Much more area is imaged using InSAR than is with leveling, however, indicating that InSAR is a desirable tool for imaging the regional subsidence around Venice.

The persistent scattering method offers an incremental benefit to the InSAR method by identifying pixels within the radar images which have exceptionally stable coherence from scene to scene (Ferretti et al., 2000, 2001). Compared to conventional InSAR, this method has the ability to track a fewer number of pixels, but is typically successful for a greater number of scenes, improving the temporal resolution. Also coherence is maintained for some points where conventional InSAR fails, resulting in an overall improvement of spatial coverage. This method has been implemented on the same data that were used to generate the other InSAR results, giving results that had overall better spatial coverage in some areas (Strozzi et al., 2003).

N	Author	Model	N_0	d	η_u	η_l
P1	MM	120_1_2	256	120	1.00	2.00
P2	MM	120_1_475	256	120	1.00	4.75
P3	MM	12011.mn	128	120	1.00	1.00
P4	MM	12012.mn	128	120	1.00	2.00
P5	MM	12015.mn	128	120	1.00	5.00
P6	MM	120110.mn	128	120	1.00	10.00
P7	MM	120p32.mn	128	120	0.30	2.00
P8	MM	120p52.mn	128	120	0.50	2.00
P9	MM	7112.mn	128	71	1.00	2.00
P10	MM	9612.mn	128	96	1.00	2.00
P11	P	VM2				
P12	P	VM4				
P13	S	S1				

Table 7: Predictions of the present-day LSL fingerprint due to post-glacial rebound

Predictions are from Mitrovica (1999, 2001, personal communication) as well the SBL web page. N_0: Cut-off degree for spherical harmonic expansion; d: is the lithospheric thickness in units of km; η_u: is the upper mantle viscosity in units of 10^{21} Pas; η_l: is the lower mantle viscosity in units of 10^{21} Pas. Ice history is for all predictions according to ICE-3G. The authors are indicated by MM: Mitrovica/Milne, P: Peltier, S: Spada. For details on the computation see, for example, Milne et al. (1999).

3.6 Model predictions of forcing factors

3.6.1 Predictions of atmospherically forced sea level

The meteorological contribution to inter-decadal sea-level trends has been quantified for the period 1958-1991 by the EC funded HIPOCAS project (Guedes Soares et al., 2002). As part of this project a barotropic version of the HAMburg Shelf Circulation Model (HAMSOM) was run over the domain 30°N to 47°N and 12°W to 35°E, which includes the Mediterranean Sea and the eastern sector of the North Atlantic ocean (Alvarez-Fanjul et al., 1997). The HAMSOM model is routinely operated by Puertos del Estado as part of the Nivmar sea-level forecast system (Álvarez-Fanjul et al., 2001), and has a resolution of $15' \times 10'$. The atmospheric forcing of the model consisted of the downscaled atmospheric pressure and wind fields produced by the atmospheric model REMO (Sotillo et al., 2005) on the basis of the reanalysis fields of the Climate Diagnostics Centre (CDC-NOAA-CIRES). The Strait of Gibraltar was represented by one grid point but the depth of the particular grid point was modified to 160 m in order to ensure that the cross section of the Strait was accurately represented (García Lafuente et al., 2002).

3.6.2 Predictions of post-glacial rebound

Geophysical models predict the present-day LSL fingerprint of the post-glacial rebound signal (PGS) fairly well (for a review, see e.g., Peltier, 1998). In order to estimate the effect of the uncertainties of the predicted PGS fingerprint in LSL, we use a suite of models to predict the PGS trend in the Upper Adriatic and to assess the uncertainties in these predictions (Table 7). In Figure 13, two PGS predictions are compared. Both predictions display maximum negative contributions close to the centers of the former ice loads in Fenoscandia and North America. However, there are also marked differences, which are solely due to different solid earth models used for the two examples. Largest differences are found in the Arctic and around Antarctica.

Moreover, as pointed out by Stocchi et al. (2005), all models suffer from a misrepresentation of the alpine ice sheet during the last ice age. This has a particularly large effect on sea level along the northern coast of the Mediterranean, which is in the near field of this former ice sheets.

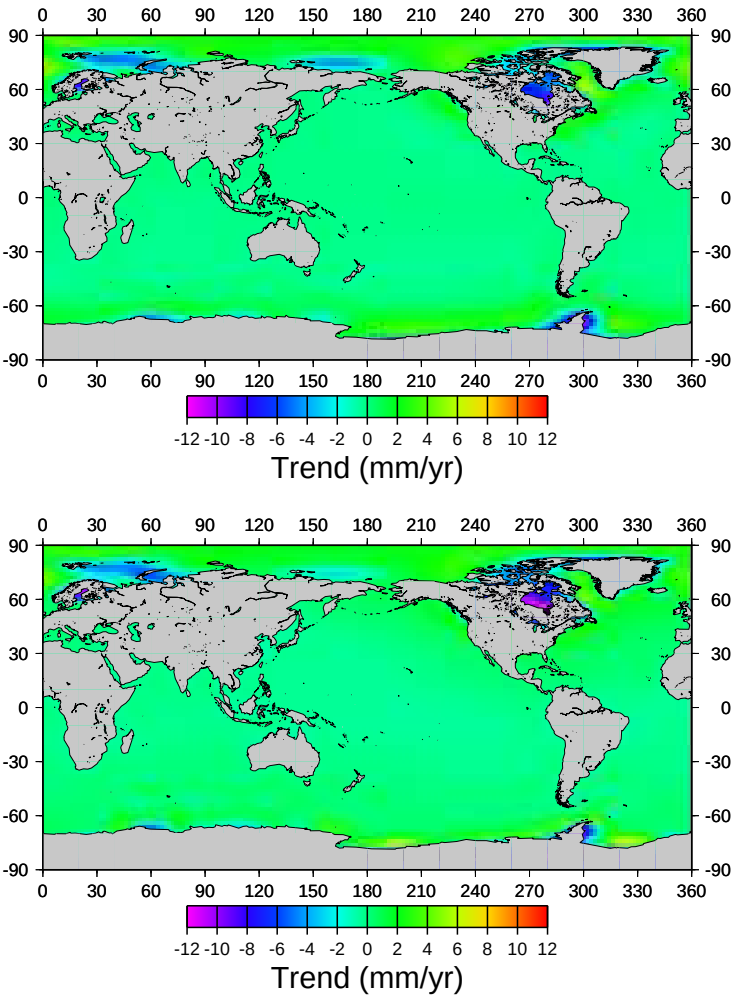

Figure 13: Spatial fingerprint of the present-day post-glacial signal in sea-level trends.
Left panel: predictions based on model P1; right panel: model P6, see Table 7.

3.6.3 Predictions of contributions from the large ice sheets

The uncertainties in the mass changes of the two largest ice sheets, namely Antarctica and Greenland, over the last five decades are too large to base the LSL fingerprints of these ice sheets on observations. Therefore, Plag & Jüttner (2001); Plag (2006a) determined for each ice sheet a fingerprint function for a constant, unit trend over the complete area of the ice sheet. These fingerprints were determined by solving the static sea-level equation derived by Farrell & Clark (1976). For time scales of up to a century, the sea-level equation can be treated elastically, and in this case, the equation can be solved analytically, resulting in the fingerprints shown in Figure 14. The Antarctic fingerprint has a distinct zonal component, while the Greenland fingerprint shows more variations with longitude, particularly in the northern hemisphere. Plag & Jüttner (2001) also determined the fingerprint for an average mass change in the ice cover of Iceland. However, this fingerprint is found to be highly correlated with the Greenland fingerprint and cannot be distinguished from the latter one on the basis of the LSL observations available.

The changes in LSL due to changes in the Greenland and Antarctic ice sheets can be computed using the respective fingerprint functions described in Plag & Jüttner (2001). From these fingerprints, we get scaling factors of 1.4 and -0.2 between the global average LSL change due to changes in the Antarctic and Greenland ice sheets, respectively, and the LSL changes in the upper Adriatic. However, it is pointed out here that the fingerprint functions strongly depend on the solid Earth model. The model used by Plag & Jüttner (2001) and Plag (2006a) is a spherically symmetric model, which in

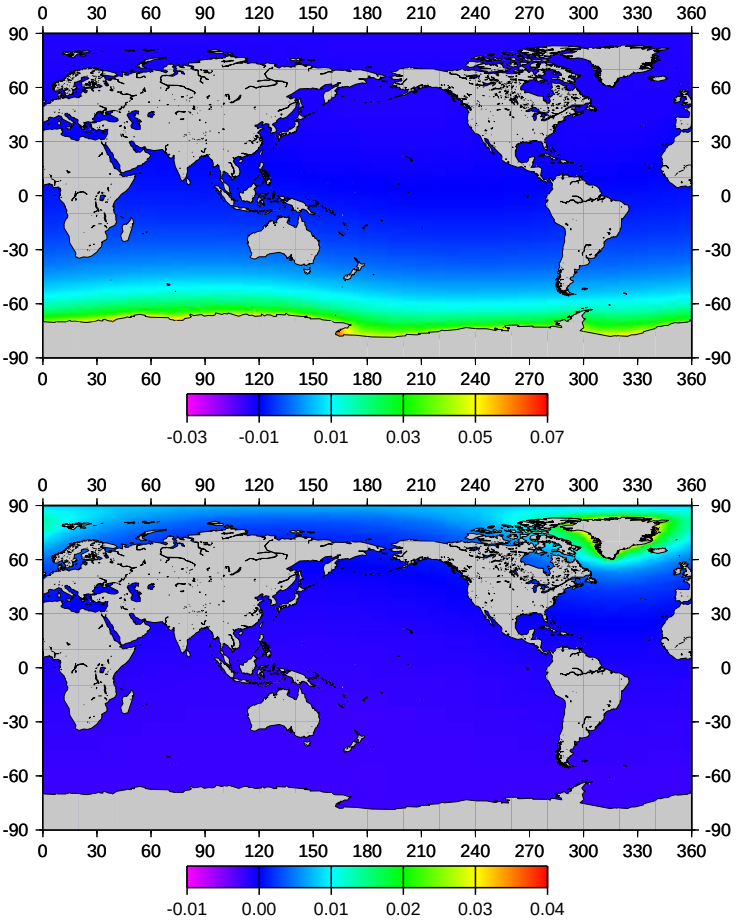

Figure 14: Spatial fingerprints of changes in the mass of the large ice sheets in LSL trends.
Upper panel: fingerprint of the Antarctic ice sheet; lower panel: fingerprint of the Greenland ice sheet. The fingerprints are based on a solution of the static sea-level equation for degree and order 72. The fingerprints are given for a unit mass change and have the same dimension as the unit mass change.

particular does not take into account lateral heterogeneities in the upper layers of the mantle and the crust. Therefore, the scaling factors have to be associated with an uncertainty which is estimated here (based on a sensitivity study using different solid Earth models) to be 1.4 ± 0.4 and -0.2 ± 0.4. Thus, a deloading of Greenland through ice melt could in fact slightly lower the sea level in the Mediterranean and the Adriatic, while a deloading of Antarctica would lead to a larger than average sea level rise in the Mediterranean and the Adriatic. These effects result from the fact that the Adriatic is in the far field of Antarctica and thus will experience a maximum sea-level rise for any melting, while with respect to the Greenland ice sheet, the Adriatic is in the intermediate field and thus experiences a strongly reduced (negative) effect from melting.

3.6.4 Predictions of other contributions due to mass exchange

Contributions from changes in continental glaciers result mainly from mass changes in small-scale sources distributed over the global land area. The resulting LSL fingerprint will be dominated by small spatial scales in the near-field of the individual glaciers and fairly constant amplitudes over most of the ocean surface.

Since the Upper Adriatic is located in the near field to the glaciers in the Alps, the melting of these glaciers is expected to induce a significant negative sea-level trend in the Upper Adriatic, which is due to a combination of a fall in the geoid due to the mass removal and an uplift of the area due to elastic rebound. Studies in the vicinity of glaciers in Alaska (Tamisiea et al., 2005) confirm this

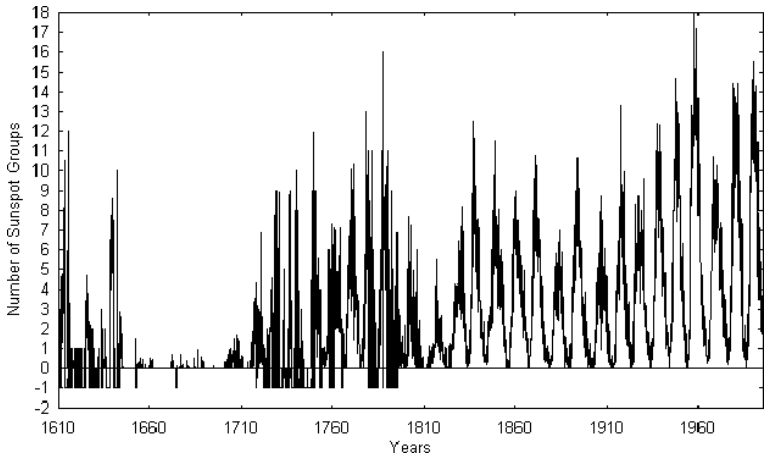

Figure 15: Original time series of sunspot groups.
Positive numbers are SGN sunspot group numbers and values of -1 indicate gaps. From Serre & Nesme-Ribes (2000).

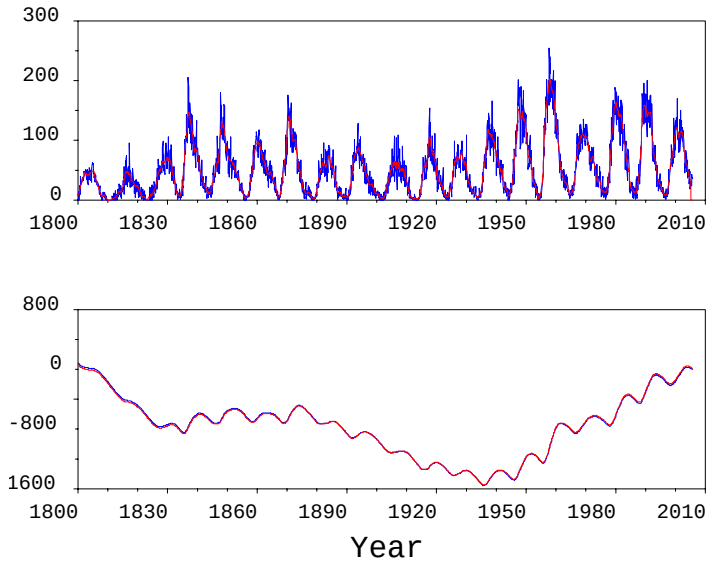

Figure 16: Monthly sunspot numbers.
Data are taken from the World Data Center for the Sunspot Index, Royal Observatory of Belgium (http://sidc.oma.be/index.php3). Upper diagram shows the monthly sunspot numbers, the lower diagram the integrated numbers using eq. (17).

understanding. However, the current mass balance models of the glaciers in the Alps are not sufficient to carry out detailed computations of this effect.

The sea-level fingerprint of the continental hydrosphere (excluding glaciers) is expected to be dominated by small spatial wave length in the vicinity of the coasts and nearly constant amplitudes in the far-field. The only exception may be due to trends in the average snow load, thawing of permafrost, and regional deforestation, which may induce considerable large scale patterns. Currently, there is no sufficient model available to account for these contributions comprehensively. Consequently, we have to neglect any near-field contribution from glaciers and the continental hydrosphere. The far field contribution can be estimated on the basis of the overall mass balance of the ocean.

It is pointed out that eq. (1) implicitly accounts for changes in the ocean basin induced by plate tectonics, sedimentation, subsidence, etc.

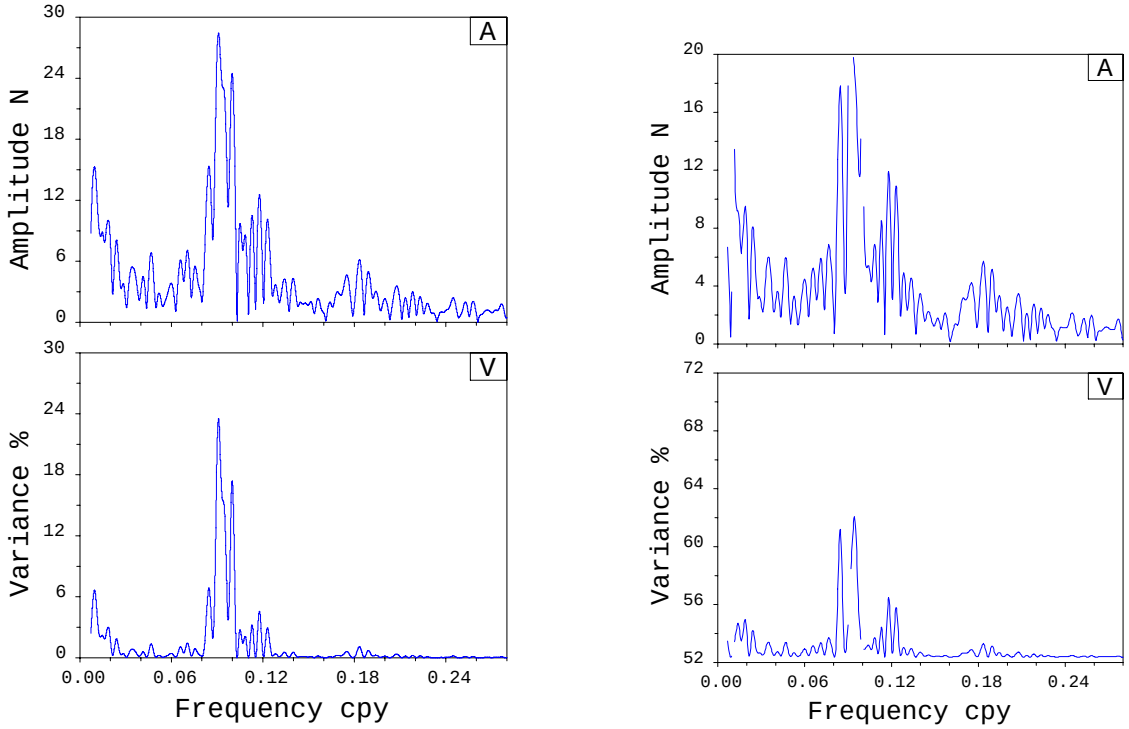

Figure 17: Spectrum of sunspot numbers.

Spectra are calculated as variance spectrum (Plag, 1988). Left: Variance spectrum without fixed harmonic constituents. Right: variance spectrum including three fixed harmonic constituents with periods of 11.0000 years, 10.0135 years and 95.877 years.

3.7 Proxy data

3.7.1 Sun spot observations

The solar cycles have a magnetic origin and manifest themselves as sunspots emerging at the solar surface. They are the result of a dynamo process that converts kinetic energy into magnetic energy taking place at the bottom of the convective zone (0.7 R_s or below). The best indicator of solar activity is provided by the sunspots, which are the seat of an intense magnetic activity. They have been observed with the naked-eye as early as two centuries B.C. in China but since the telescope era (since 1609), they have been carefully monitored. During the mid-19$^{\text{th}}$ century it was discovered that the sunspot activity followed a roughly 11 yr cycle. Shortly after, Wolf introduced an empirical indicator, that is, the sunspot number, that is now used as a solar activity index. The Wolf sunspot number (WSN) is defined as

$$WSN = 10 * SGN + ISN + f_c \tag{20}$$

where SGN is the number of sunspot groups, ISN the number of individual sunspots and f_c a corrective factor for each observer. However, Wolf adopted several simplifications: smoothing monthly fluctuations of sunspots, not using all available archives prior to 1848 and completion of observational gaps by using aurora events as a sunspot index which dangerously mixed two time series of different origins.

Recently, a new time series of sunspot numbers has been created (see Hoyt et al., 1994, and the reference therein), based on a reexamination of the whole archives. The treatment by Hoyt and co-workers differs from the Wolf 's treatment in that they used sunspot group numbers rather than individual sunspots. The new time-series is homogeneous leaving out aurora data and it contains fewer gaps with more than 350,000 observations obtained from more than 350 observers. Also, they

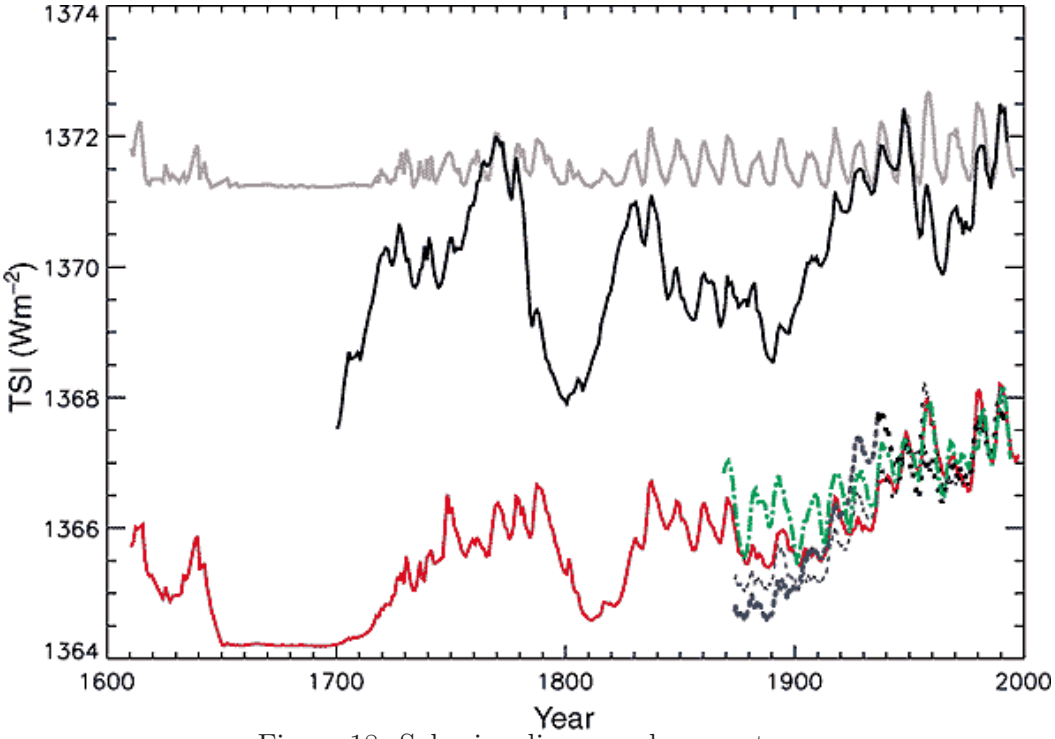

Figure 18: Solar irradiance and sunspots.

Solid red curve: reconstructions of total solar irradiance (TSI) by Lean et al. (1995); solid black curve: TSI by Hoyt & Schatten (1993), data updated to 1999 by Ramaswamy et al. (2001); dotted blue curve: TSI by Solanki & Fligge (1998), heavy dash-dot green: TSI by Lockwood & Stamper (1999), grey curve: group sunspot numbers (Hoyt & Schatten, 1998) scaled to Nimbus-7 observations for 1979 to 1993.

used a new approach by normalizing each set of data coming from different observers with the one they considered the best set, that is, the Royal Greenwich Observatory (RGO) data (1874-1976). The normalizing process can be even more complicated depending on the set considered (see their papers for details). The new SGN time-series is thus more objective, homogeneous and longer than the WSN time-series. A good match between the two time-series is obtained for the well-documented period 1874-1991 after an appropriate scaling (see details in Hoyt et al., 1994) while most differences are found prior to 1848. The Hoyt et al. time series is shown in Figure 15. The plot shows that before approximately 1800 there are numerous gaps in the record.

The leading sunspot of an individual magnetic area lasts longer than the following sunspots with several days up to one (or exceptionally two) solar rotations for the leading one and usually less than one rotation for the following one. Therefore, the lifetime of a sunspot group as a whole, is of the order of a solar rotation. Consequently, monthly means of the SGN time-series seem to be a good compromise between daily measures and yearly means that do not accurately represent the shape of a solar cycle.

For this study, we have down-loaded the monthly sunspot cycle numbers from the World Data Center for the Sunspot Index hosted by the Royal Observatory of Belgium (http://sidc.oma.be/index.php3). The unfiltered and filtered time series are shown in Figure 16. Integrating the deviation from the mean SSN level reveals an interesting fact, namely that since 1800, the SSN had four different periods with different mean levels, namely approximately from 1800 to 1830, 1830 to 1890, 1890 to 1960, and 1960 to present. This is deduced from the nearly linear segments in the integrated time series, which result from an integration over a nearly constant non-zero offset from the mean.

The spectrum of the SSN time series is dominated by the broad peak around 11 years (Figure 17).

By now, it is widely accepted that the main cycle has a period close to 11.0 years, and most of the temporal variations described by, for example, Friis-Christensen, E., Lassen, K. (1991) are attributed to problems with data quality in earlier parts of the record as well as the methodology used to create the original WSN series (Serre & Nesme-Ribes, 2000). The peak actually consists of at least two constituents, namely a major one with a period of exactly 11.000 years and a minor one with a period of very close to 10 years. Moreover, the spectrum shows a peak close to a period of 100 years. Including the two main constituents in the 11 year broad peak in the model function fro the variance spectrum, this peaks turns out to have a period of 95.877 years. Finally, including these three constituents in the model function results in a spectrum showing a low number of additional peaks, which indicate that the SSN series is a composite of a few nearly harmonic constituents. The residual peaks close to the 11 and 10 years peaks may indicate slight deviations of these constituents from purely harmonic oscillations, while the peaks around 0.12 cpy (with the main peak having a period of 8.47 years) most likely constitutes a separate oscillation. It is also interesting to note that the three main constituents account for more than 52% of the total variance of the SSN time series.

A relevant question is how the sunspot numbers are related to climate. This question is under intense scientific discussion without a clear answer. Recently, progress has been made in respect to relating the sunspot numbers to *total solar irradiance* (TSI) (see Ramaswamy et al., 2001, for a detailed discussion). According to the TAR, the change in radiative forcing due to total solar irradiance is estimated to be $+0.3 \pm 0.2$ Wm^{-2} for the period from 1700 to present. The large uncertainty and the low *Level of scientific understanding* (LOSU) assigned to this climate forcing in the TAR is due to the uncertainty in the past TSI (see Figure 18). Satellite observations show that the variations in TSI over a full sunspot cycle is about 0.08% while long-period variations may be considerably larger. Moreover, the main variations are in the ultraviolet region of the spectrum, and GCM studies show that considering the spectral distribution of the the variations is likely to increase the climate effects of TSI variations (see the discussion and references in Ramaswamy et al., 2001). The TAR discusses other mechanisms for amplification of solar forcing, including cosmic rays, which are inversely correlated with the SSN, but concludes that these mechanism are not well established. This is emphasized by Schlesinger & Ramankutty (1992) and Kelly & Wigley (1992), who study the contribution of solar forcing to the global warming over the last 100 years and reach conflicting conclusions, depending on the assumed sensitivity of the climate system to solar forcing.

3.7.2 Atmosphere-ocean oscillation indices

The NAO dominates atmospheric variability over the North Atlantic and Europe especially in winter (Hurrell, 1995). The NAO is usually measured as the atmospheric pressure difference between the Icelandic Low and the Azores High. The effects of the NAO on various meteorological parameters have been well established (Hurrell, 1995; Osborn et al., 1999), with high NAO winters being wetter, warmer and windier over northern Europe and the north Atlantic. In addition to its dominance of interannual variability, a multi-decadal positive trend occurred in the NAO index from the 1960s onwards, raising the possibility that climate change might be linked with changes in the NAO (Hurrell, 1995), a possibility that remains uncertain (Osborn et al., 1999; Osborn, 2004). The monthly mean values of the NAO are shown in Figure 20 together with the Mediterranean Oscillation Index (MOI, see below).

The effect of continuous changes in atmospheric parameters on sea-level trends have been known for long. For example wind and atmospheric pressure variations have been found to alter significantly the sea-level trend estimates even for measurements spanning half a century (see for example Tsimplis et al., 1994; Marcos et al., 2005).

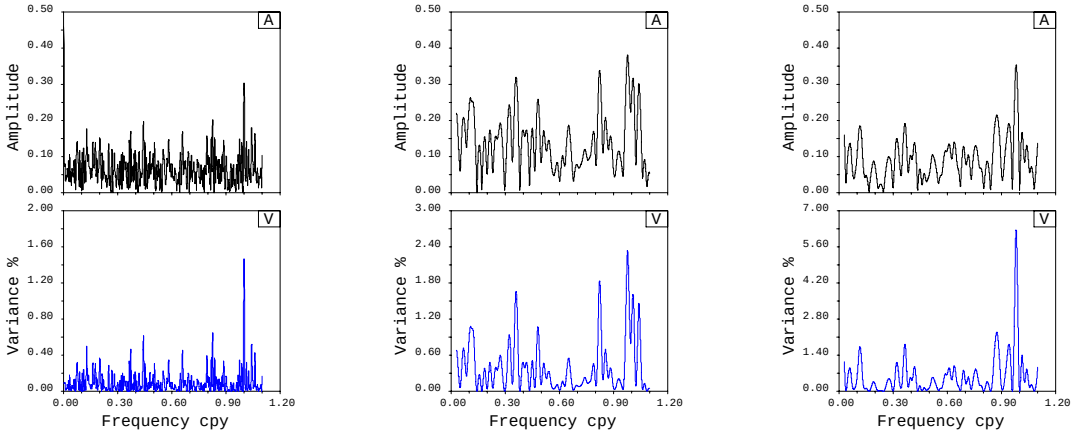

Figure 19: Spectra of NAO index and MO index.

Left diagrams are for the full NAO index series. The middle and right diagrams are for the NAO index and MO index, respectively, restricted to data after 1960.

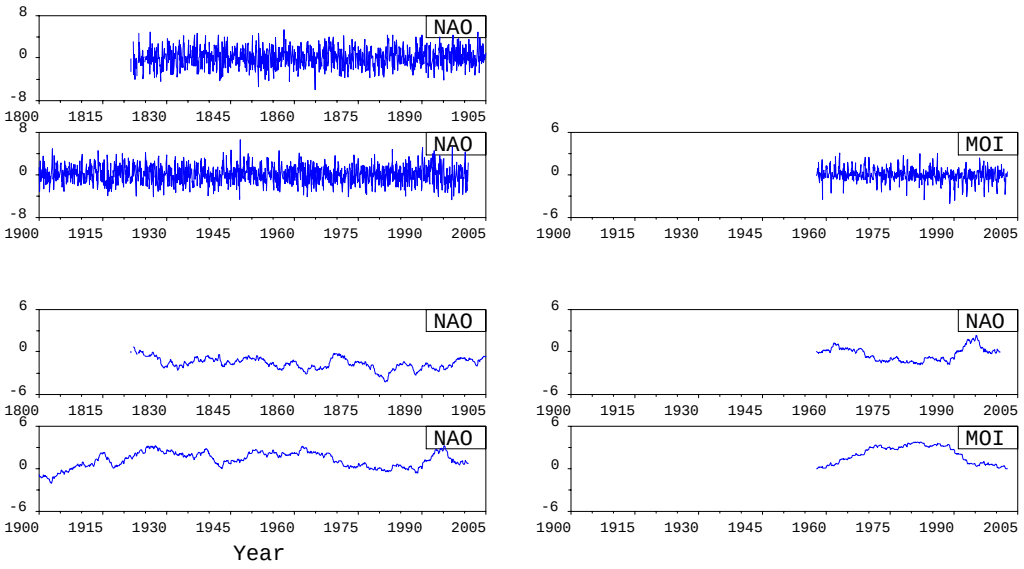

Figure 20: NAO and MO Index.

The upper diagrams show the NAO index on the left and the MO Index on the right. The lower diagrams show the time series of deviations from the mean, which have been integrated using eq. (17). The right diagram above the integrated MOI shows the NAO integrated from 1960 for comparison with the integrated MOI.

Moreover, several studies (Tsimplis & Josey, 2001; Woolf et al., 2003; Wakelin et al., 2003; Yan et al., 2004; Tsimplis et al., 2005d) have demonstrated the influence of the NAO on sea-level variability around Europe. Woolf et al. (2003) have shown that the a linear relationship between the winter sea-level anomalies and the winter NAO Index can be used to explain most of the variability in the North Sea, the Mediterranean and the eastern parts of the North Atlantic. However, the NAO affects several forcing parameters and the dominant one varies from region to region. In brief, high NAO state causes increased sea levels at the North Sea and the Baltic (Wakelin et al., 2003; Yan et al., 2004; Tsimplis et al., 2005d) mainly due to increased westerlies but also because of water temperature increases (Tsimplis et al., 2005c) while at the southern Atlantic coasts and the Mediterranean Sea

increased atmospheric pressure during winter causes reductions in sea level (Tsimplis & Josey, 2001) with additional effects caused by cooling of the upper waters and the $E - P$ balance (Tsimplis & Rixen, 2002; Tsimplis & Josey, 2001). For the Black Sea the impact of the NAO is linked to sea level in spring through variations of the river outflow but a small effect is also detectable in winter (Stanev & Peneva, 2002; Tsimplis et al., 2004).

The Mediterranean Oscillation Index (MOI) is defined as the pressure difference between mid northern Atlantic and southeastern Mediterranean(Grbec et al., 2003; Supic et al., 2004). The index is based on the Principal Component Analysis (PCA) of the atmospheric pressure fields. Tsimplis & Shaw (2005) have found that it correlates better than the NAO with the Mediterranean Sea level. It is not clear why this is so. It could be due to the fact that the PCA takes into account the shifting of the center of actions in the Atlantic, while the NAO based on station data does not. The MOI is available only for a restricted time interval (see Figure 20), while the NAO has available reconstructions for many years.

The spectrum of the long NAO Index record is dominated by an annual constituent, which, however, only accounts for slightly more than 1% of the total variance (Figure 19). Restricting the record to the interval 1960 to present reveals a few interannual signals with the most prominent ones at periods of 1.22 years and 2.78 years. The spectrum of the MO Index is rather similar to that of the NAO Index restricted to data after 1960 (Figure 19). The annual peak is a bit larger and the most prominent interannual peaks are at 1.22 years and 2.74 years.

Integrating the time series of the NAO index and the MOI reveals that the MOI contains a negative trend in the time window from 1960 to 2002, while NAO exhibits a positive trend in the same interval (Figure 20). On longer time scales, the NAO is dominated by century time scale variations with a minimum deviation from the mean around 1880 and a maximum around 1930. A minor maximum is reached around 1960 and followed by a minimum in the 1980s. The obvious anti-correlation of the integrated NAO Index and MOI on long time scales is an interesting feature not observed so far.

3.8 Overview

Table 8 gives an overview of the available observations, model predictions, and proxies discussed in this section and summarizes their main properties. Sea-level observations useful for the present study originate from tide gauges, and this emphasizes their crucial role for assessing changes in LSL. Observations and model predictions of the forcing factors are either directly related to LSL or they are given in a global, geocentric reference frame. In order to separate the vertical land motion from the other forcing factors, this factor therefore needs to be given in a geocentric reference frame, too. Consequently, the main observational source for vertical land motion is GPS, which allows to determine the vertical land motion in a geocentric reference frame.

Table 8: Overview of the sea-level related observations.

Param.	Origin	Sampling Interval	Comment	Main Signals
			LSL and sea surface	
LSL	CVN, and PSMSL	hourly and monthly	Cover up to 100 years, data quality variable in time,	Dominant signals are tides, seasonal cycle, 15-17 years signal, trends
Sea surface	Satellite altimetry	10 days or longer	Short time series of order 10 years	High spatial variability on interannual time scales
			Local meteorology	
Air pressure	CVN	subdaily	100 years, inhomogeneous in time, homogeneous since 1960	Small seasonal signal, positive trend over the last 40 years.
Temperature	CVN	subdaily	100 years, inhomogeneous in time, homogeneous since 1960	Dominated by seasonal signal, very minor positive trend over the last 40 years.
Wind	CVN	hourly	about 20 years	Interannual variability, positive trend in east component, negative trend in north component.
Precipitation	CVN	daily	100 years, temporal inhomogeneities due to relocation of institute	No dominant harmonic signals, no discernible trend in the last 40 years.
			Global meteorology	
Air pressure, air temperature, wind	era40, ECMWF	6 hours	1957 - 2002, spatial resolution 2.5×2.5 degrees, temporal inhomogeneous due to change in observations	Agreement with local observations very good for air pressure and temperature but less for wind.
			Oceanographic data	
Temperature and salinity	Medar	Episodic	Large temporal inhomogeneity in available observations, usable after approximately 1950	
steric LSL	Levitus et al.	annual	1958 to 2002, result dependent on depths interval integrated	Interannual to decadal variability, on average negative trend in the upper Adriatic
steric LSL	Ishii et al.	monthly	1958 to 2002, only available for integration from 500 m depths	Seasonal, interannual and decadal variability, on average very small positive trend in the upper Adriatic.
			Vertical land motion	
relative	Leveling	decades	Several campaigns	Most importantly, a relative subsidence of Venice and the Lagoon with respect the alpine foothills.
relative	InSAR	episodic	Several interferograms, though with large gaps	Interferograms show subsidence of Venice relative to larger surroundings in agreement with leveling.
geocentric	GPS	daily	More than 30 stations within 300 km with useful records extending up to ten eight	

Table 8: continued.

Param.	Origin	Sampling Interval	Comment	Main Signals
		Model predictions of forcing factors		
atmosphere	HAMSON model, based on NCEP	daily	44 years from 1958, model resolution $15' \times 10'$	
Post-glacial rebound	geophys. models	secular	Model predictions depend on earth model and ice history	Trend of the order of ± 0.3 mm/yr, with considerable model differences.
Ice sheet melting	geophys. models	secular	Model predictions depend on earth model and inversion for ice melt	
Other mass contributions	geophys. models	n/a	Model predictions rather uncertain due to large uncertainties in mass changes in the terrestrial hydrosphere and cryosphere.	
		Proxies		
Sunspot numbers	World Data Center for Sunspot Index	monthly	Observations start in 16010, with high quality time series since approx. 1800	Dominated by a broad peak at approximately. 11 years. Different levels can be separated with highest average level since about 1940.
NAO Index		Monthly	Since approx. 1820.	Dominated by a seasonal cycle and a few interannual signals, particularly over the last 40 years. Some multi-decadal variability, a slight positive trend of the last 40 years. Relation to TSI and climate not well understood, particularly for longer time scales.
MO Index		Monthly	Since 1957.	Dominated by a seasonal cycle, minor interannual signals, slight positive trend.

4 Observed sea-level variations

4.1 Introduction

LSL variations as observed by tide gauges display variations on a wide range of temporal scales ranging from sudden changes due to earthquakes, over seiches and tides at the high-frequency end, intra-seasonal and seasonal oscillations, interannual and decadal variations to century scale secular changes at the low frequency end captured by longest tide gauge records (Chelton & Enfield, 1986, see, e.g.,). All of these variations are highly space-dependent, and in each oceanic region, different temporal scales can dominate. In the following sections, we will discuss the different phenomena and time scales separately. In particular, we will address tides, seasonal variations, interannual and decadal variations, secular trends and extreme values due to meteorological forcings.

4.2 Tides

The tides in the Mediterranean Sea are generally small, though in the northern Adriatic Sea there is strong amplification. A general description is given in Defant (1961). He gives values for the M_2 principal lunar semidiurnal constituent amplitude of 0.235 m (at Malamoco), and of 0.183 m for the diurnal amplitude K_1. There is a well developed amphidromic system for semidiurnal tides, and a standing wave, but without an amphidrome because of the longer wavelengths, for diurnal tides.

The variance spectrum computed from a typical year of hourly tide gauge recordings at Trieste and Venice (Figure 21) show amplitudes of the order 25 cm and 19 cm for the main semi-diurnal (M_2) and diurnal (K_1) constituents, respectively, with the difference between the two sites being small. The amplitudes of the main tidal constituents at the two locations appear to be increasing over time, and the difference in amplitude between 1970 and 2000 is of the order of 2-3 cm for M_2 (Figure 21). This confirms qualitatively the results reported by Pirazzoli (1987).

The spectrum of the hourly differences between Venice and Trieste (Figure 22) reveals that the difference for the main semi-diurnal and diurnal constituents are 4 cm and 1.2 cm, respectively. The diurnal and semi-diurnal constituents are larger in Trieste and Venice, respectively (see Figure 21). It is interesting to note that these differences appear to be stable in time. Thus, the increase in the tidal constituents appears to be spatial homogeneous, which excludes the possibility of the increase being due to an effect at or near to a tide gauges.

For the question of extreme sea levels (see Section 4.7), it is important to know whether the tides are stable over time. Ocean tides depend crucially on the eigenfrequencies of the geometry of the local and global ocean basin (see, e.g., Platzman, 1983, 1984, for a more detailed discussion) and particular those harmonic tidal constituents close to a resonance frequency can change significantly if the resonance frequency changes either due to changes in mean sea level or changes in the local geometry.

The fortnightly and monthly tides (with the main constituents in each band being denoted as Mf and Mm, respectively) are zonal tides. Due to their long periods, they are generally expected to be equilibrium tides (Proudman, 1959). At the latitude of the Northern Adriatic, these tidal constituents have equilibrium amplitudes of the order of 10 mm and 7 mm, respectively (see, e.g., Lisitzin, 1974). The spectrum of the hourly sea-level variations at Venice and Trieste show that only the fortnightly tide is above the noise level (Figure 23). In the fortnightly band, the maximum amplitude is found for a frequency of 2.2280 cpm in both spectra, which is exactly the frequency of Mf in the astronomical potential. The amplitude of Mf is 9.8 mm and 9.3 mm in Venice and Trieste, respectively, and thus in perfect agreement with the expected equilibrium tide. Figure 23 also shows a significant increase of the noise level for periods long than two to three weeks, and this intra-seasonal noise covers the

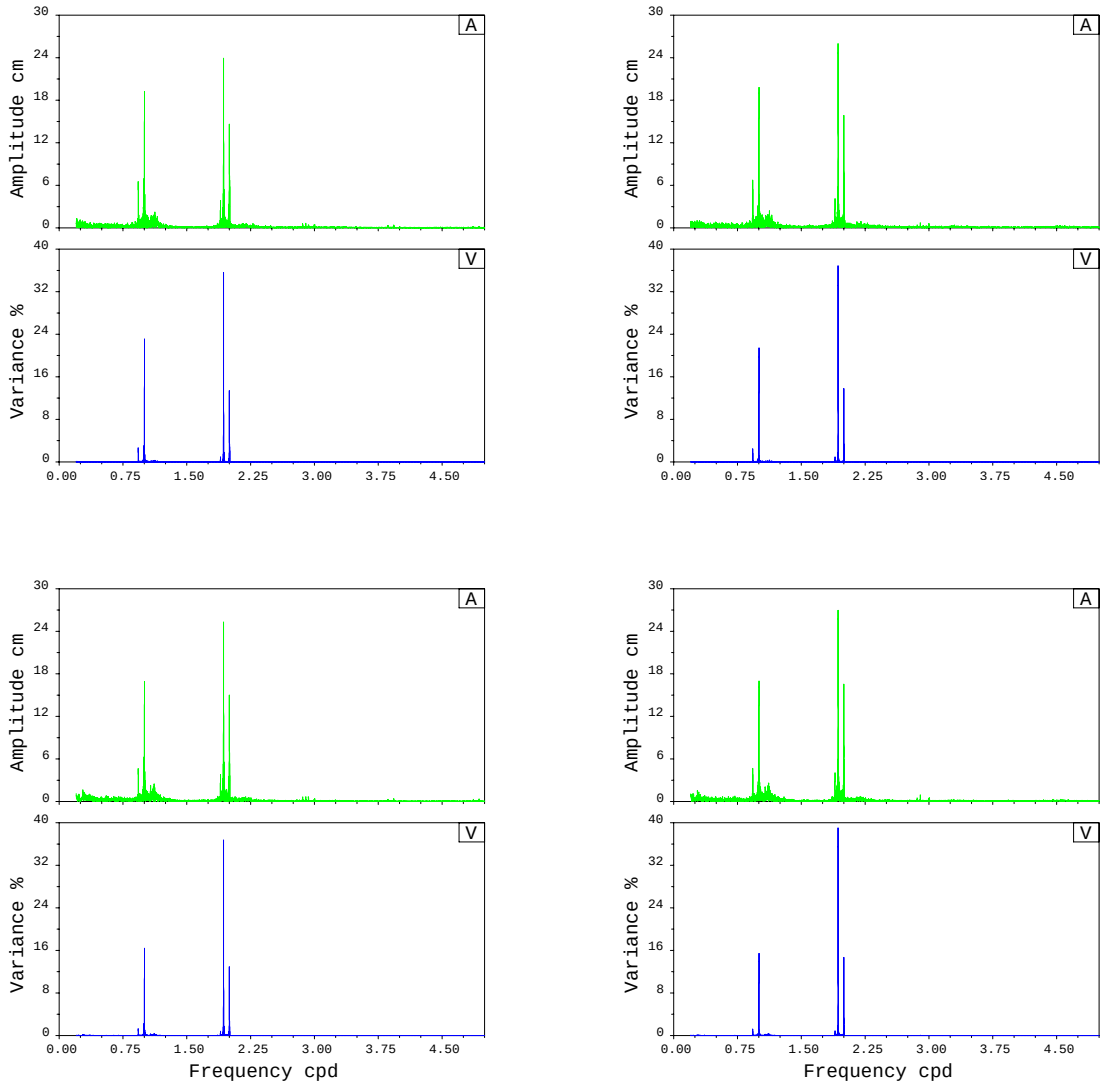

Figure 21: Spectra of the diurnal and semidiurnal tidal band for Venice and Trieste.

The spectra are variance spectra (Plag, 1988) for a full year of data computed with a frequency resolution of 0.00005 cpd. Left: Venice, right: Trieste. Upper diagrams are for 1970, lower for 2000. For each spectrum, the lower diagram shows the variance in % explained by a harmonic constant with the given frequency, and the upper diagram the resulting amplitude in cm.

monthly tidal constituents. Nevertheless, close to the frequency of Mm, which is 1.1047 cpm, a nearly identical peak is found in each of the Venice and Trieste spectra at 1.1039 cpm, with an amplitude of 7.9 mm. Again, this peak is not significantly different from an equilibrium Mm.

The annual and semi-annual astronomical tides are extremely small and at the latitude of the Northern Adriatic, the equilibrium amplitudes are of the order < 1 mm and 3 mm, respectively. Most of the observed annual and semi-annual harmonic sea-level variations are consequently due to climatological and oceanographic forcing.

In the Adriatic, the nodal tide M_N with a period of 18.667 years has an equilibrium amplitude of less than 5 mm. However, the spectra shown in Figure 24 below and the results compiled in Table 10 in Section 4.4 indicate that there is a signal close to the nodal period, which is much larger than the

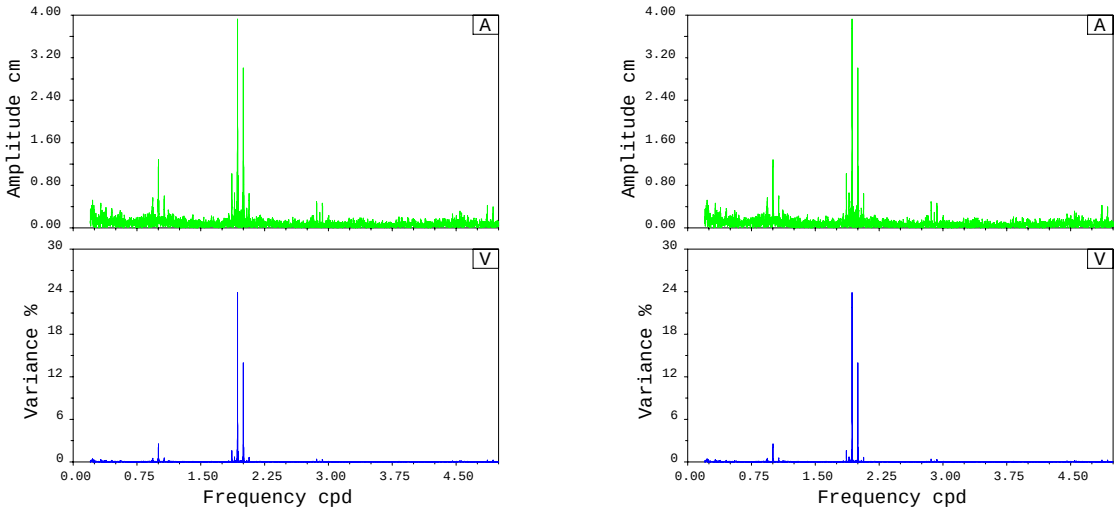

Figure 22: Differences in diurnal and semidiurnal tidal bands between Venice and Trieste.
The spectra are variance spectra (Plag, 1988) computed for the differences of the hourly sea-level values at Venice and Trieste for a full year with a frequency resolution of 0.00005 cpd. Left: for 1970, right: for 2000. For each spectrum, the lower diagram shows the variance in % explained by a harmonic constant with the given frequency, and the upper diagram the resulting amplitude in cm.

Table 9: Long period harmonic signals in sea level in Venice and Trieste.

Tentative Signal	Venice		Trieste	
	Period years	Amplitude cm	Period years	Amplitude cm
Nodal Tide (?)	16.835	3.0	17.271	2.7
Sun spot cycle (?)	8.316	2.4	8.285	1.8
FSO	1.168	1.3	1.168	1.3

equilibrium nodal tide. One possible explanation would be that the nodal tide in the ocean is actually not an equilibrium tide. However, this would be surprising and not consistent with our understanding of ocean dynamics.

Alternatively, the signal close to 18.6 years may not be the nodal tide but rather a signal forced by other factors than the astronomical potential. This option will be further explored in Section 4.5.

In order to study the temporal variations of the tides in the upper Adriatic, a moving tidal analysis should be carried out similar to the methodology discussed in, for example, Baker & Alcock (1983); Plag (1984, 1988). Some work is also suggested in Cecconi et al. (1999). The tidal analysis should not only consider the diurnal and semi-diurnal tidal constituents but also include the main fortnightly and monthly constituents.

4.3 Long-period spectrum

The long-period spectra of the two records in Venice and Trieste (Figure 24) appear to be highly coherent. The spectra are dominated by the semi-annual and annual constituents, which we will discussed in more detail in the next section.

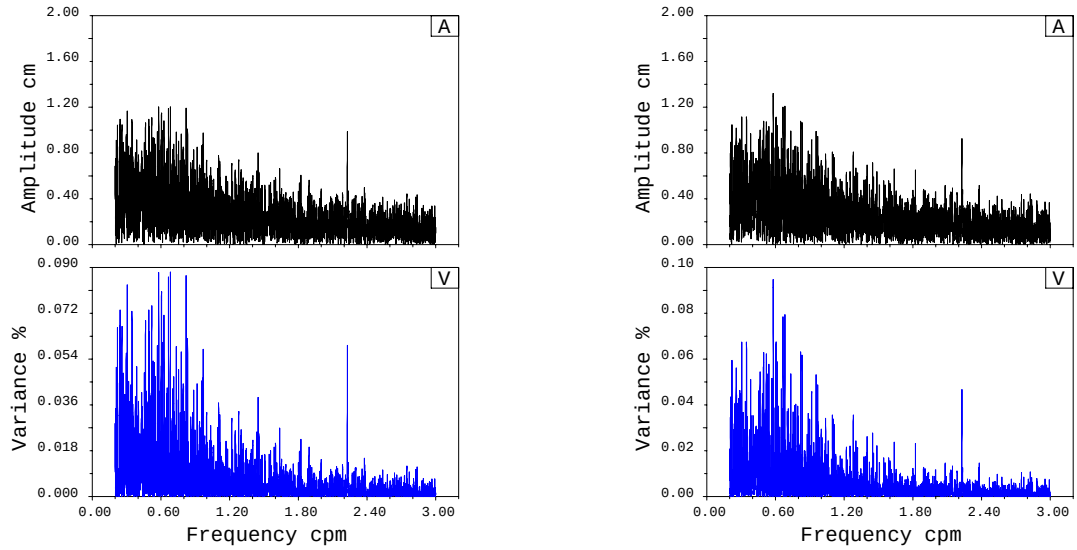

Figure 23: Fortnightly to monthly spectra for Venice and Trieste.

The spectra are variance spectra (Plag, 1988). The spectra are computed using all data given in the interval 1955-2003 and with a frequency resolution of 0.0001 cpm. Left: Venice, right: Trieste. For each spectrum, the lower diagram shows the variance in % explained by a harmonic constant with the given frequency, and the upper diagram the resulting amplitude in cm.

There are also significant peaks in the interannual to decadal part of the long-period spectrum (Table 9). The peak closest to Sa has a period of 1.168 years in the spectra of both records. This is close to the Chandler Wobble period of approximately 1.188 years. However, the difference in period is highly significant. Plag (1997) proposes a *Fourteen to Sixteen Month Oscillation* (FSO) in air pressure as the cause of this signal in sea level.

We do not discuss here in detail the peaks between 2 and 8 years, which were also identified by Plag (1988) in an analysis of the sea level along the Norwegian Coast. In a later step, a more detailed analysis of the long period spectrum should be performed similar to the one performed by Plag (1988) and Plag (1997). However, we point out that these peaks are time-dependent, as is illustrated by the dynamic spectra shown in Figure 25. Thus, in sea level we see a transient signal with a period between 14 and 16 month (0.8 to 0.9 cpy), which is particularly strong over the last 40 years. In air pressure and precipitation, a similar signal is found with nearly identical temporal behavior. In the period band of 4 to 5 years, a transient signal is most pronounced in the first half of the 20^{th} century, while the signal in the band between 15 and 20 years is strongest in the last 20 years of the time window considered.

At the low end of the spectrum, there are two peaks that are of particular interest. The peak close to the period of M_N has a period of approximately 17 years, which is significantly different from the 18.6 years period of the nodal tide. We therefore conclude that this peak is at least partly due to another forcing process.

The peak with a period of approximately 8.3 could be related to characteristic time scales in the NAO or to the sunspot cycle. In order to clarify this, the spectrum of these two proxies for the identical time interval will be compared to the sea-level spectrum.

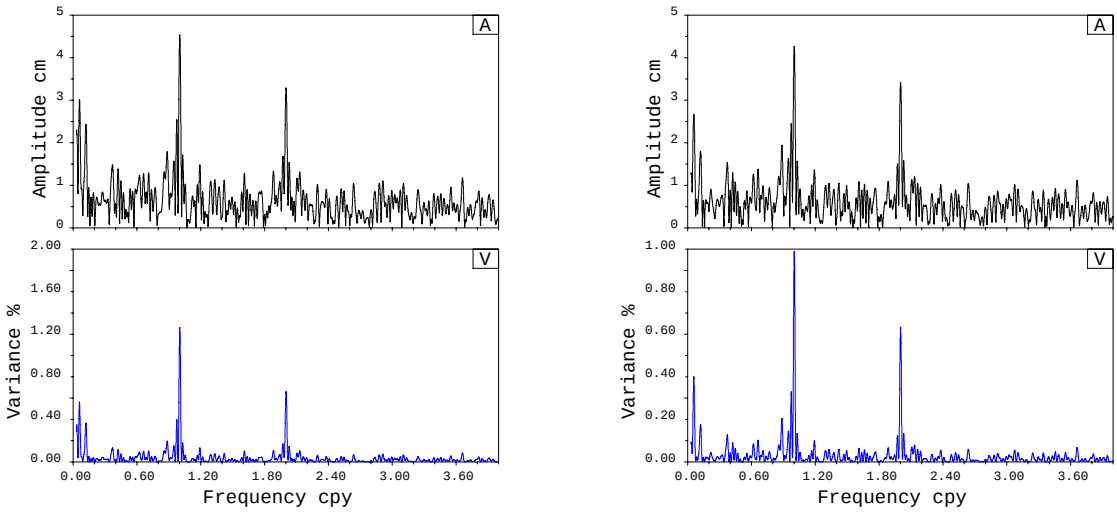

Figure 24: Long-period spectra for Venice and Trieste.

The spectra are variance spectra (Plag, 1988). The spectra are computed using all data given in the interval 1955-2003 and with a frequency resolution of 0.0001 cpy. Left: Venice, right: Trieste. For each spectrum, the lower diagram shows the variance in % explained by a harmonic constant with the given frequency, and the upper diagram the resulting amplitude in cm.

Table 10: Long-period oscillations and trends in the sea level of the Adriatic.

The stations are those currently available in the PSMSL database (see http://www.pol.ac.uk/psmsl/). Only records with more than 240 monthly values have been included (except for Venecia Arsenale). The parameters were determine through a fit of eq. 21 to the records.

Name	**Type**	N	A_{N}	ϕ_{N}	A_{Sa}	ϕ_{Sa}	A_{Ssa}	ϕ_{Ssa}	b
VENEZIA ARSENALE	RLR	159	27.8	2.188	32.7	2.798	35.3	3.237	1.1
VENEZIA (S.STEFANO)	RLR	240	23.2	2.469	31.0	2.662	38.8	3.180	2.3
VENEZIA (PUNTA DELLA	RLR	1039	0.7	4.791	41.0	2.757	32.9	3.093	2.4
TRIESTE	RLR	1092	3.4	5.047	39.0	2.989	34.2	3.098	1.2
KOPER	RLR	344	17.7	4.745	33.0	2.898	27.4	3.064	0.2
ROVINJ	RLR	532	23.8	5.078	45.8	2.748	29.2	3.042	0.2
BAKAR	RLR	708	25.8	5.485	39.7	2.317	31.6	3.004	0.4
SPLIT RT MARJANA	RLR	558	23.3	5.066	37.6	2.174	28.2	2.909	0.1
SPLIT HARBOUR	RLR	550	22.7	5.153	40.5	2.122	29.3	2.915	-0.2
DUBROVNIK	RLR	523	23.0	5.005	42.8	2.172	24.6	2.956	0.5
BAR	RLR	319	17.6	4.465	41.9	1.911	22.1	2.904	1.3

4.4 Seasonal cycle

In order to assess the seasonal cycle in the sea level of the Adriatic, the model function

$$h(t) = a + b \cdot t + A_{\mathrm{N}} \cdot \sin(\omega_{\mathrm{N}} \cdot t + \phi_{\mathrm{N}}) + A_{\mathrm{Sa}} \cdot \sin(\omega_{\mathrm{Sa}} \cdot t + \phi_{\mathrm{Sa}}) + A_{\mathrm{Ssa}} \cdot \sin(\omega_{\mathrm{Ssa}} \cdot t + \phi_{\mathrm{Ssa}}) \qquad (21)$$

where the suffix N stands for the nodal tide of 18.6 years period and Sa and Ssa for the annual and semi-annual harmonic constituents, respectively, was fitted to the monthly mean sea-level record available in the PSMSL data base. The results are compiled in Table 10. The time series together with the model functions are displayed in Figure 26 and the residuals are shown in Figure 27.

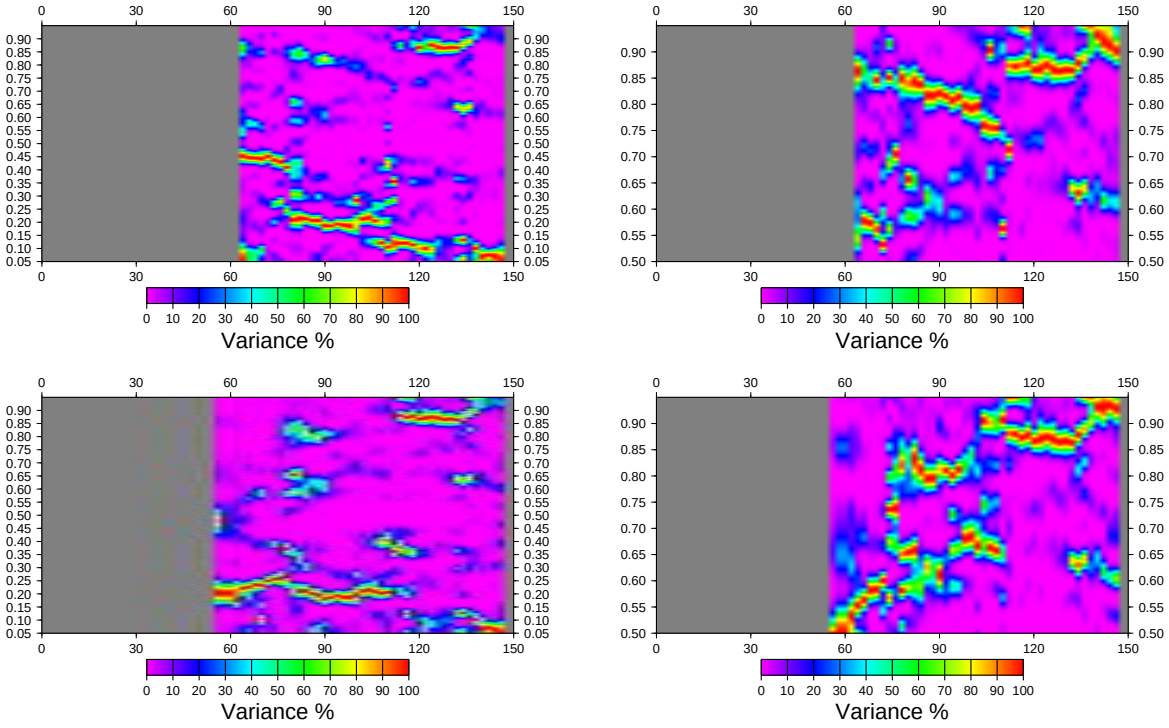

Figure 25: Dynamic spectra for sea level in Venice and Trieste.

The dynamic spectra are computed with a temporal resolution of two years on the basis of normalized variance spectra for the time interval 1850 to 2000. The seasonal cycle is taken into account in the computation of the spectra. Upper diagrams are for Venice, lower for Trieste. Left and right diagrams show the spectra from 0.05 to 0.95 cpy and 0.50 to 0.95 cpy, respectively.

Table 11: Long-period oscillations and trends in the sea level of the Adriatic for 1960 to 2000.

The table is the same as Table 10, except that the data interval has been constraint to the time window 1960 to 2000.

Name	**Type**	N	A_{N}	ϕ_{N}	A_{Sa}	ϕ_{Sa}	A_{Ssa}	ϕ_{Ssa}	b
VENEZIA (PUNTA DELLA	RLR	484	16.3	0.307	43.2	2.815	33.9	3.161	0.5
TRIESTE	RLR	492	21.6	0.282	40.8	2.961	34.9	3.164	0.4
KOPER	RLR	344	17.7	6.163	33.0	2.889	27.4	3.045	0.2
ROVINJ	RLR	477	22.4	0.370	44.7	2.729	28.1	3.102	0.0
BAKAR	RLR	480	29.5	0.542	39.5	2.429	33.2	3.051	0.2
SPLIT RT MARJANA	RLR	466	23.4	0.283	37.1	2.234	29.8	2.995	0.0
SPLIT HARBOUR	RLR	480	24.1	0.358	40.2	2.166	29.6	2.988	-0.2
DUBROVNIK	RLR	475	22.5	0.258	43.3	2.186	23.7	3.000	0.3
BAR	RLR	319	17.6	5.883	41.1	1.902	22.1	2.885	1.3

The two harmonic constituents that are used here to represent the seasonal cycle are fairly homogeneous throughout the Adriatic both in amplitude and phase, this despite the fact that the time series cover quite different time intervals (Figure 26). In Figure 28, the model functions for all stations listed in Table 10 are shown for an arbitrary year, and this figure emphasizes the spatial coherence of the seasonal cycle in the Adriatic. The maximum sea level occurs consistently in October, while a minor maximum in April is larger at the southern part of the Adriatic than in the northern part. In the southern part, the minimum occurs a little earlier in February and is lower than in the northern part.

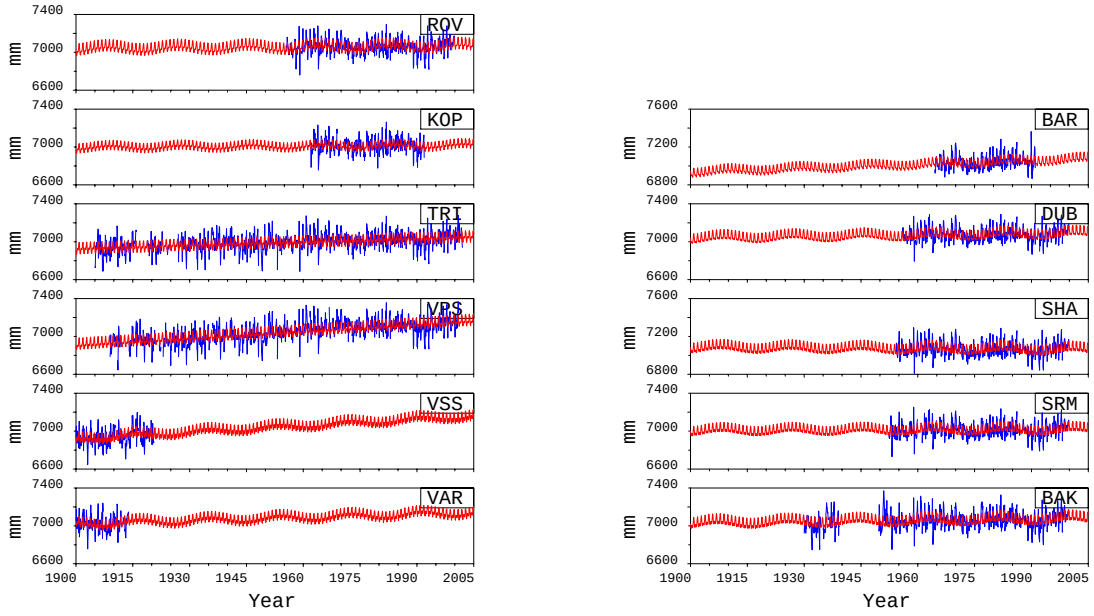

Figure 26: Monthly mean sea-level time series for Adriatic stations.

Only time series having more than 20 years of data are shown. The model function is eq. (21). Station abbreviations are as in Table 2.

4.5 Interannual to decadal variability

Table 10 also contains the parameters for the anticipated nodal tide. The nodal tide turns out to be surprisingly coherent in space both in amplitude and phase. The only exception are the records from the various tide gauges in Venice and also Trieste. The long records in Venice PS and Trieste have a phase comparable to the Eastern Adriatic stations, but a very small amplitude. The two other Venice stations have amplitudes comparable to the Eastern Adriatic stations, but phases that are nearly 180 degrees off.

The records at Venice Arsenale and S. Stefano cover only the first decades of the 20^{th} century, while all other Eastern Adriatic records cover the last half of the 20^{th} century. Only the two records of Venice PS and Trieste cover the full 20^{th} century. In order to get comparable results, eq.(21) was also fitted to all time series using only the data in the time window 1960 to 2003 (Table 11). The results for the nodal tide are now highly consistent for all stations both in amplitude and phase. Assuming that the large deviation of the apparent nodal tide for the interval 1900 to 1960 is not due to instrumental effects, we state that the apparent nodal tide is a transient phenomenon with a phase in the first half of the 20^{th} century very different from that in the second half. Thus, we can conclude that the oscillation close to 18.6 years is not the nodal tide (which is very stable in time) but rather a phenomenon at least partly due to other forcing. Consequently, the anticipated non-equilibrium nodal tide indicated by Pirazzoli & Tomasin (2002) (see also Section 4.7) is most likely not due to a non-equilibrium response of the Adriatic to the nodal tide but rather caused by other processes.

We use integration over time to emphasize the long-period variations in the sea-level records. In Figure 29, the integrated residuals (that is, the difference between the monthly means and the model function) are shown for the complete records. The two long records for Trieste and Venice Punta Salute are dominated by a higher order term, which shows that the residuals, which do not contain an overall linear trend, contain a non-linear trend term. The shorter records are all dominated by an inter-decadal variation. Constraining the time window to the data after 1960 emphasizes on the

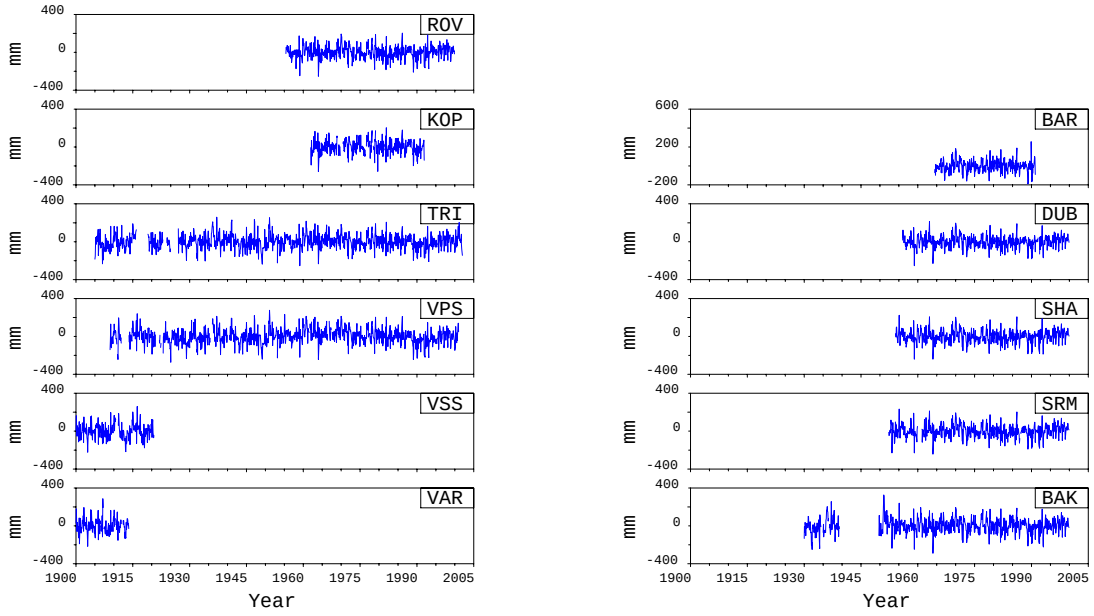

Figure 27: Residual monthly mean sea-level time series for Adriatic stations.

Only time series having more than 20 years of data are shown. The model function eq. (21) has been removed and the residuals are shown. Station abbreviations are as in Table 2.

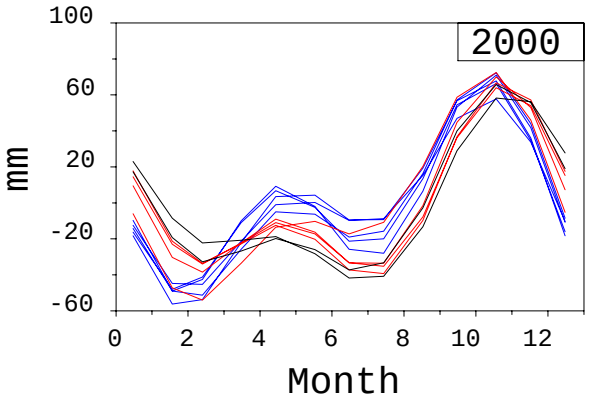

Figure 28: Seasonal cycle in the Adriatic.

The model function eq. 21 is shown for the year 2000. The Northern Adriatic stations are in blue (including Koper), the Eastern Adriatic stations are in red (from Rovinj to Split) and the Southern Adriatic stations (Dubrovnik and Bar) are in black.

one hand the dominance of this inter-decadal variation, and on the other hand its spatial coherency (Figure 29. For the records covering the complete time interval this inter-decadal variability has the same amplitude and temporal history. For the shorter records, the integration is not fully comparable, but the inter-decadal signal is still well reproduced. In total, about 2.5 to 3 cycles of this signal are contained in the time window from 1960 to present. It is interesting to note here that the amplitude of the signal appears to be increasing with time, and the signal is most pronounced after about 1970.

We also use the monthly mean sea level to emphasize the differences in sea level at the stations available in the Mediterranean, in particular the differences of the sea level in Venice compared to adjacent locations. In Figure 31, we have plotted the monthly differences between the individual stations and a base station for all long records in the Adriatic. For this comparison, first the seasonal

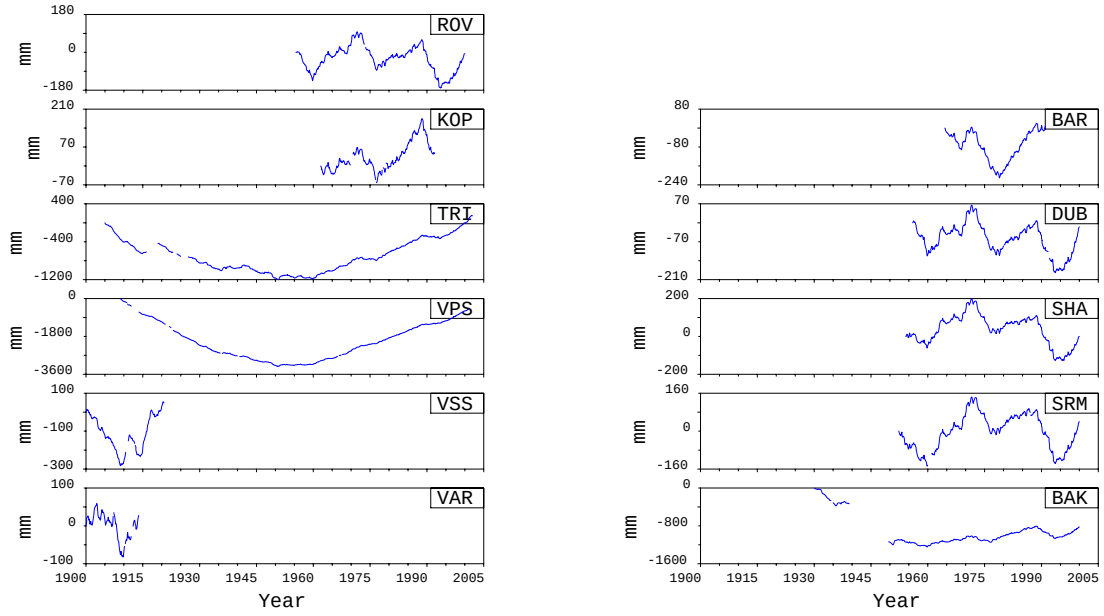

Figure 29: Integrated residual sea-level records.

The time series integrated are those shown in Figure 27. The time series are integrated using eq. (17). Station abbreviations are as given in Table 2.

cycle represented by an annual and semi-annual constituent is removed prior to the computation of the differences.

Using the record of monthly mean sea level at Trieste as a base record, the difference between this base record and the other long RLR records in the Adriatic reveal a number of interesting features (Figure 31). At intraseasonal time scales, the stations in the Upper Adriatic as well as Bar at the southern end of the Adriatic are to a very high degree coherent with the variations in Trieste, while Split and even more so Dubrovnik show deviations from Trieste at least a factor three larger. These three records also show coherent interannual variations not found in the other records. The same picture is found for Venice Punta Salute as base station.

The frequent spikes in the records before 1940 indicate data errors either in the station record or the base station. Based on a comparison of the differences for the two base stations, the actual location of a spike can easily be identified. For example, the large spike in early 1955 found in most records if Trieste is used as the base station must be attributed to a data error in the Trieste record.

In Section 3.1.1, we noted that in the interval from 1990 to 2003, sea level in Venice was rising faster than in Trieste (see Figure 5 on page 24, left side, second diagram from bottom). This feature is confirmed in Figures 31 (page 57). After 1970, the differences shows some interannual variability within a range of the order of ± 5 cm.

In order to emphasize the long-period signals in the differences, in Figure 32, we show the time series of differences after integration over time (see eq. 17 in Section 3.3.1, page 26). Since any differential linear trend in the two time series would lead to a quadratic term in the integrated differences, we have also removed the linear trends from the time series prior to differencing the series.

Rovinj, Koper, and Trieste and to a lesser extent also Bakar exhibit the same differences with respect to Venice, while the differences between Trieste and Rovinj, Koper and Bakar are rather small. This indicates that the Venice record contains some long-period variations (non-linear trends?) not found in the adjacent records. Split and Dubrovnik show the same general deviations from Venice and Trieste,

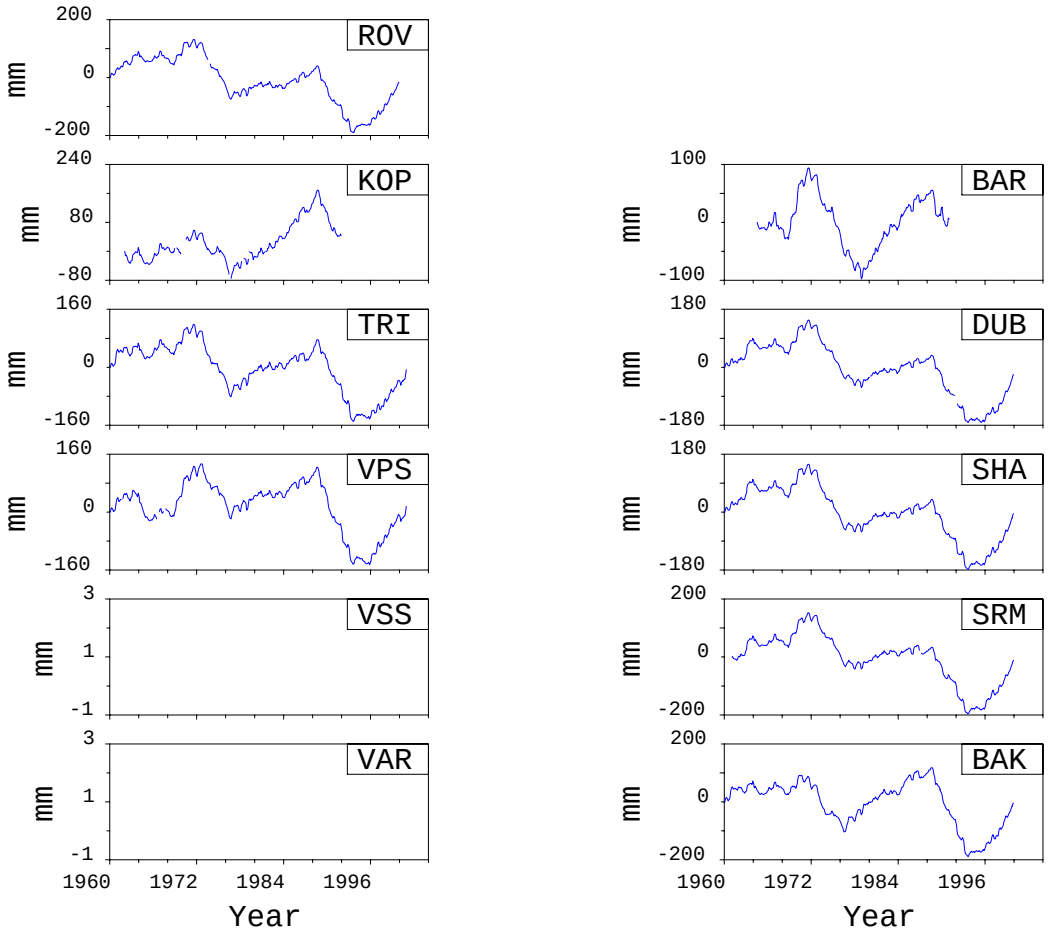

Figure 30: Integrated residual sea-level records in the time window 1960 to 2002.
Same as Figure 29 but constraint to the time window from 1960 to 2002.

though with smaller amplitudes if Trieste is used as base station. At decadal time scales, the difference for Dubrovnik, Split and particularly Bar show a signal of the order of 15 year, which may be related to spatial differences in the 16 year signal discussed above.

In general, the long-period variations in the integrated differences are larger for the base station Venice than Trieste. This supports the notion that the low-frequency part of the Venice record contains variations not found at the other stations.

4.6 Secular trends

The secular trend in Venice has been studied in detail in a number of studies (see, e.g., Emery & Aubrey, 1991; Woodworth, 2003; Carbognin et al., 2004). Most of these studies have been based on annual mean values. Considerable focus has been on the non-linear behavior of the trend in Venice, which is particularly obvious if compared to the secular trend in Trieste (see, e.g., Pirazzoli & Tomasin, 2002). The transient parts of the secular trend in Venice are due to a complex interplay of natural and anthropogenic factors influencing mainly the vertical land motion (see Woodworth, 2003, for an overview).

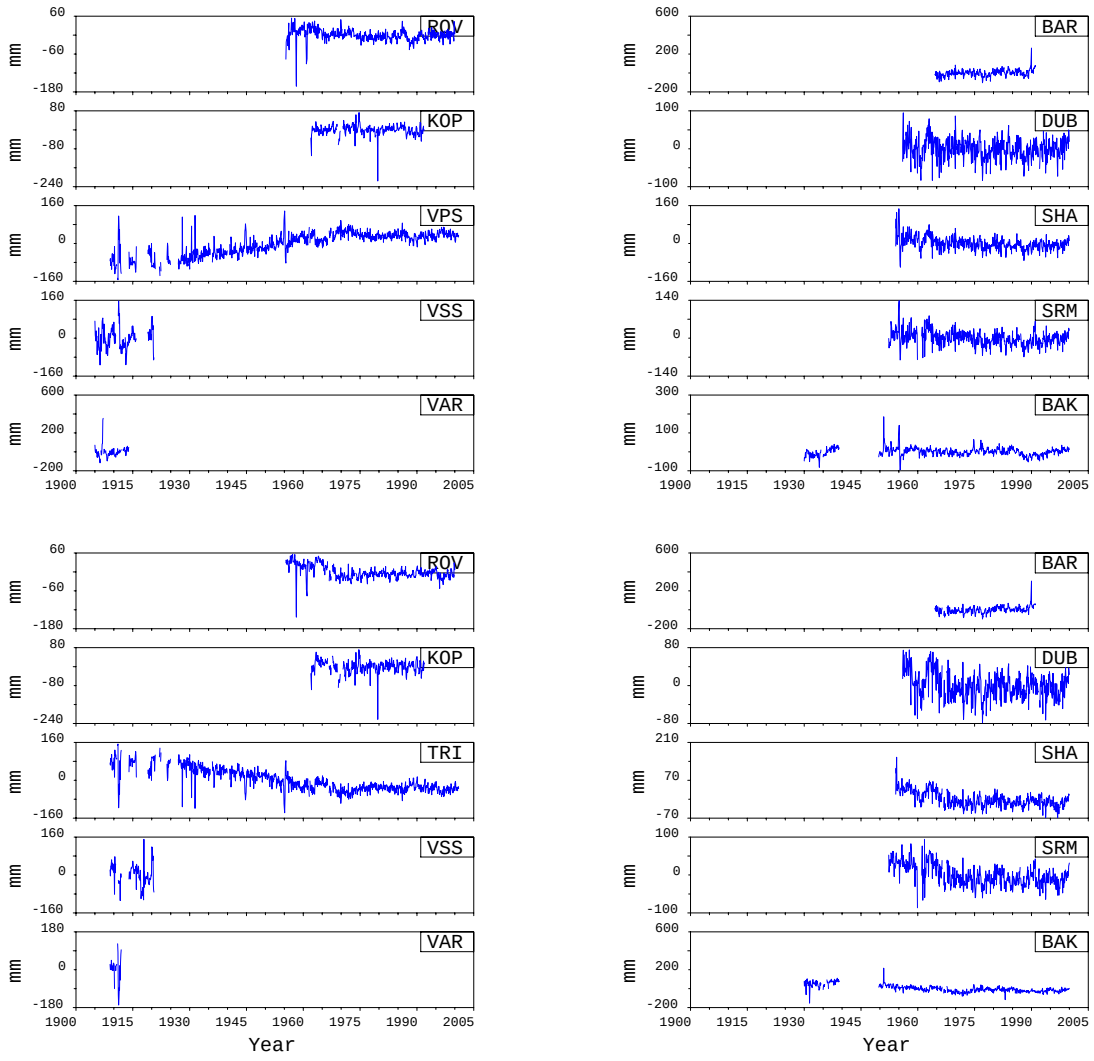

Figure 31: Differences of monthly sea-level variations in the Adriatic.

Upper two diagrams are for differences with respect to Trieste, lower two diagram with respect to Venice Punta Salute. For each station, the monthly differences to the base station Trieste are shown. The annual and semi-annual constituent was removed from all series before the differences were computed.

Here we consider monthly mean sea levels in order to understand the secular sea-level variations in the Northern Adriatic. In Tables 10 and 11, the secular sea-level rates are given for the complete time series as well as restricted to the time interval between 1960 and 2003. For the complete records, the trend pattern exhibits rather large spatial variations throughout the Adriatic, which are strongly attenuated if the data window is nearly the same for all records (Table 11). Over the 43 years considered here, LSL in the uppermost part of the Adriatic increased by approximately 0.4 to 0.5 mm/yr while along the eastern coast the values range from -0.2 to 0.3 mm/yr. An exception is the station at Bar, where a high value of 1.3 mm/yr is indicated by the observations. This particular record will require a more detailed study.

It is interesting to note here that the spatial trend pattern is in good agreement with the present-day sea-level change predicted by Di Donato et al. (1999) for the combined effect of tectonics and post-glacial rebound. Subtracting their model from the rates given in Table 11 results in a secular sea-level change caused by atmospheric and oceanographic forcing of approximately -0.2 to 0.0 mm/yr for the

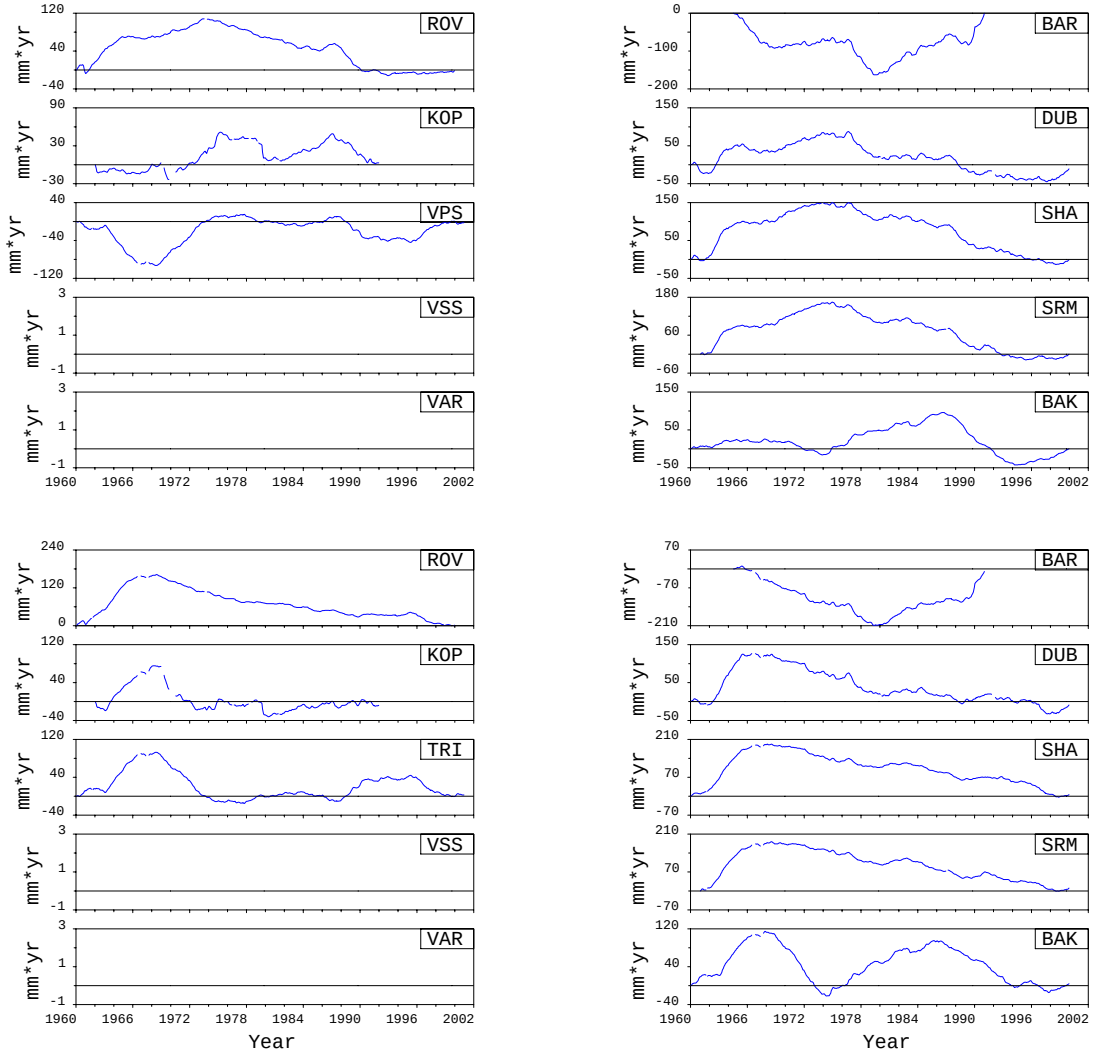

Figure 32: Long-period differences of monthly sea-level variations in the Adriatic.
Same as Figure 31 but integrated over time. Only data from 1960 to 2002 is shown.

whole Adriatic. This is again in agreement with our understanding of the influence of atmospheric and oceanic forcing as discussed in Section 5.3.

4.7 Extreme sea levels

4.7.1 Background to estimating probabilities of extreme sea levels

It is necessary to define some basic concepts and parameters common in these assessments, and the general concepts of risks and how these are calculated for extreme sea levels. Estimating these risks needs to be based on good data and a range of analysis techniques.

The probabilities of extreme sea levels and coastal flooding may be specified in several different ways. These levels, including the tide, surge and mean sea level elements, are sometimes called still water levels to distinguish them from the total levels, which include waves. Waves are usually accounted for separately in risk analysis, although more elaborate procedures may allow for some correlation between storm surges and high wave conditions.

If the probability of a level z being exceeded in a single year is $Q(z)$, that level is often said to have a return period, which is in the inverse of $Q(z)$ in years. For example, a sea level having a probability of being exceeded in a year of 0.05 would be said to have a return period of 20 years. Similarly the level that has a probability of being exceeded once in a hundred years, is called the hundred-year return level. This inversion of annual exceedance probabilities to give return periods makes the implicit assumption that the same statistics are valid for the whole period specified; since for very small probabilities, this may be many tens or hundreds of years, this can be a very big assumption. It would be absurd to say the 10^{-4} level has a 10000 year return period because MSL conditions have changed and will change substantially over that period.

The appropriate value of $Q(z)$ chosen for coastal planning will depend on the value of the property at risk. Nuclear power stations may specify 10^{-5} or 10^{-6} . For the coastal protection of the Netherlands a value of 10^{-4} is adopted, but for many British coastal protection schemes values of 10^{-3} or greater are accepted. When estimating $Q(z)$ it is very unusual for an engineer or coastal scientist to have access to the quantity or quality of data that many of the theoretical techniques available require. Estimates must be based on only limited observations, so that extrapolation of the available data in both time and space is inevitable. Skill is necessary to decide how valid it will be to use data from another location, and the best way to make the transfer.

In addition to estimating probabilities of exceeding stated levels in a particular year, other design requirements may specify the likely duration for which such exceedances may occur. Another alternative presentation is to assign a return period to some particular extreme level; several authors have done this for Venice.

For very expensive structures and major regional studies such as Venice, the most elaborate available statistical methods should be used to estimate extremes. For less expensive schemes approximate methods of estimating have been developed as cheaper alternatives.

The two most commonly used methods are a) those based on analyses of a series on the maximum levels observed in a series of years, and b) the calculations of joint-probabilities where tidal and meteorological influences on sea level are separately assesses. Fuller summaries and specific details are found in formal texts, for example Pugh (2004) and Coles (2001).

The major disadvantage of the annual maxima method is the waste of data and potentially valuable information, because a complete year of observations is being represented by a single value. If the largest positive meteorological surge for the year coincides with a low tidal level, the information is ignored despite its obvious relevance to the problem of estimating extreme level probabilities. Joint tide-surge probability estimates require substantially more work but have several additional benefits.

- Stable values are obtained from the relatively short periods of data.

- There is minimal waste of information.
- The probabilities are not based on large extrapolations.
- Estimates of low water level probabilities are also produced.

However, for this method to be successful, data must be of a good quality, with timing accuracy to better than a few minutes. If there are timing errors (old chart recorders were especially prone to these) tidal variations will appear in the non-tidal residuals. Joint tide-surge probability estimates of extremes require a high degree of analytical skill, and extra computational effort is involved.

Other methods, either similar to or extensions of the annual maxima and joint-probability methods described briefly above are often applied. One method looks at a fixed number of the maximum extreme levels in a year, typically up to ten, instead of just the single annual maximum value. Sometimes this will mean including some highest levels from one year, which are less than those not included for another year. Care is necessary to make sure that each storm is a separate and independent event, which is sometimes taken to mean that they are at least three days apart. At Venice because of the seiching in the Adriatic, longer periods of separation may be necessary for true independence. These storm levels are then fitted with an appropriate extreme value distribution

Another method, developed for river hydrology, is to look at the number of times a level exceeds some stated threshold level. Unlike the previous method, this may result in several storms being recorded in one year and few or none in another year. Total sea levels (tides plus weather effects) could be influenced by the 18.6-year cycle in tidal amplitudes. A better approach is to apply this peaks-over-threshold method to the non-tidal residuals, after removing the tides, and to use the resulting probabilities in a joint-probability calculation.

The reliability of all estimates is limited by the available data and by possible trends and changes in the regional meteorology and oceanography. The possibility of some rare unsampled event, such as a tsunami, cannot be ignored, nor is it easily incorporated into the estimates. Tsunamis are more common in the Pacific than in other oceans, but even for the Atlantic, well-documented tsunamis have occurred and the Mediterranean has recently been considered for a local tsunami warning system.

4.7.2 Total observed sea levels

Sea levels in Venice are traditionally measured relative to the datum for the tide gauge at Punta Salute. This reference is called the "tidal zero of Punta Salute" and designated Z.M.P.S. It is a mark that has never varied with respect to the ground level of the city (Rusconi, 1993). Sea-level changes referenced to this mark include oceanographic changes and vertical land movements.

In Rusconi (1993) and many other papers, the term "tide" is used to mean "total observed sea level"; however, the latter technically includes both tidal and meteorological components added to the mean sea level.

Observed sea level= mean sea level + tide + weather effects

Fortunately it is clear in the texts where the term "tide" is used in this more general and popular way. Cavaleri et al. (1991) have suggested that wave set-up is also a factor in correct sea level forcing for Venice; this will be correlated with the meteorological effects discussed below.

The mean sea level has itself increased over the period since measurements began and longer (Pirazzoli, 1987; Cecconi et al., 1999; Battistin & Canestrelli, 2001; Bonato et al., 2001a; Camuffo & Sturaro, 2003; Rusconi, 1993). Over the same period the frequency of extreme events has increased substantially. Rusconi summarizes the frequency of sea levels above 0.90 m Z.M.P.S. on a decadal basis (Table 12).

Decade	> 0.80 **m**	> 0.90 **m**
1920-1929	5.7	2.2
1930-1939	12.7	4.0
1940-1949	11.8	5.5
1950-1959	23.1	9.8
1960-1969	48.2	20.4
1970-1979	42.5	17.3
1980-1989	45.9	17.4
1990-1999	52.0	21.0

Table 12: Frequency of extreme sea levels in Venice.
From Rusconi (1993). The numbers are events per year of high water above 0.80 m and 0.90 m, respectively.

Ranking	**Date**	**Level**	**R.P.**
1	4 Nov 1966	1.94	217
2	22 Dec 1979	1.66	38
3	1 Feb 1986	1.58	23
4	15 Jan 1867	1.53	< 23
5	12 Nov 1951	1.51	
6	16 Apr 1936	1.47	
7	15 Oct 1960	1.45	
8	3 Nov 1968	1.44	
9	6 Nov 2000	1.44	
10	8 Dec 1992	1.42	
11	17 Feb 1979	1.40	
12	5 Nov 1967	1.38	
13	26 Nov 1969	1.38	
14	22 Dec 1981	1.38	
15	24 Nov 1987	1.38	

Table 13: Extreme total sea levels in Venice.
From Bonato et al. (2001b). Level is in meters above Z.M.P.S. R.P. is the "return period" in years.

More detailed statistics are in the original paper and its update (Rusconi, 1993; Bonato et al., 2001b). High water levels above 1.10 m are described as "acqua alta." The highest level recorded, 1.94 m was on 4 November 1966 (Pirazzoli, 1987). There is a strong winter seasonal dependence in the probabilities of flooding with maximum probabilities in the months November-February. This is clearly shown in Figure 7 of Cecconi et al. (1999).

Bonato et al. (2001b) tabulate recent (1867-2000) extreme total sea levels (Table 13). The return periods, given in years, are also from Bonato et al. (2001b). They estimate the "500 year" return level as 2.07 m, but caution extreme care in the deductions that should be made. Their estimates of return periods are based on a Gumbel extreme value distribution, confirmed by other procedures. It appears that they have treated the series of extreme values as a statistically stationary set. It can be argued that as the mean sea levels at Venice have increased, so too have the risks of extreme events, and so the statistics are not stationary. Similarly, future probabilities of extreme levels will depend on the longer-term mean sea-level changes; this in turn makes the concept of a "500 year" return level based on past statistics a very difficult to realize. The caution recommended by the authors reflects this.

There is also an apparent "18.6 year cycle" in extreme values as shown in Figure 3 of Pirazzoli & Tomasin (2002) among others. These amplitudes (estimated from the Figure as about 3-5 cm), are bigger than the Equilibrium Tidal signal modulations for the Nodal Tide due to changes in the lunar declination, and deserve further investigation to determine the regional extent of their amplification.

Mazzarella & Palumbo (1991) and Palumbo (1997) make adjustments to the extremes to allow for mean sea-level changes, before computing the statistics. This makes the statistics more stationary. For Venice extreme floodings using two different statistical models the values compiled in Table 14 are given in Palumbo (1997).

Height	Return period	
	EM	**FM**
1.2	4.3	4.9
1.3	7.8	9.0
1.4	10.5	16.0
1.5	23.1	27.4
1.6	25.3	45.1
1.7	45.7	72.1
1.8	82.5	112.2
1.9	268.4	170.5

Table 14: Return periods for extreme floodings in Venice.
From Palumbo (1997). Height is the height of the flooding in meters above Z.M.P.S. Return period is in years with EM for the exponential model, and FM for the fractal model.

In the above table the exponential (Gumbell) method fitted the observations better. This paper also introduces a new statistical process that takes into account the time gap and the energy released from the last event , and on the return period. The model is applicable to a general range of extreme events, and is illustrated with the example of Venice extreme levels. This work may be further developed.

Dealing with only total sea levels, and one annual maximum a year, fails to capture a lot of potentially valuable information. Smith (1986) and Tawn (1988) have applied methods of using instead the n maximum values, typically ten, in a year. See also Coles (2001).

4.7.3 Trends in individual components of sea levels: Mean sea levels

These are presented in several publications and elsewhere in this report. In summary, there have been substantial increases in the past several hundred years (Camuffo & Sturaro, 2003). From direct sea-level observations there has been a steady increase until about 1970, followed by a period of approximately no change. It is not part of this particular report to interpret these changes as they are dealt with elsewhere [insert cross reference]. However it is clear that mean sea level variations and long-term changes must affect the probabilities of extremes as the short-term daily changes are about this mean.

A comparison with Trieste is included in Battistin & Canestrelli (2001); their Figure 2 also plots means of maximum and minimum sea levels. It should be noted that the values for Venice, which the authors label as "mean sea level" are strictly the Mean Tide Levels by definition, not the true mean sea level computed from a mean of hourly or more frequent sea levels. The differences are usually small, and depend on the shallow-water M_4 and MS_4 harmonic constituents of the tides.

4.7.4 Trends in individual components of sea levels: Tidal variations

The tides in the Mediterranean Sea are generally small, though in the northern Adriatic Sea there is strong amplification (see Section 4.2). Globally and as a consequence of their astronomical origin, and dependence on the overall dimensions of ocean basins, there have been no proven changes in ocean tides over centuries. It is also unlikely that any significant changes to Adriatic tides will occur over the periods of interest here. However, local changes in tidal amplitudes and phases have often been reported, usually related to specific dredging or other changes. Pirazzoli (1987) reports that the harmonic constituents $M_2 + S_2$, which around 1920 were smaller in Venice in relation to the open sea, are now 4% greater in Venice. A systematic study of long-term tidal changes could be undertaken. Some work on this is suggested in Cecconi et al. (1999), who refer to Tomasin (1974).

4.7.5 Trends in individual components of sea levels: Meteorological components and extreme sea levels

Some authors have recently looked at the contribution of meteorological contributions to extreme levels separately, and in some cases have also looked for trends in these contributions. Cecconi et al. (1999) make a very thorough analysis of data from 1924 to 1996. Hourly water levels for Venice were provided by the National Research Council from 1955 to 1984 and from 1981 to 1996 by the Centre Previsioni Maree of the Venice Municipality. Mean sea levels and tides were removed (but not seasonal effects). Only 8 tidal harmonics were used in the tidal removal process. Four daily maximum and minimum values of water levels were extracted and by interpolation of maximum and minimum storm surge data an entire series of hourly values were computed for the period 1924 to 1996. It is not clear why the non-tidal components were not directly subtracted from annual harmonic analyses, which would also have removed annual sea-level variation, but this is possibly due to the absence of hourly measured sea levels in the earlier years. Storms were defined as residuals more than 0.30 m, positive and negative; this value is about twice the standard deviation of the residuals. The authors define two indexes of storminess: "the storm activity in terms of the annual duration of storm events (in hours) and the storm severity in terms of the annual intensity of storms (its units are meter-hours)". The paper is not specifically looking at frequencies of extremes though it is implicit that trends in these two parameters will be indicative of similar changes in the frequency of extreme events. They conclude that there is no significant secular trend in sea levels, as expressed in storm activity or storm severity during the period of their data. But there are very large inter-annual differences and inter-decadal fluctuations. This is a very thorough piece of work on which to base future assessments.

This paper is not directly referred to in either of two papers published later, both of which look for trends in the underlying meteorological conditions that generate extreme sea levels. Trigo & Davies (2002) look at conditions associated with sea surges at Venice for 1958 to 1997. They explain the general synoptic situations that precede sea surges in Venice are associated with Atlantic depression systems moving along a northwest-southeast path, towards the Bay of Biscay. The perturbations on these systems induced by mountains in Southern Europe give rise to conditions favorable for Venice extreme sea levels. They conclude that there is a general decreasing of these conditions, and specifically identify significant reductions in extreme local winds and an increase in air pressure. The latter, through the inverted barometer effects would depress sea levels. This decrease is supposed to offset increases in mean sea level, leading to stationarity in the frequency of sea surge statistics for Venice over the period. The authors point out that these trends cannot be used as evidence that any future sea-level rises will continue to be offset by reductions in meteorological extremes.

A similar analysis by Pirazzoli & Tomasin (2002) also finds meteorological trends that tend to reduce probabilities of extreme sea levels. They describe in more local terms the weather conditions that produce storm surges in Venice: the bora that blows from the east and the sirocco which blows from the southeast along the axis of the Adriatic. The bora is reported to be sharply lessening, while the sirocco is increasing in frequency. They also report a decrease in atmospheric mean pressures. They conclude that the frequency of non-tidal residuals "sea surges" in the range 0.05 to 0.30 m is increasing in the North Adriatic. These, although below the threshold set by Cecconi et al. (1999) (see above) in their work, will lead to more regular flooding of the lowest parts of the city of Venice. For Venice they used hourly records digitized for Punta Della Salute, 1940-2000. The authors state that tides are statistically independent of weather effects, and while this is generally the case in areas of extensive shallow water, for example the southern North Sea , there can be significant interaction. This independence has yet to be confirmed for Venice. In Guardiani et al. (1988) the complicating role of dynamic non-linearities for Venice sea levels is identified. Their Figure 6 shows a smooth frequency distribution of surges, with a pronounced skew towards positive surges. This could be combined

with an equivalent tidal probability density function, to estimate joint probabilities of extreme levels, though it appears that this has not been done. This is a very careful study which can form a sound basis for further work.

4.7.6 Studies of extreme sea levels in nearby locations

Pirazzoli & Tomasin (2002) also looked at sea levels and trends from Diga Sud Lido outside the Venice Lagoon, and from Trieste. In this short section we draw attention to other recent assessments of flooding risks in nearby areas. There is considerable advantage in making these local comparisons. This applies also for mean sea levels, which are considered elsewhere.

Pasaric & Orlic (2001a) have made a careful analysis of flooding potentials and extreme levels above a threshold, in the Adriatic, based on 14 years of hourly sea level data recorded at Bakar. They distinguish four driving factors: tides; storm surges and seiches; low frequency oscillations from planetary atmospheric waves, in the band 0.01 to 0.1 cycles per day; and seasonal processes. They place particular emphasis on the importance of the "planetary wave" component, which accounts for one-third of the total sea-level variability. See also Pasaric et al. (2000); Pasaric & Orlic (2002, 2001b). Their Figure 3 shows the energy spectrum of sea levels with a high degree of background energy around the diurnal and semidiurnal tidal frequencies. In their study they looked at comparisons between sea levels at Bakar and at Venice for a flooding event on 24 November 1987. The low frequency elements are very similar but the extra tidal amplification at Venice gives higher total levels there.

The general oscillations of the Adriatic Sea under meteorological forcing are described by Vilibic (2000). The largest amplitudes occur in the October to March period, but the seiche can occur strongly (but very rarely) given favorable meteorological conditions during the Summer. The period of the first mode of the seiching is around 21 hours and this accounts for the marked asymmetry in the spectrum around the diurnal tidal frequencies, shown in Figure 10a in Pasaric & Orlic (2001a). The decay time of these seiches has been estimated as 3.2 ± 0.5 days. The seiches, like the tides, have their maximum amplitude at the northern end of the Adriatic, in the region of Venice and Trieste. Maximum amplitudes there can be tens of centimeters in amplitude, and clearly they are an important component of the non-tidal signal. Any correlation between these and tidal oscillations could affect joint-probability estimates of extreme sea levels at Venice, and a more detailed study could be part of further investigations.

4.7.7 Issues for further assessments and some limitations

There have been several studies tackling the issue of extreme sea levels at Venice in different ways. However, none of the published available studies has made a systematic study of all aspects. Also new data is continuously becoming available from the sea-level gauges. One valuable action would be to collect a standard set of available edited data. It appears that hourly values are available from Punta della Salute from 1940 onwards Pirazzoli & Tomasin (2002). Also the Centro Previsioni e Segnalazoni Maree has been preparing a complete time series of extreme values (Battistin & Canestrelli, 2001) from 1872 to the present. Hourly values are preferred for surge analysis as maximum surges may not occur at high water. Battistin and Canestrelli emphasize the difficulties of correcting "mistakes". This work, uncompleted at the date of their publication, is systematic with all the editing documented.

Possible further work includes both some simple actions and some extensive investigations to get maximum benefit from the data that has been so expensively collected and maintained. The suggestions fall into two categories.

First the standard analysis of annual extreme values could be updated with the long-term trends removed. Also the "n largest in a year" analysis could be repeated as there are no some 20 years more data. The alternative, but effectively equivalent of analyzing peaks over a specified threshold may also be done again with new data.

Secondly, looking at the separate components of the total sea level suggests the following:

- Look at tides and tidal probabilities and trends since 1940
- Build on the work of Pirazzoli & Tomasin (2002) to look at the seiche and other meteorological effects separately
- Investigate possible interaction between seiches/ surges/ and tides
- Perform joint probability calculations from tidal and surge pdfs.
- Look at trends in the driving factors (tides and weather), including mean sea level, to predict changes in risks of flooding in future years. Caution is necessary in extrapolating some recent reductions in meteorological drivers as a long-term trend.
- Look at the influence of set-up on lagoon sea levels
- It would also be useful to quantify the difference between mean Tide Level and Mean Sea Level at Venice, and to clarify when these are used in long series.

4.8 Conclusions

The main characteristics of the observed LSL variations in the Adriatic are summarized in Table 15.

Table 15: Main characteristics of the LSL variations in the Adriatic.

Phenomena	Description
Diurnal and semi-diurnal tides	The tides in the upper Adriatic have amplitudes of the order of 25 cm for the main semidiurnal constituents. There appears to be a slow increase in amplitude over the last five decades.
Fortnightly and monthly tide	Appear to be equilibrium tides with no significant deviation from the equilibrium.
Seasonal cycle	The annual and semi-annual constituents have amplitudes of the order of 38 ± 8 mm and 30 ± 8 mm, respectively with the seasonal cycle having a total range of approx. 120 mm and a maximum in early November and a minimum in late February.
Nodal (18.6 years) tide	Not detectable, most likely due (see below)
Interannual to decadal variability	Dominated by a strong nearly harmonic signal with a period of 16 to 17 year. The signal is most pronounced in the last 40 to 50 years with an amplitude ranging from 16 to 29 mm.
Secular linear trends	Over the last 40 years, LSL has been remarkably stable with trends ranging from -0.2 mm/yr at Split to 0.5 mm/yr in Venice, with the only exception at Bar, where the trend reaches 1.3 mm/yr.
Non-linear trends	Most remarkably in Venice, where the trend prior to approximately 1965 exceeds 3 mm/yr, leading to a century trend of 2.4 mm/yr. Also at Trieste, the trend in the first half of the 20^{th} century was somewhat larger than in the second half, leading to a century trend of 1.2 mm/yr.
Extreme sea levels	There was an increase in number of high waters above 0.80 m and 0.90 m over the first half of the 20^{th} century with a maximum of 48 and 20 excess levels, respectively, reached in the 1960s, a slight decrease after that and a new overall maximum (52 and 21 excess levels, respectively) reached in the 1990s. This pattern is a composite of the secular trend, the 16 to 17 years oscillation, increase in tidal range, and changes in weather.

5 Local forcing of sea-level variations in the upper Adriatic Sea

5.1 Introduction

As discussed in Section 2.2, LSL is affected by a number of local, regional and global forcing factors. Scenarios for future sea levels require a good knowledge of these forcing mechanisms for sea-level change and, in addition, some knowledge about the expected changes in these forcing mechanisms. The existing global scenarios are based mainly on the assumption that heat expansion of the oceans and ice-sheet melting would be major global mechanisms for sea-level rise Church et al. (2001). However the forecasts from various models do not show the same regional variability under the same scenario assumptions. Thus, it is necessary to understand the regionally important mechanisms in order to decide on the regional applicability of global scenarios and to improve on the existing scenarios.

In this section, we will discuss the state of knowledge of the various forcing factors for sea level in the upper Adriatic Sea. For the atmospheric forcing, large scale phenomena such as the NAO and NAM come into play and introduce interannual to multidecadal variability. For the oceanographic contribution, processes in the Mediterranean need to be considered. For vertical land motion, natural processes including tectonics, sediment loading and compaction, post-glacial rebound and present-day surface loading are of importance and are supplemented by anthropogenic processes such as groundwater, gas and oil extraction. All these factors need to be understood in order to synthesize future scenarios

5.2 Atmospheric forced variations

Potentially, changes in the atmospheric circulation might induce ocean current changes. Secular variations in the spatial pattern of the mean air-pressure field introduces secular changes in sea level due to the inverted barometer (IB) response of the ocean. An analysis of the ERA40 air-pressure field available from the European Center for Medium Range Weather Forecast (ECMWF) showed that over a time window of nearly 50 years, the maximum secular trends are found to be of the order of 0.01 HPa/yr, which is equivalent to 0.1 mm/yr in IB response. Changes in the mean wind field can results in changes of sea level particularly at coastal sites. These changes will have small spatial scales due to a complex interplay of the wind field and the coastal geometry.

Tsimplis et al. (2005b) used the predictions from the HANSOM model (see Section 3.6.1) showed that the atmospheric forcing reduced sea level over the last 40 years by approximately 0.5 mm/yr in the Adriatic. This is in agreement with the results from our own regression analysis reported in Section 8, though the effect appears to be slightly larger than 0.5 mm/yr. Over the last 40 years, air pressure over the northern Adriatic increased as well as the east wind component increased, while the North component decreased (see Section 3.3.1. In combination, the effects lead to a secular negative trend in sea level. Thus, we conclude that over the last 40 years, the apparent secular trend in LSL was reduced by atmospheric forcing by > 0.5 mm/yr. However, it is likely that this contribution is rather of a cyclic nature than being actually a secular trend sustained from centuries. Schlesinger & Ramankutty (1994) detected a 65-70 years oscillation in the global climate system, which is most pronounced in the North Atlantic and adjacent areas. Similarly, Plag (2000) reported long-period variations in sea level of the North Atlantic and air pressure in Europe on the same time scale. Therefore, we consider it likely that the negative effect of the atmospheric forcing is likely to be related to such a century scale oscillation. Consequently, this trend is likely to be reversed and compensated over the next fifty or so years, leading to a potential increase in sea level of up to 25 mm (assuming a positive effect of ≈ 0.6 mm/yr as opposite to the -0.5 mm/yr over the last 40 years plus an uncertainty).

5.2.1 Seiches

The known periods for seiches in the Adriatic sea are at 22 to 23 h, 10.8 h, 7.5 to 8 h and 4 h Vilibic et al. (1999). These events are excited by wind, and have estimated decay times of 3 to 4 days (Cerovecki et al., 1997). However, depending on the prevailing wind conditions, seiches can last for more days.

5.2.2 Storm surges

Storm surges are generated by the direct atmospheric forcing, that is the wind and atmospheric pressure changes. In the Adriatic Sea the generation of seiches and the interaction with tides are also important in generating dangerously high waters. The strongest winds in the Adriatic Sea are the bora and the sirocco. The bora is a northeasterly cold katabatic wind while the sirocco blows from the southeast. Both last for days (Orlic et al., 1994). It has been known for years that the sirocco is primarily responsible for many flooding events in Venice (Orlic et al., 1994, and references therein) by pilling up waters and generating a circulation that has a general inflow at the surface and a general outflow at the bottom and with the development of a cyclonic gyre at the eastern Adriatic and an anticyclonic gyre at the western Adriatic (Orlic et al., 1994). By contrast, the bora produces a complicated system of alternating high and lows (Bergamasco & Gacic, 1996). The bora also contributing to flooding events albeit less than the sirocco (Pirazzoli & Tomasin, 2002).

The wind field over the Adriatic is generally more energetic in winter with substantial energy in the lower-than synoptic frequencies (Pasaric et al., 2000). The wind dynamics are ageostrophic thus making the use of pressure gradients inappropriate in the Adriatic Sea (Pasaric et al., 2000).

The statistical analysis of the storm surges in Venice for the past 40 years together with the prevailing synoptic condition revealed that low atmospheric pressure combined with negative north-south pressure gradient and south-southeasterly to southeasterly winds are the conditions dominating when the largest storm surges occur (Trigo & Davies, 2002). These conditions are produced when the Atlantic synoptic system is perturbed by the orography. However no trends were identified in the number of large storm surges (Trigo & Davies, 2002). (Pirazzoli & Tomasin, 2002) identify an atmospheric pressure increase as well as a reduction in bora events. Raicich (2003) finds a reduction in the highest surges. Notably, all the above characteristics are consistent with prevailing high NAO conditions rather than global warming. However, sensitivity studies with double CO2 conditions indicate no statistically significant changes in the largest storm surges (Lionello et al., 2003). Several attempt to model storm surges in the north Adriatic have taken place (see Orlic et al., 1994, and references therein). Numerical models, are, still, inferior to statistical models for forecasting purposes (Lionello, personal communication). The description of the atmospheric forcing has been considered a major problem. Simulation of the same storm surge events with three different meteorological fields have produced differences of up to 60 cm between the model outputs (Wakelin & Proctor, 2002). Better results with quite accurate reproduction of one of the largest flooding events have been achieved by Lionello (personal communication). However, there is a discrepancy of about 6 h between the model and the tide gauge data with the model being ahead.

5.2.3 Seasonal variations

The seasonal cycle is a combination of steric and mass contribution. The steric changes are due to temperature and salinity changes, while the mass contribution arises from both thermohaline circulation and atmospherically driven changes. In our own regression analysis (see Section 8), we find that taking into account the atmospheric forcing increases the amplitudes of the annual constituent to a

Data set	13.5°E, 44.5°N	14.5°E, 43.5°N
I500	0.040	0.054
L500	-0.099	-0.211
L3000	-0.103	-0.230

Table 16: LSL trends predicted on the basis of temperature data.
Datasets are those given in Table 3. Trends are for two points close to Venice and Trieste. Trends are in mm/yr.

range from 67 to 79 mm (from 33 to 45 mm) and changes the phase from roughly 150°to roughly 135°. The effect on the semi-annual constituent is a reduction of the amplitude from a range of 22 to 35 mm down to a range of 20 to 27 mm and changes the phase from roughly 170°to about 149°(compare Tables 11 and 22).

5.2.4 Interannual to decadal variations

Taking into account the local atmospheric forcing has virtually no effect on the 16 to 17 year oscillation discussed in Section 4.5, as can be seen in the residuals shown in Figure 41. Therefore, we hypothesize here that this oscillation appears to result from an internal oceanic oscillation, which in fact may be related to the EMT discussed in Section 5.3.7. However, we have no observational basis to verify this hypothesis.

5.2.5 Secular trends

The secular LSL trends in the Adriatic over the last 40 years appear to be strongly affected by local and regional atmospheric forcing. The meteorological contribution due to local wind and air-pressure forcing over the time interval from 1958 to 2001 (see Section 8 ranges from -1.331 mm/yr in Bar to -0.236 mm/yr in Bakar. For Venice, this contribution is found to be -0.844 mm/yr (see Table 22 on page 22). Taking into account this local forcing leads to 'decontaminated' secular LSL trends in the range from 0.34 mm/yr in Split to 2.61 mm/yr in Bar (see Table 21 in Section 8). At Venice, this 'decontaminated' LSL trend value is 1.34 mm/yr.

Using the steric datasets discussed in Section 3.4.1, we get the contributions to the secular trends compiled in Table 16. The Ishii et al. (2003) predictions are close to zero, while the Levitus et al. (2000) datasets for 500 m and 3000 m both predict a negative trend. In summary, we conclude that the most likely steric contribution to the LSL trend over the 1960 to 2000 period is of the order of -0.10 ± 0.15 mm/yr.

5.3 Oceanographic contribution

The Adriatic Sea is a landlocked basin with a shallow area in its northern part where the average depth is $\sim$ 35 m, and a central area with average depth of $\sim$ 140 m but with maximum depth reaching 260 m and a southern area with maximum depth of 1200 m (Artegiani et al., 1997). The Adriatic Sea connects to the deep Ionian Sea (depths $\sim$ 4000 m) through the Strait of Otranto which has a maximum sill depth of $\sim$ 800 m. The Ionian Sea in turn is linked to the Western Mediterranean through the Straits of Sicily through sills of $\sim$ 540 m deep (Gasparini et al., 2005) which in turn connects to the Strait of Gibraltar which has a sill depth of $\sim$ 280 m (Tsimplis & Bryden, 2000).

5.3.1 Tides

The local tides are a result of the astronomically forced tidal signal and the incoming tide through the Strait of Gibraltar. The relative importance of the incoming tide for the Adriatic Sea is small

(Tsimplis et al., 1995) and the reason for the relatively large signals is the astronomic forcing and basin resonance. Several models have been published with progressively increasing resolution and accuracy (Tsimplis et al., 1995; Malacic & Viezzoli, 2000; Malacic et al., 2000; Cushman-Roisin & Naimie, 2002; Janekovic et al., 2003). While in most of the Mediterranean sea-level rise will only have small effects on tides due to the size of the signal, for the Adriatic, where the tides depend on the basin resonance, a change in the length of the basin by increasing sea levels are likely to affect the observed tides significantly. In a sensitivity study, Lionello et al. (2005) suggest that a 10 m rise could result in doubling the amplitude of the semidiurnal signal and producing a total increase on the amplitudes reached in a present day storm surge + seiche + tide simulation by about 15%. However, they correctly point out that more accurate estimates will be obtained in relation to tides if the tides of the whole of the Mediterranean Sea were modeled.

5.3.2 Oceanic circulation of the Mediterranean Sea

The basic circulation of the Mediterranean Sea has long been recognized to be that of a concentration basin (Marsigli, 1681; Waitz, 1755; Nielsen, 1912). The excess evaporation over freshwater input within the basin (Garrett et al., 1993; Gilman & Garrett, 1994) is balanced by a two layer exchange at the Strait of Gibraltar comprising a relatively warm, fresh (15°C, 36.2psu) upper water inflow and a relatively cool and saltier (13.5°C and 38.4 psu) outflow to the Atlantic (Bryden et al., 1994; Tsimplis & Bryden, 2000).

The transformation of the inflowing Atlantic Water to outflowing Mediterranean water within the basin is made through a thermohaline cell that involves the whole basin and leads to the formation of the Levantine Intermediate Water (LIW). In brief, the Atlantic inflow becomes progressively more saline as it moves eastwards. During winter it becomes cooler and denser and sinks to intermediate or sometimes deep levels. The role of the intermediate waters and in particular the LIW is important because they occupy the layer that corresponds to the sill depth ($\sim$ 280 m) at the Strait of Gibraltar, thus determining the characteristics of the Mediterranean outflow.

In addition to the formation of intermediate waters, deep water formation takes place in several parts of the basin and in particular in the Gulf of Lions Stommel (1972); Mertens & Schott (1998), the Adriatic Sea (Schlitzer et al., 1991; Malanotte-Rizzoli et al., 1997) and recently in the Aegean Sea (Roether et al., 1996). Therefore the Mediterranean Sea acts as a reduced scale ocean as regards the thermohaline circulation and dense water formation (Bethoux et al., 1998; Bethoux & Gentili, 1999).

5.3.3 Exchange through Straits

The exchanges of the Mediterranean Sea both at the Strait of Gibraltar and at the Dardanelles are two way flows with salinity differences driven by the water mass characteristics of the basins and mass exchanges limited by the hydraulic control points of the Straits (Candela, 1991). The exchange at the Strait of Gibraltar is of paramount importance for the Mediterranean Sea. Candela et al. (1989) have explained up to 80% of the observed variability of the currents in the Strait on the basis of an almost barotropic mode. The inflow of Atlantic water is highly modulated by the tidal signal and the atmospheric forcing at the Strait of Gibraltar. Its barotropic component has been found to correlate well with the cross strait sea-level component (see for example Tsimplis & Bryden, 2000). Estimates of the Atlantic inflow spanning much of the 20^{th} century range between 0.72 and 1.60 Sv while outflow values range between 0.80 and 1.68 Sv. It is not clear to what extent the variability in the estimates is a reflection of changes in the freshwater balance or an artifact of the technique used for the estimates (Tsimplis et al., 2005a). However omitting the oldest estimate of Schott (1915) significantly reduces

the range to between 0.72 and 1.26 Sv. The net exchange is of the order of tenths of Sv (1 Sv = 10^6 m^3 s^{-1}).

Apart of its role in balancing the excess of evaporation E over precipitation P and river runoff R, the Strait of Gibraltar acts as a choking point on direct meteorological forcing in the Mediterranean Sea thus making the response of sea level in the basin to be under isostatic, that is, smaller in magnitude than the -1 cm per mbar of change of atmospheric pressure for pressure signals with periods smaller that 15 days (Garrett & Majaess, 1984; Lascaratos & Gacic, 1990).

The inflow of water from the Black Sea to the Mediterranean is about 2 orders of magnitude smaller than the inflow of Atlantic water through the Strait of Gibraltar. However, the salinity difference between the Black Sea and Mediterranean Sea water is of order 18 psu, that is, much larger than the ~ 2 psu differences in the Strait of Gibraltar. Because of the large salinity differences the role of the Black Sea outflow is not negligible, at least for the Aegean Sea.

5.3.4 Effect of local air-sea interaction on the circulation in the Adriatic

The general features of the air-sea interaction based on climatologies have been described in detail by Artegiani et al. (1997). Remarkably, one of their datasets showed westerly winds as prevailing during the whole year while two other datasets showed a dominant easterly component. Wind is a crucial factor in estimating heat fluxes at the air-sea interface which in turn are crucial in providing understanding the climatic system and its relation to winter convection and deep water formation (Cardin & Gacic, 2003; Josey, 2003). In the Adriatic Sea the dominant feature is a strong seasonal cycle with maximum loss to the atmosphere in January at values between -150 and -180 W/m^2 depending on the equations used to derive the estimates and the data values used (Cardin & Gacic, 2003). On top of the annual signal significant interannual variability has been observed. The mean values indicate that the Adriatic Sea generally loses heat (-17 to -24 W/m^2) to the atmosphere therefore heat must be imported by the Ionian Sea for the basin to be in balance. Heat flux estimates through the Strait of Otranto are not presently available thus the heat budget problem of the basin is not fully resolved (Cardin & Gacic, 2003).

By contrast to the whole of the Mediterranean Sea which has a negative $E - P + R$ balance, the Adriatic Sea has a positive balance due to the large river outflow that it receives which corresponds to about 1.14 m /yr (Artegiani et al., 1997). Therefore, it is a dilution basin located within a larger concentration basin (the Mediterranean Sea).

The river outflow influence on salinity is evident over the whole of the Adriatic in winter and spring (Artegiani et al., 1997). There is a clear seasonal signal in temperature with maximum values in summer while the maximum thermocline depth is achieved in winter. The inflow from the Ionian in the form of the (modified) LIW is more abundant in autumn where it has been found to occupy most of the water column in the central and southern Adriatic (Artegiani et al., 1997). The north Adriatic influences the central and southern part of the Adriatic through the formation of dense waters. However, to a first order approximation it seems to be dynamically independent (Artegiani et al., 1997).

Dense water formation takes place both at the shallow northern Adriatic and at the deep south Adriatic (see for example Mantziafou & Lascaratos, 2004, and references within) with the two mechanisms been interlinked as the dense waters formed at the north Adriatic flow to the deeper southern parts of the basin and mix with the dense waters produced there by open ocean convection processes. Modeling of the deep water processes in the basin (Mantziafou & Lascaratos, 2004) suggest that on the basis of a perpetual average climatology the mean outflow of dense waters through the Strait of Otranto is 0.28 Sv while about 0.1 Sv recirculates within the basin. The dense water formation at the shallow north

Adriatic Sea contribute about 18% of the outflowing quantity and are conditioned on the outflow of the river Po (Mantziafou & Lascaratos, 2004) while the dense water formation at the southern Adriatic Sea are not significantly affected by the river outflow but on the heat losses to the atmosphere. More importantly they suggest that the basin has memory, that is, the deep water formation on each year does not only depend on that year's heat losses but also on the actual heat content of the basin. Thus, successive years with the same heat losses do not necessarily produce the same deep water formation Mantziafou & Lascaratos (2004). This suggests that the exchanges with the Ionian are important for deep water formation.

The temperature and salinity distributions and direct measurements permit the description of the circulation of the basin (Sellschopp & Alvarez, 2003, and references therein). The Ionian waters enter from the Eastern part of the Otranto Strait and exit from the western part. The southward currents depict seasonal variability with larger values in winter and lower in the summer. The flow on the western side is intermittent and reversals have also been observed (Kovacevic et al., 1999). The circulation within the is cyclonic (anticlockwise), dominated by three major cyclonic gyres related to the major topographical features of the basin. A density-driven current (North Adriatic Current) exists along the western coastline associated with the river outflow and during winters the lowest parts of this current carry the newly formed North Adriatic Dense waters. The jet separates and one branch turns east towards the deeper parts of the central Adriatic while another branch has been observed to flow to the southern end of the Adriatic where following the topography it sinks and mixes with the waters there (Sellschopp & Alvarez, 2003). When significant dense water formation takes place then the overflow over the Strait of Otranto sinks to the deepest parts of the Eastern Mediterranean. However, even in winters that there is no dense water formation, the outflow from the Adriatic continues although the water settle above the LIW waters of the Ionian Sea Sellschopp & Alvarez (2003).

5.3.5 The influence of oceanic circulation on sea-level variability

The variation of the water characteristics within the basin is of paramount important for steric sea-level variability. These would be determined by the amount of river water, the heat fluxes and the amount and water characteristics of the intermediate waters coming in through the Strait. The pressure across the Strait of Otrando at sill depth should be in static terms the quantity relevant for sea-level variability rather than the local, close to the tide-gauge, variations in temperature T and salinity S.

Tsimplis & Rixen (2002) have found common signals in the tide-gauge and steric estimates of sea level, however they as well as Tsimplis et al. (2005b) cannot describe the observed variability on the basis of the steric estimates. Grbec et al. (2003) have found that the maximum salinity at the southern Adriatic Sea is correlated with the Mediterranean Oscillation Index, an atmospheric pressure index based on pressure gradient between the Eastern Atlantic and the Central Mediterranean Sea.

In addition, deep water formation is a major reason for the seasonality in the water characteristics and the circulation patterns observed in the Adriatic Basin.

5.3.6 Multidecadal trends in water mass characteristics in the Adriatic and the Eastern Mediterranean

Existing climatological data sets indicate that the Mediterranean Sea is not in a steady state and is potentially very sensitive to changes in atmospheric forcing. In particular, during the 20^{th} century several changes in the Mediterranean circulation have been documented. Trends in T and S of the deep waters have been found in the Western Mediterranean (Lacombe et al., 1985; Charnock, 1989;

Bethoux et al., 1990; Bethoux & Gentili, 1999; Leaman & Schott, 1991; Rohling & Bryden, 1992; Tsimplis & Baker, 2000) as well as the Eastern Basin (Tsimplis & Baker, 2000; Rixen et al., 2005) as well as in the upper waters (Painter & Tsimplis, 2003). The characteristics of the LIW have also been found to change in time (Astraldi et al., 1999; Brankart & Pinardi, 2001; Gasparini et al., 2005). Moreover sudden changes in the deep water formation sites in the Eastern Mediterranean have been documented between 1987-1995 (Roether et al., 1996).

Various causes for these trends, including anthropogenic influence, local and regional atmospheric conditions and hydrological conditions during dense water formation events, as well as the first signature of global warming have been proposed. Bethoux & Gentili (1999) argue that while the warming trend can be explained by greenhouse-effect related warming of the sea surface between 1940 and 1995, the salinity trends require a rate of increase in the water deficit of the Mediterranean of the order of 0.10 m yr^{-1}. In order to achieve such a high value, it is necessary to consider not only the damming of the major Nile (Wadie, 1984) and Ebro (Martin & Milliman, 1997) rivers, but also a small increase in evaporation and decrease of the net Black Sea outflow, mainly due to Central/Eastern European river damming. A model study (Skliris & Lascaratos, 2004), suggests that the river Nile damming could account for about 45% of the salinity increase in the WMDW.

Estimates of trends in the Eastern Mediterranean have been included in several analyses (Tsimplis & Baker, 2000; Painter & Tsimplis, 2003; Manca et al., 2004). Tsimplis & Baker (2000) identified significant increasing trends in the temperatures of the deep waters of the Eastern Mediterranean and some suggestions for trends in salinity, though they were reluctant to accept them as real due to the large scattering of the salinity values especially in the Ionian Sea. Painter & Tsimplis (2003) have found that the upper waters of the entire Eastern Mediterranean have been undergoing a sustained period of cooling throughout all seasons since about 1950. The identified trends were caused by significant reductions in the winter temperatures while the other seasons did not have in general statistically significant signals. The salinity was also found to be increasing over the same period with the strongest trends often being found at the shallowest horizontal levels examined. The upper layers of the Western Mediterranean exhibit the same salinification as seen in the Eastern Mediterranean but the temperature trend is restricted to the Eastern Mediterranean. The analysis of Painter & Tsimplis (2003) supports the suggestion made by Krahmann & Schott (1998) that the LIW is not the major contributor to changes in the deep water characteristics of the Western Mediterranean implying that changes in the local atmospheric forcing are responsible for the deep water trends. However, Manca et al. (2004), have identified trends in the deep waters of the eastern Mediterranean of similar order of magnitude as those estimated in the western basin by Bethoux et al. (1990) implying either a common atmospheric origin or a communication of the changes from one basin to the other most likely through the LIW.

Changes in the deep water characteristics are unlikely to affect the sea-level values within the Adriatic because any increase in pressure is compensated by the sides of the basin. However, changes at sill depth would immediately be reflected in sea-level changes within the basin. Thus, sea-level rise within the Adriatic Sea can be caused by a sudden pushing up of the isopycnals south of the Strait of Otranto. Mixing processes are likely to smooth out the pressure differences with time but that would depend on how vigorous they are.

5.3.7 The Eastern Mediterranean Transient

The classic view of the oceanic circulation in the Mediterranean Sea had the Adriatic Sea as the major source of the deep waters (EMDW) of the Eastern Mediterranean Pollak (1951). However, comparison of hydrographic cruises in 1987 and 1995 (Roether et al., 1996) revealed a dramatic change of the vertical structure of the deep water column of the Eastern Mediterranean. New, highly saline and rich

in oxygen waters filled the bottom layers of the Ionian and Levantine basins. These water masses were outflowing from the Straits of the Cretan Arc, "pushing" the older EMDW water mass to shallower depths. Roether et al. (1996) estimated an average rate of outflow of dense Aegean waters from the Cretan Straits of about 1 Sv for seven years (1987-1995) three times the stated values for the Adriatic Sea.

The evolution of this change which was termed the Eastern Mediterranean Transient was further clarified through analyses of various oceanographic cruises that took place in the region in the years between 1987 and 1993. The Cretan Sea gradually filled with newly-formed, more saline water, with density exceeding 29.2 kg m^{-3} (see Figure 4.11 Theocharis et al., 1999b) at a rate reaching 3 Sv in 1991-1992. This water overflowed from the Cretan Straits filling the deep Eastern Mediterranean basin. Estimates of the outflow based on current meter measurements covering 150 days in 1994 suggested rates close to 0.5 Sv (Tsimplis et al., 1997, 1999). Since then, the signature of the Aegean waters has propagated in the Ionian Sea (Manca et al., 2002). After the mid-nineties, the Cretan Sea returned to the pre-EMT condition of exporting small amounts of dense water that does not reach the bottom of the Ionian and Levantine basins, but ventilates the depths of 1500 to 2000 m (Theocharis et al., 2002), while the main contribution of dense water for the Eastern Mediterranean is once again the Adriatic Sea (Klein et al., 2000).

The development of the water mass properties within the Cretan Basin happened in two steps (Lascaratos et al., 1999; Theocharis et al., 1999a; Tsimplis et al., 1999). The first step involves increase in salinity and the second one is associated with cooling and further salinity increase. These changes have been linked with changes in the atmospheric and oceanic circulation. Local (over the southern Aegean) anomalous meteorological conditions may have been partly responsible for the shift of dense-water formation activity from the Adriatic to the Aegean Sea (Lascaratos et al., 1999; Theocharis et al., 1999b). Samuel et al. (1999) showed that the period of increased dense-water formation over the Aegean Sea coincided with change in the wind driven-circulation of the Eastern Mediterranean which supplied more LIW to the Aegean Sea (see their Figure 4.14).

Malanotte-Rizzoli et al. (1999) identify significant changes in the oceanic circulation: (1) a gyre developed in the Ionian Sea which deflected the fresher Atlantic Water from its course towards the Levantine and the Aegean Sea resulting in increased salinities in both basins (2) gyres developed east of the eastern Straits of Crete that blocked the normal progress of the LIW south of Crete and forced the LIW into moving through the eastern Cretan Straits into the Cretan Sea thus increasing the local salinity (3) this situation which was observed both in 1991 as well as 1995 (Group, 2003) also involved Cretan Intermediate Water (CIW) spreading out from the Cretan Sea towards the Sicily Strait. These changes have also been linked to changes in the atmospheric forcing (Pinardi et al., 1997).

The EMT has not yet been fully resolved and disagreements exist in relation to when it started, whether is happened at the north or southern Aegean and what is the primary cause (For reviews see Zervakis et al., 2004; Tsimplis et al., 2005a).

5.3.8 The signature of water mass and circulation changes at the tide gauges of the Northern Adriatic

Several analyses have tried to explain the observed variability and trends at the tide gauges of the Northern Adriatic. The difficulties associated with the changing trend in the Venice tide gauge around the 1970s Woodworth (2003) meant that this tide gauge was excluded from many of these studies. (Tsimplis & Josey, 2001) extract a regional sea level time series for a number of tide gauges and they find that the sea-level variability is coherent with the winter NAO index for the Adriatic and the whole of the Mediterranean Sea. They also explain the sea level reduction between 1960-1994

observed by Tsimplis & Baker (2000) as a result of increasing atmospheric pressure associated with the NAO pattern. Tsimplis & Rixen (2003) identify correlations between the NAO index and the water temperature and salinity of the upper and intermediate waters of the Adriatic. Grbec et al. (2003) find the maximum salinity of the Adriatic waters to vary with the Mediterranean Oscillation Index, an index related to the NAO index (see Section 3.7.2). Fenoglio-Marc (2002) find consistent trends in the TOPEX-POSEIDON data, tide-gauges and steric values.

However, Tsimplis & Rixen (2002) find that the reconstructed steric heights do not explain the sea-level variability at the tide gauge of Trieste. Tsimplis et al. (2005b) correct the tide gauge values for the atmospheric forcing from a 2-D model and compare the residuals to the steric estimates from the Medatlas database (MEDATLAS Group, 1997). However, the resulting sea level anomalies are inconsistent with the estimated ones.

5.4 Contributions from local vertical land motion

5.4.1 Regional Tectonics

Vertical motions of the solid Earth associated with the regional tectonics surrounding Venice and northern Italy result from the neotectonic expression of the Alpine/African collision. Secular land motion associated with this ongoing tectonic event are expected to be active on time scales between 10^5 and 10^7 years, and will thus combine with glacial rebound to cause the long term, background rate of vertical motion.

The total contraction rate across the European/African plate boundary is between 3 and 10 mm/yr, but closer to 4-8 mm/yr near the Adriatic (DeMets et al., 1994; Nocquet & Calais, 2004). The geometry of the microplates and their boundaries is complex but is separable into distinct, mostly rigid lithospheric domains (see Figure 33). Venice itself lies on a basin trapped between subduction-related thrust belts, where, according to the Quaternary stratigraphy examined with seismic profiles and drill cores, the bedrock has been subsiding on average 1 mm/yr (Kent et al., 2002; Carminati et al., 2005) over the last 1.8 Ma. However, model studies indicate that the tectonic signal should be positive and of the order of 0.1 to 0.4 mm/yr (Di Donato et al., 1999). The most recent regional GPS solutions show little, if any, contractional or shear deformation between Apennines and the Alps across the Po Plain (Serpelloni et al., 2005), suggesting that Venice lies atop a lithosphere that is horizontally stable. However, the geodynamics behind the relationship between the subsidence of the Po plain and subduction is still contentious. Lithospheric dynamics are strongly affected by local forces, likely having a source in the mantle Wortel & Spakmann (2000), as illustrated by the close proximity of strongly extensional (Apennines) and contractional domains (Dinerides).

Vertical motion of continuous GPS sites in Marinca di Revenna, and Bologna suggest they are going down with respect to the nominally stable GPS site in Trieste (Zerbini et al., 2005) However these sites could also be affected by local vertical motions not related to regional tectonics. Preferably data from these sites will be processed along with all the EUREF sites in the region inside a several hundred kilometer radius in order to place these vertical motions in a regional reference frame.

5.4.2 Postglacial rebound

Taking the two locations in Venice and Trieste as an example, in Table 17, we give the predictions for vertical land motion from several models (see Section 3.6.2 for a discussion of the models). The differences are considerable, suggesting that the uncertainties are at least of the order of ± 0.3 mm/yr. However, Woodworth (2003) quotes even larger differences between the various model predictions.

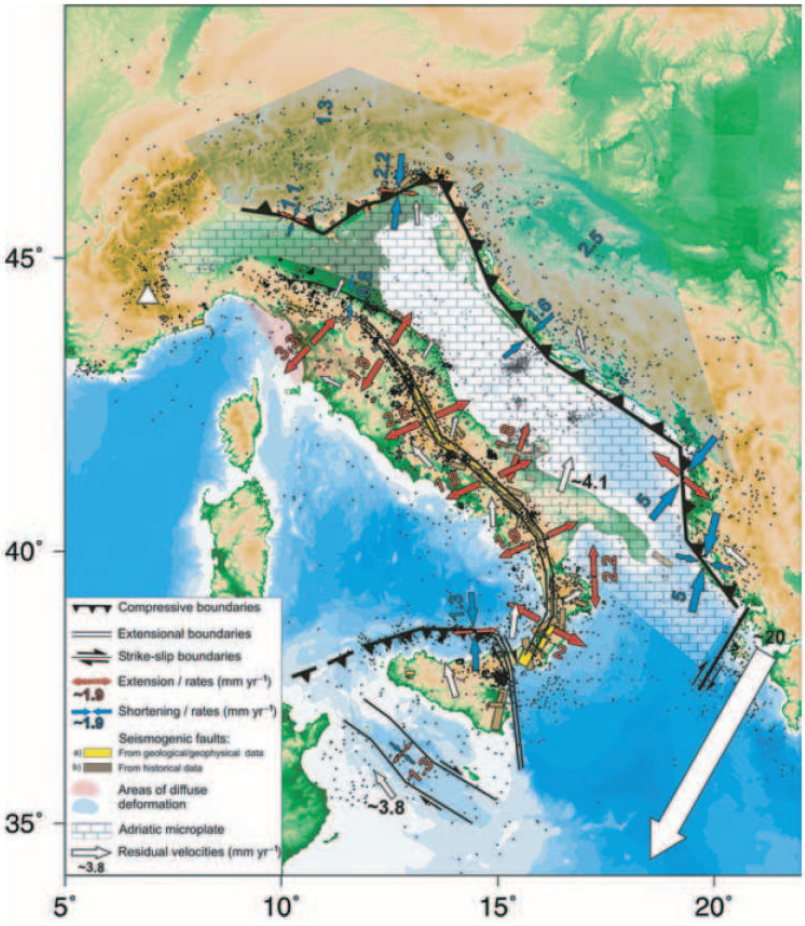

Figure 33: Regional tectonic framework around the city and Lagoon of Venice, Italy. This model shows deformation rates derived from regional continuous and campaign GPS measurements and implies horizontal rigidity of the Po Plain and region surrounding Venice (from Serpelloni et al., 2005).

Model/Author	Venice	Trieste
Peltier, VM2	0.02	0.05
Peltier, VM4	0.24	0.27
Mitrovica	-0.30	-0.28
Di Donato et al. (1999)	~ 0.35	~ 0.35
Stocchi et al. (2005), ICE1+ALP1	~ 0.35	~ 0.40
Stocchi et al. (2005), ICE3G+ALP1	~ 0.07	~ 0.07

Table 17: Predictions of vertical land motion due to post-glacial rebound.
All values in mm/yr. More details to be added.

5.4.3 Present-day mass movements

Mass exchange of the terrestrial hydrosphere with the ocean and, more generally, any mass transport in the Earth system, leads to loads on the Earth surface, which result in deformations of the Earth and associated changes in the Earth gravity field. Present-day changes in the large ice sheets as well as changes in the Alpine glaciers can induce vertical land motion in the Upper Adriatic that may be significant on a level of 0.1 mm/yr. For the Alpine glaciers, the Upper Adriatic is in the near-field, and thus melting of these glaciers is expected to result in a sea-level fall in the northern part of the Adriatic, similar to the signal around the ice sheets on Greenland and Antarctica (see, e.g., Plag, 2006a). However, the models for glacier mass changes are not comprehensive and thus, any estimate of this effect is rather uncertain.

5.4.4 Water extraction

Near the middle of the 20th century, increases in the demand for industrial and municipal water promoted rapid withdrawal of groundwater in several Po Plain localities. Water was withdrawn primarily from the uppermost 350 meters of the Quaternary formation. Between 1950 and 1970 land subsidence in the industrial zone, the southern Lagoon, and the City of Venice, and northeastern of the lagoon were 7, 6, 5, and 2 mm/yr, respectively (Carbognin et al., 2004), but reached as high as 17 mm/yr locally in the industrial zone (Brambati et al., 2003). Total subsidence between 1952 and 1969 averaged 9 cm in Venice. Regionally, this phenomenon was commonly seen in many other localities of the Po Plain as well (Bondesan et al., 2000).

By 1973 limitations on groundwater pumping reversed the trend, and dramatically slowed the anthropogenic component of subsidence. Between 1967 and 1986 subsidence of the industrial zone and Mestre, had slowed to less than 1 mm/yr (Bondesan et al., 2000), a rate that is also confirmed by leveling (1973-1993) and InSAR measurements (1993-2000) (Strozzi et al., 2003).

5.4.5 Gas Extraction

Offshore natural gas extraction fields have the potential to induce subsidence in a broad area that includes the area of the Venice Lagoon. However, modeling suggests that the planned 13 years of gas extraction from this field will result in at most 10 mm of subsidence in Chioggia (southern Lagoon littoral), and the Malmocco inlet, but less significant subsidence in Venice over 25 years (Baú et al., 2000). Most of the subsidence will occur in the Adriatic, to the east of Venice, in a zone 20 km in radius directly above the drilling, and relatively little in the vicinity of the Lagoon itself. While this may not affect the city of Venice itself, it may affect the stability of the littoral in the southern and central part of the Lagoon. This subsidence is expected to be permanent.

5.4.6 Biological/Chemical Soil Processes

The human reworking of the landscape surrounding the Venice Lagoon converted much of the land surface from marshland to farmland over the early 20th century. Dry and hot conditions that are now maintained by drainage of the soil for agriculture are ideal for oxidation of the organic content of the soil, which releases CO2 and causes mass-loss compaction subsidence of the land surface (Gambolati et al., 2005). The irreversible part of the soil chemistry change results in subsidence that has been measured and correlated to temperature and rainfall (Teatini et al., 2004). The dependence of this process on weather and farming activity makes the rate of vertical movement spatially variable and temporally variable from year to year. Between March 2002 and March 2003, approximately 20 mm of total subsidence was attributed to this process by Gambolati et al. (2005). While these effects can cover a large area, they are essentially a shallow process that will not directly affect adjacent areas that are not covered by soils, (for example, the city of Venice). They could, however, appear in remote sensing studies (for example, InSAR) of the hinterland and so the presence of this process should be considered when interpreting these results.

5.4.7 Sediment compaction and loading

The sedimentological record of the Po Plain goes back to pre-Pliocene and is consistent with periods of intermittent pervasive shoaling and transgressive encroachment of the Adriatic.

Five kilometers of Pre-Pliocene, Pliocene, Quaternary deposits include mostly sandy, silty, and clayey layers of alluvial and marine origin. An absence of a large change in porosity with depth over a 950

meter deep-drill core led Kent et al. (2002) to conclude that natural compaction in this sequence is not a major contributor to the long-term subsidence. Modeling by Gambolati & Teatini (1998), however, suggests that the contribution could be larger, as high as 0.5 mm/yr at Venice, under some circumstances, which would make it a substantial portion of the long term rate. This long-term subsidence is likely ongoing and is a part of the vertical motion budget of Venice.

The fact that the land beneath the city of Venice is today above the surface of the Adriatic is an indication that sedimentation rates, with mass sources in the Alps and Apennines, are sufficient to compensate for the long-term subsidence. This it is likely associated with tectonic contraction between the Apennines and stable Europe (Section 5.4.1), and has an average rate over the Quaternary of approximately 0.5 to 1.0 mm/yr (Kent et al., 2002; Carminati et al., 2005). The load of the sediments on the crust has a role in controlling this surface level. Their contribution is included in the long-term rate, and is likely stable from year to year, but could experience variation that is connected to precipitation and erosion rates in the sediment source region.

5.5 Overview

The contributions of the different factors to LSL are summarized in Table 18. In the following, we summarize the main local forcings, that is the LSL changes due to the atmosphere, the ocean, and the vertical land motion.

Atmospheric contribution

The main atmospheric contribution to LSL variations in Venice is at three different time scales, namely (1) a few hours to days, where meteorologically forced seiches, storm surges, and depressions contribute significantly to extreme sea levels, (2) at seasonal time scales, where the atmospheric forcing contributes more than 30% of the observed seasonal cycle, which is mainly due to steric changes in the sea water, (3) at multi-decadal time, where slow changes in the wind field and the mean pressure field induce sea-level trends on multi-decadal or longer time scales close to 1 mm/yr. On the other hand, there seems to be little contribution from the atmosphere on interannual to bi-decadal time scales.

Oceanic contribution

The oceanic and atmospheric contribution to sea level in the Adriatic depends on a) the local water mass characteristics and circulation, b) the regional meteorological forcing (the NAO index been a good proxy) and c) on the hydraulics at the Straits that interconnect it to the Eastern and Western Mediterranean and the Atlantic. The latter have been strongly affected by the sudden changes in the deep water formation in the Eastern Mediterranean (the EMT).

Local and regional forcing appears to be dominating the sea-level signal not only in the northern Adriatic but in the whole of the Mediterranean Sea during the last decades. Thus future sea levels would depend on the behavior of the above mentioned factors, namely, what would the NAO do, how would the other local meteorological patterns change and also how would the North Atlantic Ocean change. Would there be another EMT? Is it an independent phenomenon or is it part of a feedback or adjustment mechanism? We cannot say at the moment. Notably during the last decades the Mediterranean Sea has been cooling in the upper layers as higher than normal pressures prevailed during the winter due to the NAO status. At the same time sea level has been reducing mainly because of the increasing pressures but also because of the cooling. This may have contributed to the EMT which caused, in our view, the sudden rise in sea level during the 1990s. If this is true then the path the future changes will follow is far from clear. However, it is clear to us that it is the local heating of the oceans that matters thus any forecasting model should have enough resolution to show the heat changes at the various basins of the Mediterranean. In addition it should be able to give

Table 18: Local contributions to LSL variation in Venice.

Phenomena	Description	Range
	Atmospheric forcing	
Seiches	Resonant oscillations excited by meteorological forcing, longest period 22 to 23 h.	order 0.5 m amplitude
Storm surges	Meteorologically forced long waves, sub-daily to several days	up to 1.5 m
Seasonal cycle	atmospheric contribution to seasonal cycle is of the order of a few cm, but out of phase with the steric forcing	~ 3 cm
Interannual to decadal	No significant contribution	
Secular	Over the interval 1960 to 2002, negative contribution lowering sea-level rise	order -0.8 mm/yr
	Astronomically forced	
semidiurnal tides	Slightly increasing amplitude range in the 20st century	~ 25 cm in amplitude for M2
diurnal tides	Increase is not statistically significant	~ 15 cm in amplitude for main constituent
fortnightly tides	Appear to be close to equilibrium tides	~ 1 cm in amplitude
monthly tides	Masked by noise, most likely equilibrium tides	< 1 cm in amplitude
semi-annual and annual tides	Completely masked by steric and atmospheric forcing.	< 1 cm in amplitude
nodal tide	Masked by noise, most likely equilibrium	$\sim$ 0.5 cm in amplitude
	Oceanographically forced	
Steric	Changes in the temperature and salinity as observed in the interval from 1958 to 2000 indicate a small negative trend	-0.10 ± 0.15 mm/yr
Ocean circulation	Observed time series show a significant variation on time scales 16 to 17 years. This is most likely oceanographic	~ 2 cm in amplitude
	Vertical land motion	
Regional tectonics	The secular tectonic trend in vertical land motion is not clear, stratigraphy suggest subsidence, while models suggest small uplift	-1 mm/yr to 0.4 mm/yr
Post-glacial rebound	Small secular trend.	0.0 ± 0.3 mm/yr
Present-day mass movements	Can introduce non-linear signals on time scales of the mass load changes.	?, of order 0.1 mm/yr
Water extraction	Considerable non-linear trends, particularly during the first half of the 20st century	max. exceeding 10 mm/yr
Gas extraction	May contribute in the future	order 10 mm total subsidence
Soil processes	Oxidation of peat can lead to subsidence	
Sedimentation	Compaction of sediments leads to subsidence, and so does viscoelastic response to sediment loading, while sedimentation leads to an upward motion of the surface. Anthropogenic changes in sedimentation may have a significant effect but difficult to estimate.	-0.5 mm/yr for compaction

basin-wide estimates of the freshwater budget which defines the salinity of the basin. Finally such forecasts should take into account independently the role of the NAO as it is yet unclear how much of the NAO variability is linked with global warming. It is also suggested that annual values projections are not appropriate and that scenarios and models should have seasonal resolution as the danger of over topping is greater in particular seasons.

Vertical land motion

Over the 20th century, Venice has been subsiding both with respect to regional reference and also in a global reference frame. Over the first half of that century, subsidence was much larger than in the second half. Water extraction related subsidence, which was once a major problem, is now a more

minor player in the issue of Venice subsidence. Although this phenomenon has potential to play a big role in local areas where groundwater extraction is still rapid. Gas extraction is not expected to produce significant subsidence in the city of Venice, but could impact the littoral by ~ 10 mm over the course of drilling and pumping. These estimates are based on detailed modeling of deep compaction associated with the drilling, but have inherent uncertainties. Thus the actual impact could be more or less than what is expected. Chemical oxidation of soils in the hinterland of Venice, can produce significant subsidence, but these effects are shallow and likely contained to the agricultural areas. Rates of vertical movement could be as high as 20 mm/yr, but this is likely a time and spatially variable effect. Taking all these factors in to consideration, those that affect the city of Venice directly are the long-term tectonic motion, and the glacial isostatic rebound.

Table 19: Mass exchange of the ocean with other reservoirs in the global water cycle. *All values are in mm/yr.*

Contribution	Period	Sea-level rise	Source
Mountain glaciers	1960-2000	0.41	Meier & Dyurgerov (2002)
Greenland mass change	1960-2000	0.10 ± 0.05	Plag (2006a)
Antarctic mass change	1960-2000	0.35 ± 0.15	Plag (2006a)
Land water storage	1910-2000	-1.1 to 0.4	Church et al. (2001)
total		-0.24 to 1.26	

6 Global sea-level changes and their effect on the upper Adriatic Sea

6.1 Introduction

Here we consider two contributions to global sea-level changes that have not been taken into account in the previous section, namely the mass exchange of the ocean with the terrestrial hydrosphere and the cryosphere, and the global steric changes, which result from the general warming of the ocean and the freshening of the ocean due to melt water from both sea ice and continental glaciers and ice sheets.

6.2 The global ocean mass balance

Mass exchange with the terrestrial hydrosphere

The current estimates for mass exchange of the ocean with the other reservoirs in the global water cycle are summarized in Table 19. The total contribution is estimated to be between -0.24 mm/yr and $+1.26$ mm/yr.

For the last 50 years, Plag (2006a) estimated contributions of Greenland and Antarctica to a global sea-level rise of 0.10 ± 0.05 mm/yr and 0.39 ± 0.11 mm/yr, respectively. These values are well within the uncertainties of the observed contributions for Greenland and Antarctica as summarized in the Third Assessment Report (TAR) of IPCC (Church et al., 2001), which are 0.12 ± 0.15 mm/yr and 1.04 ± 1.06 mm/yr, respectively. Using the Plag (2006a) estimates and the scaling factors deduced from the fingerprints, we get contributions of -0.02 ± 0.04 mm/yr and 0.54 ± 0.45 mm/yr for the contribution of the Greenland and Antarctic ice sheets, respectively, to LSL changes in the Adriatic.

Similarly, future projected changes in the Greenland and Antarctic ice sheets can be down-scaled to the Adriatic using the scaling factors given above. However, the relatively large uncertainty of the scaling factors needs to be taken into account.

Concerning future contributions from the large ice sheets, we face considerable uncertainties. While until recently, Greenland was considered to be fairly stable, there are now indications that the Greenland ice sheet may be destabilized over a short time scale of a few decades due to melt water reaching the base of the thick ice sheets to cracks forming in the ice sheet (Richard Alley, Bob Thomas, personal communication). This could induce basal sliding and accelerate the pace of Greenland melting considerably (Zwally et al., 2002). As pointed out by Overpeck & others (2005) and Meier et al. (2005), the Arctic ocean is on a trajectory to a new, seasonally ice-free state within the next 100 years, which would transform the Earth system into a state not witnessed in at least a million years. The authors see only few, if any processes or feedback that could stop this process. The consequences

for, for example, the ocean circulation and the heat transport from lower latitudes to the polar region are not yet known.

In the past, rapid melting of Greenland ice is documented in the so-called Dansgaard-Oeschger events and these events make a rapid melting of Greenland ice under favorable conditions realistic. These events are documented in temperature proxy from three ice cores for the last 140 kyr, showing δ-O events in the northern hemisphere but not the southern hemisphere. These δ-O events are related to rapid fluxes of fresh water into the ocean. Dansgaard-Oeschger events are rapid climate fluctuations during and at the end of the last ice age. There were 23 such events identified between 110,000 and 23,000 years BP.

In the Northern Hemisphere, they take the form of rapid warming episodes, each followed by gradual cooling. The pattern in the Southern Hemisphere is different, with slow warming and much smaller temperature fluctuations. Indeed, the Vostok core was done first, and the existence of D-O events was not widely recognized until the Greenland (GRIP/GISP2) cores were done later; after which there was some reexamination of the Vostok core to see if these events had somehow been "missed." The processes behind the timing and amplitude of these events (as recorded in ice cores) are still unclear.

Dansgaard-Oeschger events are closely related to Heinrich events. Heinrich events disrupt North Atlantic Thermohaline Circulation (most likely due to fresh water fluxes into the ocean), causing cooling in the Northern Hemisphere. Cooler climate increases ice cover, consequently increasing surface albedo - more of the incoming solar energy is reflected back to space - and promoting further ice growth. There is evidence to suggest Dansgaard-Oeschger events were globally synchronous (Bond et al., 1999).

For the Antarctic ice sheet, considerable uncertainties exist with respect to the present day changes and the distribution of regions with growth and melting. Thus, Davis et al. (2005) find indications for a snowfall driven growth of the East Antarctic ice sheet, while Thomas et al. (2004) sees indication of an increased melting of the West Antarctic ice sheet.

6.3 Steric contribution

The steric contribution arise from both global warming and a freshening of the ocean due to melt water added to the ocean. From sea ice melting alone, Wadhams & Munk (2004) estimated a global signal of 0.6 ± 0.18 mm/yr, though the uncertainties may be much larger. The thermal signal alone is estimated by Lombard et al. (2005) on the basis of the steric datasets of Levitus et al. (2000) and Ishii et al. (2003) to be of the order of 0.3 ± 0.1 mm/yr for the period from 1960 to 2000, and of the order of 1.2 to 1.6 mm/yr for the time interval from 1993 to 2003.

The thermosteric signal is, however, rather complex. The warming signal over the last 40 years shows a vertical structure that varies widely over the ocean (Barnet et al., 2005), and changes in advection combine with surface forces to give the overall picture. Hegerl & Bindoff (2005) point out that there is clear evidence that the warming trend in the ocean is human-induced. In order to assess the future development, complex climate model studies are required (Barnet et al., 2005).

Taking into account that the North American and European summer climate is subject to Atlantic Ocean forcing acting on multi-decadal time scales (Sutton & Hodson, 2005), it can be expected that ocean warming has a significant long-range affect on the climate in the Adriatic and, consequently, for the development of the LSL in Venice. Only detailed regional climate studies can help to bring more light into these regional and global processes affecting the Adriatic.

6.4 Overview

Summing up the different contributions, we get a global sea-level rise due to mass and volume changes r of

$$\begin{aligned} r &= \text{mass} + \text{thermosteric} + \text{freshening} && (22)\\ &= (0.51 \pm 0.75) + (0.3 \pm 0.1) + (0.6 \pm 0.18) && (23)\\ &= (1.41 \pm 1.03) \end{aligned}$$

which is well in agreement with the observed value in the range from 0.5 to 2.0 mm/yr.

7 Reanalysis of the vertical land motion in the upper Adriatic area

In order to determine the vertical motion of the land surface with respect to the Earth's center of mass, that is, the quantity that affects LSL, we have analyze all of the available GPS data around the vicinity and region of the city of Venice. GPS data are currently available, are sufficiently precise and can be placed into local or global reference frame. The data considered include the IGS and EUREF continuous sites within 300 km of the city of Venice (see Table 5 for the 36 individual site names). These data are available on the Internet.

The interpretation based on review of other indications from geodetic, tectonic and geological study of the region of Venice suggests that we should expect a rate of subsidence of approximately 1 to 2 mm/yr. The claim of present ground stability of the city of Venice, as put forward by Tosi et al. (2002) does not contradict this, since all the data considered by them (in particular leveling, InSAR and tide gauges) only provide information concerning relative stability with respect to nearby or regional reference points, but no or very weak links to vertical motion in a global, geocentric reference frame.

In our analysis, station coordinates were estimated every 24 hours using the GIPSY/OASIS II software in the precise point positioning mode (Zumberge et al., 1997) and the precise orbits from the U.S. Jet Propulsion Laboratory. Ionosphere-free combinations of carrier phase and pseudorange were processed every 5 minutes. Estimated parameters included a tropospheric zenith bias and two gradient parameters estimated as random-walk processes, and station clocks estimated as a white-noise process. Carrier phase ambiguity resolution (Blewitt, 1989) was performed on all data to improve positioning precision, followed by transformation of the daily solutions to ITRF2000 Altamimi et al. (2002) using Jet Propulsion Laboratory GISPSY/OASIS II transformation parameters (x-files). The orbit and transformation files are all freely available on the Internet.

In this way, time series have been obtained for 36 sites out of the 43 listed in Table 5, since in some cases data were not available in the archive. The lengths of the obtained time series vary between 0.9 to 8.5 years. After the GPS data processing, raw time series were scanned for outliers that can potentially contaminate velocity estimates obtained through least-squares estimation. All point-positions with uncertainties greater than 10 mm, and all positions different than the median position by over 100 mm in horizontal or 60 mm in vertical were omitted from the analysis. The remaining time series show that in some cases significant offsets could be perceived and often associated with physical changes in the GPS receiver or antenna configuration. We omitted the sites WETT, MDEA because their time series were very short. We omitted data prior to the latest offset before calculating rates. Horizontal and vertical rates in the ITRF2000 reference frame (Table 20 and Figure 34) were obtained from these time series.

Regional filtering (Blewitt, 2004) was then performed on the time series in order to reduce the effects of daily reference frame noise on the change in shape of the network. This algorithm assumes that all sites are moving with a constant velocity. Prior to this filtering, times with fewer than 3 site positions were omitted since they have insufficient data for calculating a translation of the reference frame for that day. The algorithm also omits positions that were more than 10 times the one standard deviation uncertainty of the position away from the expected position based on the estimated velocity. As a result of the filtering, RMS scatter in the positions around the constant velocity was reduced across the network by 43%. The horizontal and vertical filtered rates are shown in Table 20.

The velocities listed in Table 20 have uncertainties that vary from 0.1 to 3.0 mm/yr. These uncertainties are conservative values that have been obtained by augmenting the formal uncertainty that were obtained based an assumption of white noise in the GPS time series, with two additional noise components. The first additional component is an estimated effect from random walk noise, a type

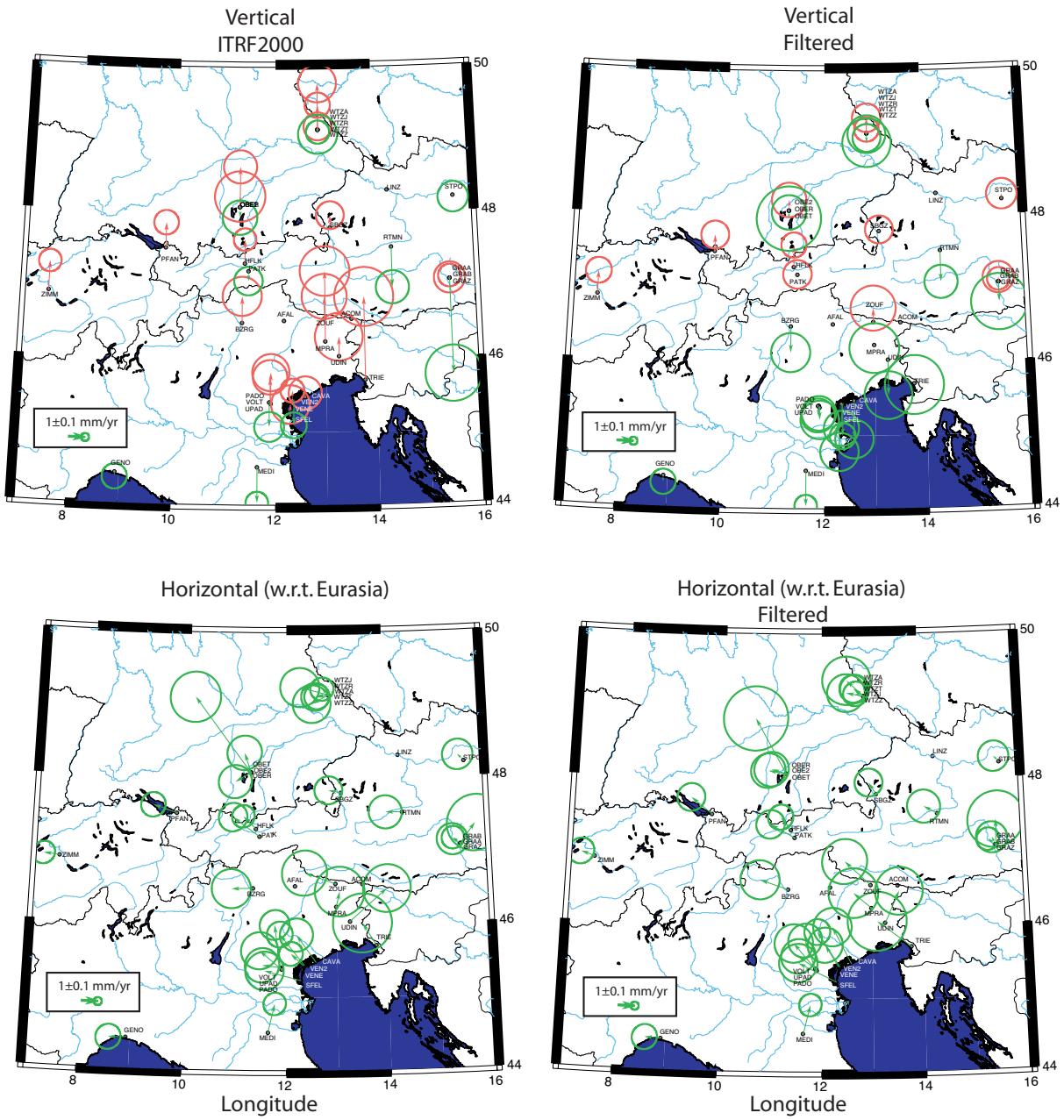

Figure 34: Velocities of GPS stations.

Left: Unfiltered velocities. Right: Filtered velocities. All velocities have been reduced by a rigid body rotation with the pole taken from Kreemer et al. (2003).

that has been shown to exist in GPS data time series and is sometimes associated with momument effects (Agnew, 1992; Langbein & Johnson, 1997; Williams et al., 2004). We use an amplitude of 1 mm/sqrt(T), where T is the length of the time series in years. It is possible that the amplitude of this annual signal varies from site to site, but we choose a constant intermediate value here of 1 mm. Site-specific values may be used in the future, once the amplitude of the seasonal signal has been estimated. Both of these noise contributions tend to increase the uncertainty of shorter time series to a greater degree than longer time series. The second noise component comes from velocity bias owing to the presence of annual signal in the GPS data that is not accounted for in the rate calculation (e.g.,

Table 20: Vertical and horizontal velocities at GPS stations.

Station	**Long.**	**Lat.**	**ITRF2000**			**Filtered**		
			Ve	**Vn**	**Vu**	**Ve**	**Vn**	**Vu**
ACOM	13.5149	46.5479	22.6 ± 1.1	16.2 ± 1.1	-5.5 ± 1.1	19.0	16.0	0.4
AFAL	12.1745	46.5271	36.3 ± 1.1	16.3 ± 1.1	-10.5 ± 1.1	32.7	15.9	-4.7
BZRG	11.3368	46.4990	19.7 ± 0.6	14.8 ± 0.6	1.3 ± 0.6	19.1	15.5	-2.3
CAVA	12.5827	45.4794	20.1 ± 0.6	16.7 ± 0.6	0.3 ± 0.6	20.3	17.3	-3.1
GENO	8.9211	44.4194	19.9 ± 0.4	15.0 ± 0.4	-0.6 ± 0.4	20.0	15.1	-0.7
GRAA	15.4935	47.0672	22.8 ± 0.9	15.7 ± 0.9	-6.7 ± 0.9	21.8	16.0	-1.3
GRAB	15.4935	47.0671	21.5 ± 0.5	14.4 ± 0.5	-0.5 ± 0.5	21.5	14.8	0.2
GRAZ	15.4935	47.0671	21.2 ± 0.3	14.7 ± 0.3	0.0 ± 0.3	21.2	14.7	0.0
HFLK	11.3861	47.3129	20.1 ± 0.4	15.7 ± 0.4	1.7 ± 0.4	20.3	15.8	1.5
MEDI	11.6468	44.5200	22.2 ± 0.3	16.8 ± 0.3	-2.8 ± 0.3	22.2	16.8	-2.8
MPRA	12.9877	46.2408	22.8 ± 0.8	15.3 ± 0.8	2.5 ± 0.8	20.1	15.7	-0.5
OBE2	11.2799	48.0862	19.5 ± 0.5	14.1 ± 0.5	2.7 ± 0.5	19.5	15.0	0.5
OBER	11.2799	48.0862	20.2 ± 0.5	16.1 ± 0.5	-0.8 ± 0.5	19.6	15.0	-0.3
OBET	11.2777	48.0843	16.8 ± 1.0	19.1 ± 1.0	1.2 ± 1.0	18.6	18.9	-1.1
PADO	11.8961	45.4112	20.0 ± 0.5	15.1 ± 0.5	1.8 ± 0.5	20.1	15.8	-0.8
PATK	11.4602	47.2080	19.2 ± 0.4	16.0 ± 0.4	-1.2 ± 0.4	19.2	15.7	-0.2
PFAN	9.7847	47.5153	18.9 ± 0.4	15.4 ± 0.4	1.6 ± 0.4	19.1	16.1	1.0
RTMN	14.3433	47.5246	20.4 ± 0.5	14.3 ± 0.5	-3.7 ± 0.5	20.5	15.0	-2.6
SBGZ	13.1104	47.8034	20.3 ± 0.4	14.7 ± 0.4	0.7 ± 0.4	20.7	15.4	-0.1
SFEL	12.2913	45.2300	18.8 ± 0.6	15.5 ± 0.6	0.9 ± 0.6	18.8	16.1	-2.7
STPO	15.6329	48.2031	21.4 ± 0.5	14.6 ± 0.5	-0.7 ± 0.5	21.1	14.7	0.2
TRIE	13.7635	45.7098	22.0 ± 0.9	16.0 ± 0.9	3.0 ± 0.9	19.1	16.5	-0.4
UDIN	13.2530	46.0372	25.1 ± 0.7	16.7 ± 0.7	-1.2 ± 0.7	22.6	16.9	-3.2
UPAD	11.8779	45.4067	21.1 ± 0.5	17.8 ± 0.5	-1.9 ± 0.5	20.7	16.8	-0.8
VENE	12.3320	45.4370	20.5 ± 0.5	15.7 ± 0.5	0.4 ± 0.5	20.5	16.3	-2.3
VOLT	11.9109	45.3846	19.8 ± 0.6	16.2 ± 0.6	2.5 ± 0.6	19.8	16.7	-1.0
WTZA	12.8789	49.1442	19.9 ± 0.4	14.4 ± 0.4	0.0 ± 0.4	20.1	15.1	-0.5
WTZJ	12.8789	49.1442	19.5 ± 0.6	14.1 ± 0.6	4.0 ± 0.6	19.6	14.9	0.1
WTZR	12.8789	49.1442	20.4 ± 0.4	14.9 ± 0.4	-0.5 ± 0.4	20.2	14.7	0.1
WTZT	12.8789	49.1442	20.0 ± 0.4	14.5 ± 0.4	1.6 ± 0.4	20.2	15.2	0.9
WTZZ	12.8789	49.1442	17.8 ± 0.7	15.6 ± 0.7	1.2 ± 0.7	19.7	15.9	-0.9
ZIMM	7.4653	46.8771	19.2 ± 0.4	15.2 ± 0.4	2.0 ± 0.4	19.3	15.4	1.5

Blewitt & Lavallée, 2002).

We tested the sensitivity of the velocities to the presence of older data and to the effect of changing the number of stations over time, since this can influence the effects of regional filtering on the vertical rates. To do this we first omitted all data prior to January 1, 2000 and repeated our analysis of the vertical motion in both ITRF2000 and in the regionally filtered solution. The results shows that the net effect of including data before year 2000 on the vertical velocity of the sites is small, that is, not significant for most sites. For 5 sites out of the 33 for which filtered rates were obtained (GENO, HFLK, MEDI, OBER, and PATK), however, significant changes in vertical rate were observed between the complete time series and the time series post January 1, 2000, possibly indicating that they did not move at a constant rate for their entire time span or that the regional filtering had a non-consistent

Figure 35: Monumentation of the sites CAVA, SFEL, VOLT and VENE.
Upper two pictures are the site VENE. Lower pictures are from left to right: CAVA, SFEL, VOLT. The site VENE sits on top of a long pole that is braced by a wooden railing which may experience seasonal swelling or shifting.

effect over time owing to the change in network strength over time. In order to determine which effect was stronger, we tested the effect of regional filtering on the vertical GPS velocity by differencing the vertical rates before and after the filtering. We found that for sites with time series greater than 4.5 years long, the rate difference is less than 1 mm/yr, however for time series less than 4 years in length the differences can be larger, up to 5 mm/yr when the time series is less than 2 years long. This indicates that shorter time series are more susceptible to the effects of noise and that it is difficult to extrapolate the true rate from the apparent rate based on shorter time series. However, in this test we also found that for time series made shorter by truncation, filtering tended to bring the velocity closer to the value obtained by considering the full time series if the GPS network was strong, but not so well if the network was weak (as in the earliest times). This implies that filtering should provide improved velocity estimates for sites with shorter time series installed after the year 2000, when a greater number of sites have offset-free time series.

The horizontal components of the velocities (Figure 34 and Table 20) are consistent with previous studies of the geodetic velocity field around Italy, southern Europe and the Mediterranean. We have

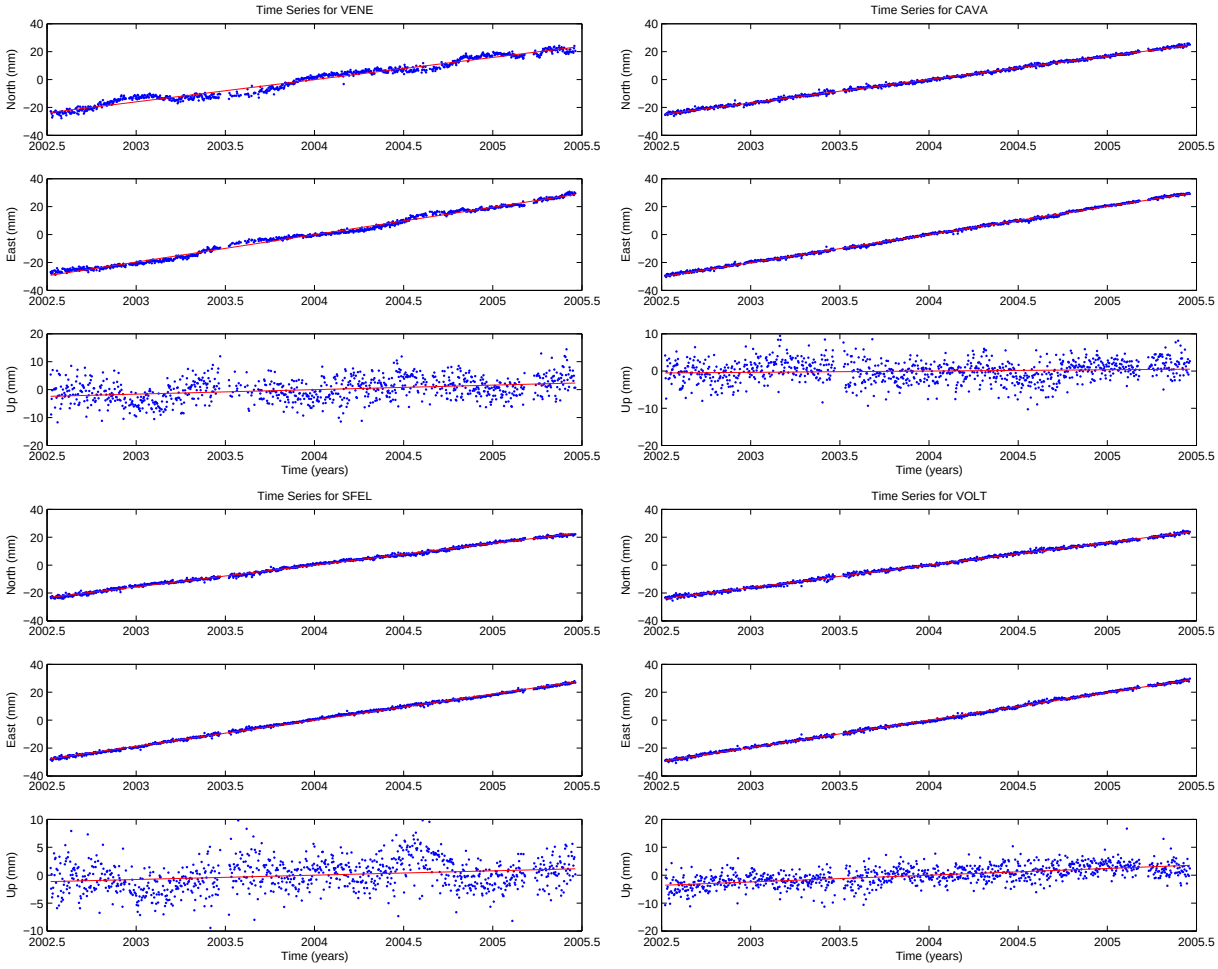

Figure 36: Time series of displacements.

Time series of horizontal and vertical displacements for VENE, CAVA, SFEL, and VOLT after regional filtering has been applied using just the position data from VOLT, CAVA and SFEL to define the daily reference frame transformation. This shows that the sites VOLT, CAVA and SFEL have very linear trends, with very little annual component of motion in the horizontal or vertical components. The site VENE has a relatively large oscillation in both horizontal and vertical components.

solved for a uniform horizontal strain field and found a barely significant approximately north-south contraction (4.5 ± 2.0 mm/yr) across the network between longitude 9°E 15°E, which is equivalent to a 2.3 mm/yr gradient in velocity across the network in the north-south direction. The velocities in Figure 34, are shown in Eurasian fixed reference frame obtained by rotating the horizontal velocities according to the pole of Kreemer et al. (2003). This rotation does not affect the vertical component of velocity and is used to make geographic changes in the horizontal GPS velocities more clear.

The vertical motion of the GPS site VENE is -1.5 mm/yr with respect to the geocenter and -1.1 mm/yr with respect to the neighboring sites VOLT on the Po Plain. This subsidence is not quite as rapid as at the northern and southern ends of the Venice Lagoon, where the sites SFEL and CAVA have vertical rates of -2.0 mm/yr and -2.4 mm/yr, respectively.

Initially, VENE was the only site in the City and island of Venice available for our analysis that is capable of quantifying vertical motion with respect to the geocenter. Thus this site takes on particular importance in the study of LSL rise in the city. InSAR and leveling results all show that some parts or all of the Venice Lagoon are subsiding by between 1 and 3 mm/yr with respect to some other points within the geographic area of the respective studies. However, all InSAR and leveling studies

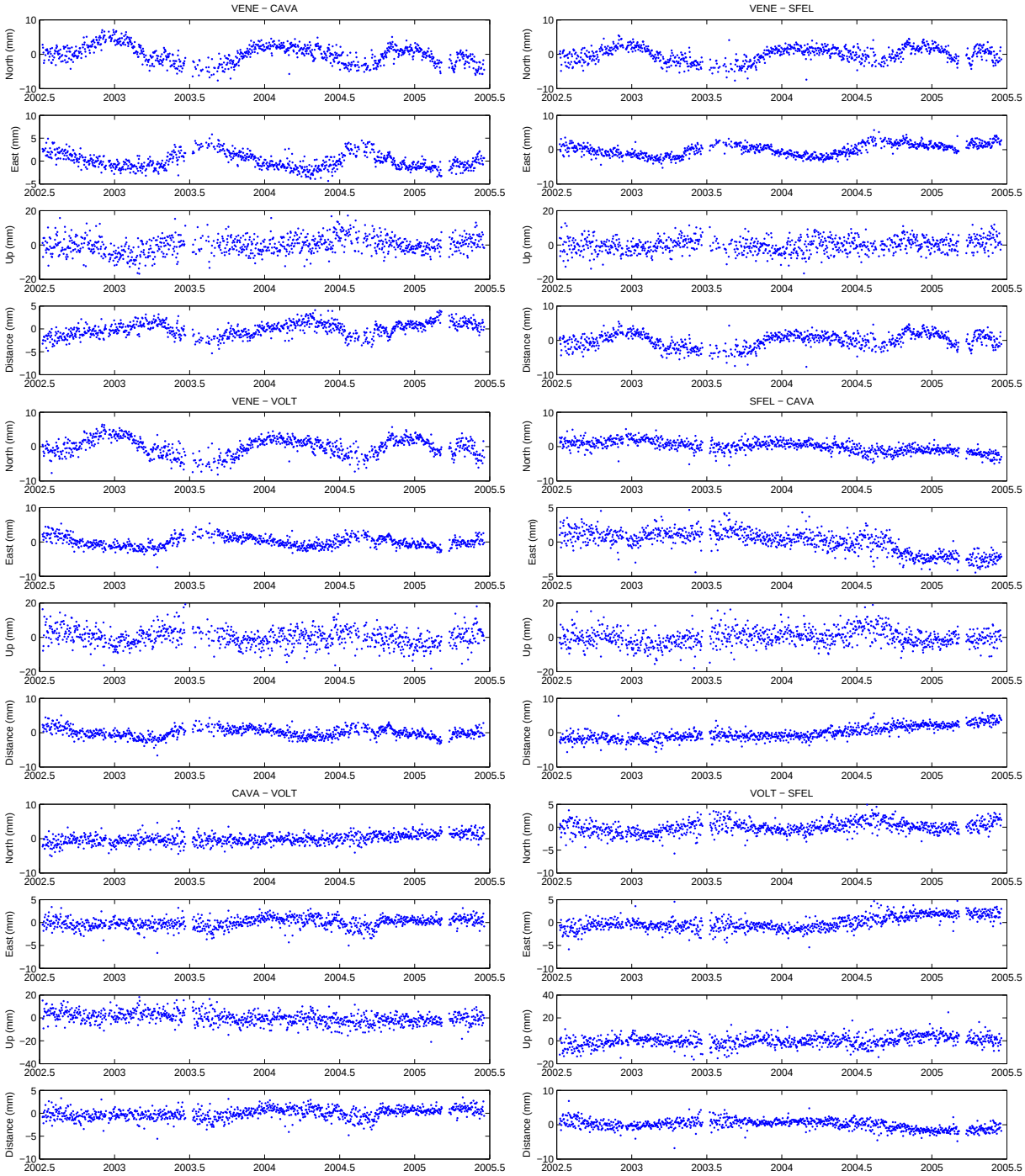

Figure 37: Time series of displacement differences.

Time series of differences of the horizontal and vertical displacements for each pair of sites in the VENE, VOLT, CAVA, SFEL cluster.

are not well connected to a global reference frame and therefore have large uncertainties with respect to the geocenter. Since the site VENE has been suspected of instability owing to the quality of its monumentation (Figure 35), we have analyzed the relative motion of VENE with respect to its three closest neighboring sites VOLT, CAVA and SFEL, which have monumentation that are considered of high quality (Figure 35).

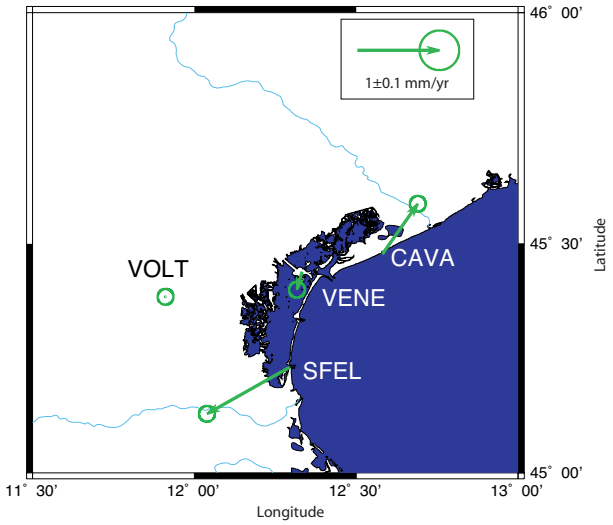

Figure 38: Velocities of Venice Lagoon GPS sites relative to VOLT. *Horizontal motion of GPS sites VENE, SFEL, CAVA, and VEN2 with respect to the site VOLT. Ellipses show the 95white noise.*

The results of this analysis suggest that the site VENE experiences a greater level of annual oscillation than most other stations, which is present in both its horizontal and vertical coordinates (Figure 36). This is consistent with the antenna being mounted on the top of a narrow pole, and braced by a wooden structure that can experience seasonal variations in its position and shape (Figure 35). The amplitude of the horizontal annual motion with respect to SFEL, CAVA and VOLT is < 10 mm peak to peak, and shows a linear trend with respect to VOLT of < 0.2 mm/yr (Figure 37). Trends of VENE with respect to CAVA and SFEL can be attributed to horizontal motion of CAVA and SFEL (Figure 38) with respect to VOLT, one another and the global frame of reference. Vertical annual oscillation of VENE with respect to SFEL, CAVA and VOLT has an amplitude of 10-20 mm peak to peak, compared to 5-10 mm peak to peak for the differences of vertical coordinate for the other three sites (Figure 37). This shows that the site VENE is likely to be the one that provides most of the oscillation in the horizontal component.

While VENE shows greater temporal variability than the sites SFEL, CAVA and VOLT, its time series are not characterized by large steps, trends, or other irregularities that can occur when a site has demonstrably unstable monumentation. Much of the annual motion of VENE could be accounted for by solving for annual terms in addition to long-term trends, that is, linear velocities, from the time series. However, the addition of a cluster of additional continuous GPS sites on highest quality monuments distributed into several different portions of the city of Venice is the best solution for long term monitoring of the city with respect to the geocenter.

Unfortunately, for the sites nearest the city of Venice (UPAD, PADO, VOLT, SFEL, VENE, CAVA) the length of the time series after adjustment for offsets were between 2.9 and 3.9 years, and therefore the consistency of vertical rates is not optimal. We recommend that in the future, when attempting to measure vertical rates, GPS equipment changes are avoided for at least 5 years, or even better, indefinitely.

For the study of the stability of VENE, CVN also made available the GPS observations from a second site in the city of Venice, which is denoted here as VEN2. We have also analyzed the data from VEN2, which spans from 1999 to 2005. The time series of VEN2 show a larger than usual annual signal in the horizontal components, comparable to those seen at VENE. This is particularly obvious in the difference between this site and the other four stations (Figure 39). The vertical component for VEN2 is rather noisy with several periods of deviation up to 20 mm from the mean. After filtering VEN2 with the regional filter defined by VOLT, CAVA, and SFEL, the vertical rate at VEN2 is found to be -2.4 ± 0.4 mm/yr, which is comparable to the vertical rates of the other sites.

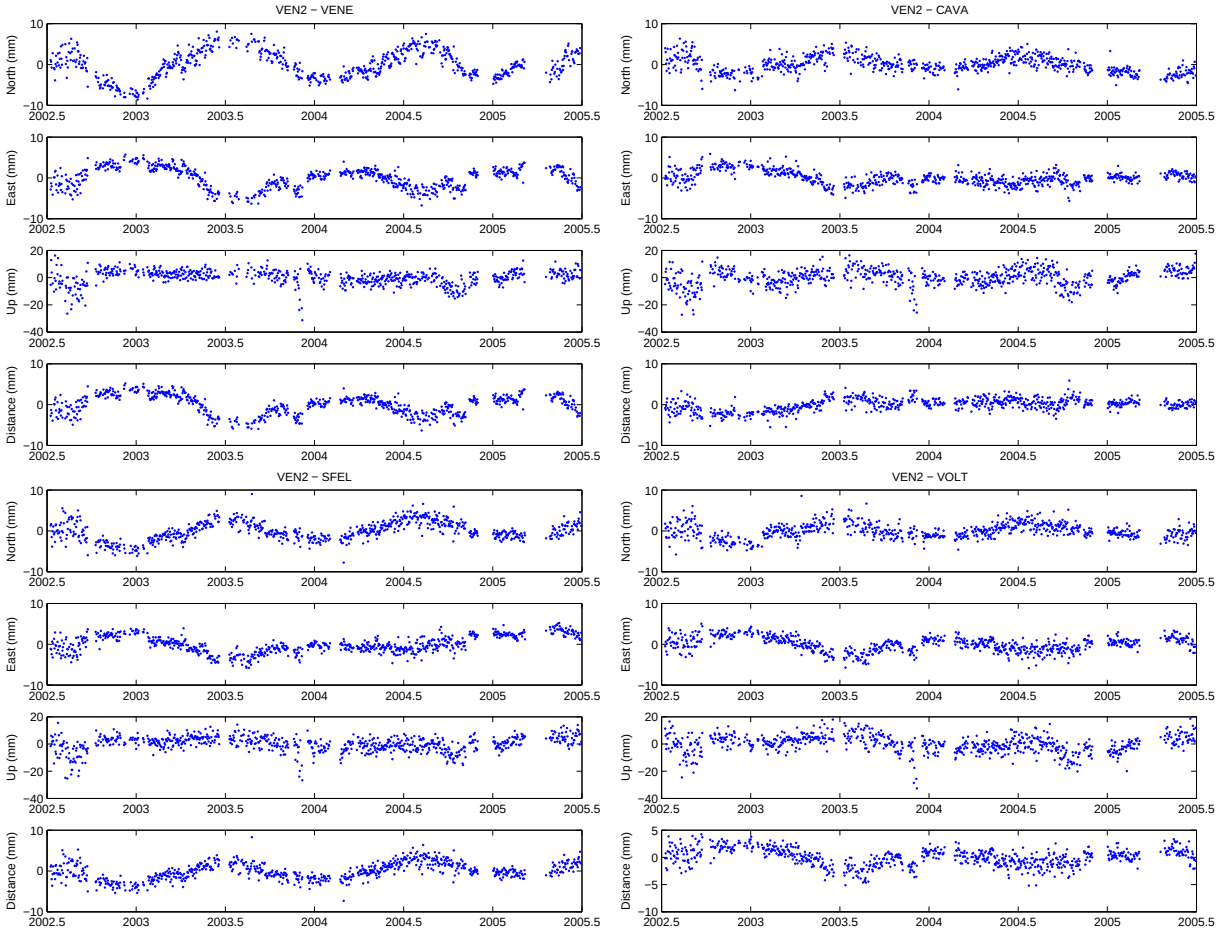

Figure 39: Time series of displacement differences with respect to VEN2.

Time series of differences of the horizontal and vertical displacements for each pair with VEN2 and one of the stations VENE, VOLT, CAVA, and SFEL.

Considering that the time series for the stations close to Venice are relatively short, we will use the filtered vertical rates in the scenarios discussed below. The regionally filtered velocities are less affected by long-period common modes and give velocities closer to the ITRF2000 velocities than those determined from the unfiltered time series.

At the GPS stations directly around Venice, the mean vertical velocity are

(24)

$$\begin{aligned} \text{CAVA} &= -2.4 \pm 0.4 \text{mm/yr} \\ \text{VENE} &= -1.5 \pm 0.3 \text{mm/yr} \\ \text{VEN2} &= -2.4 \pm 0.4 \text{mm/yr} \\ \text{SFEL} &= -2.0 \pm 0.4 \text{mm/yr} \end{aligned} \tag{25}$$

The overall average of these values is -2.0 ± 0.3 mm/yr. Thus the Lagoon of Venice appears to be moving towards the geocenter (downward) at about -2.0 mm/yr.

A rather crucial uncertainty in the GPS-determined vertical velocities originates from a significant uncertainty in the relation between ITRF and the physical geocenter, that is, the *Center of Mass* (CM) of the complete Earth system. The ITRS is defined to have its origin in the CM. However, due

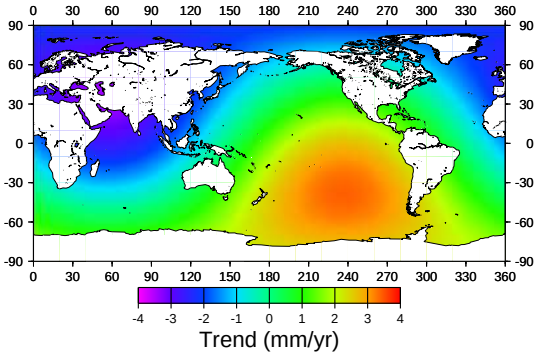

Figure 40: Effect of differential motion between the origins of ITRF and IGP-00 on local vertical motion. *The vertical motion is given for a differential velocity between the origin of ITRF2000 and IGS-P00, that is a reference frame determined by GPS alone, which is estimated by Kierulf & Plag (2006) as* $\delta\vec{v} = (-1.5, -2.2, -2.1)$ *mm/yr. The mean vertical motion over the complete surface of the ocean is 0.4 mm/yr. From Plag (2006d).*

to the particular sensitivity of the different techniques with respect to geocenter variations, there is a time-dependent difference between the origin of ITRF and the CM. This is particularly obvious in the different origins that IGS has chosen for the reference frames implicit in the different IGS products (Kierulf & Plag, 2006). The effect of the unknown differential movement between ITRF origin and CM, which is estimated to be of the order of 2 to 3 mm/yr, on observations of the surface displacements, sea level, and comparative studies between local gravity changes and vertical displacements is severe, as it demonstrated in Figure 40. This figure shows the effect on height of the translation between ITRF2000 and the frame IGS-P00, which is defined by the IGS precise products. For this frame, the vertical velocities in central Europe would be about 2 to 3 mm/yr larger than in ITRF2000. Thus, in IGS-P00, the vertical velocity of the Venice Lagoon would be close to zero.

Table 21: Results of multivariate regression analysis.

Station	N	Airpressure mm/Hpa	Wind stress, east mm/(m/s)$^(3/2)$	Wind stress, north mm/(m/s)$^(3/2)$	Trend mm/yr
VENEZIA PDS	508	-18.098 ± 0.014	-6.841 ± 0.020	8.083 ± 0.030	1.342 ± 0.004
TRIESTE	528	-17.484 ± 0.014	-7.885 ± 0.029	16.925 ± 0.048	0.966 ± 0.004
KOPER	344	-17.297 ± 0.017	-9.575 ± 0.038	17.183 ± 0.059	0.500 ± 0.006
ROVINJ	501	-16.675 ± 0.014	-8.619 ± 0.026	11.199 ± 0.040	0.591 ± 0.004
BAKAR	504	-18.334 ± 0.014	-10.344 ± 0.035	19.633 ± 0.059	0.536 ± 0.004
SPLITRTMARJANA	490	-16.593 ± 0.016	-4.389 ± 0.021	3.968 ± 0.016	0.469 ± 0.004
SPLITHARBOUR	504	-16.690 ± 0.016	-3.969 ± 0.021	4.224 ± 0.016	0.342 ± 0.004
DUBROVNIK	499	-16.126 ± 0.018	-1.956 ± 0.016	2.863 ± 0.011	0.878 ± 0.004
BAR	319	-15.892 ± 0.022	-4.102 ± 0.033	6.546 ± 0.026	2.631 ± 0.007

Table 22: Effect of atmospheric forcing on seasonal cycle.

The table gives the amplitudes and phases of the annual and semi-annual harmonic constituents as determined in the linear regression according to eq. (26). We also give the difference between the secular trend b for the fit given in Table 11 and the trend b' determined in the regression analysis, that is, $\hat{b} = b - b'$. The coefficient $\hat{b}$ describes the effect of the local atmospheric forcing on sea level.

Station	Mon.	A_{Sa}	ϕ_{Sa}	A_{Ssa}	ϕ_{Ssa}	$\hat{b}$
VENEZIA PDS	508	71.439 ± 0.098	140.075 ± 0.078	26.623 ± 0.092	148.934 ± 0.198	-0.844 ± 0.004
TRIESTE	528	69.056 ± 0.094	139.434 ± 0.078	26.266 ± 0.089	148.130 ± 0.195	-0.566 ± 0.004
KOPER	344	68.105 ± 0.119	141.000 ± 0.100	25.945 ± 0.110	144.172 ± 0.244	-0.300 ± 0.006
ROVINJ	501	71.885 ± 0.100	141.248 ± 0.080	24.585 ± 0.092	145.362 ± 0.215	-0.591 ± 0.004
BAKAR	504	76.274 ± 0.098	125.849 ± 0.074	28.171 ± 0.091	144.882 ± 0.185	-0.236 ± 0.004
SPLITRTMARJANA	490	63.732 ± 0.108	126.667 ± 0.098	24.494 ± 0.093	148.869 ± 0.217	-0.469 ± 0.004
SPLITHARBOUR	504	66.103 ± 0.107	125.021 ± 0.093	25.019 ± 0.092	147.809 ± 0.210	-0.542 ± 0.004
DUBROVNIK	499	67.813 ± 0.116	127.638 ± 0.098	20.918 ± 0.092	153.708 ± 0.253	-0.578 ± 0.004
BAR	319	69.644 ± 0.146	123.362 ± 0.121	22.718 ± 0.115	152.247 ± 0.290	-1.331 ± 0.007

8 Reanalysis of the sea-level variations in the upper Adriatic Sea

The tables and figures in this Section represent the results from a regression analysis taking into account the full local atmospheric forcing. A full description of the analysis and the interpretation of the results will be added.

Main focus in the reanalysis of the sea-level data was on the assessment of the local atmospheric contribution to the LSL variations. Plag (2006c) used an extended regression analysis to study the local atmospheric effect on secular trends on a global basis. The regression analysis uses

$$h(t) = A_{\mathrm{Sa}} \sin(\omega_{\mathrm{Sa}} + \phi_{\mathrm{Sa}}) + A_{\mathrm{Ssa}} \sin(\omega_{\mathrm{Ssa}} + \phi_{\mathrm{Ssa}}) + a + bt + \alpha p(t) + \beta\sigma_{\mathrm{E}} + \gamma\sigma_{\mathrm{N}} \qquad (26)$$

to represent the monthly mean sea-level values, which includes an annual and semi-annual harmonic constituent, a linear trend and contributions from air pressure and the two horizontal wind-stress components (as defined in eq. (18)).

Monthly mean values of the air pressure and the wind-stress components were computed from the ERA40 reanalysis data provided by the ECMWF. The ERA40 dataset has a spatial and temporal resolution of $2.5^\circ \times 2.5^\circ$ and 6 hours, respectively. Monthly means of σ_2 and σ_3 are computed as averages of the six-hourly values of these quantities.

Figure 41 shows the results of the regression analysis for each of the Adriatic stations having sufficient data in the time interval covered by the ERA40 data. At all sites, the regression model explains more than 75% of the variance of the monthly mean sea levels. At most stations, the response to air pressure is the largest single contribution. The regression coefficients for air pressure are significantly larger than the inverted barometer response of -10 mm/HPa (Table 21 and Figure 42), and indicate a dynamic response of the Adriatic to air-pressure forcing even at time scales of months and longer. For the northern Adriatic stations, the wind-induced LSL variations are larger than for the southern Adriatic stations.

Comparing the amplitudes and phases of the annual and semi-annual constituents for the regression with the atmospheric forcing included (Table 22) to those obtained for the regression without atmospheric forcing (Table 10 on page 51), we see that the atmospheric forcing reduces the amplitude of the annual constituent in sea level while increasing the amplitude of the semi-annual constituent. For both constituents, the atmospheric forcing shifts the phase to a latter maximum. Thus, the part of the seasonal cycle in LSL not attributed to local atmospheric forcing follows much closer to the annual air temperature variation than the full seasonal cycle does.

Table 22 also gives the part of the observed LSL trend that is attributed to local atmospheric forcing. For all stations, this contribution is negative and ranges from -0.2 mm/yr in Bakar to -0.8 mm/yr in Venice and even -1.3 mm/yr in Bar. The LSL trends decontaminated for the local atmospheric forcing (Table 21) thus are considerably larger than the observed LSL trends. Over the time interval from 1958 to 2001 the combined effect of air-pressure and wind forcing appears to have lowered sea level by 1 to 5 cm, thus off-setting a sea-level rise significantly.

This result is in agreement with the findings of Tsimplis et al. (2005b), who used a hydrodynamical model forced by air-pressure and wind forcing deduced from the NCEP reanalysis data to study the effect on sea-level trends in the Mediterranean. Their conclusion is that the atmospheric forcing reduced sea level in the time window considered.

In Section 3.3.1, we indicated that the fresh water influx provided, in particular, by the River Po may control some of the oceanic contributions to sea-level variations (see Figure 11 on page 30). Therefore, we also carried out a regression, where the flux was included as an additional forcing. However, the results were only marginally improved, with small contributions assigned to the fresh water forcing. In particular, the decadal variations in the residual remained largely unchanged (Figure 43). We also noted above a similarity of the integrated river flux with the decadal variation in sea level. However, using the integrated river flux in the regression instead of the actual flux observations does not improve the results (Figure 43, right diagrams).

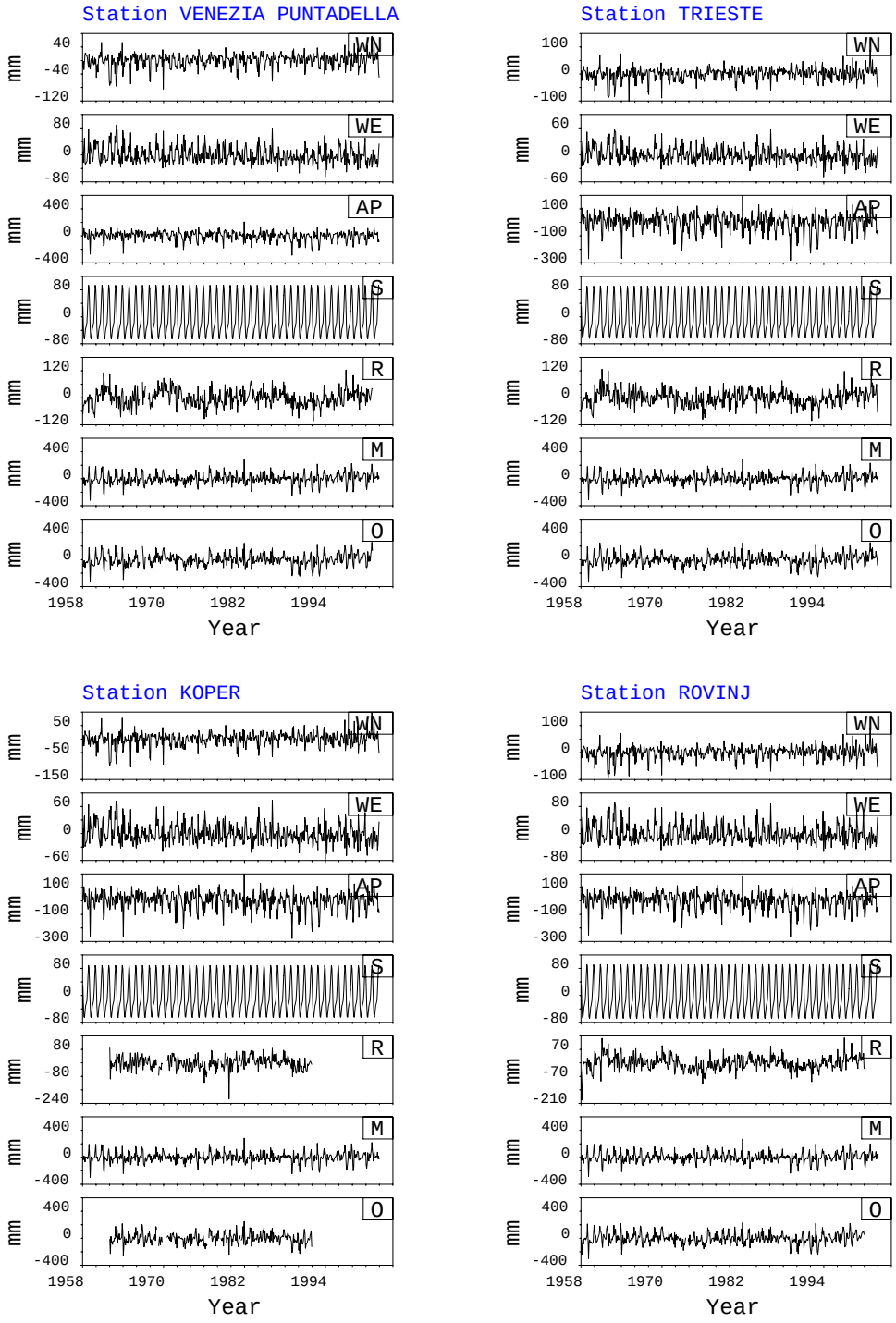

Figure 41: Multiregression models for Adriatic tide gauges.

O, M, and R give the observations, the regression model and the residual, respectively. S is the sum of the annual and semi-annual constituent, AP, WE, and WN are the contributions from air pressure, east component of wind stress, and north component of wind stress, respectively.

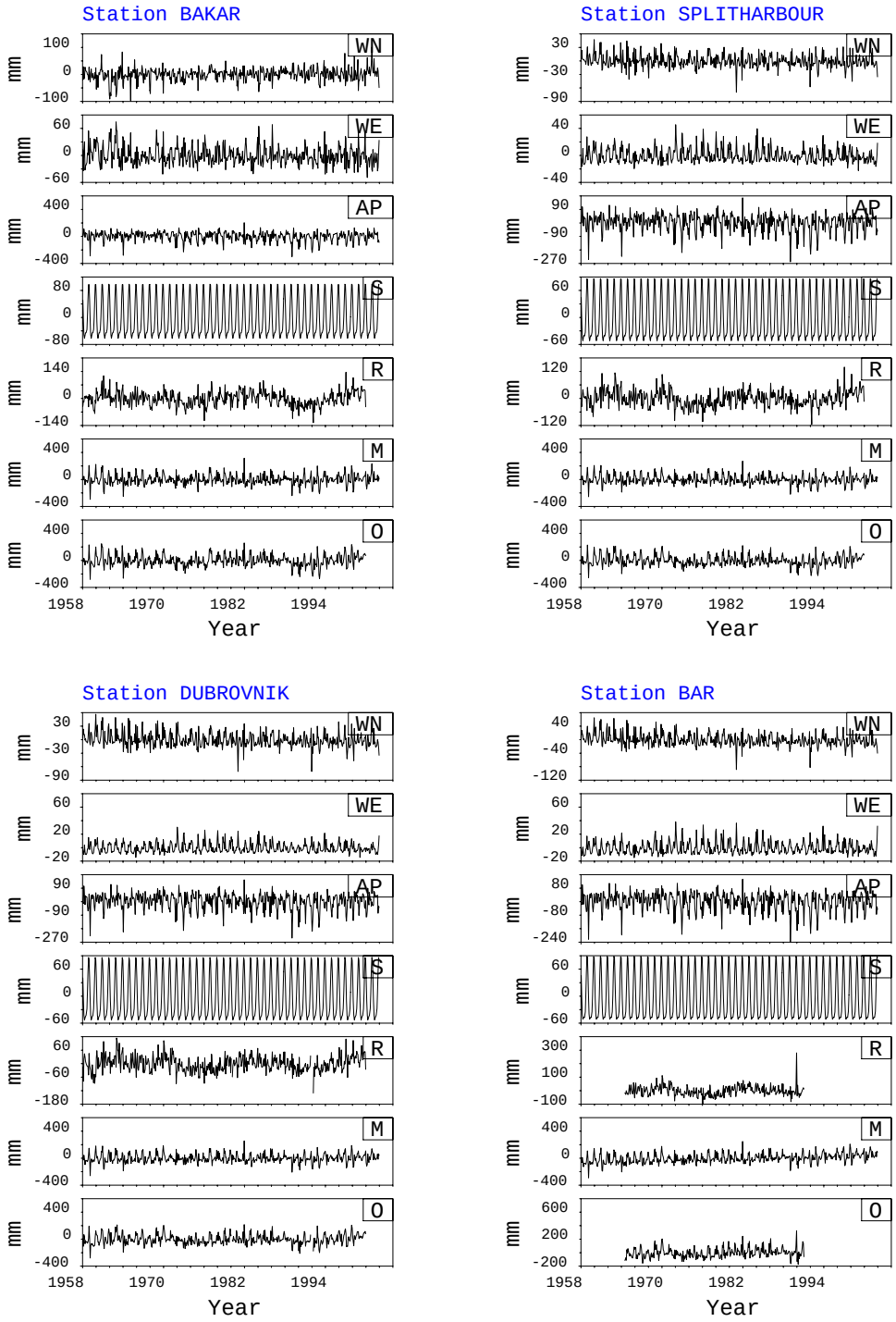

Figure 41 continued.

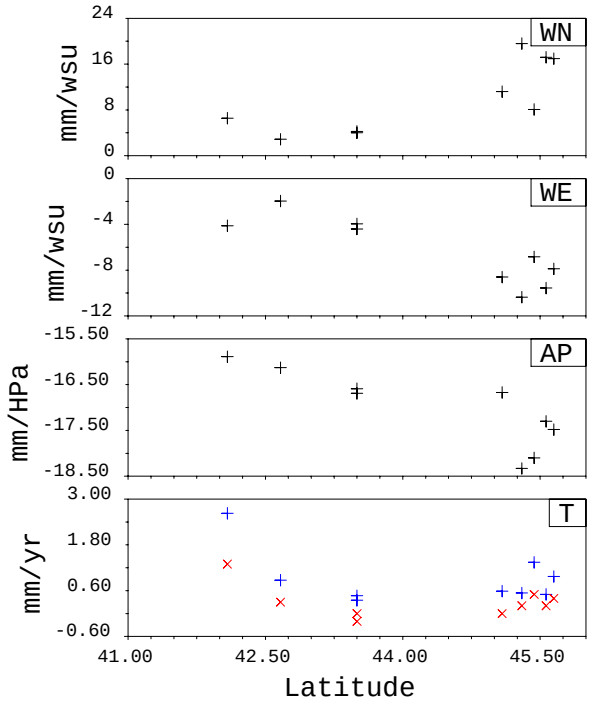

Figure 42: Multiregression coefficients.

From top to bottom, the regression coefficient for wind stress north (WN), wind stress east (WE), air pressure (AP) are shown. The lower diagram displays the trend (T) as determined in the full regression model (blue crosses). For comparison, the trends determined from the data without taking into account atmospheric forcing are shown as red x. Wsu stands for wind-stress units and is in $(m/s)^{(3/2)}$.

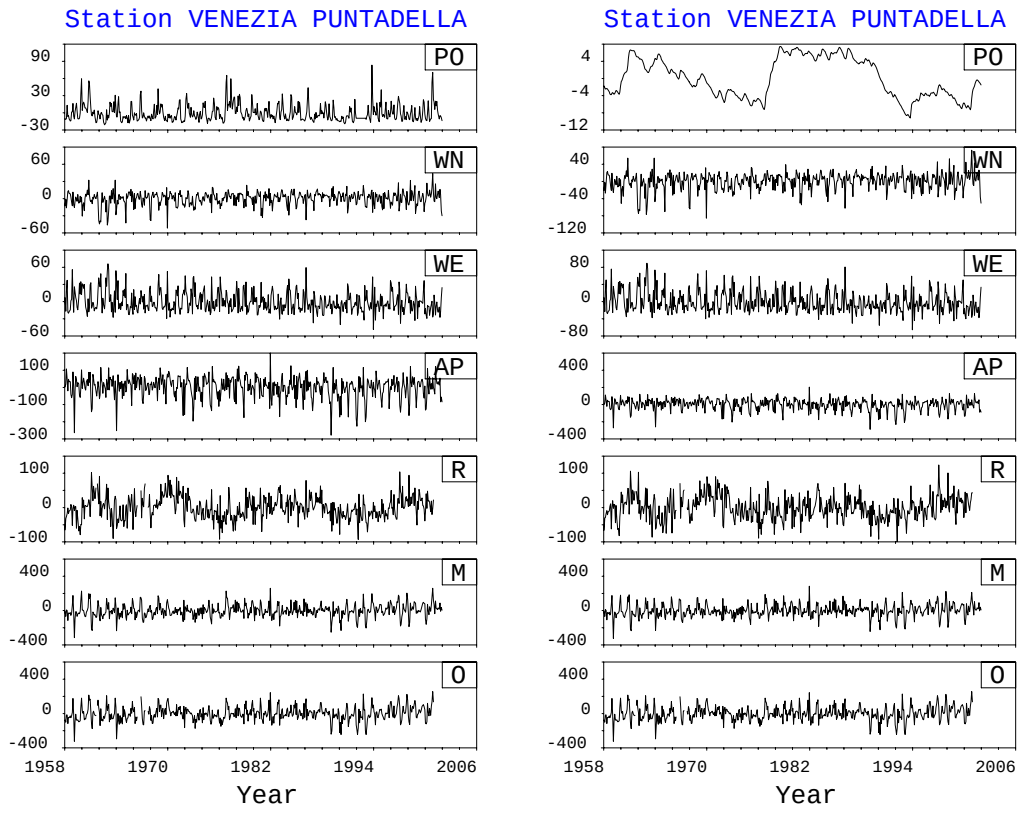

Figure 43: Regression for Venice including fresh water influx.

Model and symbols are as in Figure 41 but with the fresh water influx as indicated by the River Po influx included. The diagram denoted by PO shows the resulting contribution attributed to the river influx. Left: Regression result for a regression including the flux for River Po. Right: regression results for a regression including the integrated flux for River Po.

9 Appraisal of sea-level rise scenarios for Venice

9.1 Critical review of the current sea-level rise scenario for Venice

The current sea-level rise scenario was accepted in 1999 on the basis of a study carried out by Co.Ri.La (1999). This study had the goal to examine *the peculiar regional characteristics of the eustatic scenarios due to global change* (translation by M. Di Donato). Here the term "eustatic" is used, which today is widely considered to be inappropriate to describe sea-level variations. The spatially highly variable fingerprints of all forcing factors affecting sea level is now widely acknowledged and this nature of sea-level changes need to be taken into account in the synthesis of LSL scenarios.

The study proposed three different sea-level scenarios, which we describe here used in the terms defined in Section 2.1 (page 12):

A **Subsidence only:** Based on 20 years of data, it is deduced that there is no contribution due to oceanic and atmospheric forcing and the observed rise of 0.44 mm/yr is attributed solely to subsidence of the land. This results in an estimate of a LSL rise of 4.4 cm by 2100.

B **Subsidence and LSL as in the** 20^{th} **century:** It is assumed that in addition to subsidence there is a contribution of 1.2 to 2.0 mm/yr which is attributed to a global average sea-level rise continuing as in the 20^{th} century. This leads to a LSL increase of 16.4 to 24.4 cm by the year 2100.

C **Subsidence + sea-level rise scenarios from Warrick et al. (1996):** In addition to scenario A, different climate change effect according to the IPCC assessment (Warrick et al., 1996) are added, which leads to three different scenarios with total LSL rises of 16.4 cm (most likely for scenario IS92c), 21 to 23 cm (scenario unclear), 31.4 cm (for scenario IS92a assuming changes in aerosol after 1990), and 53.4 cm (for scenario IS92e assuming constant areosol after 1990) over the next 100 years.

The scenario proposed by Co.Ri.La (1999) for the LSL rise in Venice was then 21 to 23 cm rise by 2100.

We have the following comments on these scenarios:

A First of all, we do agree with the assessment that LSL in the Adriatic over the last approximately 40 years was stagnating or rising very slowly. In the first part of the time window, sea level was actually falling and in the last 15 years rising more rapidly. Moreover, the relative rise at the northern Adriatic locations with respect to those further south on the eastern coast is consistent with a modeled tectonic and post glacial signature in sea level of the Adriatic (Di Donato et al., 1999), though the uncertainties are too large to firmly conclude that this consistency is not accidental. Moreover, the assumption that there is no oceanic and atmospheric contribution to sea level over the last 20 to 40 years is not in agreement with the evidence from atmospheric data and modeled ocean response to atmospheric forcing. Thus, this forcing appears to have offset temporarily a larger LSL trend present before approximately 1960 (see Chapter 8).

B The global average sea-level rise of the last 100 years is a rather uncertain quantity, which may well be in the interval from 0.5 to 2.5 mm/yr (Taking the full range indicated in Church et al., 2001; Plag, 2006a). However, the specific location of the Adriatic in the semi-enclosed Mediterranean makes it very unlikely that Venice will experience a LSL rise consistent with the global average. Moreover, based on the knowledge collected since 1999 it is by now widely

accepted that over the last fifty years increasingly changes in the mass balance of the ocean have taken place, which render an extrapolation of a (poorly determined) global average into the future inappropriate.

C The authors chose to use only a subset of the scenarios from the Warrick et al. (1996) assessment, restricting the range of sea-level rise by 2100 to 12 to 49 cm, while Warrick et al. (1996) point out that the 'best estimates result in a range from 38 to 55 cm, while the total range is 20 is 96 cm. Moreover, the IPCC assessments have stated repeatedly that all scenarios have to be considered as equally likely futures. The epistemic uncertainty in our scientific understanding, which leads to a set of different plausible assumption, as well as the aleatory uncertainties associated with the randomness of the relevant processes and the models used for predictions do not provide a scientific basis for selecting one of the scenarios or a small range of them as more likely than others. It is also pointed out here, that the estimates of global sea-level rise given by Warrick et al. (1996) were in general confirmed by Church et al. (2001), who obtained a range of 0.09 to 0.88 m with a central value of 0.48 m. Today it is widely accepted that the different forcing factors will lead to spatially highly variable LSL changes in the time up to 2100 (compare, e.g., Figure 11.13 in Church et al., 2001). Therefore, we have to stress that the estimates of a global sea-level rise due to climate change can only be used to determine the boundaries of LSL rise scenario in Venice, without any reliable indication of what the actual trajectory of LSL at Venice will turn out to be during the 21^{st} century.

9.2 Critical review of global sea-level rise scenarios

In order to assess the state of knowledge with respect to the scenarios of future global sea-level changes, we can look at the changes in these scenarios over the three assessment reports addressing sea-level changes, namely Warrick & Oerlemans (1990); Warrick et al. (1996); Church et al. (2001).

In Warrick & Oerlemans (1990), main conclusions with respect to sea level in the 20^{th} century were that global sea level had been rising with 1.0 to 2.0 mm/yr, and that the main causes were thermal expansion, as well as melting of mountain glaciers and Greenland ice margin. For the 21^{st} century, scenarios for sea-level rise by 2070 had a range from 21 to 71 cm with a best estimate given as 44 cm. Most of the increase was attributed to thermal expansion, while the polar ice caps were considered as minor contributions.

In Warrick et al. (1996), past sea-level rise was consider to be in the range from 1.0 to 2.5 mm/yr, thus allowing for a slightly larger range. The possible causes for this rise included now also the ice caps and ice sheets, in addition to the causes identified by Warrick & Oerlemans (1990). Concerning projection of the sea level by 2100, the extreme range of all scenarios covered the interval from 13 to 94 cm. Using best-estimate model parameters, the range is given with 38 to 55 cm increase by 2100. The main causes were seen in thermal expansion, melting of mountain glaciers, and melting of the ice caps. The contribution from the large ice sheets was considered as minor, but a large uncertainty was attached to this contribution.

Church et al. (2001) found a sea-level rise of 1.0 to 2.0 mm/yr for the 20^{th} century, and like the two previous reports, they pointed out that this range is larger than the rise in previous centuries, while no indication for acceleration in the 20^{th} century is found. In terms of forcing factors, they consider thermal expansion as a major contribution. Mountain glaciers and ice caps as well as the Greenland and Antarctic ice sheets also contribute positively to the sea-level rise, while exchange with the continental hydrosphere comes in with a large uncertainty ranging from -1.1 to $+0.4$ mm/yr. The scenarios for the sea-level rise by 2100 are uncertain with respect to the contribution from Greenland

and Antarctica and see the major contribution in thermal expansion and mountain glacier melting. The total range is from 11 to 77 cm in sea-level rise by 2100.

In summary, we can state that the estimates for the 20^{th} century sea-level rise are remarkably stable and so are the major forcing factors consider to be responsible for this increase. Likewise, considering the large uncertainties in some of the forcing factors, particularly the large ice sheets, the scenarios for the sea-level rise in the 21^{st} century are also surprisingly stable. This stability of the estimates and scenarios from report to report can be taken as indication for a well developed point of view and approach to the problem. However, the stability does not rule out that some major uncertainties have been overlooked.

A candidate process able to introduce large changes in the scenarios could be increased melting of the two large ice sheets in Greenland and Antarctica. The discussion in the cause of the preparation of the Fourth Assessment Report seems to indicate that increasingly, the option of increased melting of both the West Antarctic ice sheet (Thomas et al., 2004) and the Greenland ice sheet Zwally et al. (2002) is considered realistic.

9.3 Possible future sea-level scenarios for Venice over the 21^{st} century

Initially, it is emphasized here that there is considerable uncertainty concerning future LSL changes and the range of possible changes that might occur over the 21^{st} century. The uncertainty arises from three different sources. The first one is the epistemic uncertainty, that is the uncertainty in our knowledge of the processes affecting LSL and how these factors will evolve in the future. Thus, we are required to make different assumptions with respect to these processes, their relevance, and their future development. Each set of assumptions will lead to a different scenario. Since these assumptions are associated with an epistemic uncertainty, we have little scientific basis to assign probabilities to these scenarios. Therefore, the scenarios derived here are "plausible futures", and similar to the IPCC assessments, we point out that all the scenarios considered here must be considered as "equally plausible". In the future, it might be possible to move to probabilistic predictions of sea-level changes.

A second source of uncertainties arises from the randomness of the processes affecting sea level. Thus, even if we would have complete knowledge of all relevant processes, their randomness would add aleatory uncertainties to the predictions and thus to the scenarios.

Finally, a third source of uncertainty comes from the errors associated with the measurements and analysis that we used to determine numbers for the individual factors contributing the sea-level changes. In particular, this is the case for the present-day contributions caused by the different factors. These uncertainties arising from measurement errors and analysis procedures can be associated with a probability distribution. In the following, we will make an attempt to distinguish between the uncertainties arising from observation errors and the aleatory uncertainties on the one side, and the epistemic uncertainties on the other side. The latter lead to different scenarios, while the former result in error bars attached to these scenarios.

We do not attempt to generate a comprehensive set of plausible scenarios. Considering that the goal of the study is an appraisal of the existing sea-level rise scenarios for Venice, we aim to establish a few plausible scenarios, which will provide the background against which the existing scenarios, and in particular the adopted scenario, can be assessed.

The scenarios set up here are based on our understanding of the past sea-level changes, as described in the previous chapters of the report. Moreover, we take the global sea-level scenarios provide in the TAR (Church et al., 2001) and consider their potential contributions to local sea-level rise in the Adriatic. A major uncertainty comes from the fact that sea-level variations in semi-enclosed and

marginal seas are likely to differ from the variability in the open ocean. For the Mediterranean, the loss of water through evaporation minus precipitation and river runoff is balanced through water entering the Mediterranean through the Strait of Gibraltar. Thus, in addition to the steric variations in the Mediterranean, addition of water mass and internal circulation, the sea level in the Mediterranean also depends on the hydraulic control of the water exchange through the Strait of Gibraltar.

The scenarios are separated into a high frequency and low frequency part, with the first one representing changes due to tides, seiches, storm surges and tsunamis, and the second one representing the changes resulting from steric changes, mass changes, and vertical land motion (see the corresponding eq. (8) and (9), respectively, on pages 14 and 15). Main weight is on the later one, describing the low-frequency changes in mean sea level, however, the importance of the former one describing the high-frequency contributions from tides and extremes is emphasized here.

We will also consider a precautionary scenario based directly on the global scenarios, adding 50% to them to allow for worst case regional oceanic fluctuations, as well as the local vertical land motion. This approach was suggested by Hulme et al. (2002) for the UKCIP02 scenarios, which were developed for climate impact assessment and adaptation planning in the U.K. This approach gives fairly plausible top-end scenarios for mean sea level. However, the current planning for the flood defense in London takes an even more conservative approach assuming a total rise in maximum flooding of 3 m by 2100 (composed of 1 m of mean sea-level rise and 2 m of increase in storm surges, Tim Reeder, Environment Agency, England, personal communication, see also Lowe & Gregory, 2005).

9.3.1 Scenario components

In the following, we will discuss detailed contributions to the scenario summing all factors with their uncertainties. We first consider the high frequency part (eq. 8) and then low frequency part (eq. 9).

For eq. (8), which describes sea-level variations around the mean LSL, we have to consider tides, surges, and seiches. Changes in these contributions to LSL lead to changes in the extreme sea levels above mean LSL. The changes in maximum total sea levels are then the sum of the maximum sea levels above the mean plus the changes in the mean.

Tides:

We anticipate an increase of 10% in amplitude for an increase of 1 m in mean sea level (derived from a doubling of amplitude for a rise of 10 m determined by Lionello et al. (2005)). This results in a total increase of the tidal amplitude of about 3.5 cm.

Surges:

From the available material, it is not clear how much of the increase in number of sea-level events exceeding a given height is due to increase of sea level and tidal range (both already taken into account) and how much results from increase in extreme weather conditions. The main increase in the number of sea-level extremes (that is, high water levels) took place in the first half of the 20^{th} century, when local mean sea level was rising above normal due to increased subsidence (see Table 12 in Section 4.7.2 on page 61). Over the second half of the 20^{th} century, the meteorological conditions changed towards less extreme winds, resulting in lower extreme sea levels above mean sea level (see, e.g., Pirazzoli & Tomasin, 2002; Raicich, 2003). Studies of the sea-level extremes under changing climate conditions do not indicate a statistically significant increase in surges. However, currently, there is little scientific evidence available that would provide a sound bases for scenarios for these extreme sea levels in the Adriatic.

Seiches:

Seiches are also related to meteorological conditions, that is, the occurance of Bora. Their maximum height as well as the frequency depends on these conditions (see, e.g., Vilibic, 2000). Over the 20$^{\text{th}}$ century, the frequency of the Bora has sharply decreased at Trieste and also in Venice (see Pirazzoli & Tomasin, 2002, and the reference therein). However, it is not clear whether the maximum amplitudes have also decreased.

In summary, we have to state that scenarios for the high frequency part of LSL changes are rather uncertain. Besides a slight increase in the tidal range, past observational evidence indicates that the number of extreme sea level above the mean due in particular to storm surges and seiches have decreased over the interval from 1960 to at least 1990. Meteorological studies show that conditions for storm surges have decreased. Nevertheless, as significant increase in the number and amplitude of extreme sea levels above mean LSL over the 21$^{\text{st}}$ century cannot be excluded. In fact, model studies indicate an increase of extreme weather conditions over the 21$^{\text{st}}$ century leading to more frequent extremes. Thus, for the high-frequency part, scenarios from no increase in number and amplitude of extreme sea level above mean LSL to an increase of a few tens of centimeters appear realistic.

It is worthwhile to mention that the number of events with total LSL (that is, high frequency plus low frequency part) exceeding certain thresholds has been more or less constant over the period from 1960 to 1990 with a slight increase afterwards (see Table 12 on page 61. Thus, it appears that a slow LSL increase has counterbalanced any decreasing number and magnitude of storm surges.

Any increase in mean LSL will inevitably increase the number of events where LSL exceeds a certain threshold. The impact of a mean LSL rise on extreme total LSLs can be easily demonstrated by comparing the number of events exceeding a certain threshold for a given observational period to the number of extremes we get by shifting the record to a level corresponding to an assumed LSL rise.

Turning to the lower frequency part, we have to consider all factors given in the corresponding equation, that is, eq. (9) (see page 15):

Steric contribution:

The global predictions for the steric contributions given in Table 11.11 in TAR indicate that based on the IS92a scenario, the global steric effect is of the order of 0.09 to 0.37 m by the years 2090, which we here express as 0.23 ± 0.14 m. This effect is difficult to down-scale to the Adriatic. Adding an uncertainty of $\pm 50\%$ for these estimates for regional amplifications results in a value of 0.23 ± 0.21 m as a plausible estimate for the steric contribution.

Ocean currents:

The observational evidence for changes in the ocean currents indicates that on a multi-decadal time scales, we can expect variations of several cm in the Adriatic, which are most likely caused by phenomena such as the EMT. There is little evidence that these changes would lead to larger effects on the decadal mean sea level. Therefore, we assume an effect of 0.00 ± 0.03 m for the effect of current changes.

Atmospheric circulation:

Over the past 40 years, atmospheric circulation has contributed up to -2.5 cm to the sea-level changes. This is likely to be part of a century scale oscillation. Therefore, we assume a contribution of 0.03 ± 0.03 m cause by changes in the atmospheric circulation.

Ice sheets:

The TAR reports a contribution of 0.01 to 0.03 m for Greenland and -0.07 to -0.01 m for Antarctica. The uncertainty of these values are rather larger, so that we here assume globally averaged contributions of 0.02 ± 0.02 m for Greenland and -0.04 ± 0.04 m for Antarctica. Using the scaling factors discussed in Section 3.6.3 of 1.4 and -0.2 for the Antarctic and Greenland contributions, respectively,

we get for Venice IPCC-based predictions of -0.004 ± 0.004 m and -0.056 ± 0.056 m for the Greenland and Antarctic contributions, respectively.

It is pointed out here that Plag (2006a) found the contribution of of the Antarctic and Greenland ice sheets to globally averaged sea-level changes over the time window 1958 to 2000 to be 0.39 ± 0.11 mm/yr and 0.10 ± 0.05 mm/yr, respectively. These values are in agreement with the IPCC estimates for the past contribution of the ice sheets. Compared to these estimates, the predicted contributions appear to be considerably smaller. Moreover, these predicted values do not include any instability of the West Antarctic ice sheet or increased melting of the Greenland ice sheet. In order to account for these case, we also consider the values of 0.50 m and 0.25 m for the contribution of the Greenland and Antarctic contribution, respectively, as still rather conservative estimates for these plausible events. For the two accelerated events, we get -0.10 m and 0.35 m for Greenland and West Antarctic contribution.

Glaciers:

The IPCC TAR gives in Table 11.12 a range of 0.05 to 0.15 m from melting of continental glaciers. The uncertainty is estimated to be 40%, so that we here assume a value of 0.10 ± 0.07 m as the contribution from continental glaciers. Considering that only a minor amount comes from the glaciers in the Alps, the local amplification is not large and we assume here $\pm 20\%$ for the local amplification, leading to 0.10 ± 0.10 m.

Changes in the terrestrial hydrosphere:

Here we consider only regional and global effects, while local effect are assumed to be included in the vertical land motion estimates. Extrapolating the estimates for the past 100 years (Table 11.8 in TAR) into the future results into a contribution of -0.035 ± 0.075 m by 2090. Allowing $\pm 50\%$ for local amplification gives an estimate of -0.035 ± 0.113 m.

Vertical land motion:

As discussed in Section 7, the vertical motion of the Venice Lagoon as determined by GPS in ITRF2000 is on average about -2.0 ± 0.5 mm/yr, where the uncertainty results from the determination of the trends on the basis of the GPS time series. However, due to the considerable uncertainty in the relation between the ITRF2000 origin and the geocenter, the actual uncertainty of the vertical motion with respect to the geocenter is much larger. Moreover, the comparison of ITRF2000 to a GPS-only determined reference frame indicates that the ITRF2000 trends in the Adriatic may be biased to lower values. Therefore, we will consider two scenarios for the vertical land motion, namely the ITRF2000 scenario with a vertical motion of -2.0 ± 2.0 mm/yr, and a IGS-P00 scenario with a vertical motion of 0.0 ± 2.0 mm/yr.

Extrapolating these two rates forward over the next 100 years we obtain the contributions of the vertical land motion to LSL rise of $+0.20 \pm 0.20$ m and 0.00 ± 0.20 m for ITRF2000 and IGS-P00, respectively. Here we assume that the vertical land motion observed over the last three years with GPS is representative for the next 100 years.

However, the past was dominated by anthropogenic effects, inducing considerable subsidence. The distance of Venice from earthquake generating fault systems suggests that non-linear seismic cycle effects are not to be expected. Thus the largest potential source of vertical perturbation is from human activity, through reactivated pumping of groundwater. Although legal controls on ground water extraction are now in place, we cannot anticipate how future possible needs of additional water might be pursued. For example a future severe drought could change society's priorities and motivate a return to pumping. If this were to happen then a vertical rate that was observed in the past could return (for example, 9 cm in 17 years or ≈ 0.5 cm/yr). This extreme scenario could cause subsidence of 5.0 mm/yr, but it is not clear if subsidence of this rate could be sustained for one century, which

would produce surface subsidence of one half meter. Nevertheless, the numbers given here emphasize the importance of keeping the current regulations of groundwater extraction sustained.

Another non-linear contribution to vertical land motion can result from present-day or past mass transports in the vicinity of the Lagoon. Potential candidates are regional deloading due to groundwater and oil extraction as well as melting of the Alpine glaciers. Changes in sedimentation also introduces a non-linear component in vertical land motion due to loading. Furthermore, geochemical processes in the subsurface can cause additional subsidence (Gambolati et al., 2005).

In summary, the contribution from vertical land motion has to be considered as rather uncertain. The two scenarios considered here may therefore not capture all plausible contributions.

Precautionary scenario:

The precautionary scenario is based on the IPCC estimates plus 50% for worst case regional modification and the land movements. The scenarios summarized in Figure 11.11 of the TAR exhibit a range of 0.15 to 0.70 m of sea-level rise by 2100. Adding 50% to this range, results in a range of 0.23 to 1.05 m by 2001.

Summary of scenarios

An overview of the scenarios considered here is given in Table 23. These scenarios are based on the following considerations:

A **Composite of factors:** The composite of all factors discussed above leads to a LSL rise of 0.47 ± 0.61 m and 0.27 ± 0.61 m including vertical land motion in ITRF2000 and IGS-P00, respectively. However, this scenario does not include any allowance for increased uncertainties in the regional alterations, nor does it include any additional effects due to increasingly likely melting of Greenland or the West-Antarctic ice sheet.

B **A plus 50% increased uncertainty for regional alterations:** Increasing the uncertainty for the contributions from expansion, continental glaciers, and terrestrial hydrosphere, leads to an increased uncertainty of 0.47 ± 0.74 m and 0.27 ± 0.74, respectively.

C **Increased Greenland melting:** Replacing the IPCC estimate for Greenland by the accelerated value changes scenario A into 0.37 ± 0.61 m and 0.17 ± 0.61 m, respectively.

D **Increased contribution from West Antarctica:** Replacing the IPCC estimate for Antarctica by an accelerated value changes scenario A into 0.87 ± 0.61 m and 0.67 ± 0.61 m, respectively.

E **IPCC plus 50% plus local atmospheric contribution plus vertical land motion:** The precautionary scenario results into an estimate of a range from 0.46 m to 1.28 m total sea-level rise by 2100, if we assume vertical land motion as given in ITRF2000, and a range from 0.26 m to 1.08 m, if IGS-P00 is the reference frame. These values include already the uncertainty of the global scenarios and their down-scaling but not the uncertainties in the estimates of the vertical land motion, the local atmospheric forcing, and the ocean currents. Therefore, we have to add an additional uncertainty of ± 0.28 m.

Without considering the uncertainties of the individual factors, the plausible scenarios considered here cover a total range of LSL rise by 2100 from 0.17 m to 1.28 m (Figure 44. All of these scenarios have to be considered as equally possible sea-level changes over the next 100 years. In particular, the mean of the range is not more plausible than any other value in this range. The scenarios are partly based on range estimates (for example, the atmospheric contribution), extrapolations of current trends (for example, the vertical land motion) or model runs (global scenarios as well as, for example, the steric

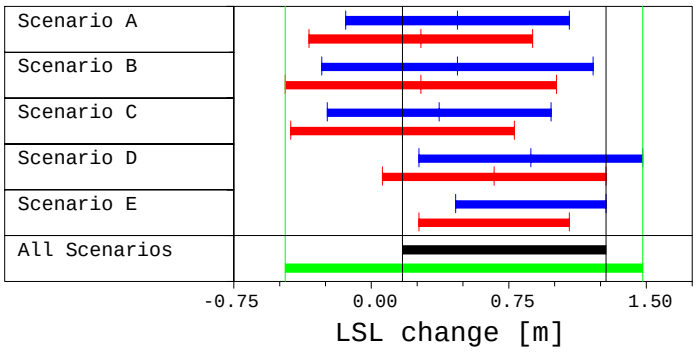

Figure 44: Scenarios for LSL changes in Venice in the 21st century.

The Scenarios are A: Composite of best estimates for forcing factors, B: same as A but with 50% increased uncertainty, C: A plus increased Greenland melting, D: A plus increased melting of West Antarctica, E: IPCC range plus 50% for local amplification. Blue and red bars are for scenarios with vertical land motion in ITRF2000 and IGS-P00, respectively. The black and green bars give the total range of the scenarios without and with the uncertainty of the individual scenarios include.

Table 23: Overview of the LSL scenarios for Venice.

The scenarios A to E are as described in the text. The values are sea-level change by 2100 in meters. The contribution from the vertical land motion is given for ITRF2000 and IGS-P00, respectively, and Sum1 and Sum2 are the sums of all other factors plus the vertical land motion in ITRF2000 and IGS-P00, respectively.

Factor	A	B	C	D	E
Steric	0.23 ± 0.14	0.23 ± 0.21	0.23 ± 0.14	0.23 ± 0.14	
Ocean curr.	0.00 ± 0.03	0.00 ± 0.03	0.00 ± 0.05	0.00 ± 0.05	0.00 ± 0.05
Atmosphere	0.03 ± 0.03	0.03 ± 0.03	0.03 ± 0.03	0.03 ± 0.03	0.03 ± 0.03
Greenland	-0.004 ± 0.004	-0.004 ± 0.004	-0.10	-0.004 ± 0.004	
Antarctica	-0.056 ± 0.056	-0.056 ± 0.056	-0.056 ± 0.056	0.35	
Glaciers	0.10 ± 0.07	0.10 ± 0.10	0.10 ± 0.07	0.10 ± 0.07	
Terr. Hydro.	-0.035 ± 0.075	-0.035 ± 0.113	-0.035 ± 0.075	-0.035 ± 0.075	
Global					0.23 to 1.05
ITRF2000	0.20 ± 0.20	0.20 ± 0.20	0.20 ± 0.20	0.20 ± 0.20	0.20 ± 0.20
IGS-P00	0.00 ± 0.20	0.00 ± 0.20	0.00 ± 0.20	0.00 ± 0.20	0.00 ± 0.20
Sum 1	0.47 ± 0.61	0.47 ± 0.74	0.37 ± 0.61	0.87 ± 0.61	0.46 to 1.28
Sum 2	0.27 ± 0.61	0.27 ± 0.74	0.17 ± 0.61	0.67 ± 0.61	0.26 to 1.08

contribution). Most factors cannot be assumed to vary linearly over the next hundred years and our scenarios therefore cannot be used to deduce any intermediate LSL values. However, most IPCC scenarios exhibit a characteristic curvature with larger changes in the second half of the 21st century.

The uncertainties given in Table 23 are conservative estimates. The uncertainties of the sums are maximum estimates, which are likely to be too large, since some of the uncertainties are correlated. Taking into account the complete range of uncertainties leads to a range starting from 0.17 ± 0.74 to the upper end of 1.28 ± 0.74 m. This wide range of plausible LSL scenarios and the large uncertainties attached to these underlines the importance of a continuous monitoring of the actual trajectory of LSL in the Venice Lagoon as well as the individual factors contributing to the sea-level changes with a dedicated multi-parameter sea-level observation system.

Moreover, the range estimates given here do not include any high-frequency effects, potentially leading

Table 24: Impact of mean LSL rise on number and duration of high water events.

All values are for a threshold for water levels of 90 cm above Z.M.P.S. The values are means over the time interval from 1955 to 2002. The parameters considered are the number of annual events exceeding the given threshold of 90 cm, the number of hourly values exceeding this threshold in a year, and the mean duration of the high water events in a year. Note that two events separated by only up to two samples below threshold are considered to be one event.

Parameter	observed	+25 cm	+50 cm	+75 cm
Mean of number of events per year	17	141	479	517
Mean of number of hourly values	49	458	2323	5144
Mean duration (samples)	2.85	3.23	4.83	10.00
Maximum duration (samples)	27	36	73	235

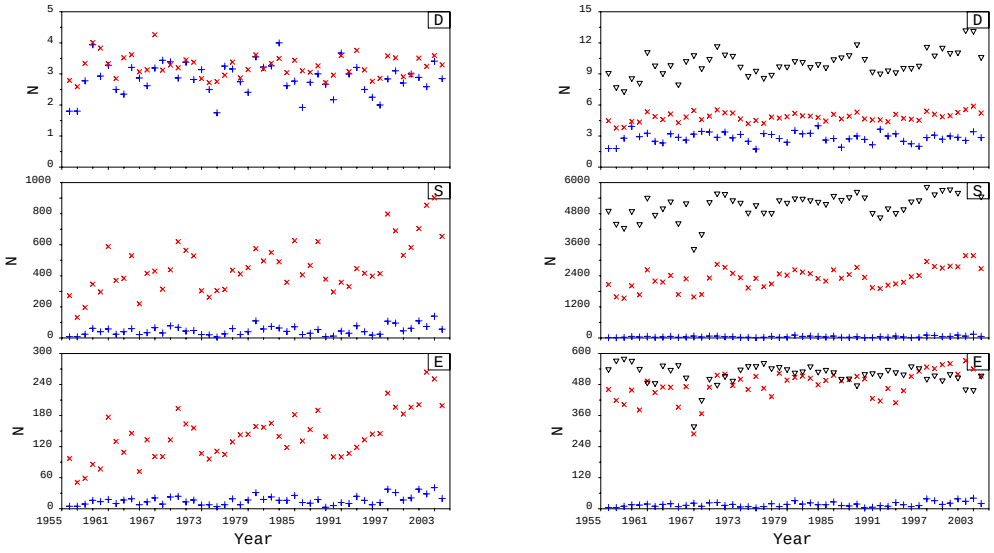

Figure 45: Impact of mean local sea level rise on high water events.

The symbols are for E: Number of high water events per year, S: Number of high water samples in a year, D: mean duration of a high water event in a year. Blue '+' are for the observed world. In left diagram, red 'x' are for the '+25 cm' World. Right diagrams: Red 'x' are for the '+50 cm' world; and black inverted tringles for the '+75 cm' world.

to additional increases in the maximum flood level. Therefore, additional studies focusing on scenarios for maximum flood levels are recommended.

It is interesting to note, that the estimate of mean sea level change of 1 m applied for the planning of the mitigation for the London flood defence (Tim Reeder, personal communication) is the upper 1/3 of the range estimated here.

9.4 Impact of mean LSL rise on high water levels

As mentioned in the previous section, the database for estimating future changes in surges and seiches leading to changes in extreme sea level above a future mean LSL is sparce. Except for an expected increase in tidal range of a few cm, the current knowledge is not sufficient to set up more sophisticated scenarios for the high-frequency part of the future LSL. For that, detailled model studies of storm surges under changing climate conditions would have to be carried out, comparable to the study by Lowe & Gregory (2005).

However, it is interesting to assess the impact of a mean increase of LSL on the number of events

exceeding a certain high-water mark and the mean duration of these event. Therefore, we have carried out a simple experiment, where we assume that for the sea level from 2055 to 2102, the overall statistics of the sea level variations have not changed compared to the same time window in the 20th century, except for the increase in the mean. As one sample, we assume that the tide gauge record at Venice from 2055 to 2102 is identical to the observed tide gauge record from 1955 to 2002, except for a constant offset due to mean sea level rise at 2100. For the experiment, we have chosen a threshold water level of 90 cm. Moreover, events separated by only two hourly samples below the threshold are considered as one event. Assuming an increased LSL at 2100 of only 25 cm results in a dramatic increase of the number of events per year as well as the number of hourly values exceeding this threshold (Figure 45). Both the number of events and the number of hourly values in a "+25 cm world" are roughly 9 times and 12 times, respectively, larger than in the observed world. However, the mean duration of these high-water events increases only from 2.85 hourly samples to 3.23 hourly samples (Table 24). Thus, most of these events are associated with high tides combined with meteorological surges on longer times scales.

Assuming a mean sea level increase of 50 cm by 2100, again increases the number of events and hourly samples, and for almost all years, we have now more than 360 events. Almost 30% of the hourly samples are above the threshold. However, the mean duration of the highwater events increases relatively moderately to 4.83 hourly samples.

A dramatic change in the duration of the events occurs if we assume a sea level rise of 75 cm by 2100. Then the mean duration of the high water events is 10.00 hourly samples, and on average almost 60% of the hourly samples are above the threshold. Further increases of the LSL would lead to a reduction of the number of individual events but a dramatic increase of the mean duration of these events.

The maximum duration of a high-water event in the 47 years considered here is 27 hourly samples for the observed record. For the "+25 cm world" this does not changes very much (Table 24). However, for the "+50 cm" and "+75 cm" worlds, the maximum duration increases significantly, and in our experiment we get values of 73 and 235 hourly samples, respectively.

This simple experiment shows the complex dependency of the parameters describing high water events on mean LSL increases. This information is relevant for the planning of mitigation, and a more elaborated study should be carried out, including also storm surge models under changing climate conditions.

9.5 Reducing the uncertainties

In setting up the sea-level scenarios for Venice, we face considerable uncertainties with respect to both mean LSL changes and extreme sea levels. These uncertainties result partly from gaps in our knowledge of the main forcing factors and their relative contributions to LSL in Venice. Uncertainties arise also from a considerable degree of randomness of some of the factors forcing the LSL changes, which make it difficult to predict their trajectories throughout the 21st century. Finally, for extrapolations of the present secular trends of some of the factors expected to be linear, the errors associated with our measurements of the present secular trends introduce also significant uncertainties.

The first type of uncertainty, that is, the epistemic uncertainties can only be reduced to basic studies of Earth system processes. Recognizing that sea level is a fundamental output of the Earth system, affected by nearly all Earth system processes, it is clear that a better understanding of sea-level variations on local, regional and global scales requires elaborated studies taking a system approach. Studies based on coupled atmosphere-ocean circulation models suitable to predict sea-level variations may help to bring more light into the processes on seasonal to multi-decadal time scales. Inter-model difference require, however, that different models are used and compared to each other.

The second type of uncertainties, that the aleatory uncertainties associated with the randomness of the climate and oceanic processes, can be addressed for example by ensemble studies with the climate models using different initial conditions. For short time scales from sub-daily to weekly time scales, extensive model studies with storm surge models, also under changing climate conditions, would help to better understand the generation of surges and seiches and to identify the conditions leading to changes in extreme sea level as a consequence of climate change.

The third uncertainty, which hampers the extrapolation of those factors that can be assumed to be linear in nature, that is, the uncertainty in our measurement of their present-day rates, can only be reduced to a better observation system. Moreover, such a system would also improve the database of the model studies required for the reduction of the first two types of uncertainties. The monitoring system is also fundamental for a control of the LSL scenarios, which only can be a subset of all plausible scenarios, which may or may not include the true trajectory the LSL in Venice will follow throughout the 21st century. In the next section, we consider the necessary monitoring system in more detail.

9.6 A local integrated sea-level monitoring system

Here we provide basic considerations and recommendations for local sea-level monitoring, with focus on recommendations for improvements of the monitoring particularly through integration of the various available techniques. These recommendations take into account that considerable efforts have been made in the past to set up a comprehensive sea-level monitoring system in the Lagoon and focus on necessary improvements that became obvious in the frame of the present study.

Multiple processes on various spatial and temporal scales contribute to LSL changes in Venice, and this needs to be reflected in the design requirements of a system that monitors sea level. Thus, we recommend an observing system that has features of multiple data acquisition systems. Continuous GPS and tide gauges have high temporal resolution that can identify transient events, while InSAR can obtain high spatial resolution to identify local subsidence features associated with, for example, hydrological basin-scale or anthropogenic activity. In addition, campaign GPS data can provide a complimentary constraint that has a greater spatial coverage, but with lesser temporal resolution.

9.6.1 Tide gauges

Tide gauges are a crucial component of the LSL monitoring system. In order to ensure that any given tide gauge is representative for a larger area, it is important to co-locate the tide gauge with GPS/GNSS and to ensure that relative motions of the tide gauge with respect to the GPS station are monitored with an accuracy of 1 mm (Plag et al., 2000).

If proper operation of a tide gauge is ensured, then this tide gauge can be representative for a larger area, in particular if longer time scales are considered. This is nicely demonstrated by the high spatial coherency of the monthly mean sea levels discussed in Section 4.6. However, in order to get from one tide gauge reasonable estimates of LSL trends in adjacent areas, appropriate monitoring of the vertical land motion there is needed since in many locations vertical land motion is dominated by much smaller spatial scales than the long-period or secular contribution to sea-level variations from oceanographic and atmospheric forcing.

In order to ensure that a given tide gauge is operating properly, special care needs to be take with the operational routines. If redundancy is required, tide gauges with two sensors located in the same area and connected to the same GPS station should be considered.

9.6.2 Oceanographic and meteorological measurements

In order to be able to separate the factors contributing to LSL variations, it is mandatory to have a sufficient number of oceanographic and meteorological observation sites in the Lagoon and the adjacent Adriatic Sea. Profiles of sea water temperature and salinity are necessary in order to determine the LSL variations caused by steric changes. Of particular importance are long time series at a few carefully selected reference sites.

Meteorological observations, in particular air pressure and wind, are crucial for the determination of local atmospherically forced LSL variations. Alternatively, these variations can be computed from hydrodynamical models forced by the regional atmospheric fields. However, the latter may result in considerable deviations in areas like the Venice Lagoon. Therefore, long, homogeneous local time series of air pressure and wind are of considerable importance. Efforts should be made to integrate these time series into a sea-level related data base easily accessible for researchers.

9.6.3 GPS

In order for GPS data to best isolate the separate processes contributing to the vertical motion, the spatial distribution of the sites should be adequate to characterize both regional and local phenomena. The existing regional network of continuously recording sites is adequate to characterize processes that act on spatial scales of the order of 50 to 100 km. Supplementary campaign networks with greater spatial density provide constraints on local processes. Campaign sites are usually surveyed less frequently, and hence have larger uncertainties because less data are collected and because of the presence of additional noise associated with tripod setup. However, the advantages of higher spatial sampling can outweigh this if the local surface deformation is highly heterogeneous or has a large amplitude. The needs of the city of Venice require characterization of surface motion on both these spatial scales.

The regional data should be complemented by a small number (approximately 5) of new permanently deployed GPS receivers. Considering the large uncertainty connected to the vertical motion, and taking into account that reliable vertical velocity estimates require time series of several years length, the establishment of these new sites should have highest priority. GPS vertical motions are 3 to 4 times less precise that horizontal measurements, and thus high quality monuments are mandatory in order to reduce noise. Maximally stable sites should be identified. Permanent deployments have greater stability (and hence higher precision) because of consistency in the antenna and receiver configuration, and removal of tripod setup uncertainty. GPS offers the best reference for other geodetic techniques. If it is difficult or impossible to identify true bedrock sites in a landscape covered by soft sediments and agricultural activity, then low aspect ratio buildings or other stable land can offer an adequate substitute.

Campaign GPS data acquisition can greatly enhance the spatial scope of the network and provide flexibility to respond to any events that deform the surface of the Earth (for example, seismic, water table pumping). We recommend that the present and proposed campaign GPS networks be surveyed at least every second year. Where possible, it should be considered to installing monuments in a way allowing for precise repositioning (< 1 mm) of the antenna (Figure 46b). Changing the position and type of antenna from survey to survey can complicate processing of the data, even if antenna heights above the benchmark are carefully measured and offsets accounted for. This can result from changes in the multipath environment that introduce apparent position changes that are not the result of geometric position change of the antenna phase center. Using very precisely repeatable antenna installations can almost completely remove a component of noise associated with tripod setup that is typically on the order of 2 mm/yr RMS.

Figure 46: Examples of GPS monuments.
Drilled and cross-braced style monument of the Basin and Range Geodetic Network (BARGEN) of the western United States (left). Among the most stable type of monument, these isolate the antenna from the shallow surface by over-coring the top several meters of the bracing. Semi-continuous or campaign-style monuments can be made more precise by permanently fixing a steel pin with an antenna coupling to a rock or building (right). This provides very precise repositioning and orientation of the antenna for subsequent surveys.

To resolve the processes of interest on an experimental time scale of a few years, the velocity precision should be better than 1 mm/yr. This level of precision can be obtained in continuous or semi-continuous deployments within 2 years. For campaigns the time required to achieve this precision depends on the frequency and length of observation, and also the characteristics of the noise in the time series Mao et al. (1999); Williams (2003) perhaps in as little as 5 years. Achieving this precision in the vertical component requires a longer time span of observation.

When targeting long-term or regional-scale process (for example, tectonics or post-glacial rebound) that have rates on the order of 1 mm/yr for measurement with GPS, careful characterization of the surface geology and placement of the GPS antenna must considered. It is most desirable to place the antenna on a monument that is connected directly to bedrock, and is not affected by non-tectonic short-term loads (for example, mining, ground water extraction, etc.). The geological environment surrounding the Venice Lagoon may make this difficult or impossible. However, some forms of stabilization, such as Wyatt-type deep drill braced monuments (Figure 46a), decouple the antenna from the upper few meters of the surface to reduce noise associated with thermal changes, water, or bioturbation. An effort should be made to identify sites with clear sky visibility above the satellite elevation cutoff, and are relatively free of disruption within 10 meters of the antenna in order to eliminate change sin the multipath environment. Alternatively, when deep drilling is not possible or prohibitively expensive, very precise repositioning of the antenna can be achieved with steel pins mounted in bedrock or highly stable buildings (Figure 46b).

GPS data should be acquired from these regionally distributed sites and processed routinely with the newly deployed Venice network continuous sites and also the available campaign data. Data should be processed under homogeneous software and placed the same reference frame so that all the results can be directly compared in order to quantify relative motions within the network.

Considering the importance of GPS observations, it is also important to ensure that observations from all GPS sites installed in the Venice area for research and other purposes are made available freely

for sea-level related studies. It is difficult to understand that observations from some stations are restricted, considering the general importance of these observations for the public.

9.6.4 Leveling

In theory leveling surveys can be effectively replaced by campaign GPS surveys of the same benchmarks used in the leveling if there are sufficient GPS receivers and logistical resources to mount GPS campaigns over the leveling routes. If not, a subset of the roughly 1000 leveling benchmarks in place in the region (Carbognin & Tosi, 2003) should be surveyed. GPS positioning is inherently three-dimensional and is not subject to geoid changes or position uncertainties that vary with distance along the line. Furthermore GPS data can be processed simultaneously with regional GPS sites (for example, EUREF), in order to assess vertical motions of Venice in a regional reference frame. This can be vital when separating the relative contributions from regional tectonics and local subsidence.

If leveling routes are maintained, as proposed by Strozzi et al. (2003) then their utility could be enhanced as a reference for InSAR and GPS-derived vertical motions by extending additional lines into relatively stable bedrock areas, for example, the alpine foothills. Previous results (Carbognin et al., 2004) show that much of the subsidence recorded by the single line connecting the basin and foothills occurs between Treviso and the Alps, suggesting that subsidence could be a broad (> 50 km) feature, possibly affecting the entire leveling network. Surveying leveling marks with campaign GPS is also recommended in order to tie the GPS and leveling together into an integrated surface motion solution that is regionally referenced.

9.6.5 InSAR

InSAR scenes should be routinely acquired, processed and integrated with the GPS data as part of ongoing monitoring. More often than is specified in Table 3 of the Subsidence Monitoring Service (Strozzi et al., 2003). They specified 5 years, but it has been shown in numerous studies (e.g., Bawden et al., 2001; Gourmelen & Amelung, 2003) the value of stacking of large numbers of interferograms in order to reduce noise.

InSAR images record the change in range between the satellite and surface of the Earth, which for ERS and ENVISAT data is typically 23°from vertical. Thus some horizontal motion can be mapped into an interferogram, and could be mistaken for vertical deformation. The presence of GPS control inside the radar scene can remove this ambiguity, and thus it is recommended that InSAR be interpreted in conjunction with GPS data.

Furthermore, comparisons of InSAR results to geologic and other geophysical data (for example, gravity, magneto-telluric, active tectonic fault surveys) can lead to insights about the cause for specific subsidence features (Bell et al., 2005). Therefore it is also recommended that results from InSAR surveys be compared to geology and subsurface geophysics, thickness of Quaternary sediments, etc., in order to maximize their benefit.

9.7 Future updates of the sea-level rise scenarios

The LSL scenarios discussed in Section 9.3 cover a wide range and are associated with considerable uncertainties. Partly, the range is due to uncertainties in the scenarios for the global climate development and the impact this will have on global sea level. Additional uncertainties come from local factors and their potential development over time. A large uncertainty is associated with vertical land motion.

It can be expected that the next IPCC assessment will provide new insight in global processes, particularly those associated with warming of the ocean and changes in the large ice sheets. Therefore, modified scenarios may already be possible after the new IPCC assessment becomes available. The comparison of the sequence of IPCC assessments will also elucidate the actual state of knowledge with respect to global and regional sea-level changes.

The uncertainty in the relation between reference frame origin and geocenter will be addressed in the frame of the *Global Geodetic Observing System* (GGOS), and improvements can be expected already for ITRF2004, which is expected to be released in the near future. Longer GPS time series for the stations in the vicinity of the Venice Lagoon will also help to reduce the uncertainties in the vertical land motion. Combined with GPS campaign data and an improved analysis of InSAR observations, it will be possible to determine the spatial pattern of vertical motion with better resolution and precision.

The LSL scenarios for Venice should be updated regularly when significant new information becomes available. Such information includes, but is not limited to new IPCC assessments, significantly improved new versions of the ITRF, and significant new studies providing new insight in the processes affecting LSL in Venice.

Considering the presently large uncertainties, the LSL scenarios should be reconsidered at least every five years. If possible, the next appraisal should be scheduled to be carried out after a new IPCC assessment becomes available in four to five years from now.

10 Main conclusions and recommendations

10.1 Conclusions

Local sea level at any location on Earth is the result of complex processes Earth system processes interacting on a wide range of temporal and spatial scales. In order to understand the past LSL variations in relation to the forcing processes and to be able to set up plausible scenarios of future sea-level changes, it is important to base the analysis of past as well as the prediction of future sea levels on a physically consistent theory and a set of terms that are well defined in this frame. We were able to set up an equation that explains the LSL variations as a sum of largely independent contributions arising from processes in the atmosphere, the ocean and the solid Earth as well as their interactions. This equation (and several simplifications) provide the basis for the analysis of the observations of both LSL and quantities related to the forcing processes and this equation is used to set up a set of scenarios for future sea levels.

The analysis of the LSL variations in Venice and the Adriatic over the last 50 years documents that the available LSL observations in the Upper Adriatic are of high quality, with high spatial coherency of not only the long-period variations but also variations down to hourly values. A large fraction of the intra-seasonal to interannual LSL variations are due to local atmospheric forcing, while the residual LSL variations are dominated by long-period oscillations with characteristic time scales of 16 to 17 years, which appear to be caused by oceanic processes. However, a full explanation of the LSL changes in terms of forcing factors is uncertain due to uncertainties in the local, regional and global factors contributing to vertical land motion.

The observed LSL changes in the Adriatic over the last five decades of the 20^{th} century are small (order 0.5 mm/yr). This is partly due to a negative effect the local atmospheric forcing, which reduced sea-level rise (temporarily?) by up to 1.3 mm/yr. This effect is most likely of a cyclic nature, which implies larger sea-level rise in the next few decades.

Future LSL scenarios for the 21^{st} century are set up here by summing up plausible futures for each of the contributing factors, which have been estimated independently. The resulting scenarios cover a large range of LSL changes by 2100 (see Figure 44 on page 106).

Moreover, we face the risk that there may be dramatic changes in the global climate system over the 21^{st} century, but we have no basis to assess the probability of such non-linear events. One of the risks, which became obvious recently is a catastrophic disintegration of the Greenland ice sheet, which is considered possible in the time frame of the next fifty to one hundred years (Zwally et al., 2002). The present trends in the Arctic sea ice further enhance this risk (Overpeck & others, 2005). However, we have no sound scientific basis to assess the risk. The planning of mitigation will have to consider these risks.

10.2 Main recommendations

10.2.1 Observations

The continuation of high-quality tide gauges observations in the Venice Lagoon and the adjacent Adriatic Sea are mandatory for the monitoring of the LSL variations, both in order to provide a better database for studies of the sea-level variations as well as the monitoring of LSL variation in an area so sensitive to even slight changes in the mean LSL. The importance of the tide gauges cannot be overemphasized.

The absence of a sufficient number of continuous GPS stations is a serious deficiency of the current sea-level observation system. It is strongly recommended to establish of the order of five permanently recording GPS sites distributed throughout the City of Venice. We are aware of the problems of finding suitable sites in the City, however, without a reasonable network, it will not be possible to constrain the important contribution from vertical land motion, which needs to be known in a geocentric reference frame, to better than ±2 mm/yr.

A densification of the permanent GPS network with campaign-type GPS observations is strongly recommended. However, for such measurements it is important to take care with antenna monuments, the appropriate frequency of the campaigns, and the establishment of a dense enough network, that is able to capture the short wave length in the vertical motion.

The co-location of tide gauges with GPS is mandatory for the separation of the different factors contributing to LSL changes. The tide gauges in Venice seem to be co-located with GPS, however, the observations were not available for this study and do not seem to be available publicly. Every effort should be made to ensure that these crucial data are made available freely for research.

Absolute gravity measurements at the tide gauges should be considered. In combination with co-located GPS measurements, the absolute gravity observations would provide information on changes in the gravity field, which directly affect LSL.

10.2.2 Database related recommendations

It is recommended that all relevant data are compiled in a high quality, homogeneous database and made available freely for scientific studies. The database should include tide gauges data (hourly as well as monthly time series), GPS observations, local meteorological and oceanographic data, information about relevant regional and global data sets, as well as relevant model predictions.

10.2.3 Data analysis

It is recommended to facilitate data analyses that will provide a better picture of the spatial pattern of vertical land motion in the Venice Lagoon and the adjacent land areas. In particular, InSAR analysis with the permanent scattering method are recommended in order to get time series of the land motion. A combined analysis of GPS and InSAR observations are also considered promising.

A detailed study of extreme LSL base on several stations should be carried out. The availability of hourly sea-level data from most of the Adriatic tide gauges through the ESEAS provides the observational basis for such studies. A combined analysis of LSL and meteorological observations would give further insight into the processes causing the long-term variations in extreme water levels (see, e.g., Raicich, 2003).

10.2.4 Research studies

It is recommended that the development of surges under past, present and future climate conditions is studied in more detail in order to complement the mean LSL scenarios by scenarios for sea-level extremes. These studies should comprise both, statistical studies of observations of LSL and relevant meteorological parameters and storm surge models (see, e.g., Lowe & Gregory, 2005). For the latter, it is important to take into account that both models and observations tend to underestimate the extreme surges (see, e.g., van den Brink et al., 2005).

10.2.5 Updates of the LSL Scenarios

It is recommended to reconsider the LSL scenarios set up here briefly after the next IPCC Assessment becomes available in 2007. It is expected that the new assessment will provide new insight into the global scenarios for sea-level rise as well as new information concerning the potential risks associated with increased melting or disintegration of the Antarctic and Greenland ice sheets.

Moreover, in the near future, the increasing observational database particularly for vertical land motion should be analyzed frequently (on a five year basis) and the LSL scenarios should be updated, if required by the analysis results.

References

Agnew, D. C., 1992. The time-domain behavior of power law noises, *Geophys. Res. Lett.*, **19**, 333–336.

Altamimi, Z., Sillard, P., & Boucher, C., 2002. A new release of the International Terrestrial Reference Frame for earth science applications, *J. Geophys. Res.*, **107**, 2214, doi: 10.1029/2001JB000561.

Altiner, Y., 2001. The contribution of GPS data to the detection of the earth's crust deformations illustrated by GPS campaigns in the Adria Region, *Geophys. J. Int.*, **xx**, yy.

Alvarez-Fanjul, E., Pérez, B., & Rodríguez, I., 1997. A description of the tides in the Eastern North Atlantic, *Progr. Oceanogr.*, **40**, 217–244.

Álvarez-Fanjul, E., Pérez, B., & Rodríguez, I., 2001. NIVMAR: A storm-surge forecasting system for Spanish waters, *Sci. Mar.*, **60**, 145–154.

Anzidei, M., Baldi, P.and Casula, G., Galvani, A., Mantovani, E., Pesci, A., Riguzzi, F., & Serpelloni, E. E., 2001. Insights into present-day crustal motion in the central Mediterranean area from GPS surveys, *Geophys. J. Int.*, **146**, 98–100.

Artegiani, A., Bregant, D., Paschini, E., Pinardi, N., Raicich, F., & Russo, A., 1997. The Adriatic sea general circulation. 1. Air-sea interactions and water mass structure, *J. Phys. Ocanogr.*, **27**(8), 1492–1514.

Astraldi, M., Balopoulos, S., Candela, J., Font, J., Gacic, M., Gasparini, G. P., Manca, B., Theocharis, A., & Tintoré, J., 1999. The role of straits and channels in understanding the characteristics of Mediterranean circulation, *Progress in Oceanography*, **44**(1-3), 65–108.

Baker, T. F. & Alcock, G. A., 1983. On the time variation of ocean tides, in *Proceedings of the Ninth International Symposium on Earth Tides*, edited by J. Kuo, pp. 341–350, E. Schweitzerbart'sche Verlagsbuchhaltung, Stuttgart.

Barnet, T. P., Pierce, D. W., AchutaRao, K. M., Gleckler, P. J., Santer, B. D., & Gregory, J. M., 2005. Penetration of human-induced warming into the world's oceans, *Science*, **309**, 284–287.

Battistin, D. & Canestrelli, P., 2001. Statistical study on the time series of extremal tide values measured in Venice from 1872 to 2000, in *Book of Extended Abstracts, Final Workshop of COST Action 40*, pp. 71–74, Hydrographic Institute of the Republic of Croatia - Split.

Baú, D., Gambolati, G., & Teatini, P., 2000. Can gas withdrawal from Chioggia-mare field affect the stability of the Venetian littoral?, in *Proceedings of the Sixth international Symposium on Land subsidence, Ravenna Italy, Sept. 24-29, 2000*, edited by L. Carbognin, G. Gambolati, & A. I. Johnson, vol. II of **Land Subsidence**, pp. 421–433, ISBN 88-87222-06-1.

Bawden, G. W., Thatcher, W., Stein, R. S., Hudnut, K. W., & Peltzer, G., 2001. Tectonic contraction across Los Angeles after removal of groundwater pumping effects, *Nature*, **412**, 812–815.

Bell, J. W., Amelung, F., Bianchi, M., Ferretti, A., Novali, F., & Bawden, G. W., 2005. InSAR reveals aquifer system response in heavily pumped basins in nevada: A tool for groundwater resource management, *EOS Trans. AGU*, **86**(18), Jt. Assem. Suppl., Abstract G14A–03.

Bergamasco, A. & Gacic, M., 1996. Baroclinic response of the Adriatic Sea to an episode of bora wind, *J. Phys. Oceangraphy*, **26**(7), 1354–1369.

Bethoux, J. P. & Gentili, B., 1999. Functioning of the Mediterranean Sea: past and present changes related to freshwater input and climate changes, *J. Marine Sys.*, **20**, 33–47.

Bethoux, J. P., Gentili, B., Raunet, J., & Taillez, D., 1990. Warming trend in the Western Mediterranean Deep Water, *Nature*, **347**, 660–662.

Bethoux, J. P., Gentili, B., & Tailliez, D., 1998. Warming and freshwater budget change in the Mediterranean since the 1940s, their possible relation to the greenhouse effect, *Geophys. Res. Lett.*, **25**, 1023–1026.

Blewitt, G., 1989. Carrier phase ambiguity resolution for the Global Positioning System applied to geodetic baselines up to 2000 km, *J. Geophys. Res.*, **94**(B8), 10187–10283.

Blewitt, G., 2004. Lower crustal transients and surface mass transport: Time series filtering for signal detection at two spatial extremes, *Eos Trans. AGU*, **85**(47), Fall Meet. Suppl., Abstract G51D–02.

Blewitt, G. & Lavallée, D., 2002. Effect of annual signals on geodetic velocity, *J. Geophys. Res.*, **107**, DOI 10.1029/2001JB000570.

Bonato, N., Egiatti, G., Ferla, M., & Fillipi, M., 2001. Tidal observations in the Venetian lagoon. Update on sea level change from 1872 to 2000, in *Book of Extended Abstracts, Final Workshop of COST Action 40*, pp. 97–105, Hydrographic Institute of the Republic of Croatia - Split.

Bonato, N., Ferla, M., Umgiesser, G., & Zen, G., 2001. High water level events in the Venice Lagoon, in *Book of Extended Abstracts, Final Workshop of COST Action 40*, p. 75, Hydrographic Institute of the Republic of Croatia - Split.

Bond, G. C., Showers, W., Elliot, M., Evans, M., Lotti, R., Hajdas, I., Bonani, G., & Johnson, S., 1999. The North Atlantic's 1-2 kyr climate rhythm: relation to Heinrich events, Dansgaard/Oeschger cycles and the little ice age, in *Mechanisms of Global Change at Millennial Time Scales*, edited by P. U. Clark, R. S. Webb, & L. D. Keigwin, vol. 112 of **Geophysical Monograph**, pp. 59–76, American Geophysical Union, Washington DC.

Bondesan, M., Gatti, M., & Russo, P., 2000. Subsidence in the eastern Po plain (Italy), in *Proceedings of the Sixth international Symposium on Land subsidence, Ravenna Italy, Sept. 24-29, 2000*, edited by L. Carbognin, G. Gambolati, & A. I. Johnson, vol. II of **Land Subsidence**, pp. 193–204, ISBN 88-87222-06-1.

Brambati, A., Carbognin, L., Quaia, T., Teatini, P., & Tosi, L., 2003. The Lagoon of Venice; geological setting, evolution and land subsidence, *Episodes*, **26**(3), 264–268.

Brankart, J. M. & Pinardi, N., 2001. Abrupt cooling of the Mediterranean Levantine Intermediate Water at the beginning of the 1980s: Observational evidence and model simulation, *J. Phys. Oceanogr.*, **31**(8), 2307–2320.

Brasseur, P., 1995. Free data offered to researchers studying the Mediterranean, *Eos, Trans. Am. Geophys. Union*, **76**(37), 363.

Bryden, H. L., Candela, J., & Kinder, T., 1994. Exchange through the Strait of Gibraltar, *Progress in Oceanography*, **33**, 201–248.

Camuffo, D. & Sturaro, G., 2003. Sixty-cm submersion of Venice discovered thanks to Cabaletto's paintings, *Climate Change*, **58**, 333–343.

Candela, J., 1991. The Gibraltar Strait and its role in the dynamics of the Mediterranean Sea, *Dynamics of Atmospheres and Oceans*, **15**(3-5), 267–299.

Candela, J., Winant, C. D., & Bryden, H. L., 1989. Meteorologically forced subinertial flows through the strait of Gibraltar, *J. Geophys. Res.*, **94**(C9), 12667–12679.

Carbognin, L. & Tosi, L., 2003. Il progetto ises per l'analisi dei processi di intrusione salina e subsidenze nei territori meridionali delle province di padova e venzia, Tech. rep., Grafiche Erredici, Padova, 96pp.

Carbognin, L., Teatini, P., & Tosi, L., 2004. Eustacy and land subsidence in the Venice Lagoon at the beginning of the new millenium, *J. Marine Systems*, **51**, 345–353.

Cardin, V. & Gacic, M., 2003. Long-term heat flux variability and winter convection in the Adriatic Sea, *J. Geophys. Res.*, **108**(C9), art. no. 8103.

Carminati, E., Doglioni, C., & Scrocca, D., 2005. Magnitude and causes of long-term subsidence of the po plain and venetian region, in *Flooding and Environmental challenges for Venice and its Lagoon: State of Knowledge*, edited by C. A. Fletcher & T. Spencer, pp. ??–??, Cambridge University Press.

Cartwright, D. E. & Edden, A. C., 1973. Corrected tables of tidal harmonics, *Geophys. J. R. Astron. Soc.*, **33**, 253–264.

Cavaleri, L., Bertotti, L., Canestrelli, P., & Lionello, P., 1991. Extreme storms in the Adriatic Sea, in *Proceedings of the 22nd Coastal Engineering Conference, 1990*, vol. 1, pp. 218–226, American Society of Civil Engineers, New York.

Cecconi, G., Canestrelli, P., Corte, C., & Di Donato, M., 1999. Climate record of storm surges in Venice, in *The impact of climate change on flooding and sustainable river management*, edited by P. Balabanis, A. Bronstert, R. Casale, & P. Samuels, pp. 149–156, European Commission, EUR 18287 EN.

Cerovecki, I., Orlic, M., & Hendershott, M. C., 1997. Adriatic seiche decay and energy loss to the Mediterranean, *Deep-Sea Research*, **44**, 2007–2029.

Charnock, H., 1989. Temperature and salinity changes in the deep water of the western Mediterranean basin, in *3rd POEM Scientific Workshop, Harvard, Cambridge, USA*.

Chelton, D. B. & Enfield, D. B., 1986. Ocean signals in tide gauge records, *J. Geophys. Res.*, **91**, 9081–9098.

Church, J. A., Gregory, J. M., Huybrechts, P., Kuhn, M., Lambeck, K., Nhuan, M. T., Qin, D., & Woodworth, P. L., 2001. Changes in sea level, in *Climate Change 2001: The Scientific Basis. Contribution of Working Group I to the Third Assessment Report of the Intergovernmental Panel on Climate Change*, edited by J. T. Houghton, Y. Ding, D. J. Griggs, M. Noguer, P. J. van der Linden, X. Dai, K. Maskell, & C. A. Johnson, pp. 639–693, Cambridge University Press, Cambridge.

Clark, J. A., Farrell, W., & Peltier, W. R., 1978. Global changes in postglacial sea level: A numerical calculation., *Quatern. Res.*, **9**, 265–287.

Coles, S., 2001. *An introduction to statistical modelling extreme values*, Springer Verlag, Berlin.

Co.Ri.La, 1999. Scenari di crescita del livello del mare per la Laguna di Venezia, Vol. I, November 1999, Consorzio per la Gestione del Centro di Coordinamento dell Attività di Ricerca Inerenti il Sistema Lagunare di Venezia.

Cushman-Roisin, B. & Naimie, C. E., 2002. A 3-d finite-element model of the Adriatic tides, *J. Marine Sys.*, **37**(4), 279–297.

Davis, C. H., Li, Y., McConnell, J. R., M., F. M., & Hanna, E., 2005. Snowfall-driven growth of the East Antarctic ice sheet mitigates recent sea-level rise, *Science*, **308**, 1898–1901.

Defant, A., 1961. *Physical Oceanography*, vol. Volume II, Pergamon Press, Oxford.

DeMets, C., Gordon, R. G., Argus, D. F., & Stein, S., 1994. Effect of recent revisions to the geomagnetic reversal time scale on estimates of current plate motions, *Geophys. Res. Lett.*, **21**, 2191–2194.

Di Donato, G., Negredo, A. M., Sabadini, R., & Vermeersen, L. L. A., 1999. Multiple processes causing sea-level rise in the Central Mediterranean, *Geophys. Res. Lett.*, **26**(12), 1769–1772.

Doodson, A. T. & Warburg, H. D., 1941. *Admiralty Manual of Tides*, His Majesty's Stationary Office, London, 270pp.

Douglas, B. C., 1991. Global sea level rise, *J. Geophys. Res.*, **96**, 6981–6992.

Douglas, B. C., 1997. Global sea level rise: a redetermination, *Surveys Geophys.*, **18**, 279–292.

Emery, K. O. & Aubrey, D. G., 1991. *Sea Levels, Land Levels, and Tide Gauges*, Springer, Berlin.

et al., M., 2000. Global positioning constraints on plate kinematics and dynamics in the eastern Mediterranean and Caucasus, *J. Geophys. Res.*, **105**, 5695.

Farrell, W. E. & Clark, J. A., 1976. On postglacial sea level, *Geophys. J. R. Astron. Soc.*, **46**, 647–667.

Fenoglio-Marc, L., 2002. Long-term sea level change in the Mediterranean Sea from multi-satellite altimetry and tide gauges, *Phys. Chem. Earth*, **27**(32-34), 1419–1431.

Ferretti, A., Prati, C., & Rocca, F., 2000. Measuring subsidence with SAR Interferometry: applications of the permanent scatterers technique, in *Proceedings of the Sixth international Symposium on Land subsidence, Ravenna Italy, Sept. 24-29, 2000*, edited by L. Carbognin, G. Gambolati, & A. I. Johnson, vol. II of **Land Subsidence**, pp. 67–79, ISBN 88-87222-06-1.

Ferretti, A., Prati, C., & Rocca, F., 2001. Permanent scatterers in SAR interferometry, *IEEE TGRS*, **39**, 8–20.

Friis-Christensen, E., Lassen, K., 1991. Length of the Solar Cycle: An Indicator of Solar Activity Closely Associated with Climate, *Science*, **254**, 698–700.

Gambolati, G. & Teatini, P., 1998. Natural land subsidence due to compaction coastal morphodynamics of the upper Adriatic Sea basin, *IGEA*, **11**, 29–40.

Gambolati, G., Putti, M., Teatini, P., Camporese, M., Ferraris, S., Gasparetto Stori, G., Nicoletti, V., Silvestri, S., Rizzetto, F., & Tosi, L., 2005. Peat land oxidation enhances subsidence in the Venice watershed, *Eos, Trans. Am. Geophys. Union*, **86**(23), 217,220.

García Lafuente, J., ´varez Fanjul, E., Vargas, E. J. M., & Ratsimandresy, A. W., 2002. Subinertial variability in the flow through the Strait of Gibraltar, *J. Geophys. Res.*, **107**(C10), 3168, doi:10.1029/2001JC001104.

Garrett, C. & Majaess, F., 1984. Nonisostatic response of sea level to atmospheric pressure in Eastern Mediterranean, *J. Phys. Oceanogr.*, **14**, 656–665.

Garrett, C., Outbridge, R., & Thompson, K., 1993. Interannual variability in Mediterranean heat and buoyancy fluxes, *J. of Climate*, **6**, 900–910.

Gasparini, G. P., Ortona, A., Budillon, G., Astraldi, M., & Sansone, E., 2005. The effect of the Eastern Mediterranean Transient on the hydrographic characteristics in the Strait of Sicily and in the Tyrrhenian Sea, *Deep-Sea Res. I*, **52**, 915–935.

Gill, A. E., 1982. *Atmosphere-Ocean Dynamics*, Academic Press.

Gilman, C. & Garrett, C., 1994. Heat flux parameterizations for the Mediterranean Sea: The role of atmospheric aerosols and constraints from the water budget, *J. Geophys. Res.*, **99**, 5119–5134.

Gornitz, V., Rosenzweig, C., & Hillel, D., 1996. Effects of anthropogenic intervention in the land hydrological cycle on global sea level rise, *Global and Planetary Change*, **14**, 147–161.

Gourmelen, N. & Amelung, F., 2003. Anomalous crustal deformation in the Central Nevada Seismic Belt detected by InSAR, *Eos Trans. AGU*, **84**(46).

Grbec, B., Morovic, M., & Zore-Armanda, M., 2003. Mediterranean oscillation index and its relationship with salinity fluctuations in the adriatic sea, *Acta Adriatica*, **44**, 61–76.

Grenerczy, G. andKenyeres, A. & Fejes, I., 2000. Present crustal movement and strain distribution in central Europe inferred from GPS measurements, *J. Geophys. Res.*, **105**, 21,835 – 21,846.

Group, T. L., 2003. The Levantine Intermediate Water Experiment (Liwex) Group, Levantine basin–a laboratory for multiple water mass formation processes, *J. Geophys. Res.*, **108**(C9), 8101, doi:10.1029/2002JC001643.

Guardiani, G., Ostili, M., Salusti, E., & Sparnocchia, S., 1988. On a nonlinear regression method as applied to "aqua alta" of Venice, *Ocean Modelling*, **79**, 6–8.

Guedes Soares, C., Carretero Albiach, J. C., Weisse, R., & Alvarez-Fanjul, E., 2002. A 40 years hindcast of wind, sea level and waves in European waters, in *Proceedings of the OMAE2002, Oslo*.

Hammond, W. C. & Thatcher, W., 2004. Contemporary tectonic deformation of the Basin and Range province, western United States: 10 years of observation with the Global Positioning System, *J. Geophys. Res.*, **109**, 1–21.

Hecht, A. & Gertman, I., 2001. Physical features of the eastern Mediterranean resulting from the integration of POEM data with Russian Mediterranean Cruises, *Deep-Sea Research, I*, **48**, 1847–1876.

Hegerl, G. C. & Bindoff, N. L., 2005. Warming the world's oceans, *Science*, **309**, 254–255.

Hoyt, D. V. & Schatten, K. H., 1993. A discussion of plausible solar irradiance variations, 1700-1992, *J. Geophys. Res.*, **98**, 18895–18906.

Hoyt, D. V. & Schatten, K. H., 1998. Group sunspot numbers: a new solar activity reconstruction, *Solar Physics*, **181**, 491–512.

Hoyt, D. V., Schatten, K. H., & Nesmes-Ribes, E., 1994. The one hundredth year of Rudolf Wolf's death: do we have the correct reconstruction of solar activity?, *Geophys. Res. Lett.*, **21**, 2067–2070.

Hulme, M., Xianfu Li, Tumpenny, J., Mitchell, T., Jenkins, G., Jones, R., Lowe, J., Murphy, J., Hassel, D., Boorman, P., McDonald, R., & Hills, S., 2002. Climate Change Scenarios for the United Kingdom: The UKCIPO2 Scientific Report, Tech. rep., Tyndall Centre fro Climate Change Research, School of Environmental Sciences, University of East Anglia, Norwich, UK, 120 pp.

Hurrell, J. W., 1995. Decadal trends in the North Atlantic Oscillation: regional temperatures and precipitation, *Science*, **269**, 676–679.

Hurrell, J. W. & van Loon, H., 1997. Decadal variations in climate associated with the North Atlantic Oscillation, *Climatic Change*, **36**, 301–326.

IOC, 2000. *Manual on Sea Level Measurement and Interpretation. Volume 3 – Reappraisals and Recommendations as of the year 2000*, vol. 14 of **Manual and Guides**, Intergovernmental Oceanographic Commission, UNESCO, available at http://www.pol.ac.uk/psmsl/manuals/.

Ishii, M., Kimoto, M., & Kachi, M., 2003. Historical ocean subsurface temperature analysis with error estimates, *Monthly Weather Rev.*, **131**, 51–73.

Janekovic, I., Bobanovic, J., & Kuzmic, M., 2003. The Adriatic Sea M-2 and K-1 tides by 3D model and data assimilation, *Est. Coast. Shelf Sci.*, **57**(5-6), 873–885.

Josey, S. A., 2003. Changes in the heat and freshwater forcing of the Eastern Mediterranean and their influence on deep water formation, *J. Geophys. Res.*, **108**(C7), 3237, doi:10.1029/2003JC001778.

Kelly, P. M. & Wigley, T. M. L., 1992. Solar cycle length, greenhouse forcing and global climate, *Nature*, **360**, 328–330.

Kent, D. V., Rio, D., Massari, F., Kukla, G., & Lanci, L., 2002. Emergence of Venice during the Pleistocene, *Quaternary Science Reviews*, **21**, 1719–1727.

Kierulf, H. P. & Plag, H.-P., 2006. Precise point positioning requires consistent global products, in *EUREF Publication No. 14*, edited by J. A. Torres & H. Hornik, vol. BKG 35 of **Mitteilungen des Bundesamtes für Kartografie und Geodäsie**, pp. 111–120, Bundesamtes für Kartografie und Geodäsie, Frankfurt am Main.

Klein, B., Roether, W., Civitarese, G.and Gaĉić, M., Manca, B. B., & Ribera D'alcala, M., 2000. Is the Adriatic returning to dominate the production of Eastern Mediterranean deep water?, *Geophys. Res. Lett.*, **27**(20), 3377–3380.

Kovacevic, V., Gacic, M., & Poulain, P. M., 1999. Eulerian current measurements in the Strait of Otranto and in the Southern Adriatic, *J. Marine Sys.*, **20**(1-4), 255–278.

Krahmann, G. & Schott, F., 1998. Longterm increases in Western Mediterranean salinities and temperatures: anthropogenic and climatic sources, *Geophys. Res. Lett.*, **25**(22), 4209–4212.

Kreemer, C., Holt, W. E., & Haines, A. J., 2003. An integrated global model of present-day plate motion and plate boundary deformation, *Geophys. J. Int.*, **154**, 8–34.

Lacombe, H., Tchernia, P., & Gamberoni, L., 1985. Variable bottom water in the western Mediterranean Basin, *Progress in Oceanography*, **14**, 319338.

Langbein, J. & Johnson, H., 1997. Correlated errors in geodetic time series; implications for time-dependent deformation, *J. Geophys. Res.*, **102**, 591–604.

Lascaratos, A. & Gacic, M., 1990. Low-frequency sea-level variability in the Northeastern Mediterranean, *Deep-Sea Research*, **20**(4), 522–533.

Lascaratos, A., Roether, W., Nittis, K., & Klein, B., 1999. Recent changes in deep water formation and spreading in the mediterranean sea: a review, *Progress in Oceanography*, **44**(1-3), 5–36.

Leaman, K. D. & Schott, F. A., 1991. Hydrographic structure of the convection regime in the Gulf of Lions: winter 1987, *J. Phys. Oceanography*, **21**, 575–598.

Lean, J., Beer, J., & Bradley, R. S., 1995. Reconstruction of solar irradiance since 1610: Implications for climate change, *Geophys. Res. Lett.*, **22**, 3195–3198.

Levitus, S., Stephens, C., Antonov, J., & Boyer, T., 2000. Yearly and year-season upper ocean temperature anomaly field, 1948-1998, Tech. rep., U.S. Gov. Printing Office, Washington, D.C.

Lionello, P., Nizzero, A., & Elvini, E., 2003. A procedure for estimating wind waves and storm-surge climate scenarios in a regional basin: the Adriatic Sea case, *Climate Research*, **23**, 217–231.

Lionello, P., Mufato, R., & Tomasin, A., 2005. Sensitivity of free and forced oscillations of the Adriatic Sea to sea level rise, *???*, **xx**, yy.

Lisitzin, E., 1974. *Sea-Level Changes*, Elsevier Scientific Publishing Company, Amsterdam.

Lockwood, M. & Stamper, R., 1999. Long-term drift of the coronal source magnetic flux and the total solar irradiance, *Geophys. Res. Lett.*, **26**, 2461–2464.

Lombard, A., Cazenave, A., Le Traon, P.-Y., & Ishii, M., 2005. Contribution of thermal expansion to present-day sea level change revisited, *Global and Planetary Change*, **47**, 1–16, DOI: 10.1016/j.gloplacha.2004.11.016.

Lowe, J. & Gregory, J. M., 2005. The effects of climate change on storm surges around the united kingdom, *Phil. Trans. Royal Soc. A*, **363**, 1313 – 1328.

Maillard, C., Balopoulos, E., Fichaut, M., Giorgetti, A., Iona, A., Latrouite, A., & Manca, B., 2001. Mater data manual version 3, vol. 1: Data management structure, inventories, formats and codes, quality assurance, Rap. Int. IFREMER/TMSI/IDM/ SISMER/01-058, IFREMER, 67 pp.

Malacic, V. & Viezzoli, D., 2000. Tides in the northern Adriatic Sea - the Gulf of Trieste, *Nuovo Cimento Della Societa Italiana Di Fisica C-Geophysics And Space Physics*, **23**(4), 365–382.

Malacic, V., Viezzoli, D., & Cushman-Roisin, B., 2000. Tidal dynamics in the northern Adriatic Sea, *J. Geophys. Res.*, **105**(C11), 26265–26280.

Malanotte-Rizzoli, P., Manca, B. B., Ribera Dacala, M., Theocharis, A., Bergamasco, A., Bregant, D., Budillon, G., Civitarese, G., Georgopoulos, D., Michelato, A., Sansone, E., Scarazzato, P., & Souverrmezoglou, E., 1997. A synthesis of the Ionian hydrography, circulation and water mass pathways during poem–phase i, *Progr. in Oceanogr.*, **39**, 153–204.

Malanotte-Rizzoli, P., Manca, B. B., D'acala, M., Theocharis, A., Brenner, S., G., B., & Özsoy, E., 1999. The eastern Mediterranean in the 80s and in the 90s: the big transition in the intermediate and deep circulations, *Dynamics of Atmospheres and Oceans*, **29**, 365–395.

Manca, B., Burca, M., Giorgetti, A., Coatanoan, C., Garcia, M.-J., & Iona, A., 2004. Physical and biochemical averaged vertical profiles in the Mediterranean regions: an important tool to trace the climatology of water masses and to validate incoming data from operational oceanography, *J. Marine Sys.*, **48**(1-4), 83–116.

Manca, B. B., Kovacevic, V., Gacic, M., & Viezzoli, D., 2002. Dense water formation in the Southern Adriatic sea and spreading into the Ionian Sea in the period 1997 to 1999, *J. Marine Sys.*, **33–34**, 133–154.

Mantziafou, A. & Lascaratos, A., 2004. An eddy resolving numerical study of the general circulation and deep-water formation in the Adriatic Sea, *Deep-Sea Research, Part I*, **51**(7), 921–952.

Mao, A. C., Harrision, G. A., & Dixon, T. H., 1999. Noise in GPS coordinate time series, *J. Geophys. Res.*, **104**, 2797–2816.

Marcos, M., Gomis, D., Monserrat, S., Alvarez-Fanjul, E., Perez, B., & Garcia-Lafuente, J., 2005. Consistency of long sea-level time series in the northern coast of spain, *J. Geophys. Res.*, **110**(C3).

Marsigli, L. F., 1681. Osservazioni lntomo al Bosforo Tracio o vero Canale di Constantinopli rappresentate in lettera alla Sacra Real Maesta di Cristina Regina di Svezia Nicolb Angelo Tinassi, Rome. Reprinted in, *Bollettino di pesca, di piscicoltura e di idrobiologia*, **Anno Xl**(Fast. 5, Settembre-Ottobre 1935), 734–758.

Martin, J. M. & Milliman, J. D., 1997. EROS 2000 European chRiver Ocean System. The western Mediterranean: an introduction, *Deep-Sea Research*, **44**, 521–529.

Mazzarella, A. & Palumbo, A., 1991. Effect of sea level time variations on the occurrence of extreme storm-surges: an application to the northern Adriatic Sea, *Bollettino di Oceanologia Teorica ed Applicata*, **9**, 33–38.

MEDATLAS Group, 1997. MEDATLAS 1997 database and climatological atlas of temperature and salinity, Three cd-roms and www server, IFREMER Ed.

Meier, M. F., 1984. Contribution of glaciers to global sea level, *Science*, **226**, 1418–1421.

Meier, M. F. & Dyurgerov, M. B., 2002. How Alaska affects the world, *Science*, **297**, 350–351.

Meier, W., Stroeve, J., Fetterer, F., & Knowles, K., 2005. Reduction of Arctic sea ice cover no longer limited to summer, *Eos, Trans. Am. Geophys. Union*, **86**, 326.

Mertens, C. & Schott, F., 1998. Interannual variability of deep water formation in the Northwestern Mediterranean Sea, *J. Phys. Oceanogr*, **28**, 1410–1424.

Miller, L. & Douglas, B., 2004. Mass and volume contributions to the 20th century global sea level rise, *Nature*, **428**, 406–408.

Milne, G. A., Mitrovica, J. X., & Davis, J. L., 1999. Near-field hydro-isostasy: the implementation of a revised sea-level equation, *Geophys. J. Int.*, **139**, 464–482.

Mitrovica, J. X., Tamisiea, M. E., Davis, J. L., & Milne, G. A., 2001. Recent mass balance of polar ice sheets inferred from patterns of global sea-level change, *Nature*, **409**, 1026–1028.

Nakada, M. & Lambeck, K., 1987. Glacial rebound and relative sea-level variations: a new appraisal., *Geophys. J. R. Astron. Soc.*, **90**, 171–224.

Nielsen, J. N., 1912. Hydrography of the Mediterranean and adjacent seas, in *Danish Oceanographic Expeditions 1908–10*, vol. Report I, pp. 72–191.

Nocquet, J.-M. & Calais, E., 2004. Geodetic measurements of crustal deformation in the western Mediterranean and Europe, *P. Applied, Geophys.*, **161**, 661–681.

Oldow, J. S., Ferranti, L., Lewis, D. S., Campbell, J. K., D'Argenio, B., Catalano, R., Pappone, G., Carmignani, L., Conti, P., & Aiken, C. L. V., 2002. Active fragmentation of Adria, the north Africa promontory, central Mediterranean orogen, *Geology*, **30**, 779–782.

Orlic, M., Kuzmic, M., & Pasaric, Z., 1994. Response of the Adriatic Sea to the bora and sirocco forcing, *Continental Shelf Research*, **14**, 91–116.

Osborn, T. J., 2004. Simulating the winter North Atlantic Oscillation: the roles of internal variability and greenhouse forcing, *Climate Dynamics*, **22**, 605–623.

Osborn, T. J., Briffa, K. R., Tett, S. F. B., Jones, P. D., & Trigo, R. M., 1999. Evaluation of the North Atlantic Oscillation as simulated by a coupled climate model, *Climate Dynamics*, **15**, 685–702.

Overpeck, J. T. & others, ., 2005. Arctic system on trajectory to new, seasonally ice-free state, *Eos, Trans. Am. Geophys. Union*, **86**, 309,312–313.

Painter, S. C. & Tsimplis, M. N., 2003. Temperature and salinity trends in the upper waters of the Mediterranean Sea as determined from the MEDATLAS dataset, *Continental Shelf Res.*, **23**, 1507–1522.

Palumbo, A., 1997. A new methodological contribution to forecast extreme damaging events: an application to extreme marine floodings in Venice, Italy, *J. Coastal Research*, **13**, 890–894.

Pasaric, M. & Orlic, M., 2001. Long-term meteorological preconditioning of the North Adriatic coastal floods, *Continental Shelf Research*, **21**, 263–278.

Pasaric, M. & Orlic, M., 2001. Effects of mean sea level rise on the flooding of the North Adriatic coast, in *Book of Extended Abstracts, Final Workshop of COST Action 40*, pp. 80–82, Hydrographic Institute of the Republic of Croatia - Split.

Pasaric, M. & Orlic, M., 2002. Response of the Adriatic sea level to the planetary-scale atmospheric forcing, in *Sea level changes: determination and effects*, edited by P. e. a. Woodworth, no. 69 in Geophysical Monograph, pp. 29–39, American Geophysical Union.

Pasaric, M., Pasaric, Z., & Orlic, M., 2000. Response of the Adriatic sea level to the air pressure and wind forcing at low frequencies (0.01 - 0.1 cpd), *J. Geophys. Res.*, **105**, 11423–11439.

Peltier, W. R., 1998. Postglacial variations in the level of the sea: implications for climate dynamics and solid-earth geophysics, *Reviews of Geophysics*, **36**, 603–689.

Philander, S. G. H., 1990. *El Niño, La Niña and the Southern Oscillation*, Academic Press, San Diego, CA.

Pinardi, N., Korres, G., Lascaratos, A., Roussenov, V., & Stanev, E., 1997. Numerical simulation of the interannual variability of the Mediterranean Sea upper ocean circulation, *Geophys. Res. Lett.*, **24**(4), 425–428.

Pirazzoli, P. A., 1986. Secular trends of relative sea level (RSL) changes indicated by tide gauge records, *J. Coastal Res.*, **81**, 1–26.

Pirazzoli, P. A., 1987. Recent sea-level changes and related engineering problems in the Lagoon of Venice (Italy), *Prog. Oceanog.*, **18**, 323–346.

Pirazzoli, P. A. & Tomasin, A., 2002. Recent evolution of surge-related events in the Northern Adriatic area, *J. Coastal Research*, **18**(3), 537–554.

Plag, H.-P., 1984. Water level changes along the Norwegian coast, *Mar. Geophys. Res.*, **7**, 283–297.

Plag, H.-P., 1988. A regional study of Norwegian coastal long-period sea-level variations and their causes with special emphasis on the Pole Tide, *Berl. Geowiss. Abhandl. Reihe A*, **14**, 1–175.

Plag, H.-P., 1997. Chandler wobble and pole tide in relation to interannual atmosphere-ocean dynamics, in *Tidal Phenomena*, edited by H. Wilhelm, W. Zürn, & H.-G. Wenzel, no. 66 in Lecture Notes in Earth Sciences, pp. 183–218, Springer.

Plag, H.-P., 1998. Sea level and ice sheets: What can tide gauges tell us?, in *The Ninth General Assembly of the Working group of European Geoscientists for the Establishment of Networks for Earth-science Research - Second revised edition*, edited by H.-P. Plag, pp. 98–101, Norwegian Mapping Authority, ISBN 82-90408-76-5.

Plag, H.-P., 2000. Large-scale phenomena on interannual to interdecadal time scales detected from tide gauges and atmospheric data, in *Ocean Circulation Science derived from the Atlantic, Indian and Arctic Sea Level Networks*, edited by G. Mitchum, Workshop Report No. 171, pp. 4–8, Intergovernmental Oceanographic Commission.

Plag, H.-P., 2006. Recent relative sea level trends: an attempt to quantify the forcing factors, *Phil. Trans. Roy. Soc. London, A*, **364**, 1841–1869.

Plag, H.-P., 2006. Concepts in global and local sea level studies, *Global Planetary Change*, In preparation.

Plag, H.-P., 2006. Estimating recent global sea level changes, in *Dynamic Planet – Monitoring and Understanding a Dynamic Planet with Geodetic and Oceanographic Tools*, edited by P. Tregoning & C. Rizos, vol. 130 of **International Association of Geodesy Symposia**, pp. 39–46, Springer Verlag, Berlin.

Plag, H.-P., 2006. GGOS and it user requirements, linkage and outreach, in *Dynamic Planet – Monitoring and Understanding a Dynamic Planet with Geodetic and Oceanographic Tools*, edited by P. Tregoning & C. Rizos, vol. 130 of **International Association of Geodesy Symposia**, pp. 711–718, Springer Verlag, Berlin.

Plag, H.-P. & Jüttner, H.-U., 2001. Inversion of global tide gauge data for present-day ice load changes, in *Proceed. Second Int. Symp. on Environmental research in the Arctic and Fifth Ny-Ålesund Scientific Seminar*, edited by T. Yamanouchi, no. Special Issue, No. 54 in Memoirs of the National Institute of Polar Research, pp. 301–317.

Plag, H.-P. & Tsimplis, N., 1999. Temporal variability of the seasonal sea-level cycle in the North Sea and Baltic Sea in relation to climate variability, *Global and Planetary Change*, **20**, 173–203.

Plag, H.-P., Axe, P., Knudsen, P., Richter, B., & Verstraeten, J., eds., 2000. *European Sea Level Observing System (EOSS): Status and future developments*, vol. EUR 19682, Office for Official Publication of the European Communities, Luxembourg, 72 pages.

Platzman, G. W., 1983. World ocean tides synthesized from normal modes, *Science*, **220**, 602–603.

Platzman, G. W., 1984. Normal modes of the world ocean. Part iv: Synthesis of diurnal and semidiurnal tides, *J. Phys. Oceanogr.*, **14**, 1532–1550.

Pollak, M. I., 1951. The sources of deep water in the eastern Mediterranean Sea, *J. Marine Research*, **10**, 128–152.

Press, W. H., Teukolsky, S. A., Vetterling, W. T., & Flannery, B. P., 1992. *Numerical Recipes in FORTRAN*, Cambridge University Press.

Proudman, J., 1959. The condition that a long-period tide shall follow the equilibrium law, *Geophys. J. R. Astr. Soc.*, **?**, 244–249.

Pugh, D., 2004. *Changing sea level: effects of tides, weather and climate*, Cambridge University Press, Cambridge, 265 pages.

Quinlan, G. & Beaumont, C., 1982. The deglaciation of Atlantic Canada as reconstructed from the post glacial relative sea-level record, *Can. J. Earth Sci.*, **19**, 2232–2246.

Raicich, F., 2003. Recent evolution of sea-level extremes at Trieste (Northern Adriatic), *Continental Shelf Research*, **23**, 225–235.

Ramaswamy, V., Boucher, O., Haigh, J., Hauglustaine, D., Haywood, J., Myhre, G., Nakajima, T., Shi, G. Y., & Solomon, S., 2001. Radiative forcing of climate change, in *Climate Change 2001: The Scientific Basis. Contribution of Working Group I to the Third Assessment Report of the Intergovernmental Panel on Climate Change*, edited by J. T. Houghton, Y. Ding, D. J. Griggs, M. Noguer, P. J. van der Linden, X. Dai, K. Maskell, & C. A. Johnson, pp. 349–416, Cambridge University Press, Cambridge.

Rixen, M., Beckers, J.-M., Brankart, J.-M., & Brasseur, P. A., 2001. A numerically efficient data analysis method with error map generation, *Ocean Modelling*, **2**(1-2), 45–60.

Rixen, M., Beckers, J.-M., Levitus, S., Antonov, J., Boyer, T., Maillard, C., Fichaut, M., Balopoulos, E., Iona, S., Dooley, H., Garcia, M. J., Manca, B., Giorgetti, A., Manzella, G., Mikhailov, N., Pinardi, N., Zavatarelli, M., & the Medar Consortium, 2005. The Western Mediterranean deep water: a proxy for climate change, *Geophys. Res. Lett.*, p. in press.

Roether, W., Manca, B. B., Klein, B., Bregant, D., Georgopoulos, D., Beitzel, V., Kovacevic, V., & Luchetta, A., 1996. Recent changes in eastern Mediterranean deep waters, *Science*, **271**, 333–335.

Rohling, E. J. & Bryden, H. L., 1992. Man-induced salinity and temperature increases in Western Mediterranean deep water, *J. Geophys. Res.*, **97**, 11191–11198.

Rusconi, A., 1993. The tidal observations in the Venice lagoon - the variations in sea level observed in the last 120 years, in *Sea level changes and their consequences for hydrology and water management*, pp. 115–132, Bundesanstalt für Gewässerkunde, IHP/OHP Secretariat, Koblenz.

Sahagian, D. L., Schwartz, F. W., & Jacobs, D. K., 1994. Direct anthropogenic contribution to sea level rise in the twentieth century, *Nature*, **367**, 54–57.

Samuel, S. L., Haines, K.and Josey, S. A., & S. A. Myers, S. A., 1999. Response of the Mediterranean Sea thermohaline circulation to observed changes in the winter wind stress field in the period 1980-93, *J. Geophys. Res.*, **104**, 5191–5210.

Schlesinger, M. E. & Ramankutty, N., 1992. Implications for global warming of intercycle solar irradiance variations, *Nature*, **360**, 330–333.

Schlesinger, M. E. & Ramankutty, N., 1994. An oscillation in the global climate system of 65-70 years, *Nature*, **367**, 723–726.

Schlitzer, R., Roether, W., Oster, H., Junghans, H., Hausmann, M., Johannsen, H., & Michelato, A., 1991. Chlorofluoromenthane and oxygen in the Eastern Mediterranean, *Deep-Sea Research*, **38**, 1531–1555.

Schott, G., 1915. Die gewässer des mittelmeeres, *Annal. der Hydrographie und maritimen Meteorologie*, **43**(1-18), 63–79.

Schureman, P., 1958. Manual of harmonic analysis and prediction of tides, Coast and Geodetic Service Special Publication (Revised) 58, US Government Printing Office, Washington, D.C.

Sellschopp, J. & Alvarez, A., 2003. Dense low-salinity outflow from the Adriatic Sea under mild (2001) and strong (1999) winter conditions, *J. Geophys. Res.*, **108**(C9), art. no. 8104.

Serpelloni, E., Anzidei, M., Baldi, P., Casula, G., & Galvan, A., 2005. Crustal velocity and strain-rate fields in Italy and surrounding regions: new results from the analysis of permanent and non-permanent GPS networks, *??*, **161**(3), 861, doi:10.1111/j.1365–246X.2005.02618.x.

Serpelloni, E. e. a., 2002. Combination of permanent and non-permanent GPS networks for the evaluation of the strain-rate field in the central Mediterranean area, *Boll. Geof. Teor. Appl.*, **43**, 195–219.

Serre, T. & Nesme-Ribes, E., 2000. Nonlinear analysis of solar cycles, *Astron. Astrophys.*, **360**, 319–330.

Skliris, N. & Lascaratos, A., 2004. Impacts of the Nile River damming on the thermohaline circulation and water mass characteristics of the Mediterranean Sea, *J. Marine Sys.*, **52**, 121–143.

Smith, K. D., Seggern, D. v., Blewitt, G., Preston, L., Anderson, J. G., Wernicke, B. P., & Davis, J. L., 2004. Evidence for deep magma injection beneath Lake Tahoe, Nevada-California, *Science*, doi:10.1126/science.1101304.

Smith, R. L., 1986. Extreme value theory based on the r largest annual events, *J. Hydrology*, **86**, 27–43.

Solanki, S. K. & Fligge, M., 1998. Solar irradiance since 1874 revisted, *Geophys. Res. Lett.*, **25**, 341–344.

Sotillo, M. G., Ratsimandresy, A. W., Carretero, J. C., Bentamy, A., Valero, F., & Gonzalez-Rouco, F., 2005. A high-resolution 44-year atmospheric hindcast for the Mediterranean Basin: contribution to the regional improvement of global reanalysis, *Climate Dynamics*, pp. doi 10.1007/s00382–005–0030–7.

Spencer, N. E. & Woodworth, P. L., 1993. Data holdings of the Permanent Service for Mean Sea Level, Tech. rep., Permanent Service for Mean Sea Level, Bidston, UK, 81pp.

Stanev, E. V. & Peneva, E. L., 2002. Regional response to global climatic change: Black Sea examples, *Global and Planetary Change*, **32**, 33–47.

Stein, S., 1993. Space geodesy and plate motion, in *Contributions of Space Geodesy in Geodynamics: Crustal Dynamics*, edited by D. E. Smith & D. L. Turcotte, vol. 23 of **AGU Geodynamics Series**, pp. 5–20, AGU.

Stocchi, P., Spada, G., & Cianetti, S., 2005. Isostatic rebound following the Alpine deglaciation: impact on the sea level variations and vertical movements in the Mediterranean region, *Geophys. J. Int.*, **162**, 137–147.

Stommel, H., 1972. Deep winter-time convection in the Western Mediterranean Sea, in *Studies in Physical Oceanography*, edited by A. L. Gordon, vol. 2, pp. 207–218, Gordon and Breach, New York.

Strozzi, T., Webmuller, U., Tosi, L., Bitelli, G., & Spreckels, V., 2001. Land subsidence monitoring with Differential SAR Interferometry, *Photogrammatic Engineering & Remote Sensing*, **67**(11), 1261–1270.

Strozzi, T., Wegmüller, U., Werner, C., Wiesmann, A., Tosi, L., Teatini, P., & Carbognin, L., 2003. Venzia: Subsidence monitoring service in the Lagoon of Venice for regional administrative and water authorities data user programme (DUP), II Period - Executive Summary, Tech. rep., Gamma Remote Sensing, Muri, Switzerland, and Istituto di Scienze Marine, Venezia, Italy, Available at http://dup.esrin.esa.it/projects/psummaryp33.asp.

Supic, N., Grbec, B., Vilibic, I., & Ivancic, I., 2004. Long-term changes in hydrographic conditions in northern Adriatic and its relationship to hydrological and atmospheric processes, *Annales Geophysicae*, **22**, 733–745.

Sutton, R. T. & Hodson, D. L. R., 2005. Atlantic Ocean forcing of North American and European summer climate, *Science*, **309**, 115–118.

Tamisiea, M. E., Leuliette, E. W., Davis, J. L., & Mitrovica, J. X., 2005. Constraining hydrological and cryospheric mass flux in southeastern Alaska using space-based gravity measurements, *Geophys. Res. Lett.*, **32**, L20501, doi:10.1029/2005GL023961.

Tamura, Y., 1987. A harmonic development of the tide-generating potential, *Bull. Inf. Marées Terrestres*, **99**, 6813–6855.

Tawn, J., 1988. An extreme value theory model for dependent observations, *J. Hydrology*, **101**, 227–250.

Teatini, P., Putti, G., Gambolati, G.and Ferraris, S., & Camporese, M., 2004. Reversible/irreversible peat surface displamements and hydrological regime in the Zennare basin, Venice, in *Scientific research and safeguarding of Venice - Research Programme, 2001-2003*, edited by P. Campostrini, pp. 93–106, CORILA, Venice, Italy.

Theocharis, A., Balopoulos, E., Kioroglou, S., Kontoyiannis, H., & Iona, A., 1999. A synthesis of the circulation and hydrography of the South Aegean Sea and the Straits of the Cretan Arc (March 1994 – January 1995), *Progress in Oceanography*, **44**, 469–509.

Theocharis, A., Nittis, K., Kontoyiannis, H., Papageorgiou, E., & Balopoulos, E., 1999. Climatic changes in the Aegean Sea influence the Eastern Mediterranean thermohaline circulation, *Geophys. Res. Lett.*, **26**(11), 1617–1620.

Theocharis, A., Klein, B., Nittis, K., & Roether, W., 2002. Evolution and status of the Eastern Mediterranean Transient (1997-1999), *J. Marine Sys.*, **33**, 91–116.

Thomas, R., Rignot, E., Casassa, G., Kanagaratnam, P., Acuna, C., Akins, T., Brecher, H., Frederick, E., Gogineni, P., Kabill, W., Manizade, S., Ramamoorthy, H., Rivera, A., Russell, R., Sonntag, J., Swift, R., Yungle, J., & Zwally, J., 2004. Accelerated sea-level rise from West Antarctica, *Science*, **306**, 255–258.

Thompson, D. W. J. & Wallace, J. M., 2001. Regional climate impacts of the Northern Hemisphere annular mode and associated climate trends, *Science*, **293**, 85–89.

Tomasin, A., 1974. Recent changes in the tidal regime in Venice, *Rivista Italiana di Geophysica*, **XXIII**, 275–278.

Tosi, L., Carbognin, L., Teatini, P., Strozzi, T., & Wegmüller, U., 2002. Evidence of the present relative land stability of Venice, Italy, from land, sea, and space observations, *Geophys. Res. Lett.*, **29**(12), DOI: 10.1029/2001GL013211.

Trigo, I. F. & Davies, T. D., 2002. Meteorological conditions associated with the sea surges in Venice: a 40 year climatology, *Int. J. Climatol.*, **22**, 787–803.

Trupin, A. & Wahr, J. M., 1990. Spectroscopic analysis of global tide gauge sea level data, *Geophys. J. Int.*, **100**, 441–453.

Tsimplis, M., Zervakis, V., Josey, S., Peneva, E., Struglia, M. V., Stanev, E., Lionello, P., Malanotte-Rizzoli, P., Artale, V., Theocharis, A., Tragou, E., & Oguz, T., 2005. Changes in the oceanography of the Mediterranean Sea and their link to climate variability, in *Mediterranean Climate Variability*, edited by P. Lionello, P. Malanotte-Rizzoli, & R. Boscolo, in press.

Tsimplis, M. N. & Baker, T. F., 2000. Sea level drop in the Mediterranean Sea: an indicator of deep water salinity and temperature changes?, *Geophys. Res. Lett.*, **27**(12), 1731–1734.

Tsimplis, M. N. & Bryden, H. L., 2000. Estimation of the transports through the Strait of Gibraltar, *Deep-Sea Research I*, **47**, 2219–2242.

Tsimplis, M. N. & Josey, S. A., 2001. Forcing of the Mediterranean Sea by atmospheric oscillations over the North Atlantic, *Geophys. Res. Lett.*, **28**(5), 803–806.

Tsimplis, M. N. & Rixen, M., 2002. Sea level in the Mediterranean Sea: the contribution of temperature and salinity changes, *Geophys. Res. Lett.*, **29**(3), art. no. 2136.

Tsimplis, M. N. & Rixen, M., 2003. Variability of Mediterranean and Black Sea sea level and its forcing, in *Proceedings of the Second International Conference on the Oceanography of the Eastern Mediterranean and Black Sea: Similarities and Differences of Two Interconnected Basin*, in press.

Tsimplis, M. N. & Shaw, A. G. P., 2005. The forcing of sea level variability around Europe, *Phys. Chem. Earth*, In review.

Tsimplis, M. N., Flather, R. A., & Vassie, J. M., 1994. The North Sea Pole Tide described through a tide-surge numerical model, *Geophys. Res. Lett.*, **21**, 449–452.

Tsimplis, M. N., Proctor, R., & Flather, R. A., 1995. A two-dimensional tidal model for the Mediterranean Sea, *J. Geophys. Res.*, **100**, 16,223–16,239.

Tsimplis, M. N., Velegrakis, A. F., Theocharis, A., & Collins, M. B., 1997. Low frequency current variability at the straits of Crete, Eastern Mediterranean, *J. Geophys. Res.*, **102**(C11), 25005–25020.

Tsimplis, M. N., Velegrakis, A., Drakopoulos, P., Theocharis, A., & Collins, M., 1999. Cretan deep water outflow in the Eastern Mediterranean, *Progress in Oceanography*, **44**(4), 531–551.

Tsimplis, M. N., Josey, S. A., Rixen, M., & V., S. E., 2004. On the forcing of sea level in the Black Sea, *J. Geophys. Res.*, **109**(C8), art. no. C08015.

Tsimplis, M. N., Álvarez-Fanjul, E., Gomis, D., Fenoglio-Marc, L., & Pérez, B., 2005. Mediterranean sea level trends: Atmospheric pressure and wind contribution, *Geophys. Res. Lett.*, **32**, doi:10.1029/2005GL023867.

Tsimplis, M. N., Shaw, A. G. P., Flather, R. A., & Woolf, D. K., 2005. The influence of the North Atlantic Oscillation on the sea level around the northern European coasts reconsidered: the thermosteric effects, *Phil. Trans. Roy. Soc., A*, In press.

Tsimplis, M. N., Woolf, D. K., Osborn, T. J., Wakelin, S., Wolf, J., Flather, R. A., Shaw, A. G. P., Woodworth, P., Challenor, P., Blackman, D., Pert, F., Yan, Z., & Jevrejeva, S., 2005. Towards a vulnerability assessment of the UK and northern European coasts: the role of regional climate variability, *Phil. Trans. Roy. Soc., A*, **doi:10.1098**, pp 1–31.

Tushingham, A. M. & Peltier, W. R., 1992. Validation of the ICE-3G model of Würm-Wisconsin deglaciation using a global data base of relative sea level histories, *J. Geophys. Res.*, **97**, 3285–3304.

van den Brink, H. W., Können, G. P., & Opsteegh, J. D., 2005. Uncertainties in extreme surge level estimates from observational records, *Phil. Trans. Royal Soc. A*, **363**, 1377 – 1386.

Vilibic, I., 2000. A climatological study of the uninodal free oscillation in the Adratic Sea, *Acta Adriatica*, **41**, 89–102.

Vilibic, I., Leder, N., & Smircic, A., 1999. Forced and free response of the Adriatic sea level, *Nuovo Cimento Della Societa Italiana Di Fisica C-Geophysics And Space Physics*, **21**(4), 439–451.

Wadhams, P. & Munk, W., 2004. Ocean freshening, sea level rising, sea ice melting, *Geophys. Res. Lett.*, **31**, doi:10.1029/2004GL020039.

Wadie, W. F., 1984. The effect of regulation of the Nile River discharge on the oceanographic conditions and productivity of the southeastern part of the Mediterranean Sea, *Acta Adriatica*, **25**, 29–43.

Waitz, J. S., 1755. Undersokning om orsaken, hvarföre vattnet i Atlantiska hafvet altid strömar in uti medelhafvet genom Sundet vid Gibraltar, *Kungliga Svensk.a Vetenskupsakademiens Handlingar*, **16**, 27–50.

Wakelin, S. L. & Proctor, R., 2002. The impact of meteorology on modelling storm surges in the Adriatic sea, *Glob. Plan. Change*, **34**(1-2), 97–119.

Wakelin, S. L., Woodworth, P. L., Flather, R. A., & Williams, J. A., 2003. Sea-level dependence on the NAO over the NW European Continental Shelf, *Geophys. Res. Lett.*, **30**(7), doi: 10.1029/2003GL017041.

Warrick, R. & Oerlemans, J., 1990. Sea level rise, in *Climatic change. The IPCC scientific assessment*, edited by J. T. Houghton, G. J. Jenkins, & J. J. Ephraums, pp. 257–282, Cambridge University Press.

Warrick, R. A., Provost, C. l., Meier, M. F., Oerlemans, J., & Woodworth, P. L., 1996. Changes in sea level, in *Climate Change 1995–The science of climate change*, edited by J. T. Houghton, L. G. Meira Filho, B. A. Callander, N. Harris, A. Kattenberg, & K. Maskell, pp. 359–405, Cambridge University Press, Cambridge, UK.

Williams, S. P. D., 2003. The effect of coloured noise on the uncertainties of rates estimated from geodetic time series, *J. Geodesy*, **76**, 483–494.

Williams, S. P. D., Bock, Y., Fang, P., Jamason, P., Nikolaidis, R. M., & Prawirodirdjo, L., 2004. Error analysis of continuous GPS position time series, *J. Geophys. Res.*, **109**, B03412, doi:10.1029/2003JB002741.

Woodworth, P. & Player, R., 2003. The Permanent Service for Mean Sea Level: an update to the 21st century, *J. Coastal Research*, **19**, 287–295.

Woodworth, P. L., 2003. Some comments on the long sea level records from the Northern Mediterranean, *J. Coastal Res.*, **19**, 212–217.

Woolf, D., Shaw, A. G. P. S., & Tsimplis, M. N., 2003. The influence of the North Atlantic Oscillation on sea level variability in the North Atlantic Region, *The Global Atmosphere and Ocean System*, **9**(4), 145–167.

Wortel, M. J. R. & Spakmann, W., 2000. Subduction and slab detachment in the Mediterranean-Carpathian region, *Science*, **290**, 1910–1917.

Yan, Z., Tsimplis, M. N., & Woolf, D., 2004. An analysis of relationship between the North Atlantic Oscillation and sea level changes in NW Europe, *Intern. J. Climatol.*, **24**, 743–758.

Zerbini, S., Cecconi, G., Colombo, D., Matonti, F., Richter, B., Rocca, F., & van Dam, T., 2005. Monitoring natural and anthropogenic subsidence in the northern Adriatric area with space and terrestrial techniques, *Geophys. Res. Abstracts*, **7**, EGU05–A–03176.

Zervakis, V., Georgopoulos, D., Karageorgis, A. P., & Theocharis, A., 2004. On the response of the Aegean Sea to climatic variability: A review, *Int. J. Climatology*, **24**, 1845–1858, DOI: 10.1002/joc.1108.

Zumberge, J. F., Heflin, M. B., Jefferson, D. C., & Watkins, M. M., 1997. Precise point positioning for the efficient and robust analysis of GPS data from large networks, *J. Geophys. Res.*, **102**, 5005–5017.

Zwally, H. J., Abdalati, W., Herring, T., Larson, K., Saba, J., & Steffen, K., 2002. Surface melt-induced acceleration of Greenland ice-sheet flow, *Science*, **297**, 218–222.

A Acronyms and Abbreviations

CGPS	Continuous GPS
CTRS	Conventional Terrestrial Reference System
DST	Dynamic Sea surface Topography
ECMWF	European Center for Medium Range Weather Forecast
EMT	Eastern Mediterranean Transient
EOP	Earth Orientation Parameters
ERP	Earth Rotation Parameter
EUREF	European Reference Frame
GEO	*ad hoc*Group on Earth Observations
GEOSS	Global Earth Observation System of Systems
GGFC	(IERS) Global Geophysical Fluid Center
GLONASS	Global Navigation Satellite System
GMES	Global Monitoring of Environment and Security
GNSS	Global Navigation Satellite System
GOM	Global Ocean Mass
GOV	Global Ocean Volume
GPS	Global Positioning System
GRS80	Geodetic Reference System 80
IAG	International Association of Geodesy
IAU	International Astronomic Union
IERS	International Earth Rotation and Reference Systems Service
IGS	International GNSS Service
ITRF	International Terrestrial Reference Frame
ITRS	International Terrestrial Reference System
IUGG	International Union of Geodesy and Geophysics
LSL	Local Sea Level
NAM	Northern Hemisphere Annular Mode
NAO	North Atlantic Oscillation
PPP	Precise Point Positioning
SBL	(IERS GGFC) Special Bureau for Loading
SO	Southern Oscillation
SOC	Satelitte Orbits and Clocks
SOW	Statement of Work
TAR	Third assessement report of the IPCC
VLBI	Very Long Baseline Interferometry

END OF DOCUMENT